Gondwana Research 126 (2024) 129–201

Contents lists available at ScienceDirect

Gondwana Research

journal homepage: www.elsevier.com/locate/gr

GR Focus Review

Plate tectonic cross-roads: Reconstructing the Panthalassa-Neotethys Junction Region from Philippine Sea Plate and Australasian oceans and orogens

Suzanna H.A. van de Lagemaat *, Douwe J.J. van Hinsbergen

Deparment of Earth Sciences, Utrecht University, Utrecht, the Netherlands

ARTICLE INFO

Article history:
Received 6 June 2023
Revised 19 September 2023
Accepted 21 September 2023
Available online 29 September 2023
Handling Editor: M. Santosh

Keywords:
Kinematic reconstruction
Plate tectonics
GPlates
Junction Region
Philippine Sea Plate

ABSTRACT

The plate tectonic history of the Junction Region, which separated the Panthalassa and Tethys realms, is notoriously challenging to reconstruct. The region has been dominated by intra-oceanic subduction zones, which has led to a sparsely preserved geological record because not only the down-going plates but also the overriding plates were lost to subduction. Even though most lithosphere that was present in the Junction Region during the Mesozoic has been lost to subduction, orogenic records preserve sparse geological data that provide information for a plate tectonic reconstruction. Here we present a kinematic reconstruction of the Junction Region back to the Jurassic, based on the present-day geological record of the circum-Philippine Sea Plate and Australasian regions, and sparse paleomagnetic data. We provide a comprehensive review of orogenic and oceanic architecture from Japan to the SW Pacific region and use a systematic reconstruction protocol for a plate kinematic restoration back to the Jurassic. Based on our reconstruction, we propose that the Molucca Sea Plate formed as an Eocene back-arc basin behind a north-dipping subduction zone that consumed Australian oceanic lithosphere. We find that the Jurassic oceanic lithosphere preserved in the Philippines originated from the northern Australian margin when a back-arc basin formed. By placing our reconstruction in mantle reference frames, we identify multiple cases of slab dragging and suggest that the lithospheric collapse that led to Izu-Bonin Mariana forearc extension may have been a trigger for the absolute plate motion change of the Pacific Plate that formed the Hawaii-Emperor Bend. Finally, we show that there is no need for spontaneous subduction initiation at the Izu-Bonin Mariana trench. Instead, subduction initiation was more likely forced through a change in Pacific-Australia relative plate motion around 62 Ma. Subduction started along a pre-existing Mesozoic subduction zone that had accommodated mostly transform motion since about 85 Ma.

Contents

* Corresponding author.
E-mail address: s.h.a.vandelagemaat@uu.nl (S.H.A. van de Lagemaat).

https://doi.org/10.1016/j.gr.2023.09.013
1342-937X/

1. Introduction

Kinematic reconstructions of the modern oceans and orogens have revealed how since the formation of the supercontinent Pangea in the late Paleozoic, the Earth's plate tectonic system has been organized in two main plate tectonic realms. In the Tethyan realm, enclosed by Pangean continents, oceanic lithosphere formed and subducted along predominantly E-W trending ridges and trenches, and in the Panthalassa realm, surrounding the Pangea continents, subduction occurred predominantly radially away from the ocean, below Pangean continental margins and marginal basins (e.g., Larson and Chase, 1972; Engebretson et al., 1985; Stampfli and Borel, 2002; Seton et al., 2012; Torsvik and Cocks, 2017). In the Junction Region between these two realms, located between Australia and Eurasia (Fig. 1), these two plate systems interacted, forming a complex plate boundary system with long- and short-lived subduction zones and marginal basins (Seton and Müller, 2008; Hall, 2002, 2012; Zahirovic et al., 2014). The interaction between these plate systems holds many clues for the understanding of the drivers of plate tectonics and the formation and demise of oceans and subduction zones. However, much of these subduction zones in the Junction Region were intra-oceanic, which has a much lower propensity to leaving geological records of subduction than active continental margins do, because not only the downgoing, but also the overriding plates are eventually lost to subduction.

Kinematic restorations typically focus on regional tectonic problems of the Junction Region, such as the formation and evolution of the Philippine Sea Plate (e.g., Zahirovic et al., 2014; Wu et al., 2016; Liu et al., 2023). Such reconstructions give plate tectonic and paleogeographic context to present-day geological records of the region but focus less on the kinematic context of the wider region reconstructed in less detail. These reconstructions vary widely between authors and are difficult to connect to the global plate circuit. On the other hand, reconstructions that focused on hemispheric scales are schematic and conceptual and do not display in detail where modern geological records restore (e.g., Seton et al., 2012; Müller et al., 2019; Scotese, 2021). In this paper, we aim to bridge this gap, and provide a kinematic restoration of the Junction Region in which present-day geological records are reconstructed into the plate kinematic framework of the entire region back to Mesozoic times.

To this end, we provide a comprehensive review of the modern oceanic basins and orogenic architecture of the entire Junction Region, spanning from Japan to New Zealand (Fig. 1), following the approach of Van Hinsbergen et al. (2020a) and Boschman et al. (2021a), and connected to the recent reconstruction of SE Asian orogenic and plate tectonic evolution of Advokaat and Van Hinsbergen (2023), and Pacific Basin evolution as summarized in Van de Lagemaat et al. (2023a). Based on this review, we systematically reconstruct the Junction Region in the context of the entire plate tectonic system of the west Panthalassa and eastern Neotethyan realms. Our reconstruction goes back to the oldest records of intra-oceanic subduction that are preserved in the Junction Region, on the Philippines, i.e., back to the latest Jurassic (Dimalanta et al., 2020). We will discuss the implications of our reconstruction for the formation and destruction of plate boundaries and interpretation of modern mantle structure.

2. Reconstruction approach

To kinematically restore the Junction Region, we thoroughly review the ocean floor structure and age of marginal basins and the surrounding orogenic architecture, of the Philippine Sea Plate, New Guinea, and their surroundings. We review previously published geological and geophysical data that provide kinematic information as input for our reconstruction. This reconstruction is made using GPlates, a freely available plate reconstruction software (www.gplates.org; Boyden et al., 2011; Müller et al., 2018).

Fig. 1. Map of the Pangea-Tethys and Panthalassa plate tectonic realms separated by the Juction Region. Present-day plate boundaries are red (modified from Bird, 2003), relevant former plate boundaries are gray. Dark shaded areas behind colored realms are present-day subaerially exposed crust, the light shaded areas are submerged continental crust and thickened oceanic crust, i.e.,oceanic plateaus and island arcs.

To ensure that our reconstruction is reproducible, we use a systematic reconstruction hierarchy (Boschman et al., 2014; Van Hinsbergen et al., 2020a), which also makes our reconstruction easily adaptable when new kinematic data become available.

The first step in the reconstruction hierarchy aims at establishing the relative motions of the major plates surrounding the Junction Region (Eurasia, Australia, Pacific) using the most recent marine magnetic anomaly and fracture zone data. For the age of polarity chrons (intervals of geologic time with a normal or reversed field) and magnetic field reversals, we use the geomagnetic polarity time scale of Ogg (2020). Marine magnetic anomaly and fracture zone data of marginal ocean basins within the Junction Region are reviewed, which provide information about the timing, amount, and direction of their opening.

Our plate reconstruction has its root in Africa, of which the motion can be described relative to an independent reference frame, i.e., the spin axis or the mantle. Prior to the formation of the Pacific-Antarctic Ridge (~84 Ma), there is no plate circuit connection between the Panthalassa and Indo-Atlantic realms. Following Boschman et al. (2019), we use the Pacific mantle reference frame of Torsvik et al. (2019) combined with the slab reference frame of Van der Meer et al. (2010) to reconstruct Panthalassa plate motions before 84 Ma.

Next, we review the architecture of accretionary orogens that contain relics of now-subducted lithosphere and their overriding plates, and their subsequent deformation. We follow the reconstruction philosophy of Van Hinsbergen and Schouten (2021), by reconstructing upper/intraplate deformation and crustal accretion separately. Upper/intraplate deformation is reconstructed based on estimates of displacement accommodated by crustal extension, strike-slip faults, and tectonic shortening obtained from structural geology. This provides a plate kinematic model that must be geo-

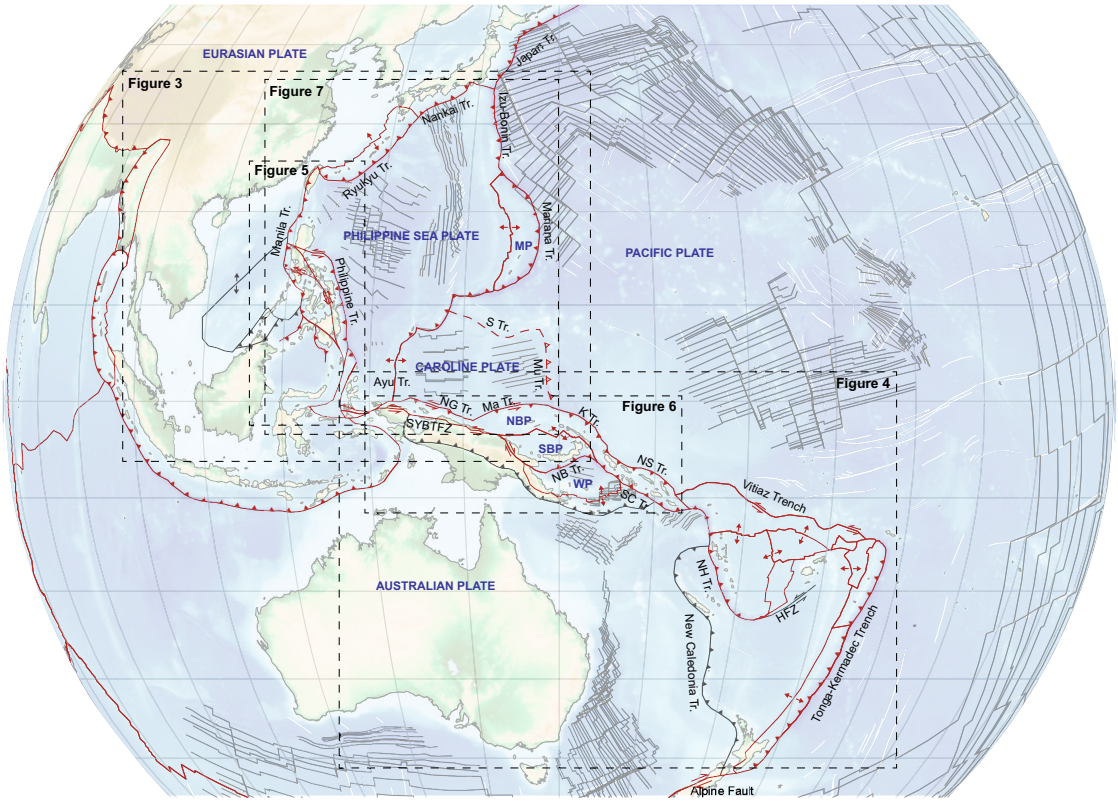

Fig. 2. Map of the reconstructed region. A0 geographic and tectonic maps of the region are provided in the supporting information as Figures S1 and S2. Present-day plate boundaries are red (modified from Bird, 2003), relevant former plate boundaries are gray. Marine magnetic anomalies are indicated by black lines, fracture zones are indicated by white lines (both based on the GSFML database, Matthews et al., 2011; Seton et al., 2014; Wessel et al., 2015, and references therein). Background image is ETOPO 2022 15 Arc-Second Global Relief Model (NOAA, 2022). HFZ = Hunter Fracture Zone; K Tr = Kilinailau Trench; Ma Tr = Manus Trench; MP = Mariana Plate; NB Tr = New Britain Trench; NBP = North Bismarck Plate; NG Tr = New Guinea Trench; NH Tr = New Hebrides Trench; NS Tr = North Solomon Trench; S Tr = Sorol Trough; SBP = South Bismarck Plate; SC Tr = San Cristobal Trench; SYBTFZ = Sorong-Yapen-Bewani-Torricelli Fault Zone; WP = Woodlark Plate.

metrically consistent, without any large over- or underlaps when there is no geological evidence, and that follows the basic rules of plate tectonics, which means that all plates are surrounded by plate boundaries that end in triple junctions (Cox and Hart, 1986).

We then reconstruct the nature and geological history of the large portions of lithosphere that have been lost to subduction, based on information preserved in accretionary complexes and ophiolites. The analysis of the stratigraphy and metamorphic history of accreted ocean-plate derived units (Ocean Plate Stratigraphy (OPS); Isozaki et al., 1990, Wakita and Metcalfe, 2005; Wakita, 2015) allows us to determine the age and geological history of the subducted oceanic lithosphere. Similarly, accreted Continental Plate Stratigraphy (CPS) allows restoration of passive margins and microcontinents that were entrained in subduction zones (Van Hinsbergen and Schouten, 2021). Key constraints for the history of oceanic basins also comes from oceanic upper plate lithosphere preserved as ophiolites and overlying volcanic arcs. Because ophiolites provide key information for the study of subduction initiation and cessation (e.g., Guilmette et al., 2018; Stern and Gerya, 2018; Crameri et al., 2020; Lallemand and Arcay, 2021; Van Hinsbergen et al., 2021), we carefully include them in our reconstruction to provide regional kinematic context for these processes. In addition, the geochemical composition of ophiolites provides insight into the tectonic setting of formation of the oceanic lithosphere. We review tectonic interpretations based on geochemistry, to facilitate the interpretation of the reconstruction, but we do not use this information to build the reconstruction for which we only use kinematic data. Finally, we test our reconstruction against a compilation of paleomagnetic data from the Philippine Sea Plate (Van de Lagemaat et al., 2023b), using the paleomagnetic reference frame of Vaes et al. (2023), and iterate where necessary, to ascertain that the reconstruction is in accordance with paleomagnetic constraints.

Fig. 3. Geographic (A) and tectonic (B) maps of the Philippine Sea Plate region. Present-day plate boundaries are red (modified from Bird, 2003), relevant former plate boundaries are gray. Marine magnetic anomalies are indicated by white lines, fracture zones are indicated by black lines (both based on the GSFML database, Matthews et al., 2011; Seton et al., 2014; Wessel et al., 2015, and references therein). AP = Amami Plateau; ASB = Amami-Sankaku Basin; BbIG = Babuyan Island Group; BHP = Bird's Head Peninsula; BTF = Bewani-Torricelli Fault; BtIG = Batan Island Group; CC = Central Cordillera; CIR = Caroline Islands Ridge; ELTF = East Luzon Transform Fault; ELTr = East Luzon Trench; GR = Gagua Ridge; HTr = Halmahera Trench; HB = Huatung Basin; KB = Kikai Basin; KDB = Kita-Daito Basin; KG = Kerama Gap; LI = Lanyu Island; MAE = Minami-Amami Escarpment; MDB = Minami-Daito Basin; MS = Molucca Sea; Ne Tr = Negros Trench; OI = Okinawa Island; OT = Ogasawara Trough; RIG = Romblon Island Group; RMF = Ramu-Markham Fault; Sa Tr = Sangihe Trench; SCDL = Sindangan-Cotabato-Daguma Linemaent; SMR = Sierra Madre Range; SP = Snellius Plateau; SSF = Sibuyan Sea Fault; Su Tr = Sulu Trench; WCR = West Caroline Rise; ZP = Zamboanga Peninsula.

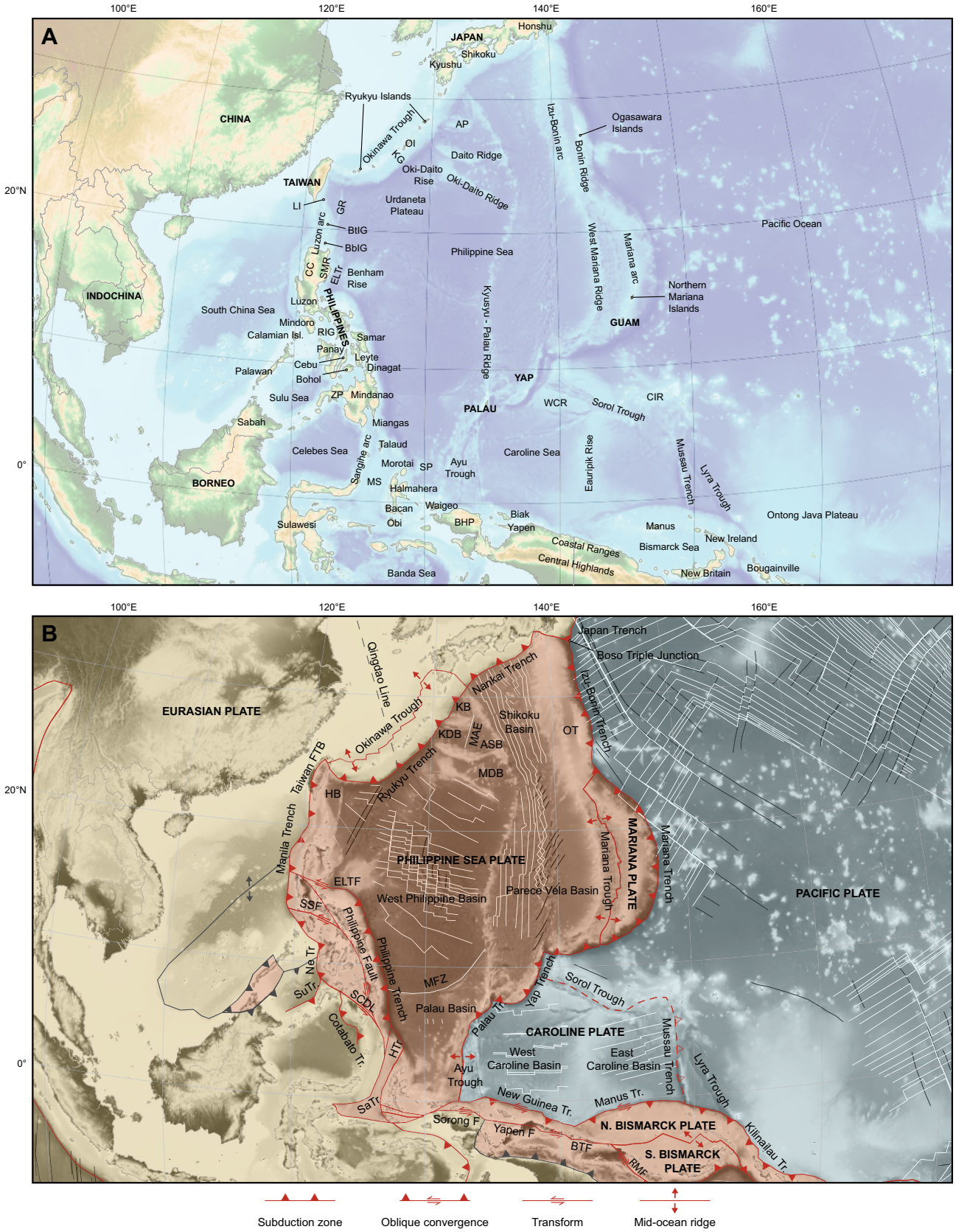
A
100°E
120°E
140°E
160°E
20°N
0°
JAPAN
Honshu
Shikoku
Kyushu
Ryukyu Islands
CHINA
Okinawa Trough
AP
Izu-Bonin arc
Ogasawara Islands
Bonin Ridge
OI
KG
Daito Ridge
Oki-Daito Rise
Oki-Daito Ridge
TAIWAN
LI
GR
Urdaneta Plateau
Luzon arc
BtlG
BblG
CC
SMR
ELTr
Benham Rise
Philippine Sea
West Mariana Ridge
Mariana arc
Pacific Ocean
Northern Mariana Islands
GUAM
INDOCHINA
South China Sea
Luzon
PHILIPPINES
Mindoro
Calamian Isl.
RIG
Samar
Panay
Leyte
Cebu
Dinagat
Palawan
Bohol
Kyusyu - Palau Ridge
YAP
Sulu Sea
ZP
Mindanao
PALAU
WCR
Sorol Trough
CIR
Sabah
Miangas
Celebes Sea
Talaud
Sangihe arc
Morotai
SP
Ayu Trough
Caroline Sea
Eauripik Rise
Mussau Trench
Lyra Trough
BORNEO
MS
Halmahera
Bacan
Waigeo
Sulawesi
Obi
BHP
Biak
Yapen
Ontong Java Plateau
Manus
New Ireland
Bismarck Sea
Coastal Ranges
Central Highlands
New Britain
Bougainville
Banda Sea
B
100°E
120°E
140°E
160°E
20°N
0°
Japan Trench
Boso Triple Junction
Izu-Bonin Trench
Nankai Trench
Qingdao Line
EURASIAN PLATE
Okinawa Trough
KB
Shikoku Basin
OT
KDB
MAE
ASB
Taiwan FTB
Ryukyu Trench
MDB
HB
Manila Trench
MARIANA PLATE
Mariana Trench
PHILIPPINE SEA PLATE
Mariana Trough
PACIFIC PLATE
ELTF
West Philippine Basin
Parece Vela Basin
SSF
Philippine Faultlt
Philippine Trench
Ne Tr
SuTr
MFZ
Yap Trench
Sorol Trough
SCDL
Palau Basin
Palau Tr
Coabalo Tr
HTF
CAROLINE PLATE
West Caroline Basin
East Caroline Basin
Mussau Trench
Lyra Trough
Ayu Trough
New Guinea Tr.
Manus Tr.
SaTr
Sorong F
Yapen F
N. BISMARCK PLATE
Kilinailau Tr.
BTF
S. BISMARCK PLATE
RMF
Subduction zone
Oblique convergence
Transform
Mid-ocean ridge

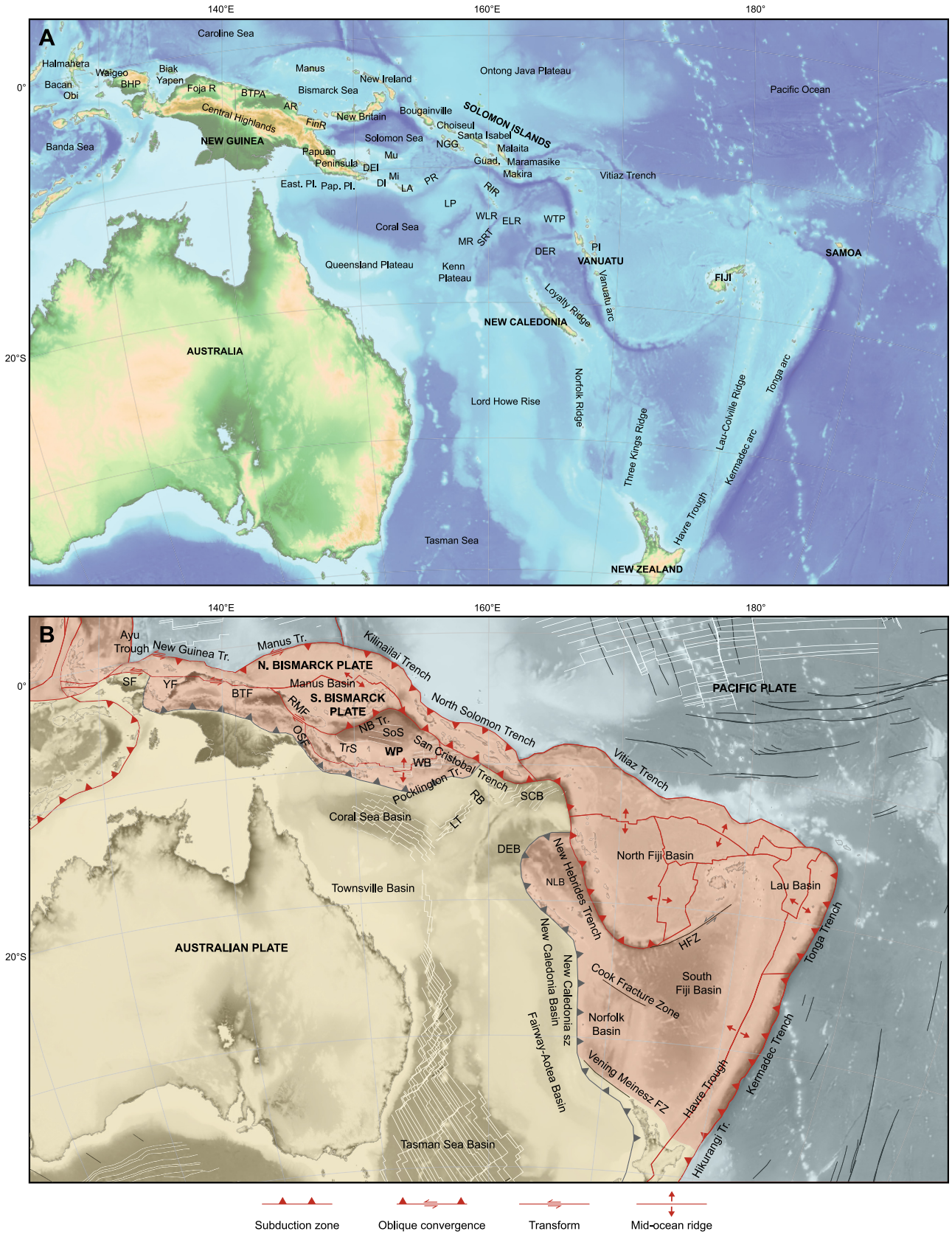
A
140°E
160°E
180°
0°
20°S
Caroline Sea
Halmahera
Waigeo
Biak
Yapen
Bacan
Obi
BHP
Foja R
BTPA
Central Highlands
AR
FinR
Manus
New Ireland
Bismarck Sea
New Britain
Bougainville
SOLOMON ISLANDS
Choiseul
Santa Isabel
Malaita
Guad.
Maramasike
Makira
Solomon Sea
NGG
Mu
Mi
DI
DEI
Papuan Peninsula
East. Pl.
Pap. Pl.
PR
RIR
LA
LP
WLR
ELR
WTP
Coral Sea
MR
SRT
DER
PI
VANUATU
Vitiaz Trench
Ontong Java Plateau
Pacific Ocean
Banda Sea
NEW GUINEA
Queensland Plateau
Kenn Plateau
Loyalty Ridge
Vanuatu arc
NEW CALEDONIA
FIJI
SAMOA
AUSTRALIA
Lord Howe Rise
Norfolk Ridge
Three Kings Ridge
Lau-Colville Ridge
Kermadec arc
Tonga arc
Havre Trough
Tasman Sea
NEW ZEALAND
B
140°E
160°E
180°
0°
20°S
Ayu Trough
New Guinea Tr.
Manus Tr.
Kilinailai Trench
N. BISMARCK PLATE
Manus Basin
S. BISMARCK PLATE
SF
YF
BTF
RMF
OSF
NB Tr.
SoS
TrS
WP
WB
San Cristobal Trench
Pocklington Tr.
RB
SCB
LT
North Solomon Trench
PACIFIC PLATE
Vitiaz Trench
Coral Sea Basin
DEB
New Hebrides Trench
NLB
North Fiji Basin
Lau Basin
Townsville Basin
AUSTRALIAN PLATE
HFZ
Tonga Trench
New Caledonia Basin
New Caledonia sz
Cook Fracture Zone
South Fiji Basin
Norfolk Basin
Fairway-Aotea Basin
Vening Meinesz FZ
Havre Trough
Kermadec Trench
Hikurangi Tr.
Tasman Sea Basin
Subduction zone
Oblique convergence
Transform
Mid-ocean ridge

3. Review of continental, oceanic, and orogenic architecture

To reconstruct the plate tectonic history of the Philippine Sea Plate and New Guinea region, we first define and review the boundaries of the region of interest for our reconstruction (Figs. 1 and 2; A0 versions of the geographic and tectonic maps are provided in the Supporting Information as Figures S1 and S2). The Junction Region as we will use it throughout this study encompasses the following region: The Philippine Sea and Caroline plates and their plate boundaries, the Philippine archipelago and the northern Molucca Islands, New Guinea and surrounding islands and intervening basins, the Melanesian borderlands, which includes the Solomon Islands, Vanuatu, Fiji, and oceanic basins such as the Bismarck Sea and the Solomon Sea, and the SW Pacific region, which comprises the series of ridges and oceanic basins to the east of Australia (Figs. 3–7, Figures S1 and S2).

Surrounding the Junction Region are three major, mostly rigid tectonics plates: the Eurasian, Australian, and Pacific plates that are connected in a plate circuit (Fig. 2). To also be able to use absolute plate motion frames, the plate circuit has its root in Africa, whose motion relative to the Earth's mantle or spin axis is available through e.g., hotspot and paleomagnetic reference frames (O'Neill et al., 2005; Torsvik et al., 2008, 2012; Doubrovine et al., 2012; Vaes et al., 2023). The plate circuit that we use in our reconstruction is Eurasia – North America – Africa – Antarctica – Australia/Pacific, whereby we follow the circuit described in Vaes et al. (2023).

In addition to these rigid plates, there are also deformed regions that border the Junction Region. These are the region west of the Philippine archipelago, i.e., the circum-South China Sea region, as well as the Sulu, Celebes, and Banda Sea, and surrounding islands (Fig. 3). This part of SE Asia contains continental fragments that were derived from Gondwana and migrated to and collided with Eurasia during opening and closure of Tethyan ocean basins (Hall, 2012; Advokaat and Van Hinsbergen, 2023; Metcalf, 2013). We refer to this orogenic collage as the SE Asian Tethysides. The south of the study region is the SW Pacific realm, hosting extensional basins and fold-thrust belts east of Australia (Fig. 4).

For the reconstruction of the rigid plates that are part of the global plate circuit and for the deformed SE Asian and Zealandia regions, we use previously published reconstructions, as reviewed below. The reconstruction of the circum-Junction Region provides a net area change of the Junction Region through time, which serves as the plate kinematic boundary condition of our new reconstruction of the Junction Region itself. Below, we first describe the plate circuit and the kinematic data that describe the relative motions that are incorporated in our reconstruction. Next, we give a short overview of the deformed regions adjacent to the Junction Region, and, finally, we provide an extensive review the orogenic architecture of the Junction Region itself.

3.1. Plate circuit

The upper plate to the Junction Region is the Eurasian continent. The Eurasian Plate is currently essentially rigid but is an amalgamation of formerly independently moving tectonic plates. The North and South China blocks have moved in unison since the Triassic, but relative motion between the China blocks and Siberia/Eurasia continued into the Cretaceous, until the closure of the Mongol-Okhotsk oceanic basin (Klimetz, 1987; Kravchinsky et al., 2002; Cogné et al., 2005; Van der Voo et al., 2015). For the motion of the China blocks relative to Eurasia before the Cretaceous, we incorporate the plate model of Torsvik and Cocks (2017), which builds on the reconstruction of Van der Voo et al. (2015).

Our reconstruction uses the global plate circuit used by Vaes et al. (2023) as basis for their paleomagnetic reference frame. In this plate circuit, the Eurasian Plate is reconstructed relative to the North American Plate, based on marine magnetic anomalies that formed in the North Atlantic Ocean. We use the rotation poles of DeMets et al. (2015), Vissers and Meijer (2012a, b), and Srivastava and Roest (1996). The North American Plate is reconstructed relative to Africa, also based on marine magnetic anomalies in the Atlantic Ocean. In our reconstruction, we use the rotation poles of DeMets et al. (2015), Müller et al. (1999), Gürer et al. (2022), and Van Hinsbergen et al. (2020a).

The other two rigid plates, the Australian and Pacific plates, are both reconstructed relative to Antarctica, which is in turn reconstructed relative to Africa. East Antarctica is reconstructed relative to Africa based on rotation poles derived from marine magnetic anomalies that formed along the Southwest Indian Ridge. We use the rotation poles of Bernard et al. (2005), Cande et al. (2010), Mueller and Jokat (2019), and DeMets et al. (2021) for this relative motion. The Australian Plate is reconstructed relative to East Antarctica based on marine magnetic anomalies that formed through spreading along the Southeast Indian Ridge. We incorporate the finite rotation poles of Cande and Stock (2004), Whittaker et al. (2007, 2013), and Williams et al. (2011). The Pacific Plate is reconstructed back to 83.7 Ma relative to West Antarctica based on marine magnetic anomalies that formed along the Pacific-Antarctic Ridge, for which we use the rotation poles of Croon et al. (2008) and Wright et al. (2015, 2016). The motion of West Antarctica relative to East Antarctica is based on marine magnetic anomaly constraints and continental extension estimates based on crustal thicknesses, for which we use the rotation poles of Cande and Stock (2004), Granot et al. (2013), Granot and Dyment (2018), and Van de Lagemaat et al. (2023a). Before the formation of the Pacific-Antarctic Ridge, the Pacific Plate is disconnected from the plate circuit, and is instead reconstructed in a separate Pacific absolute plate motion frame, for which we use the hotspot frame of Torsvik et al. (2019).

Fig. 4. Geographic (A) and tectonic (B) maps of the Melanesian – SW Pacific region. Present-day plate boundaries in red (modified from Bird, 2003), relevant former plate boundaries in gray. Marine magnetic anomalies are indicated by white lines, fracture zones are indicated by black lines (both based on the GSFML database, Matthews et al., 2011; Seton et al., 2014; Wessel et al., 2015, and references therein). AR = Adelbert Range; BTF = Bewani-Torricelli Fault; BTPA = Bewani-Torricelli-Prince Alexander Mountains; BHP = Bird's Head Peninsula; DEB = D'Entrecasteaux Basin; DEI = D'Entrecasteaux Islands; DER = D'Entrecestaux Ridge; DI = Deboyne Islands; ELR = East Laperouse Rise; East. Pl. = Eastern Plateau; FinR = Finisterre Range; Foja R = Foja Range; Guad. = Guadalcanal; HFZ = Hunter Fracture Zone; LA = Louisiade Archipelago; LP = Louisiade Plateau; LT = Louisiade Trough; MR = Mellish Rise; Mi = Misima Island; Mu = Muyua/Woodlark Island; NB Tr = New Britain Trench; NGG = New Georgia Group; NLB = North Loyalty Basin; OSF = Owen-Stanley Fault; Pap. Pl. = Papuan Plateau; PI = Pentecost Island; PR = Pocklington Rise; RMF = Ramu-Markham Fault; RB = Rennell Basin; RIR = Rennell Islands Ridge; SCB = Santa Cruz Basin; SoS = Solomon Sea; SF = Sorong Fault; SRT = South Rennell Trough; TrS = Trobriand Scarp; WLR = West Laperouse Rise; WTP = West Torres Plateau; WP = Woodlark Plate; YF = Yapen Fault.

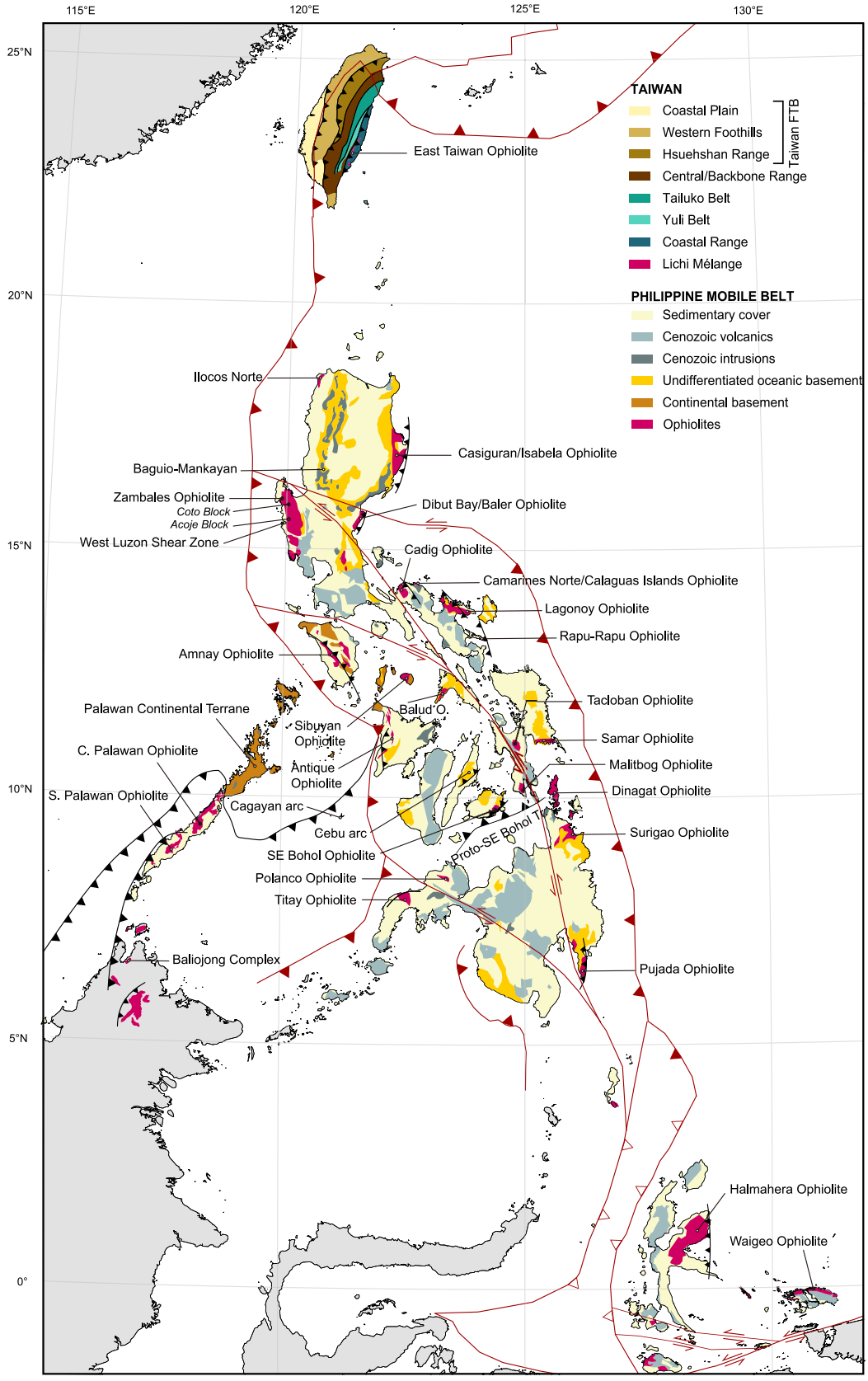

Fig. 5. Geological map of Taiwan, the Philippines, and the northern Molucca Islands. Based on Ren et al. (2013). FTB = Fold-and-Thrust Belt.

After its birth in the Panthalassa Ocean around 190 Ma, the Pacific Plate was surrounded by mid-ocean ridges and was actively spreading with three oceanic plates: the Farallon Plate in the east, the Phoenix Plate in the south, and the Izanami Plate and subsequently the Izanagi Plate in the west (Engebretson et al., 1985; Nakanishi et al., 1992; Nakanishi and Winterer, 1998; Seton

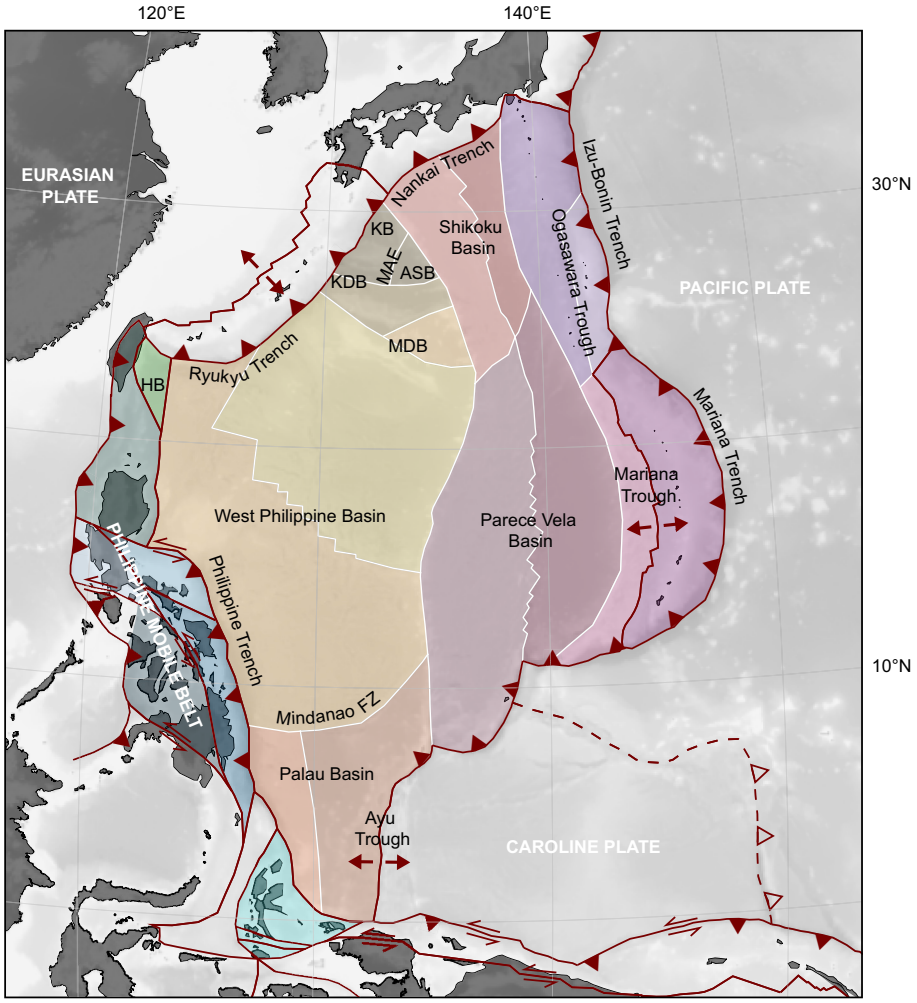

Fig. 6. Tectonic map of the Philippine Sea Plate, highlighting the different microplates that formed as a result of oceanic spreading at different spreading centers. Present-day plate boundaries are red (modified from Bird, 2003), former plate boundaries are white. KB = Kikai Basin; KDB = Kita-Daito Basin; MAE = Minami-Amami Escarpment; ASB = Amami-Sankaku Basin; MDB = Minami-Daito Basin; HB = Huatung Basin.

et al., 2012; Boschman and Van Hinsbergen, 2016; Boschman et al., 2021a). Marine magnetic anomalies that record spreading between the Pacific and Izanami/Izanagi plates between polarity chrons M5-M35 (127.5–160.9 Ma) are preserved on the Pacific Plate (Nakanishi et al., 1992). Spreading between the Pacific and Phoenix plates is recorded by marine magnetic anomalies that formed during chrons M1 and M29 (123.8 – 160.9 Ma; Nakanishi et al., 1992). The Pacific oceanic crust that is currently subducting at the Izu-Bonin-Mariana trench is oceanic crust that formed along the Pacific-Izanami/Izanagi ridges and is younging northwards. The oldest crust that is currently subducting at the Izu-Bonin-Mariana subduction zone in the south is Jurassic in age (c. 160 Ma), while Early Cretaceous (c. 130 Ma) oceanic crust is currently subducting below the northernmost Izu-Bonin Mariana subduction zone and below Japan. Pacific oceanic crust that formed through spreading with the Phoenix Plate is in the west overlain by the Ontong Java Plateau, a Large Igneous Province (LIP) that erupted at about 120 Ma (Mahoney et al., 1993; Larson, 1997; Chambers et al., 2004). The emplacement of the Ontong Java LIP led to the break-up of the Phoenix Plate around 120 Ma (Taylor, 2006; Chandler et al., 2012; Van de Lagemaat et al., 2023a). We incorporate the evolution of the western Panthalassa oceanic basin using the reconstruction of Van de Lagemaat et al. (2023a) for the Pacific and Phoenix plates, that of Boschman et al. (2021a, b) for the Izanami and Izanagi plates, and of Vaes et al. (2019) for the deformation of the Eurasian margin forming the Japan Sea between 23 and 15 Ma.

3.2. Deformed border regions

3.2.1. SE Asian Tethysides

We here briefly summarize the tectonic evolution and architecture of the SE Asian Tethysides that is overthrusted westwards by the Cretaceous and Cenozoic ophiolites of the Philippine Mobile Belt (Rangin, 1991). We refer to Advokaat and Van Hinsbergen (2023) for a detailed review of the SE Asian Tethysides and its tectonic reconstruction since the Mesozoic, which we incorporate into our model.

The northernmost basin of this region is the South China Sea, which is an uppermost Eocene to middle Miocene oceanic basin that formed after an Eocene phase of rifting that separated a Cretaceous and older accretionary prism from the South China Block (Faure and Ishida, 1990; Briais et al 1993; Li et al., 2014a; Cao et al., 2021). The opening of the South China Sea basin occurred while Borneo was converging with South China (Advokaat et al., 2018), which was accommodated by southward subduction of a Cretaceous lithosphere that became trapped between Borneo and South China in the Late Cretaceous: the so-called proto-South China Sea (Van de Lagemaat et al., 2023c). On Palawan, this subduction zone was associated with the formation of a supra-

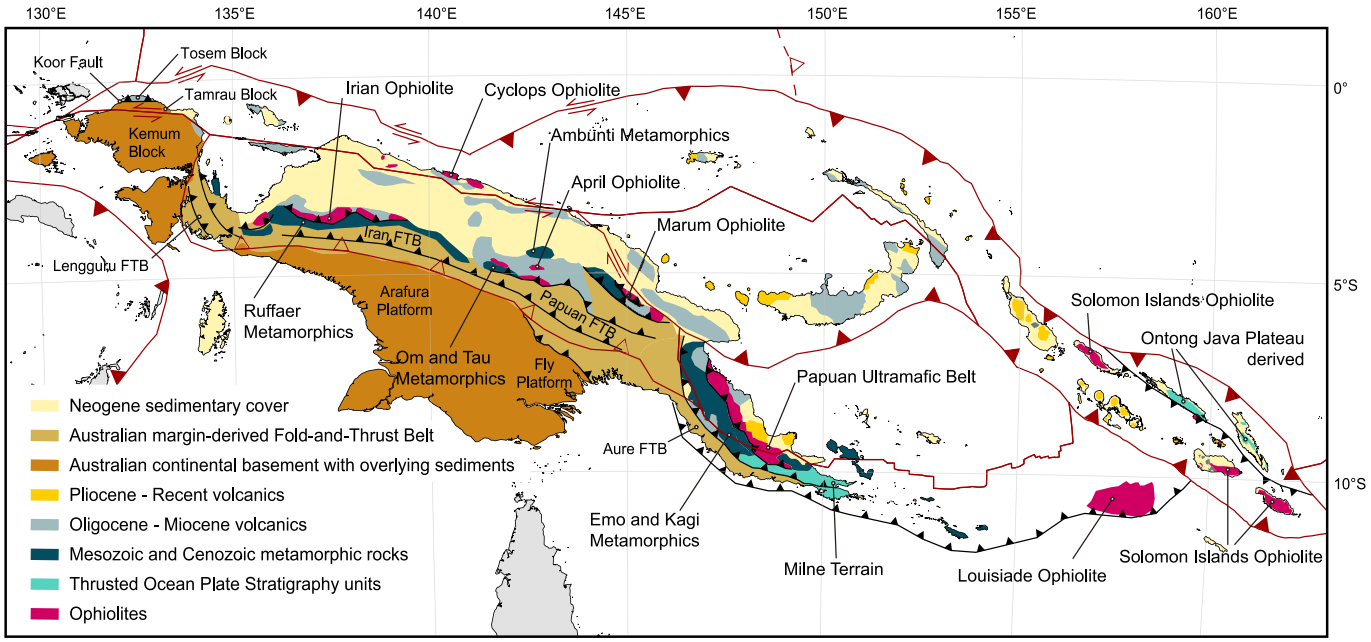

Fig. 7. Geological map of New Guinea and the Solomon Islands, based on Davies (2012); Tejada et al. (1996); Petterson et al. (1999); Tapster et al. (2014). FTB = Fold-and-Thrust Belt.

subduction zone ophiolite (the Central Palawan Ophiolite; Fig. 5) of which a plagiogranite was dated to 40.0 ± 0.5 Ma using U-Pb zircon geochronology (Dycoco et al., 2021) and basaltic flows were dated to 43.8 ± 2.2 Ma using K-Ar whole-rock dating (Fuller et al., 1991). $^{40}Ar/^{39}Ar$ and U-Pb dating of the metamorphic sole associated with the ophiolite yielded ages of c. 34 Ma (Schlüter et al., 1996; Aurelio et al., 2014; Keenan et al., 2016; Dycoco et al., 2021). The Central Palawan Ophiolite overlies an accretionary prism that contains OPS of Cretaceous (c. 100 Ma) ocean island basalt (OIB) and island arc basalts (IAT), referred to as the Southern Palawan or Calatuigas Ophiolite (Fig. 5; Almasco et al., 2000; Aurelio et al., 2014; Dycoco et al., 2021) and a fragment of the Cretaceous accretionary prism that rifted off the South China margin, known as the Palawan Continental Terrane (Rangin, 1991; Zamoras and Matusoka, 2001, 2004; Aurelio et al., 2014; Shao et al., 2017; Cao et al., 2021; Advokaat and Van Hinsbergen, 2023).

The Palawan ophiolites are to the north of the Cagayan arc, and likely formed in its forearc (Advokaat and Van Hinsbergen, 2023). The Cagayan arc is a mostly submerged magmatic arc that formed on continental basement correlated to the SW Borneo mega-unit, that is thought to have broken off Australia in the early-mid Mesozoic (Advokaat and Van Hinsbergen, 2023, and references therein). The arc was active in Oligocene to Miocene time during and likely related to the subduction of the Proto-South China Sea lithosphere during the opening of the South China Sea (Bellon and Rangin, 1991; Silver and Rangin, 1991; Hutchison et al., 2000). The Cagayan arc and its underlying continental basement share a passive margin with the Sulu Sea oceanic basin to the south, a Miocene (~24–10 Ma) back-arc basin that formed by N-S extension behind the Cagayan arc (Roeser, 1991; Schlüter et al., 1996). The Sulu Sea ocean floor becomes younger southward, towards the Sulu Trench where a well-developed accretionary prism separates the Sulu Sea ocean floor from the Sulu arc, which is built on continental crust to the south (Schlüter et al., 1996; Advokaat and Van Hinsbergen, 2023, and references therein). The conjugate of the sea floor of the Sulu Sea is interpreted to have subducted at the Sulu Trench (Roeser, 1991). To the east, the Sulu Sea subducts eastward below the Philippine Mobile Belt along the Negros Trench (Fig. 3).

The Sulu arc is built on continental crust that is also thought to correlate to the SW Borneo Mega-Unit (Advokaat and Van Hinsbergen, 2023). The available ages from the Sulu arc give Miocene-Pliocene ages, ~18–3 Ma, and stratigraphic ages indicate volcanism may have started in the late Oligocene (Bergman et al., 2000; Rangin et al., 1990). To the south, the Sulu arc shares a passive margin with the Eocene Celebes Sea oceanic basin. Oceanic crust of the Celebes Sea basin is being subducted towards the east below southwestern Mindanao at the Cotabato Trench (Fig. 3). The Celebes Sea is underlain by oceanic crust with magnetic anomalies that young southward to the North Sulawesi Trench and were interpreted to have 46–36 Ma ages (Weissel, 1980; Beiersdorf et al., 1997; Gaina and Müller 2007). The conjugate seafloor to the south is likely represented by ophiolites that are exposed on eastern and southeastern Sulawesi and that underlie the volcanic arc of the Sulawesi North Arm (Monnier et al., 1995; Advokaat et al., 2017). The ophiolites are underlain by units accreted from northward subducted Australian plate-derived oceanic and continental units (Advokaat and Van Hinsbergen, 2023, and references therein). The North Sulawesi Trench formed at approximately 8.5 Ma (Smith et al., 1990; Nichols and Hall, 1999) and may have reactivated the former spreading ridge of the Celebes Sea (Advokaat and Van Hinsbergen, 2023).

The most important events in the kinematic reconstruction of the SE Asian Tethysides for the Junction Region occurred prior to the Late Cretaceous, when the SW Borneo Block and associated continental fragments were converging with Eurasia and diverging from Australia, and since the Eocene, when the SE Asian tectonic collage was deformed, oceanic back-arc basins opened, and the South China Sea formed (See Advokaat and Van Hinsbergen for details). During the Eocene, at c. 45 Ma, the northward motion of the Australian Plate accelerated which resulted in the interaction between the Australian Plate and southern Sundaland resulting in large-scale counterclockwise rotation of Borneo in the Eocene and Miocene (Advokaat et al., 2018). This rotation caused convergence between Borneo and South China that led to subduction of the proto-South China Sea below northern Borneo and the Cagayan arc, while the South China Sea opened in its wake (Rangin et al.,

1990; Rangin and Silver, 1991; Hinz et al., 1991; Lee and Lawver 1994, 1995; Hall 1996, 2002; Hall and Breitfeld, 2017). In the Mesozoic, the proto-South China Sea region is thought to have been occupied by a paleo-Pacific Plate that subducted northwards, westwards, and southwards below the South China, Indochina and northern Borneo margins (e.g., Jahn et al., 1990; Lapierre et al., 1997; Hall and Breitfeld, 2017; Nong et al., 2021). Evidence for this subduction zone is formed by arcs and accretionary prisms. Such prisms formed during the Jurassic to Late Cretaceous (~85 Ma) in a northwest dipping subduction zone below South China, exposed in Taiwan and on Palawan and the Calamian Islands (Zamoras and Matsuoka, 2001, 2004; Yui et al., 2012). In addition, evidence for extensive continental arc magmatism is found in South China, Vietnam, and SW Borneo (e.g., Li et al., 2012; Liu et al., 2020; Nong et al., 2022; Breitfield et al., 2017; Batara and Xu, 2022). Mesozoic subduction of the paleo-Pacific Plate is thought to have ceased around 85 Ma, based on the end of magmatism (Breitfeld et al., 2017; Liu et al., 2020; Nong et al., 2022; Qian et al., 2022), and the widespread deposition of upper Cretaceous-Eocene synrift sediments (Shao et al., 2017; Breitfield et al., 2018; Conand et al., 2020; Cao et al., 2021, 2023). Subduction continued below Japan (e.g., Isozaki et al., 1990; Vaes et al., 2019; Boschman et al., 2021a, b; Wu et al., 2022) and the boundary between the ongoing and ceased subduction is the so-called Qingdao Line (Wu et al., 2022). The Qingdao line represents the location of a hypothesized plate boundary that was located between the northern and southern Ryukyu islands (around the Kerama Gap; Fig. 3) that separated ongoing Panthalassa oceanic plate subduction to the east from a Proto-South China Sea surrounded by passive margins to the west during the late Mesozoic and Early Cenozoic (Wu et al., 2022). It has been suggested that the end of subduction in the proto-South China Sea embayment was related to the arrival of an oceanic plateau in the subduction zone (e.g., Xu et al., 2022; Van de Lagemaat et al., 2023c), after which relative motion between Pacific realm plates and Eurasia must have been accommodated at a plate boundary to the east of the Proto-South China Sea, from the Qingdao Line southwards.

3.2.2. SW Pacific extensional basins

The northeastern and eastern Australian margin is deformed by extensional basins resulting in a mostly submerged mosaic of basins and rises that consist of continental fragments separated from Australia, as well as fragments of arc and LIP crust (Fig. 4). Below the Coral Sea are several oceanic plateaus separated by basins. The largest of these basins is the Coral Sea Basin, where oceanic spreading was active between 62.5 and 52.9 Ma, during polarity chrons C27-C24 (Gaina et al., 1999). Opening of the Coral Sea Basin led to the separation of the Papuan and Eastern plateaus from northeastern Australia (Fig. 4). This opening may have been related to opening of the Tasman Sea to the south, where oceanic spreading had been propagating northwards since c. 84 Ma, after rifting had started c. 95 Ma (Gaina et al., 1998; Grobys et al., 2008). Opening of these basins separated various plateaus from the Australian margin, including the Eastern, Papuan, Louisiade, and Kenn plateaus and the Lord Howe, Pocklington, and Mellish rises (Gaina et al., 1999; Collot et al., 2012; Van den Broek and Gaina, 2020; Mortimer et al., 2017) (Fig. 4).

The difference in spreading direction between the N-S opening Coral Sea and the E-W opening Tasman Sea was accommodated by extension, crustal thinning, and in places formation of oceanic crust in the northeastern part of the system. Short-lived oceanic spreading occurred in the Louisiade Trough between the Louisiade Plateau and Mellish Rise between 62.5 and 59 Ma (Gaina et al., 1999). The northeast Australian margin also contains evidence for even older extension: the Queensland Plateau, between the Coral Sea and Australia, rifted off Australia in the Cretaceous or possibly the Late Jurassic, accommodated by extension in the Townsville Basin (Falvey and Taylor, 1974; Struckmeyer and Symonds, 1997).

To the east of the Louisiade Plateau and Mellish Rise is an additional set of rises and troughs. The nature of the bathymetric highs is mostly unknown. The Rennell Ridge, West Torres Plateau, and Lapérouse rises (Fig. 4) have been interpreted as continental fragments, remnant island arcs, oceanic crust, or LIPs (Landmesser et al., 1973; Weissel and Watts, 1979; Yan and Kroenke, 1993; Schellart et al., 2006; Seton et al., 2016). Seton et al. (2016) obtained an $^{40}Ar/^{39}Ar$ ages of 42.8 ± 1.2 Ma from a dredged basalt sample from the Rennell Ridge, with an E-MORB geochemical signature. In addition, a low-quality 38 ± 5 Ma $^{40}Ar/^{39}Ar$ age was obtained from a primitive arc tholeiitic basalt sample dredged from the western margin of the Rennell Ridge (Mortimer et al., 2014a). Dredged basalt from the western margin of the West Torres Plateau had N-MORB geochemistry and a 26.2 ± 0.8 Ma $^{40}Ar/^{39}Ar$ age and a dredged basalt from the East Lapérouse Rise yielded a 39.1 ± 1.2 Ma $^{40}Ar/^{39}Ar$ age with E-MORB geochemistry (Seton et al., 2016).

The Rennell Ridge is separated from the Louisiade Plateau by the Rennell Basin. Direct age constraints for the Rennell Basin are lacking, but an Eocene to Miocene age was inferred from seismic reflection lines (Récy et al., 1977). Additionally, based on the structure of the basin, it was suggested that the basin formed an east-dipping trench of a subduction zone below the Rennell Ridge (Récy et al., 1977; Weissel and Watts, 1979).

The West Torres Plateau is separated from the Rennell Ridge by the Santa Cruz Basin (Fig. 4). Seton et al. (2016) identified marine magnetic anomalies C20-C13 (43.5–33.7 Ma) in the Santa Cruz Basin. They infer that the basin opened between 48 and 28 Ma, based on the possible existence of marine magnetic anomaly C21 (47.8 Ma). The end of spreading is based on 29.3 ± 1.6 Ma and 28 ± 3 Ma $^{40}Ar/^{39}Ar$ plagioclase ages of dredged basalts from the ridge crest of the South Rennell Trough (Mortimer et al., 2014a), which is interpreted as the southern continuation of the Santa Cruz Basin spreading center (Seton et al., 2016). Based on this interpretation, spreading in the South Rennell Trough was also active between c. 48 and 28 Ma (Mortimer et al., 2014a; Seton et al., 2016). The South Rennell Trough is flanked by the West and East Lapérouse rises (Fig. 4), and their elevated nature is thought to be the result of the interplay between magma supply and extension (Seton et al., 2016).

The East Lapérouse Rise and Lord Howe Rise are separated from the West Torres Plateau by the D'Entrecasteaux Basin. The age and geochemistry of the oceanic crust that underlies the D'Entrecasteaux Basin remains unknown. Lapouille (1982) interpreted Cretaceous marine magnetic anomalies, but this interpretation was rejected by Seton et al. (2016), as the interpreted anomalies cross-cut structural trends of the basin. No new interpretation of anomalies was made due to the lack of continuity of magnetic anomaly patterns between magnetic profiles. Instead, Seton et al. (2016) suggested that the D'Entrecasteaux Basin formed as part of the South Loyalty Basin, which is a hypothesized Cretaceous oceanic basin that was lost to subduction at the New Caledonia subduction zone in the Eocene-Oligocene (e.g., Cluzel et al., 2001).

To the east of the Lord Howe Rise are an additional set of ridges separated by oceanic basins (Fig. 4). The tectonic history of these basins was reviewed and reconstructed by Van de Lagemaat et al. (2018a), and we incorporate their reconstruction with updates of Van de Lagemaat et al. (2021, 2023a) into our model. We here briefly summarize the formation history of these basins.

To the east of the Lord Howe Rise is the New Caledonia-Fairway-Aotea basin, which separates the Norfolk Ridge from the Lord Howe Rise (Fig. 4). The Norfolk Ridge forms the easternmost part of Zealandia (Mortimer et al., 2017) and consists of Late

Mesozoic and older accretionary complexes overlain by foreland basin clastics that can be traced into New Zealand and New Caledonia (Mortimer et al., 1998; Cluzel et al., 2012a; Maurizot et al., 2020a). The age of opening of the New Caledonia-Fairway-Aotea basin remains uncertain (e.g., Lafoy et al., 2005; Collot et al., 2009), but it likely opened in tandem with the Tasman Sea, between 85 and 56 Ma (Lafoy et al., 2005; Van de Lagemaat et al., 2018a).

East of the Norfolk Ridge is the Norfolk Basin. Due to the absence of marine magnetic anomalies, the age of the oceanic crust has been debated (Launay et al., 1982; Mortimer et al., 1998; Sdrolias et al., 2003), but a late Oligocene to late Miocene age of formation was inferred from a 23 ± 0.1 Ma $^{40}Ar/^{39}Ar$ age of a dredged seafloor tholeiite (Sdrolias et al., 2003). The opening direction of the Norfolk Basin is constrained by the Cook and Vening Meinesz fracture zones (Fig. 4), which form the northern and southern limits of the basin (Herzer and Mascle, 1996; Sdrolias et al., 2004a). The Norfolk Basin is bounded in the east by the Three Kings Ridge, which is offset from the Loyalty Ridge by the Cook Fracture Zone. The Three Kings Ridge is interpreted as a remnant volcanic arc that formed during the Eocene-Oligocene above the east-dipping New Caledonia subduction zone (Kroenke and Eade, 1982; Whattam et al., 2006, 2008). Recently, latest Oligocene to earliest Miocene (25–22 Ma) and two Eocene (39–36 Ma) $^{40}Ar/^{39}Ar$ ages were obtained from dredged lavas from the Loyalty and Three Kings Ridges (Gans et al., 2023).

To the east of the Three Kings Ridge is the South Fiji Basin (Fig. 4). This basin formed in the Oligocene-Miocene as a back-arc basin above the Tonga-Kermadec subduction zone (e.g., Sdrolias et al., 2003). The age of formation of the basin is constrained by marine magnetic anomalies, but different interpretations have been suggested (Watts et al., 1977; Malahoff et al., 1982; Sdrolias et al., 2003; Mortimer et al., 2007). Using additional age constraints obtained from $^{40}Ar/^{39}Ar$ dating, which yielded ages between 19.3 and 25.9 Ma, Mortimer et al. (2007) suggested that the marine magnetic anomalies formed during chrons C9 and C6B (27.4–21.9 Ma), which is younger than previous interpretations. Spreading in the South Fiji Basin is thought to have ceased around 15 Ma (Herzer et al., 2009, 2011, Mortimer et al., 2007, 2014a).

The South Fiji Basin is bounded in the east by the Lau-Colville Ridge (Fig. 4), which formed part of the active arc above the Tonga-Kermadec subduction zone, until the arc split around 7 Ma when the Lau Basin and Havre Trough started opening (Ruellan et al., 2003; Yan and Kroenke, 1993). The Lau Basin-Havre Trough system is the currently active back-arc basin above the Tonga-Kermadec subduction zone, where westward subduction of the Pacific Plate is accommodated since the Eocene or Oligocene (Seton et al., 2012; Van de Lagemaat et al., 2018a, 2022; Sutherland et al., 2017).

3.3. Junction Region oceanic domain

3.3.1. Philippine Sea Plate

The Philippine Sea Plate is an oceanic plate mostly surrounded by subduction zones, whose oceanic crust formed at multiple spreading ridges since the Cretaceous (Fig. 6; Hilde and Lee, 1984; Deschamps and Lallemand, 2002; Yamazaki et al., 2003; Sdrolias et al., 2004b; Hickey-Vargas et al., 2013). In the east, the Philippine Sea Plate is in an upper plate position relative to the Pacific Plate that is subducting along the Izu-Bonin-Mariana Trench (Figs. 2 and 6). The well-studied forearc above the Izu-Bonin-Mariana subduction zone reveals a magmatic stratigraphy with geochemical compositions ranging from MORB-like to arc-like that is widely interpreted as the product of catastrophic extension (for instance, extension rates in the Oman ophiolite that is thought to have formed in a similar setting, were as high as 20 cm/a; Rioux et al., 2013), associated with foundering of the nascent slab shortly after Pacific subduction initiation below Izu-Bonin-Mariana (Stern and Bloomer, 1992; Stern, 2004; Stern et al., 2012). The oldest age of this sequence is dated at ~ 52 Ma (Ishizuka et al., 2011a; Reagan et al., 2013, 2019), which is often interpreted as the age of inception of subduction at the Izu-Bonin-Mariana trench (Stern et al., 2012; Arculus et al., 2015), although examples elsewhere showed that similar catastrophic extension may postdate incipient subduction by some 10 Ma (Guilmette et al., 2018). Close to the modern trench is the Omachi seamount that consists of serpentinite that includes exhumed eclogite blocks. These eclogites have not been dated, but are overlain by upper Eocene to lower Oligocene andesite, showing that by late Eocene, mature subduction was underway (Ota and Kaneko, 2010).

To the west of the Izu-Bonin-Mariana trench lies the Izu-Bonin-Mariana magmatic arc. This arc is in places emergent and exposes a stratigraphy that goes back to the Eocene (e.g., on Guam and the Ogasawara Islands; Meijer et al., 1983; Reagan et al., 2008; Ishizuka et al., 2006). To the west of the active arc are remnant arcs that form submarine ridges and that are separated from the active arc by back-arc basins. Upper plate extension in the Izu-Bonin segment in the north is restricted to the Ogasawara Trough (Nishimura, 2011). This basin separates the Bonin Ridge, an uplifted section of the forearc, from the currently active Izu-Bonin arc (Fig. 3). Based on the interpretation that volcaniclastics, dredged from the eastern slope of the Ogasawara Trough, were deposited before a c. 44–42 Ma episode of volcanism, Ishizuka et al. (2006) suggested that the Ogasawara Trough opened during the Eocene, as a narrow back-arc basin behind the Izu-Bonin-Mariana subduction zone. To the south, however, the Mariana Trough is an active back-arc basin that separates the West Mariana Ridge, a remnant arc, from the active Mariana arc (Fig. 3). The Mariana Trough has been opening since magnetic anomaly chron C3 (~5 Ma) that was identified in the northern half of the basin (Yamazaki et al., 2003), consistent with the youngest volcanic rocks known from the West Mariana Ridge remnant arc, which are 6–4 Ma based on biostratigrapy and $^{40}Ar/^{39}Ar$ whole-rock ages of dredged basalts (Karig, 1971; Kroenke et al., 1981; Ishizuka et al., 2010).

To the west of the West Mariana Ridge and Izu-Bonin arc are the Oligocene to Miocene Shikoku and Parece Vela basins (Fig. 3). These basins separate the more recent Izu-Bonin and Mariana arcs from the Kyushu-Palau Ridge to the west, which forms another remnant arc (Fig. 3). Sdrolias et al. (2004b) identified a conjugate set of marine magnetic anomalies in the Shikoku Basin mirrored in a mid-basin high that is interpreted as an extinct spreading ridge. These were interpreted in combination with radiometric ages of dredge samples as C7-C5B (24–15 Ma) (Sdrolias et al., 2004b). In the western portion of the Parece Vela Basin, marine magnetic anomalies interpreted as C9-C5D (27–15 Ma) were identified (Sdrolias et al., 2004b). Magnetic anomalies were not identified elsewhere in this basin, but clear fracture zones provide additional constraints for reconstructing its opening. These fracture zones are S-shaped and reflect a change in spreading direction within the basin from E-W to NE-SW (Fig. 3; Sdrolias et al., 2004b). A 15.6 ± 0.1 Ma $^{40}Ar/^{39}Ar$ whole-rock age was obtained from a basalt lava that was dredged from the Parece Vela extinct ridge (Ishizuka et al., 2010), providing a constraint for the end of spreading.

In the south, the extinct mid-ocean ridge of the Parece Vela basin is continuous with the Yap Trench (Fig. 3). To the west of the Yap Trench lies oceanic crust that is contiguous with the western Parece Vela Basin, younging eastwards towards the Yap Trench (Sdrolias et al., 2004b). There is currently no active volcanism and

little seismicity at the Yap trench (Sato et al., 1997). The basement of Yap Island consists of a metamorphic igneous complex of greenschist to amphibolite-facies rocks (Shiraki, 1971; Hawkins and Batiza, 1977). Ages of metamorphism were obtained from dredged greenschists and amphibolites from south of the Yap Islands, which returned a titanite U-Pb weighted mean age of 21.4 ± 0.9 Ma and $^{40}Ar/^{39}Ar$ amphibole ages of 20.7 ± 0.1 Ma and 22.0 ± 2.1 Ma (Zhang and Zhang, 2020). Based on geochemistry, the protoliths of the metamorphic rocks are interpreted to be of fore-arc basin basalt, ocean island basalt, and island-arc tholeiite affinity, but the age of the protolith remains unknown (Zhang and Zhang, 2020). The metamorphic complex is underthrusted by Miocene mélange, which contains fragments of these metamorphic rocks as well as other volcanic and sedimentary rocks of unknown age (Shiraki, 1971; Rytuba and Miller, 1990). The metamorphic complex and mélange are both overlain by Miocene andesitic lava flows and tuffs, which is the youngest volcanism on the Yap Islands (Shiraki, 1971; Rytuba and Miller, 1990). Collectively, these data show that contractional deformation, burial, and metamorphism at the Yap Trench must have been underway by ~ 21 Ma, i.e., while the Parece Vela Ridge to the north was still active. This suggests that during the opening of the Parece Vela basin in the north, the southern part was compressed, and the back-arc ridge inverted into a subduction zone that consumed the eastern forearc plate.

The western boundary of the Shikoku and Parece Vela basins is the Kyushu-Palau Ridge, another remnant arc built on lithosphere of the eastern West Philippine Basin (Fig. 3). Radiometric dating based on an extensive suite of $^{40}Ar/^{39}Ar$ ages of dredged and drilled samples along the length of the ridge shows that it was active from at least 48 to about 25 Ma (Ishizuka et al. 2011b), after which the Shikoku and Parece Vela Basins started opening. The southernmost extension of the Kyushu-Palau Ridge forms the Palau arc, immediately west of the Palau Trench. The arc is not associated with active volcanism, and subduction seismicity is shallow and weak (Kobayashi et al., 1997). The Palau Islands consist mostly of basalt and andesite lavas, flow breccias, and tuffs overlain by Mio-Pliocene lignite and limestones (Meijer et al., 1983; Rytuba and Miller, 1990; Hawkins and Ishizuka, 2009). Reported K-Ar whole-rock ages are mostly in the range of 30–34 Ma (Meijer et al., 1983; Cosca et al., 1998), with the oldest reliable K-Ar whole-rock age being 37.7 ± 3.1 Ma (Haston et al., 1988). A late Eocene age was also assigned based on foraminifera and nannofossils in interbedded tuffaceous marls and limestones (Cole, 1950; Meijer et al., 1983). The youngest age derived from volcanic rocks is a K-Ar whole-rock age of 20.1 ± 0.5 Ma (Meijer et al., 1983).

To the west of the Kyushu-Palau Ridge is the West Philippine Basin, the largest of the Philippine Sea Plate basins (Fig. 3). Marine magnetic anomalies interpreted to have formed during polarity chrons C26 to C13 (~59–34 Ma) were identified by Hilde and Lee (1984). Deschamps and Lallemand (2002) revised the model for the oldest part of the basin based on improved bathymetric data and suggest spreading started at c. 54 Ma instead. Based on new marine magnetic anomaly interpretations, Sasaki et al. (2014) suggested that spreading in the basin already ceased around 36 Ma, and that formation of oceanic crust during the initial stages of the basin (south of anomaly C21; 48 Ma) was disorganized, which resulted in a lack of formation of clear marine magnetic anomalies. Nonetheless, the onset of spreading of the West Philippine Basin is likely older than, and spreading occurred more or less perpendicular to, the rapid extension of the Izu-Bonin-Mariana forearc and the associated formation of boninites at 52 Ma (Ishizuka et al., 2011a; Reagan et al., 2013, 2019).

Oceanic crust of the West Philippine Basin is overlain by the Benham Rise, Urdaneta Plateau and the Oki-Daito Rise. The Benham Rise and Urdaneta Plateau are located south and north of the extinct West Philippine Basin spreading center, roughly at equal distance. The Oki-Daito Rise is located north of the Urdaneta Plateau. $^{40}Ar/^{39}Ar$ dating yielded ages of 35.6 ± 0.4 Ma and 36.2 ± 0.5 Ma from the Benham Rise (Hickey-Vargas, 1998), and an average of 37.9 ± 0.1 Ma from the Urdaneta Plateau (Ishizuka et al., 2013). An older age of 40.5–44.4 Ma was obtained from the Oki-Daito Rise, which is further away from the extinct spreading ridge, north of the Urdaneta Plateau (Ishizuka et al., 2013). All three plateaus have OIB-like geochemistry, and based on this and the age progression, it was suggested that a mantle plume (referred to as the Oki-Daito Plume) triggered opening of the West Philippine Basin and that the West Philippine Basin spreading center remained fixed on the plume for about 10 Ma (Ishizuka et al., 2013). Similarly, Wu et al. (2016) suggested that the Cenozoic Philippine Sea Plate nucleated above the Manus Plume and as Ishizuka et al. (2013) do not link the Oki-Daito Plume to a mantle structure, their Oki-Daito Plume may reflect the Manus Plume.

To the north of the West Philippine Basin is a series of E-W trending ridges separated by basins. These are, from south to north, the Oki-Daito Ridge (which is different from the Oki-Daito Rise), the Minami-Daito Basin, the Daito Ridge, the Kita-Daito Basin, the Amami Plateau, and the Kikai Basin. The Amami Plateau and the Kita-Daito Basin are bound to the east by the Minami-Amami Escarpment that separates them from the Amami-Sankaku Basin (Fig. 3). The age of the basement of southernmost ridge, the Oki-Daito Ridge, remains unknown, but dredged volcanics overlying the ridge yielded 40.5 ± 0.3 – 48.4 ± 0.1 $^{40}Ar/^{39}Ar$ whole-rock ages (Ishizuka et al., 2013). Dredged and drilled basalt samples showed that the Daito Ridge contains andesites, which yielded much older, 116.9–118.9 Ma $^{40}Ar/^{39}Ar$ ages (Ishizuka et al., 2011b). Eocene $^{40}Ar/^{39}Ar$ ages from the Daito Ridge were obtained by Hickey-Vargas et al. (2013), with a 49.3 ± 0.5 plagioclase age obtained from a basalt clast and ages between 44.7 and 48.0 of hornblende and biotite from volcaniclastic sediments. Basalts and tonalites dredged from the Amami Plateau, again gave Cretaceous, 115.8–117.0 Ma $^{40}Ar/^{39}Ar$ ages (Hickey-Vargas, 2005). Based on their geochemical signature, the Amami Plateau and Daito Ridge are interpreted as extinct Mesozoic arc remnants (Hickey-Vargas, 2005; Ishizuka et al., 2011b, 2022; Hickey-Vargas et al., 2013; Morishita et al., 2018). Even though the oldest volcanics and sediments recovered from the Oki-Daito Ridge are of Eocene age, based on a similar stratigraphy, it was inferred that the Oki-Daito Ridge is also a remnant Mesozoic arc (Ishizuka et al., 2022).

Dredged and drilled OIB-like basalt samples yielding 51.3–42.8 $^{40}Ar/^{39}Ar$ ages were recovered from the Minami-Daito Basin (Hickey-Vargas, 1998; Ishizuka et al., 2013). 45.8–41.0 Ma $^{40}Ar/^{39}Ar$ and 43 Ma U-Pb zircon ages were reported from andesites recovered from the Kita-Daito Basin (Ishizuka et al., 2022). Similar $^{40}Ar/^{39}Ar$ whole-rock ages, between 49.3 and 46.8 were obtained from drilled lava flows of the Amami-Sankaku Basin (Ishizuka et al., 2018) Collectively, these basins and ridges reveal that during the Eocene formation of the West Philippine Basin, smaller basins also formed to the north, within an oceanic lithosphere that contained ~ 118–116 Ma oceanic crust, or arc of that age built on even older crust. In other words, the West Philippine Basin formed by breaking oceanic lithosphere that was at least 60 Ma old at the moment of inception of extension.

In the northwest of the Philippine Sea Plate, east of Taiwan, lies the Huatung Basin, separated from the West Philippine Basin by the Gagua Ridge (Fig. 3). Hilde and Lee (1984) originally interpreted marine magnetic anomalies identified in the Huatung Basin as C19 to 16 (41 – 36 Ma), younging northward, an interpretation recently repeated by Doo et al. (2015). However, Deschamps et al. (2000) showed that the ocean floor of the Huatung Basin has an Early Cretaceous age: they obtained 114.7 ± 4.0 and 124.1 ± 2.5 Ma $^{40}Ar/^{39}Ar$ ages from amphibole of dredged gabbros from the Huatung Basin. They consequently reinterpreted the anomalies as M10-M1

(130.6–123 Ma), younging towards the south (Deschamps et al., 2000). These Early Cretaceous ages were confirmed by a mean U-Pb age of 130.3 ± 1.0 Ma obtained from 18 zircon grains from the same dredged gabbro sample (Huang et al., 2019). The Cretaceous marine magnetic anomaly ages correspond well to Lower Cretaceous (Barremian) radiolarian assemblages collected from the nearby Lanyu Island (Deschamps et al., 2000; Yeh and Cheng, 2001). The original extent of the Huatung Basin, as well as the timing of onset and cessation of spreading remains unknown, as no extinct spreading center has been identified. Much of the originally surrounding lithosphere must have been consumed by subduction, e.g., at the Ryukyu and East Luzon trenches (Deschamps et al., 2000). From the Gagua Ridge, Cretaceous lavas were recovered (Qian et al., 2021). These lavas yielded 124.06 ± 0.27 and 123.99 ± 0.24 Ma $^{40}Ar/^{39}Ar$ ages of plagioclase and have a subduction-related arc geochemical signature (Qian et al., 2021). The Gagua Ridge thus likely originally formed as a Cretaceous arc that was used in the Eocene to form a transform plate boundary that separated the Cretaceous Huatung Basin from the actively spreading West Philippine Basin.

The southern boundary of the West Philippine Basin is formed by the Mindanao Fracture Zone, which separates it from the southern part of the Philippine Sea Plate known as the Palau Basin (Fig. 3). In this basin, Sasaki et al. (2014) identified short segments of N-S trending marine magnetic anomalies, roughly perpendicular to the anomalies of the West Philippine Basin. These anomalies were tentatively interpreted as the eastern flank of a spreading center that formed during chrons C18-C15 (40–35 Ma) (Sasaki et al., 2014). The correlation is based on a 40.4 Ma $^{40}Ar/^{39}Ar$ age of a dolerite sample from the Mindanao Fracture Zone, located north of the magnetic survey lines (Sasaki et al., 2014; Ishizuka et al., 2015). This N-S trending ridge must have ended against the Mindanao Fracture Zone. In the west, oceanic crust of the Palau Basin is subducting below the Philippines, which consumed at least part of the western conjugate lithosphere of the Palau Basin. The southeastern margin of the Palau Basin is the ultra-slowly spreading Ayu Trough mid-oceanic ridge that separates the Philippine Sea Plate from the Caroline Plate and that to the north transitions to the Palau Trench in the Caroline-Philippine Sea Plate Euler pole of rotation (e.g., Weissel and Anderson, 1978; Fujiwara et al., 1995). The total amount of rotation since the formation of the Ayu Trough is estimated at ~ 25° based on the angle between the Ayu Trough rift margins (Figs. 3 and 6). A crude estimate for the age of onset of Ayu Trough spreading is 15–25 Ma based on the sediment thickness within the basin and estimated sedimentation rates that are extrapolated from a nearby borehole (Weissel and Anderson, 1978; Fujiwara et al., 1995). K-Ar whole rock dating of dredge samples recovered from 62 km east of the Ayu Trough rift axis yielded 19.9 ± 0.7, 20.5 ± 1.5 and 25.2 ± 1.1 Ma ages (Kumagai et al., 1996). These dredge samples are high-alkali andesites with an island arc geochemical signature (Kumagai et al., 1996), which suggest that the eastern margin of the Ayu Trough was a subduction zone at least until c. 20 Ma.

3.3.2. ***Caroline*** *Plate*

The Ayu Trough forms the western boundary of the Caroline Plate, separating it from the Philippine Sea Plate (Figs. 3 and 6). The Caroline Plate is bounded to the Pacific Plate in the north and east by the Sorol Trough and Mussau Trench. Whether the Caroline Plate is currently moving relative to the Pacific Plate is uncertain due to its poorly understood plate boundaries and scarce kinematic data (DeMets et al., 2010). The Mussau Trench may be the site of incipient subduction of the Caroline Plate below the Pacific Plate (Hegarty et al., 1983; Gurnis et al., 2004). The southern boundary of the Caroline Plate is formed by the New Guinea and Manus trenches, which separate the Caroline Sea from the New Guinea orogen and from the Bismarck Sea basin.

The Caroline Plate hosts an eastern and a western basin, both with E-W trending marine magnetic anomalies (Gaina and Müller, 2007), separated by the Eauripik Rise (Fig. 3). Gaina and Müller (2007) interpreted marine magnetic anomalies in the eastern basin as chrons C15r to C8n (c. 35–25 Ma) and in the western basin as chrons 16n to 8r (c. 36–25 Ma). While the eastern basin contains a symmetric set of anomalies, mirrored in a single extinct spreading ridge, the extinct spreading ridge in the western basin is not located in the center but well to the north. Close to this extinct spreading ridge, a conjugate set of anomalies from chron C8 is interpreted (Gaina and Müller, 2007). To the north of the extinct spreading ridge, the next anomaly is interpreted to have formed during chron C15. To the south of the extinct spreading ridge, two marine magnetic anomalies from chron C10 are interpreted, then two anomalies from chron C11, and then the southern anomaly of chron C15, which is interpreted to be the conjugate of the C15 anomaly in the north of the basin (Gaina and Müller, 2007). This marine magnetic anomaly pattern is interpreted to be the result of several ridge-jumps during opening of the western Caroline Basin (Gaina and Müller, 2007).

The Eocene-Oligocene oceanic crust of the Caroline Plate is juxtaposed in the north and east with Jurassic oceanic crust of the Pacific Plate across the Sorol Trough and Mussau Trench (Fig. 3). The northern boundary between the Caroline and Pacific plates is overlain by the West Caroline Rise and Caroline Islands Ridge, collectively known as the Caroline Ridge, separated from each other by the Sorol Trough (Altis, 1999). The Caroline Ridge is interpreted as a large igneous province, with an age-progressive seamount chain to the east, on the Pacific Plate (Zhang et al., 2020). K-Ar and $^{40}Ar/^{39}Ar$ ages from different sites on the Caroline Ridge yielded ages between 8.1 ± 0.8 Ma and 23.9 Ma ± 1.2 Ma (Ridley et al., 1974; Zhang et al., 2020). Based on the emplacement of the Caroline Ridge onto the Caroline and Pacific Plates, it was inferred that there has only been minor motion between the two plates since at least the Miocene (Wu et al., 2016).

Based on its morphology, the Sorol Trough was interpreted as a transtensional feature, whereby extensional motion along the Sorol Trough was proposed to have split a once-contiguous, plume-related Caroline Ridge into the West Caroline Rise and Caroline Islands Ridge (Weissel and Anderson, 1978, Altis, 1999; Dong et al., 2018). The southern margin of the Sorol Trough has large normal faults, but the northern margin is less distinctively faulted and the crust within the trough is highly disrupted (Weissel and Anderson, 1978). Bracey and Andrews (1974) suggested that the Sorol Trough formed as an interarc basin behind a north-dipping subduction zone that was interpreted from a bathymetric trough along the southern margin of the West Caroline Rise. If the Sorol Trough is an extensional feature, its modern width shows that it would have accommodated less than 100 km of extension since the early Miocene (Weissel and Anderson, 1978; Altis, 1999; Dong et al., 2018). A recent K-Ar age of 23.8 ± 0.7 Ma was obtained from basalt samples collected from a site that was interpreted to represent the age of extension in the Sorol Trough (Yan et al., 2022). We find it more likely, however, that this age represents volcanics from one of the Caroline ridges as the limited amount of extension that occurred in the Sorol Trough is unlikely to have formed new oceanic crust. At present, the Sorol Trough likely forms the current plate boundary between the Caroline and Pacific plates, with very minor relative transform motion (Weissel and Anderson, 1978; Dong et al., 2018).

The Mussau Trench represents the present-day eastern plate boundary between the Caroline and Pacific plates, where the Caroline Plate is starting to subduct below the Pacific Plate (Hegarty et al., 1983; Gurnis et al., 2004). The Lyra Trough, to the east of

the Mussau Trench, however, may represent a former plate boundary (Hegarty et al., 1983; Gaina and Müller, 2007; Wang et al., 2022) and is thought to have been a transform fault during opening of the Caroline Sea basin (Hegarty and Weissel, 1988; Gaina and Müller, 2007).

3.4. Junction Region orogenic domain

Orogenic belts with accreted and deformed relics of now-subducted lithosphere, and remains of forearcs are located along the Eurasian margin, on the Philippines, and in the Melanesian and Polynesian regions. In this section, we review the orogenic architecture and the constraints they provide for the tectonic and geological history of the lithosphere that was lost to subduction.

3.4.1. Southwest Japan (Southwest Honshu, Shikoku, Kyushu, Ryukyu Islands)

At the Boso triple junction, the Izu-Bonin-Mariana trench meets with the Japan and Nankai trenches that accommodate subduction of the Pacific and Philippine Sea Plate below the islands of Japan, respectively (Fig. 3). The islands of Japan comprise a long-lived accretionary orogen, where accretion of OPS occurred episodically during a subduction history of c. 500 million years (Isozaki et al., 1990, 2010). The southwestern part of Japan, west of the Boso triple junction, exposes foreland-younging thrust units that accreted in the late Permian the Middle-Late Jurassic, the Late Cretaceous, the Eocene (around 50 Ma), and during the Miocene, alternating with episodes of subduction without accretion, or with subduction erosion (Isozaki et al., 1990). Throughout this history, arc magmatism remained active (Isozaki et al., 2010). This accretion occurred at the continental margin of the South China Block, and within the accretionary orogen, the Japan Sea back-arc basin opened in Early Miocene time (Jolivet et al., 1994; Martin, 2011; Van Horne et al., 2017). The accretionary orogen of southwest Japan is intersected by the Median Tectonic Line, a major E-W striking fault, juxtaposing the older Inner Zone against the younger Outer Zone. The Inner Zone comprises Permian-Jurassic accretionary complexes intruded by Cretaceous granitoids, while the Outer Zone is dominated by Jurassic-Paleogene accretionary complexes (e.g., Ito et al., 2009; Isozaki et al., 2010; Wallis et al., 2020) The Median Tectonic Line is currently a right-lateral strike-slip fault (Okada, 1973; Sugiyama, 1994), but is thought to have been the site of subduction during the Early to Late Cretaceous that may have consumed a former back-arc basin (Boschman et al., 2021a, and references therein).

Towards the west, the Nankai Trench connects with Ryukyu Trench and the accretionary complexes are traced from the main islands of Japan to the Ryukyu Islands (Kizaki, 1986; Wallis et al., 2020). There is a marked difference between the geology of the northern and southern Ryukyu Islands, which are separated from each other by the Kerama Gap (Fig. 3). The youngest part of accretionary complex exposed on the northern Ryukyu Islands is exposed along the southeast coast of Okinawa Island and is composed of trench-fill turbidites of Eocene age (Kizaki, 1986; Miki, 1995; Ujiie, 1997, 2002; Hou et al., 2022). On the other hand, farther northwards, on southern Kyushu, the youngest part of the accretionary complex, also mainly composed of trench-fill turbidites, is of Early Miocene age (Taira et al., 1982; Kiminami et al., 1994; Raimbourg et al., 2014). The Eocene accretionary complex on the Ryukyu Islands does not expose OPS sequences, but Paleocene to early Eocene radiolarians were derived from blocks of OPS within an Eocene mélange complex in Shikoku (Taira et al., 1988) and lower middle Eocene mudstone associated with blocks of basalt are embedded in mid-middle Eocene terrigenous trench-fill deposits on Kyushu (Saito, 2008). The southern Ryukyu Islands, to the south of the Kerama Gap, on the other hand, have a basement of Late Paleozoic to Jurassic accretionary complexes correlated to the Inner Zone, overlain by Eocene limestones, sandstones, pyroclastics, and andesite lavas and Lower Miocene sandstones and limestones (Kizaki, 1986). The deposition of Upper Miocene to Pleistocene siltstones, sandstones and tuff is the first evidence of a shared geological history between the north and south Ryukyu Islands (Kizaki, 1986). This has been used to suggest that the Izu-Bonin-Mariana trench, and therefore the Boso trench-trench-trench triple junction, most likely migrated from a location in the central Ryukyu Islands, at or near the Kerama Gap, towards the northeast since the Miocene (e.g., Kimura et al., 2014).

The Ryukyu Islands are separated from continental crust of South China by the Okinawa Trough (Fig. 3). The Okinawa Trough is a young, currently active, extensional back-arc basin underlain by thinned continental (Lee et al., 1980; Sibuet et al., 1987, 1995; Arai et al., 2017), or possibly in places oceanic crust (Liu et al., 2016). Extension in the Okinawa Trough is thought to have started in the late Miocene, based on the oldest sediments above an unconformity over basement and may amount c. 100 km (Lee et al., 1980; Letouzey and Kimura, 1986; Sibuet et al., 1987; Fabbri et al., 2004; Tanaka and Nomura, 2009; Gungor et al., 2012).

3.4.2. Taiwan

The Ryukyu Trench ends in a complex plate boundary zone that surrounds the Taiwan orogen, where the polarity of subduction changes, and where continental crust of the South China margin is underthrust below oceanic lithosphere of the Philippine Sea Plate (Fig. 3). The geology of Taiwan is divided into five roughly N-S trending tectonostratigraphic terranes, separated by major east-dipping faults (Fig. 5; e.g., Huang et al., 2006; Brown et al., 2011, 2017; Camanni and Ye, 2022). The three western terranes (the Coastal Plain, Western Foothills, and the Hsuehshan Range) make-up the mostly non-metamorphic Taiwan fold-and-thrust belt, and together with the metamorphic Central Range that lies adjacent to the suture with the Philippine Sea Plate, forms a series of nappes that were accreted from the subducted South China margin. The Coastal Range in the east comprises Miocene volcanic and volcaniclastic rocks that are interpreted to be part of the Luzon arc built on the Philippine Sea Plate (Huang et al., 2018; Brown et al., 2022).

The Taiwan fold-and-thrust belt comprises westward-younging Eocene to upper Miocene clastic sediments interpreted to have formed on the South China passive margin, overlain by upper Miocene foreland basin sediments interpreted to derive from the approaching orogen (Huang et al., 1997; Alvarez-Marron et al., 2014; Brown et al., 2022). No crystalline basement rocks are exposed within the fold-and-thrust belt (Brown et al., 2022). Based on balanced cross-sections, shortening estimates for the fold-and-thrust belt vary from 10 to 30 km (Mouthereau et al., 2001; Yang et al., 2007, 2016; Mouthereau and Lacombe, 2006; Rodriguez-Roa and Wiltschko, 2010; Brown et al., 2022), to up to ~ 120 km (Suppe, 1980).

The fold-and-thrust belt underthrusts the Central Range, comprising of the Tananao metamorphic complex, which has been subdivided into the Tailuko and Yuli belts (e.g., Chen et al., 2016, 2017). The Tailuko Belt comprises a schist unit, a marble unit associated with metabasite, and a granitoid unit, which were metamorphosed to greenschist- to amphibolite-facies (Yui et al., 2012). Based on the occurrence of metabasite, marble, and chert, the Tailuko Belt is interpreted as metamorphosed OPS (Yui et al., 2012). Permian ages were obtained for the marbles, based on forams, corals, and Sr-isotope data (Jahn et al., 1984, 1992). The age of quartz-mica schist from the Tailuko Belt, interpreted as *meta*-foreland basin clastics, was determined from dinoflagellate assemblies, which yielded Late Jurassic to Early Cretaceous ages (~155–120 Ma; Chen, 1989 in Yui et al., 2012). More recently, U-Pb detri-

tal zircon ages yielded 120–110 maximum depositional ages for the schist formation in the Tailuko Belt (Chen et al., 2016). Based on these ages, as well as zircon-provenance data, it was inferred that the Tailuko Belt represents a Late Jurassic to Late Cretaceous accretionary complex, where Upper Permian oceanic crust was accreted at a northwest-dipping subduction zone below the South China continental margin (Yui et al., 2012). The Tailuko Belt is locally intruded by Upper Cretaceous granitic intrusions, which may belong to the youngest magmatic suite southwest of the Qingdao Line/Kerama Gap (Wintsch et al., 2011; Yui et al., 2012; Wintsch and Li, 2014; Wu et al., 2022). The Tailuko Belt is overlain by *syn*-rift sediments, which comprises Eocene shallow-marine sandstones, conglomerates, and limestones and Miocene deep-marine argillite with thin layers of sandstones, now metamorphosed at lower greenschist facies because of the late Neogene Taiwan orogenesis. These are interpreted as passive margin sediments of the South China margin that formed after the Late Cretaceous end of subduction zone and formation of the Tailuko accretionary prism (Ho, 1986; Fisher et al., 2002; Conand et al., 2020). A similar stratigraphic sequence is known from the northern margin of the South China Sea to the west (Shao et al., 2017; Advokaat and Van Hinsbergen, 2023).

The Yuli Belt is to the east and structurally above the Tailuko Belt and comprises greenschist facies, carbonaceous, quartz-micaschists, with allochthonous blocks of blueschist facies metabasites (Zhang et al., 2020). Detrital zircon U-Pb geochronology showed that the Yuli Belt comprises a mixture of host-rocks with ages between the Cretaceous and Miocene (Chen et al., 2017). A middle Miocene maximum depositional age was inferred for the Yuli Belt from the mean 15.6 ± 0.3 Ma crystallization age of youngest zircons in blueschist samples (Chen et al., 2017). The age of peak metamorphic conditions was determined for a retrogressed blueschist sample to be 5.1 ± 1.7 Ma based on a Lu-Hf garnet age (Sandmann et al., 2015). Based on these constraints, the Yuli Belt was interpreted to have formed as the most distal part of the Miocene South China margin, which was subsequently incorporated in a Miocene accretionary prism (Sandmann et al., 2015; Chen et al., 2017).

To the east of and structurally above the Yuli Belt is the Lichi Mélange (Fig. 5), the unmetamorphosed equivalent of the Yuli Belt (e.g., Chen et al., 2017). The Lichi Mélange comprises a Pliocene matrix with blocks of andesite volcanics derived from the Luzon arc to the east, Miocene turbidites, and oceanic crust sequences with overlying deep-marine sediments (Jahn, 1986; Lo et al., 2020). The blocks of oceanic crust are commonly referred to as the East Taiwan Ophiolite (Chung and Sun, 1992). Zircons from radiolarian cherts and gabbros of the East Taiwan Ophiolite yielded U-Pb ages of 14.7 ± 0.2 Ma and 17.8 ± 0.4 Ma, respectively (Lo et al., 2020). U-Pb zircon ages of 16.7 ± 0.2 Ma and 16.1 ± 0.6 Ma were obtained from blocks of pegmatitic gabbro and plagiogranite (Lin et al., 2019). A 14.8 ± 1.2 Ma $^{40}Ar/^{39}Ar$ whole-rock age was obtained from a pillow basalt sample (Lo et al., 2020). MORB geochemical signatures further support that the oceanic crust of the East Taiwan Ophiolite formed part of the South China Sea basin, which was subsequently accreted by nappe-stacking to the Luzon forearc during subduction along the Manila trench (Lin et al., 2019). U-Pb zircon crystallization ages of 17.4–16.9 Ma were derived from metaplagiogranites in the Yuli Belt (Lo et al., 2022). These ages were interpreted to be derived from the forearc crust that formed in a supra-subduction zone environment, providing an estimate for the age of subduction initiation of the Eurasian Plate below the Philippine Sea Plate (Lo et al., 2022).

The easternmost, and uppermost, tectonostratigraphic terrane, the Coastal Range, is formed by the northernmost extension of the Luzon arc and forearc. Two Oligocene and early Miocene K-Ar ages have been reported from volcanics of the Coastal Range (Ho, 1969; Richard et al., 1986), but these have been considered unreliable due to scattered results and possible alteration (e.g., Lo et al., 1994). Therefore, the volcanism in the Central Range section of the Luzon arc is thought to have started around 16 Ma, based on 16.4–15.4 Ma zircon fission-track dating (Yang et al., 1995), and a 16.0 ± 0.2 $^{40}Ar/^{39}Ar$ whole-rock age of andesites (Lo et al., 1994). These ages correspond to the oldest volcaniclastic forearc sediments (c. 18 Ma; Suppe and Chi, 1985). The youngest volcanic activity in the Central Range was dated at 4.2 Ma ± 0.1, obtained from $^{40}Ar/^{39}Ar$ groundmass dating (Lai et al., 2017), which corresponds to the earliest stages of underthrusting of the continental South China margin and the accretion of the western nappe systems of the Taiwan orogen.

3.4.3. The Philippines

3.4.3.1. Cretaceous Ophiolites: Luzon; Mindoro; Romblon; Panay. The Luzon arc continues from Taiwan over Luzon southwards, associated with subduction of oceanic crust of the South China Sea basin at the Manila Trench (Fig. 3). The Babuyan and Batan island groups, between Taiwan and Luzon, expose Late Miocene to recent volcanics (Defant et al., 1989, 1990). The Luzon arc on the island of Luzon comprises 14 Ma to recent calc-alkaline basalts and andesites, exposed in the Central Cordillera, the western mountain range of northern Luzon to the north of the Philippine fault (Maleterre et al., 1988; Defant et al., 1990).

Motion on the 1200 km long Philippine Fault is thought to have started in the Pliocene, around 4 Ma, contemporaneous with subduction initiation at the Philippine Trench (Aurelio et al., 1991; Barrier et al., 1991; Aurelio, 2000). Estimates for total displacement on the fault vary between 110 and 200 km (Mitchell et al., 1986; Cole et al., 1989).

The Luzon arc was built on oceanic crust. At the northern end of the Central Cordillera, in the Ilocos Norte region (Fig. 5), a mélange is exposed that contains blocks of radiolarian cherts, peridotite, and subordinate metamorphic rocks in a serpentinite matrix (Queaño et al., 2017a). Based on radiolarian biostratigraphy, the chert was assigned an uppermost Jurassic to Lower Cretaceous age, the age of the matrix is unknown (Queaño et al., 2017a). Ultramafic and mafic clasts within the mélange have an island arc and MORB geochemical signature and are interpreted to have formed in a supra-subduction zone setting (Pasco et al., 2019). The mélange is thrust over an Eocene volcaniclastic unit, with at its base interbeds of sandstones and siltstones that conformably overly pillow basalts with an arc geochemical signature (Queaño et al., 2017a, 2020). Other occurrences of oceanic basement are exposed in the southern Central Cordillera, in the Baguio-Mankayan region (Fig. 5), as pillow basalts and basaltic feeder dikes, sporadically intercalated with undated radiolarian chert, and unconformably overlain by epiclastic rocks, including volcaniclastics and turbidites (Ringenbach et al., 1990; Encarnación et al., 1993; Queaño et al., 2008). The basement has not been dated directly, but the oldest sedimentary formation overlying the basement in the Central Cordillera are volcaniclastics of Eocene age (Ringenbach et al., 1990; Encarnación et al., 1993). The pillow basalts have a transitional MORB-IAT geochemical affinity and are therefore interpreted to have formed in a back-arc basin environment (Queaño et al., 2008).

The Central Cordillera is intruded by the Central Cordillera Diorite Complex, with active magmatism since the late Oligocene (e.g., Hollings et al., 2011; Deng et al., 2020). This complex intruded in several magmatic phases, of which a 26.8 ± 0.4 U-Pb zircon age from a quartz diorite (Encarnación et al., 1993) is the oldest reported age. Other ages from the Central Cordillera Diorite Complex are between 23 and 0.5 Ma (MMAJ-JICA. 1977; Bellon and Yumul, 2000; Imai, 2001; Waters et al., 2011). Late

Oligocene-early Miocene (c. 20–27 Ma) magmatic rocks with an island-arc geochemical signature are also found to the east of the Central Cordillera Diorite Complex (MMAJ-JICA, 1977; Knittel, 1983; Hollings et al., 2011).

Along the east coast of Luzon, several complete ophiolite complexes are exposed (Fig. 5), which include, from north to south, the Casiguran/Isabela, Dibut Bay/Baler, Montalban, Camarines Norte/Calaguas Islands/Cadig, Lagonoy, and the Rapu-Rapu ophiolites (e.g., Encarnación, 2004; Dimalanta et al., 2020). Major and trace element geochemistry revealed transitional MORB to IAT geochemical signatures in these ophiolites and a back-arc basin setting of formation is generally inferred (Geary, 1986; Geary et al., 1988; Geary and Kay, 1989; Billedo et al., 1996; Tamayo et al., 1998; Tejada and Castillo, 2002; Andal et al., 2005). Radiolarian biostratigraphy from the chert sedimentary carapace of the northernmost, Casiguran Ophiolite yielded Lower Cretaceous (upper Barremian-Albian) ages (Queaño et al., 2013), i.e., similar as the ages of cherts on Lanyu Island (Deschamps et al., 2000; Yeh and Cheng, 2001), the ages of the ocean floor of the Huatung Basin (Huang et al., 2019) and the Gagua Ridge arc lavas (Qian et al., 2021) to the north. For the other ophiolites, the sedimentary carapace is either absent or has not been dated (Encarnación, 2004; Dimalanta et al., 2020). However, radiometric ages have been reported for some of the ophiolites exposed in eastern Luzon, which in all cases are minimum ages. A 92.0 ± 0.5 $^{40}Ar/^{39}Ar$ amphibole age was obtained from a foliated amphibolite from the metamorphosed Dibut Bay Ophiolite, which is interpreted as the age of metamorphism (Billedo et al., 1996). A similar metamorphic amphibole age of 99.9 ± 7.0 Ma was obtained from amphibolite of the structurally disrupted Camarines Norte ophiolite, using $^{40}Ar/^{39}Ar$ dating of a metagabbro (Geary et al., 1988). Ultramafic, metamorphic, and gabbroic rocks of the Camarines Norte Ophiolite are juxtaposed on east-dipping thrust faults (Geary and Kay, 1989). Estimates for the P-T conditions during formation of the amphibolites are 500-550° and 2–4 kbar (Geary and Kay, 1989). There are no interpretations about the cause of metamorphism, so it remains unknown whether the metamorphism occurred as seafloor metamorphism during extension of the ophiolite, in which case the metamorphic ages essentially represent the age of formation of the oceanic crust, or whether metamorphism occurred during a later phase of upper plate shortening, in which case the metamorphic ages may be much younger than the formation of the oceanic crust.

In contrast to the Late Cretaceous metamorphic ages obtained from the Dibut Bay and Camarines Nortes ophiolites, the Lagonoy Ophiolite yielded $^{40}Ar/^{39}Ar$ ages of 150.9 ± 3.3 and 156.3 ± 2.0 Ma, obtained from amphiboles from a metagabbro and metaleucodiabase sample (Geary et al., 1988), i.e., as much as 25–30 Ma older than the crust of the Huatung Basin. Whether these ages represent magmatic, metamorphic crystallization, or cooling ages remains unknown, and they were thus regarded as the minimum age of the ophiolite (Geary et al., 1988). No interpretations were made about possible causes of metamorphism. In addition, a 122.7 ± 4.0 Ma K-Ar whole-rock age was obtained from a gabbro of the Lagonoy Ophiolite (David et al., 1997), although this age may have suffered from Ar loss (Encarnación, 2004). Undated metamorphic rocks, interpreted as a metamorphic sole, are exposed on easternmost Rapu-Rapu island, below the (undated) Rapu-Rapu Ophiolite towards the west (Yumul et al., 2006). To the southwest, on the island of Masbate to the west of the Philippine Fault, lies another Early Cretaceous ophiolite: the Balud Ophiolite contains mafic magmatic rocks, including pillow lavas with subordinate isotropic gabbros and diabase dikes (Manalo et al., 2015), although no ultramafic rocks have been reported. The basalts are overlain by Lower-Upper Cretaceous (Aptian-Cenomanian) radiolarian chert and has a transitional MORB-IAT geochemistry (Manalo et al., 2015).

The ophiolites of southeastern Luzon and neighboring Calaguas and Rapu-Rapu islands are unconformably overlain by Upper Cretaceous sedimentary sequences. Unconformably overlying the Lagonoy Ophiolite are Upper Cretaceous volcanic sequences interpreted to be arc-related, consisting of andesitic volcanics including pillow basalts, volcaniclastics, and hemipelagic limestone interbedded with radiolarian chert (David et al., 1997). A 91.1 ± 0.5 Ma $^{40}Ar/^{39}Ar$ was obtained from amphibole separates of a basalt flow (David et al., 1997). Finally, a diorite pluton that intruded into the harzburgites of the Rapu-Rapu Ophiolite, yielded a 77.1 ± 4.6 Ma K-Ar whole-rock age and may represent a plutonic equivalent of the Upper Cretaceous arc sequence (David et al., 1997). The Camarines Norte Ophiolite to the north of the Lagonoy Ophiolite is unconformably overlain by a sedimentary sequence of graywacke, arkose, and mudstone, with minor spilite, which is possibly a distal equivalent of the Upper Cretaceous arc sequence overlying the Lagonoy Ophiolite (Encarnación, 2004).

The Upper Cretaceous arc sequences of the East Luzon ophiolites are overlain by middle to upper Eocene volcanics, volcaniclastics, limestones, and turbidite sequences, interpreted as an arc sequence that is separate from the Cretaceous sequence (David et al., 1997; Billedo et al., 1996; Encarnación, 2004; Queaño et al., 2020). The Eocene volcaniclastics are the equivalent of volcaniclastics exposed in the northernmost part of Central Cordillera in the Ilocos Norte region (Queaño et al., 2020). The Sierra Madre range of East Luzon is intruded by Eocene (49–43 Ma) and Oligocene-earliest Miocene batholiths (33–22 Ma; MMAJ-JICA, 1977, 1987; Billedo et al., 1996; Encarnación, 2004; Hollings et al., 2011). Also, the Balud Ophiolite of Central Luzon is overlain by Eocene volcanics that consist of basaltic and andesitic flows with minor sandstones and mudstones (Manalo et al., 2015; MMAJ-JICA, 1986). The Late Cretaceous and the Eocene arc sequences of the Bicol region, to the south of the Sierra Madre range, are intruded by Oligocene plutons which yielded K-Ar and $^{40}Ar/^{39}Ar$ ages between 36 and 30 Ma (David et al., 1997; Encarnación, 2004).

3.4.3.2. Eocene ophiolites: Zambales; Angat; Sibuyan; Antique. In contrast to northern and eastern Luzon, western Luzon exposes Eocene ophiolites (Fig. 5). These ophiolites are in the hanging wall of the eastward subduction zone that consumes the South China Sea crust, and the SE Asian tectonic mosaic including the Palawan accretionary prism and ophiolite. The northernmost of these ophiolites is the Zambales Ophiolite, which is subdivided into the Acoje and Coto blocks, which have transitional MORB-IAT and IAT geochemical signatures, respectively (Hawkins and Evans, 1983; Yumul, 1989), showing they were formed in or adjacent to the Eocene arc (e.g., Hawkins and Evans, 1983; Encarnación et al., 1993; Yumul et al., 2000a). The Acoje Block yielded a 44.1 ± 3 Ma K-Ar whole rock on sill cutting pillow lavas (Fuller et al., 1989) and 44.2 ± 0.9 Ma U/Pb zircon age on plagiogranite (Encarnación et al., 1993), whereas the Coto block gave a whole-rock K-Ar age of 46.6 ± 5.1 Ma from a diabase dike intruding gabbros (Fuller et al., 1989) and a plagiogranite 45.1 ± 0.5 Ma U/Pb zircon age (Encarnación et al., 1993). The Coto Block is overlain by Eocene pelagic limestone interbedded with tuffaceous turbidites (Garrison et al., 1979; Schweller et al., 1983). Emergence of the Zambales Ophiolite occurred prior to the Early Miocene, based on the presence of ophiolite clasts in a conglomerate and sandstone formation unconformably overlying the ophiolite, interpreted to result from activity of the Manila Trench (Yumul et al., 2020). Miocene sedimentary rocks overlying the Acoje Block rework Upper Jurassic to Lower Cretaceous radiolarian cherts (Queaño et al., 2017b).

To the west of the Zambales Ophiolite are isolated outcrops of a mélange with a matrix of sheared serpentinite containing blocks of

Lower Cretaceous radiolarian chert and quartz-sericite-chlorite schist, referred to as the West Luzon Shear Zone (Karig, 1983). This was interpreted as a major left-lateral strike-slip fault zone that became inactive before the end of the Oligocene, based on the lack of shearing in unconformably overlying upper Oligocene sediments (Karig, 1983).

The incomplete and structurally disrupted Angat Ophiolite, to the southeast of the Zambales Ophiolite, yielded a 48.1 ± 0.5 zircon U-Pb age from a plagiogranite (Arcilla et al., 1989; Encarnación et al., 1993). The ophiolite comprises gabbros, a sheeted dike complex and pillow basalts. The Eocene Angat Ophiolite is in fault contact with pillow basalts associated with Upper Cretaceous radiolarian chert overlain by Eocene volcaniclastics, referred to as the Montalban Ophiolite (Encarnación et al., 1993). Similar to the Eocene ophiolites to the north, the Angat Ophiolite is overlain by arc-derived sediments (Karig, 1983) and has a geochemistry displaying MORB and IAT characteristics (Yumul, 1993).

To the southeast of Mindoro is the Sibuyan Ophiolite, on the Romblon Island Group. The Sibuyan Ophiolite is exposed as tectonic slices separated by west-dipping thrust faults (Dimalanta et al., 2009). A 43.2 ± 2.5 K-Ar whole rock age was obtained from a diorite sample (Dimalanta et al., 2009). Jurassic to Cretaceous radiolarians were reported from cherts intercalated with pillow lavas (Maac and Ylade, 1988). However, these may be derived from a mélange, analogous to the West Luzon Shear Zone exposed to the west of the Zambales Ophiolite (Karig, 1983). The ophiolite is intruded by 18–20 Ma andesites and rhyolites (Bellon and Rangin, 1991). The ophiolite is structurally above a tectonic mélange to the northeast that comprises clasts of ophiolitic material and metasediment in a sheared serpentinite and red mudstone matrix (Dimalanta et al., 2009). In addition, the ophiolite is structurally above a metamorphic unit comprising mostly plagioclase-quartz-mica schist. K-Ar mica age determinations from a quartz-mica schist and a mica schist yielded ages of 12.3 ± 0.2 Ma and 12.2 ± 0.2 Ma (Dimalanta et al., 2009). U-Pb zircon dating of the protolith of the metamorphic unit yielded a c. 110 Ma maximum depositional age (Knittel et al., 2017).

South of the Romblon Island Group is the island of Panay, which exposes the Antique Ophiolite. The ophiolite comprises a mantle and crustal section and is exposed in thrust slices along SE dipping thrust faults (Tamayo et al., 2001). U-Pb ages constrain the crystallization age of the ophiolite to 44–42 Ma (Mesalles et al., 2018). Calcarenites with Early Eocene foraminifera comformably overly the pillow basalts (Rangin et al. 1991; Tamayo et al., 2001), but Late Jurassic to Early Cretaceous and Late Cretaceous radiolarians have also been found in the area, in unknown tectonic context (McCabe et al., 1982; Rangin et al., 1991). The geochemistry of the ophiolite is intermediate between MORB and IAT (Tamayo et al., 2001; Yumul et al., 2013). The ophiolite body is thrust towards the west over Middle Miocene clastic sediments, and these volcaniclastics, conglomerates, sandstones, and minor carbonates also unconformably cover the ophiolite. To the east of the ophiolite is a mélange with blocks of ophiolite material in a Middle Miocene matrix, but the contact between the mélange and the ophiolite is not exposed (Tamayo et al., 2001). The mélange underthrusts to the east an Oligocene-Early Miocene volcanic arc sequence (K-Ar ages of 30–21 Ma; Bellon and Rangin, 1991) with overlying marine sediments (Tamayo et al., 2001).

There is no evidence that the belt of Eocene ophiolites of the northwest Philippines is separated from the Cretaceous ophiolites by a major thrust fault that may represent a former subduction zone. Instead, they more likely represent Eocene oceanic crust that formed within the Cretaceous oceanic crust exposed on the eastern Philippines. Their geochemistry and overlying Eocene arc-derived sediments suggest that they formed above a subduction zone, that is related to the Eocene and younger arc rocks that unconformably overlie the Cretaceous ophiolites to the east. The associated trench was likely to the west, since no evidence exists that there was an Eocene trench between the Philippines and the Philippine Sea Plate.

Finally, to the west of the Eocene ophiolites, on Mindoro Island, lies the Amnay Ophiolite, on a ridge that forms the eastern continuation of Palawan orogenic belt (Fig. 5). The Amnay Ophiolite has been interpreted to have formed in the forearc of the subduction zone that consumed the proto-South China Sea oceanic lithosphere (Yu et al., 2020), and has been correlated to the Palawan Ophiolite (Advokaat and Van Hinsbergen, 2023). A Middle Oligocene age was assigned to the ophiolite based on foraminifera in siltstone intercalated with pillow basalts (Rangin et al., 1985; Sarewitz and Karig, 1986). Zircon U-Pb dating of two metagabbro samples yielded zircon ages of 23.3 ± 0.2 Ma and 23.6 ± 0.4 Ma (Yu et al., 2020). These ages are considered magmatic crystallization ages based on the structure and chemical composition of the zircon grains. A fresh gabbro sample, on the other hand, yielded a 33.0 ± 0.8 Ma zircon U-Pb age (Yu et al., 2020). The geochemistry of the ophiolite is dominantly MORB with a minor subduction-related component (Yumul et al, 2009). Structurally below the Amnay Ophiolite are Jurassic siltstones and Upper Cretaceous (Campanian-Maastrichtian) black shales that are unconformably overlain by Middle Eocene-Lower Oligocene *syn*-rift clastic sediments and Upper Oligocene-Lower Miocene post-rift clastic sediments and carbonates, correlated to the Palawan Continental Terrane (Marchadier and Rangin, 1990; Advokaat and Van Hinsbergen, 2023).

3.4.3.3. Southern Philippines ophiolites; Cebu arc, southeast Bohol accretionary prism and trench; mindanao; Halmahera. The central and southern Philippines are divided by the Philippine Fault Zone into an eastern belt with a NNW-SSE structural grain, and a western belt with a nearly perpendicular, ENE-SWS structural grain. The eastern zone contains several prominent ophiolite complexes, from north to south including the Samar, Tacloban, Malitbog, Dinagat, Surigao, and Pujada ophiolites. The western zone from north to south includes the Cebu arc, the SE Bohol Ophiolite and accretionary prism, the proto-SE Bohol Trench, and on Mindanao, the Polanco and Titay ophiolites (Fig. 5).

The Samar Ophiolite is exposed on southernmost Samar Island (Fig. 5). Based on radiolarian biostratigraphy of chert intercalating with pillow basalts, the Samar Ophiolite was assigned a Late Cretaceous or possibly Early Cretaceous age. This age is supported by K-Ar whole-rock dating of two basalt samples that yielded ages of 100.2 ± 2.7 Ma and 97.9 ± 2.8 Ma (Balmater et al., 2015). Based on its geochemistry, the Samar Ophiolite has a supra-subduction zone signature and is thought to have formed in an intra-arc or forearc setting (Guotana et al., 2017, 2018). Unconformably overlying the ophiolite are Upper Oligocene to Lower Pliocene sediments that incorporate fragments of successively deeper parts of the ophiolitic sequence and that were likely deposited adjacent to an active arc (Pacle et al., 2017).

Just west of the Samar Ophiolite is the Tacloban Ophiolite, exposed on Leyte Island (Fig. 5). Zircon U-Pb dating of a gabbro from the ophiolite complex yielded two very different ages: 145.1 ± 3.2 Ma and 124.7 ± 3.3 Ma (Suerte et al., 2005). The Tacloban Ophiolite is unconformably overlain by Upper Miocene to Lower Pliocene sediments with clasts derived from the ophiolite (Suerte et al., 2005). On southern Leyte Island lies the Malitbog Ophiolite (Fig. 5). The different units of the ophiolite are separated by northeast trending thrust faults (Dimalanta et al., 2006). An early Late Cretaceous age was assigned based on foraminifera in limestones that overlie the ophiolite (Dimalanta et al., 2006). Based on geochemistry of the mantle peridotites, the Tacloban and Malitbog

ophiolites were inferred to have formed in a backarc basin setting (Guotana et al, 2018).

To the east of the Malitbog Ophiolite, on Dinagat Island lies the Dinagat Ophiolite, which is also exposed in northeastern Mindanao (where it is also known as the Surigao Ophiolite; e.g., Yumul, 2003, 2007). The Dinagat Ophiolite comprises a complete mantle-crustal section, and sporadically, the basalt flows are intercalated with tuffs, tuffaceous sandstones, siltstones, and shales (Dimalanta et al., 2020). The age of the ophiolite was inferred from an 84.4 ± 4.2 Ma K-Ar whole rock age (MMAJ-JICA, 1986), although the dated rock type is not clear. Geochemical analyses revealed a transitional MORB-IAT and supra-subduction zone affinity of the mantle and volcanic sections (Tamayo et al., 2004; Yumul et al., 1997). In the west, structurally below the ophiolite are metamorphic rocks consisting of amphibolite schist, quartzo-feldspathic schist, biotite schist, and metacherts, presumed by Santos (2014) to be Late Cretaceous in age, although no radiometric ages were reported. The ophiolite is unconformably overlain by Upper Eocene conglomerates interbedded with calcareous sandstone and mudstone (Santos, 2014). First clasts of the ophiolite appear in clastic sedimentary rocks of Upper Miocene age (Santos, 2014).

The Pujada Peninsula of southeastern Mindanao exposes the Pujada Ophiolite (Fig. 5) of which zircon U-Pb geochronology from three gabbro samples yielded ages of 90.9 ± 2.7, 90.2 ± 2.0, and 88.4 ± 7.6 Ma (Olfindo et al., 2019). A back-arc basin setting was interpreted for the generation of the ophiolite, based on its geochemistry (Olfindo et al., 2019). The ophiolite is thrusted eastwards over amphibolites, which are in turn thrust over greenschist-facies metamorphosed mafic rocks with an eastward decreasing metamorphic grade (Hawkins et al., 1985). This partly metamorphosed volcano-sedimentary section has a distinct island arc affinity (Olfindo et al., 2019). Based on radiolarian and foraminiferal content, a Late Cretaceous age was assigned to the island-arc volcano-sedimentary sequence (Yumul et al., 2003; Olfindo et al., 2019). Basalts of the ophiolite are unconformably overlain by Eocene limestones (Mitchell et al., 1986). Ophiolite clasts of the Pujada ophiolite first appear in an overlying Upper Miocene–Pliocene turbidite succession (Queaño, 2005).

In summary, the southeastern Philippines ophiolites to the east of the Philippine Fault systematically reveal Cretaceous ages, perhaps younging southward from ~ 100 to ~ 90 Ma although some outlying ages of 125 or 145 are reported (Tacloban Ophiolite; Suerte et al., 2005), with geochemical signatures suggesting arc, back-arc, or forearc chemistries. In places, these are thrusted over metamorphosed volcano-sedimentary rocks with Cretaceous protoliths and presumably Late Cretaceous ages metamorphic ages that suggest a period of upper plate shortening above a subduction zone. There is no record of Eocene arc volcanism reported from the southeastern Philippines, in contrast to Luzon in the northern Philippines, but instead, this period is characterized by limestone sedimentation. The southeastern Philippine ophiolites became uplifted and emergent in the late Miocene.

To the west of the Philippine Fault Zone, the central Philippine island of Cebu exposes a metamorphic basement composed of metavolcanics, greenschists, amphibolite schists and siliceous metasediments consistent with metamorphosed ophiolitic mafic crust and overlying pelagic sediments (Diegor, 1996; Dimalanta et al., 2006; Rodrigo et al., 2020). This sequence is intruded and overlain by a Cretaceous volcanic arc sequence (Deng et al., 2015). Ages of the protoliths of the metamorphic rocks are unknown and were originally inferred to be Jurassic, but zircons extracted from amphibolite schist yielded a U/Pb mean age of 120.4 ± 0.3 Ma suggesting an Early Cretaceous age instead (Rodrigo et al., 2021). The metamorphic rocks are overlain by Lower Cretaceous limestones and arc volcanics, and an Upper Cretaceous succession of interbedded sandstone–siltstone, conglomerates, carbonaceous mudstones, and rare siliceous mudstones, which rework the deeper sequence (Rodrigo et al., 2020; Rodrigo and Schlagintweit, 2022). The volcanic arc sequence was dated through zircon U-Pb geochronology of a porphyritic andesite and a pyroclastic rock, yielding ages of 126.2 ± 2.4 Ma and 118.5 ± 1.2 Ma, respectively (Deng et al., 2015). In addition, U-Pb dating of zircons from diorite intrusions yielded weighted mean ages between 107.3 ± 1.0 Ma and 110.3 ± 4.1 Ma (Deng et al., 2017, 2019), consistent with K-Ar and U-Pb ages of 101–108 Ma and 109 ± 2 Ma (Walther et al., 1981). Moreover, detrital zircons from river sands vary in age between 100 and 140 Ma, with a peak at 118 Ma (Deng et al., 2015). Using zircon U-Pb dating on a variety of rocks interpreted to belong to the arc sequence, Gong et al. (2021) also yielded several Early Cretaceous crystallization ages (between 120.0 ± 4.7 Ma and 107.5 ± 1.6 Ma). In addition, a mean 89.1 ± 1.4 Ma crystallization age was obtained from two andesite samples (Gong et al., 2021) suggesting that arc magmatism may have continued for ~ 30 Ma. Cebu Island also contains Eocene-early Oligocene and Miocene volcanics: andesites and pyroclastics yielded ages between 43 and 30 Ma, as well as a 14.2 ± 0.7 Ma age (Gong et al., 2021). The Cebu Island arc samples contain Permian to Triassic xenocrysts in the Cretaceous samples and mainly Mesozoic with minor early Paleozoic and Archean xenocrysts in the Cenozoic samples, which suggest that the arc resurfaces continent-derived subducted sediments, perhaps from the SE Asian Tethysides (Gong et al., 2021).

To the south of the Cebu arc, the island of Bohol exposes the SE Bohol Ophiolite (Fig. 5). The pillows of the ophiolite sequence are overlain with Upper Cretaceous radiolarian chert (Faustino et al., 2003; Dimalanta et al., 2020) which gives a minimum age for the ophiolite's crust. The ophiolite thrusts towards the southeast over non-metamorphosed mélange, comprising ophiolite-derived chaotically disrupted rock units in a serpentinite matrix (De Jesus et al., 2000). Structurally below the mélange are metamorphic rocks, including chlorite schists, quartz-sericite schists, and amphibolites (De Jesus et al., 2000). Collectively, these units were interpreted as a Late Cretaceous forearc and accretionary prism that formed at the proto-SE Bohol Trench, which forms a prominent, but tectonically inactive depression to the southeast of the island (Yumul et al., 2000b; Faustino et al., 2003). The Upper Cretaceous units are unconformably overlain by lower Miocene to Pleistocene clastics, carbonates, and igneous units (Faustino et al., 2003). Clasts of the ophiolite are present in middle Miocene clastics of the overlying sedimentary sequences (Faustino et al., 2003). Zircon U-Pb dating from pyroclastics and andesites yielded ages between 42.5 ± 1.3 Ma and 30.7 ± 0.2 Ma (Gong et al., 2021), showing that Eocene-Oligocene magmatism also affected the Bohol region.

To the south of the SE Bohol Trench, on the Zamboanga Peninsula of western Mindanao are the Titay and Polanco ophiolites, both of unknown age. The Titay Ophiolite complex is thought to be emplaced onto continental basement that also underlies the Sulu arc (e.g., Pubellier et al., 1991; Tamayo et al., 2000; Yumul et al., 2004), correlated to the SW Borneo Mega-Unit of the SE Asian Tethysides (Advokaat and Van Hinsbergen, 2023). The Titay Ophiolite is in the north underlain by metamorphic rocks, including metagreywackes, amphibolites, and quartz-mica schists (Tamayo et al., 2000). A latest Oligocene to early Miocene age of metamorphism was inferred from 24.6 ± 1.4 and 21.2 ± 1.2 Ma K-Ar ages of amphibole separates from amphibolites (Tamayo et al., 2000; Yumul et al., 2004). This episode of metamorphism and associated Miocene volcanism may be related to the Miocene subduction of the Sulu Sea below the Zamboanga Peninsula along the Sulu Trench (Yumul et al., 2004).

The Zamboanga Peninsula is underlain by continental basement, correlated to the SW Borneo mega-unit (Advokaat and Van Hinsbergen, 2023). The Titay Ophiolite complex is separated from

the Polanco Ophiolite to the east by the Sindangan-Cotabato-Daguma lineament, a transform fault that is referred to as the Siayan-Sindangan Suture Zone in the north, and that links to the Negros Trench at the eastern Sulu Sea margin (Pubellier et al., 1991; Yumul et al., 2004) (Fig. 3). This zone is characterized by serpentinite-matrix mélange with ophiolite-derived clasts and a middle Miocene shale-matrix mélange with clasts of sandstone, andesite, and metamorphic rocks, interpreted as a Miocene subduction interface (Yumul et al., 2004). An upper Miocene formation comprising limestone, basalt lavas, and tuffaceous sediments, and a clastic sequence straddles the mélange and is also exposed on either side of it, providing a minimum age for the emplacement of the Polanco Ophiolite over the SE Asian continental basement (Yumul et al., 2004). To the southwest of the Siayan-Sindangan Suture Zone, southwestern Mindanao comprises oceanic crust of unknown age, which is suggested to have formed as part of the Eocene Celebes Sea (Honza and Fujioka, 2004).

Central Mindanao is underlain by oceanic basement and volcanics of unknown age, overlain by upper Oligocene to lower Miocene limestones, upper Miocene clastic sedimentary rocks, and Pliocene to recent volcanic rocks (Quebral et al, 1996; Sajona et al., 1997). K-Ar whole-rock dating of andesite samples from central Mindanao yielded ages of 19.9 ± 0.4 Ma and 16.3 ± 0.9 Ma (Sajona et al., 1997), related to the subduction of the Celebes Sea below Central Mindanao at the Cotabato Trench.

Towards the south, the Sindangan-Cotabato-Daguma lineament transitions southward into an east-dipping back-thrust to the west of the Sangihe arc (Fig. 3). The Sangihe arc formed above a west-dipping subduction zone that consumed the western part of the Molucca Sea Plate and that is dipping below the Eocene lithosphere of the Celebes Sea (e.g., Rangin et al., 1999). K-Ar dating of andesites of the Sangihe arc yielded ages between 15.6 and 0.9 Ma (Morrice et al., 1983) suggesting Miocene subduction, contemporaneous with the convergence between the Philippine Mobile Belt and the SE Asian Tethysides, but with opposite polarity. The forearc of the Sangihe subduction zone is exposed on Talaud Island (Fig. 5) and consists of an ophiolite of unknown age (Moore et al., 1981) with a MORB-BABB geochemical signature (Evans et al., 1983). This ophiolite is thrust westwards over middle Miocene-Pliocene marine volcaniclastics and andesitic volcanics (Moore et al., 1981; Rangin et al., 1996), emplaced onto a mélange comprising blocks of ophiolitic rocks and marine sediments, including Eocene (Lutetian) radiolarian chert (Moore et al., 1981). The cherts are interpreted as accreted from subducted Molucca Sea Plate lithosphere, which therefore must have had an Eocene minimum age.

The Molucca Sea Plate was also subducted eastwards, below Halmahera. The forearc of the Halmahera subduction zone is currently being underthrusted westwards below the forearc of the Sangihe subduction zone, which means that all oceanic lithosphere of the Molucca Sea has been consumed (Silver and Moore, 1978; McCaffrey et al., 1980). Arc magmatism related to the eastward subduction of the Molucca Sea Plate found on Halmahera is young, 8 Ma and younger, and slightly older on Obi to the south of Halmahera, dated at 11.8 ± 0.7 Ma using K-Ar whole rock dating (Baker and Malaihollo, 1996). On eastern Halmahera, and the islands of Morotai to the north, Obi to the south, and Waigeo to the east, ophiolitic rocks are exposed, including peridotites, gabbros, and few pillow basalts (Hall et al., 1988). From these ophiolitic rocks, $^{40}Ar/^{39}Ar$ ages of 87.3 ± 7.0 and 73.8 ± 1.5 Ma were obtained from hornblende minerals from diorite samples (Ballantyne, 1990, 1991). The ophiolitic rocks of the basement complex of Halmahera are tectonically intercalated with Upper Jurassic/Lower Cretaceous and carbonaceous turbidites, Upper Cretaceous (Campanian-Maastrichtian) volcaniclastics, and Eocene pelagic and shallow marine limestones (Hall et al., 1988). This sequence was interpreted as an east-facing forearc, with ophiolites of similar age and origin as on the southern Philippines (Hall et al., 1988), such as the Pujada Ophiolite (Olfindo et al., 2019). Oligocene-Miocene sedimentation on Halmahera is dominated by marine marls and limestones without evidence for magmatism, until the occurrence of volcaniclastics and lavas in the Miocene (Hall et al., 1988). On Waigeo, to the east of Halmahera, the ophiolites are deformed and intercalated with Lower Eocene radiolarian chert (Charlton et al., 1991; Ling et al., 1991) and unconformably overlain by sandstone with ophiolitic detritus, Lower Oligocene volcaniclastic sandstone, Upper Oligocene calc-alkaline island arc basalt, and Lower Miocene–Pliocene deep marine limestone (Charlton et al., 1991), showing that here arc magmatism was active since at least early Oligocene time.

The connection of the bivergent subduction complexes of the Sangihe and Halmahera trenches to the trenches southwest and southeast of Mindanao is diffuse and complex. Pubellier et al. (1999) showed that the connections are essentially two relay ramps. The thrust displacement on the Sangihe trench decreases northward, and between the islet of Miangas and southeast Mindanao connects to the Philippine Fault Zone. The convergent motion is northward increasingly accommodated by the east-dipping Cotabato Trench below southwest Mindanao (Fig. 3). The east-dipping subduction below Halmahera also decreases northward and is traced towards the Snellius Plateau, which may represent a submerged volcanic arc of Oligocene age (Pubellier et al., 1999) perhaps correlated to the Oligocene arc sequence of Waigeo (Pubellier et al., 2004). To the east of the Snellius Plateau, the Philippine Trench accommodates westward underthrusting of the Philippine Sea Plate, which gradually disappears southward towards northern Halmahera (Fig. 3) (Pubellier et al., 1999).

To the south of Halmahera, metamorphosed continental basement of Australian affinity is exposed on southern Bacan and Obi islands. This basement consists of diorite with a U-Pb age of 329.8 ± 2.7 Ma, micaceous quartzites with a maximum depositional age of 159 Ma, and metasedimentary gneiss with a maximum depositional age of 87 Ma (Hall et al., 1988; Malaihollo and Hall, 1996; Decker et al., 2017). The continental basement was detached from the Australian continent and is now juxtaposed against the forearc basement of the Miocene Halmahera subduction zone by a splays fault of the Sorong Fault Zone (Saputra et al., 2014). This left-lateral fault system bounds the Sangihe and Halmahera trenches in the south and continues eastwards onto the Bird's Head Peninsula of New Guinea (Figs. 3 and 4).

3.4.4. New Guinea

Southern New Guinea forms the northernmost margin of Australian continental basement, overthrusted from the north by plates of the Junction Region (Figs. 1, 4, and 7). In the southern part of central New Guinea, Precambrian and Paleozoic basement of the Australian foreland is exposed (Davies, 2012). This basement is overlain by a series of clastic sediments interpreted as a foreland basin to advancing nappes from the north. This foreland basin has been referred to as the Arafura and Fly Platforms (e.g., Pigram and Symonds, 1991). In the western part, on the Arafura Platform (Fig. 7), the Precambrian basement is overlain by mostly conformable sedimentary sequences that span the upper Proterozoic or Cambrian to the mid to upper Cenozoic (Davies, 2012). These sediments show a history of shelf sedimentation up to the late Paleozoic or early Triassic, intruded by Permian-Triassic continental arc magmatism (Amiruddin, 2009; Crowhurst et al., 2004; Webb and White, 2016; Jost et al., 2018). This was followed by rifting of the continental margin, which led to the deposition of mudstones, sandstones, and conglomerate, associated with rift-related volcanism in the Middle Triassic to Early Jurassic (Home et al., 1990; Pigram and Symonds, 1991). Post-rift passive margin subsidence in the Late Jurassic to Early Cretaceous led to the deposition

of marine shales interbedded with quartz-rich sandstones. The latest Cretaceous and most of the Cenozoic was dominated by the deposition of carbonates, with short intervals of clastic sedimentation interpreted to reflect periods of eustatic sea-level fall (Cloos et al., 2005). Around 30 Ma, an influx of clastic sediments occurred, which was interpreted as the onset of foreland basin formation in response to an approaching active margin in the north (Pygram and Symons, 1991; Quarles van Ufford and Cloos, 2005). Since the late Miocene, thick packages of terrestrial continental clastic sediments were deposited related to uplift of an advancing Papuan and Irian Jaya fold-and-thrust belt from the north (Davies, 2012).

The Fly Platform in the east (Fig. 7), where the basement is of Permian age, has a similar Mesozoic and Cenozoic stratigraphy as the Arafura Platform. However, a phase of uplift and erosion led to a widespread Upper Cretaceous to Eocene hiatus that is not seen in other parts of New Guinea (Davies, 2012). This uplift is thought to have occurred as a precursor to the opening of the Coral Sea Basin in the Paleocene (Pygram and Symonds, 1991; Davies, 2012).

3.4.4.1. Bird's Head Peninsula. The Sorong Fault that forms the plate boundary between the Philippine Sea Plate and northwestern New Guinea runs across the northwestern tip of the Bird's Head Peninsula (Figs. 4 and 7). To the north of the Sorong Fault, the Bird's Head Peninsula exposes a similar Oligocene-Miocene oceanic island arc sequence as on Waigeo: basaltic-andesitic lava, agglomerate and volcaniclastics that yielded K-Ar ages of 31.5–10.5 Ma, sometimes intercalated with limestone and gabbro intrusions (Pieters et al., 1983, 1989). These island arc volcanics (known as the Tosem Block) are thrusted along the Koor Fault over an allochthonous unit of Upper Jurassic to Lower Cretaceous age (known as the Tamrau Block; Fig. 7), which consist of partly metamorphosed shales, siltstones, and sandstones, interpreted as continental slope deposits of the Australian passive margin. The Mesozoic passive margin sediments are unconformably overlain by Eocene to middle Miocene limestones (Webb et al., 2019). Both the Mesozoic and Eocene to Miocene sediments are intruded and overlain by Miocene granitoids and lavas, including andesitic, dacitic and basaltic tuffs and lavas, volcaniclastics and intercalated limestones, as well as middle Miocene calcareous mudstones and sandstones (Webb et al., 2019). K-Ar ages of 20–9 Ma and U-Pb zircon ages of 18–10 Ma were obtained from the Miocene volcanics (Bladon, 1988; Webb et al., 2020). Based on their dominantly calc-alkaline nature, it was interpreted that these volcanics formed as part of a continental arc (Webb et al., 2020). The Koor Fault is sealed by Plio-Pleistocene sediments, which constrains the timing of thrusting of the Philippine Sea Plate and overlying arc onto the northern Bird's Head to late Miocene to Pliocene (Webb et al., 2019). The Tosem and Tamrau blocks are separated from autochthonous Australian basement (Kemum Block) by the Sorong Fault (Fig. 7). Correlations across the fault based on detrital zircon ages, stratigraphy, and structural data suggested that the northern tip of the Bird's Head Peninsula was displaced westwards by about 300 km along the Sorong Fault since the late Miocene-Pliocene (Webb et al., 2019).

South of the Sorong Fault, Bird's Head Peninsula exposes Paleozoic basement of the Australian continent (the 'Kemum Block') intruded by plutons that yielded K-Ar biotite, muscovite, and hornblende ages between 225 and 295 Ma (Pieters et al., 1983), and overlain by Paleozoic turbidites, Permian and Mesozoic platform carbonates, Paleocene to Miocene limestone and Miocene to recent siliciclastics (Pieters et al., 1983; Davies, 2012). In the Bird's Neck isthmus to the southeast of the Bird's Head, this sequence is deformed and locally metamorphosed in the Lengguru fold-and-thrust belt (Fig. 7), a west-verging, N-S striking fold-and-thrust belt that formed in a short time span of a few million years after 11 Ma, of which the total amount of shortening is uncertain (Bailly et al., 2009). During formation of the fold-and-thrust belt some of the transform motion on the Sorong Fault stepped southward towards a transform fault on Central New Guinea (see below). This was followed by Pliocene E-W extension leading to core complex exhumation (Bailly et al., 2009).

3.4.4.2. Central New Guinea. The Australian foreland of the Arafura and Fly Platforms is overthrusted from the north by the roughly WNW-ESE trending fold-and-thrust belt, comprising north-dipping, south-verging thrust faults, referred to as the Papuan fold-and-thrust belt in Papua New Guinea and the Irian Jaya/Western fold-and-thrust belt in Indonesia (Fig. 7). It comprises thrust sheets that incorporate Australian basement that is overlain by sediments of up to Late Miocene age (Hill, 1999; Cloos et al., 2005). The onset of deformation that formed the southern, continent-derived fold-and-thrust belt was in the Late Miocene, based on the incorporation of Miocene sediments in the entire fold-and-thrust belt and on fission-track thermochronology (Hill and Gleadow, 1989; Hill, 1991; Hill and Raza, 1999).

The continent-derived fold-and-thrust belt is underthrusted to the north below a belt of metamorphic rocks, ophiolites (the Irian, April, and Marum ophiolites), and island arc volcanics and intrusives (Fig. 7; Hill and Hall, 2002; Davies, 2012). Here we review the different ophiolites, which most likely formed part of a coherent oceanic lithosphere.

The Irian Ophiolite is exposed in the western part of Central New Guinea (Fig. 7). It is mainly composed of serpentinized peridotites: crustal sections such as gabbros, sheeted dikes and pillow basalts have not been reported (Weiland, 1999). The ophiolite is thrusted southwards over mélange that includes metamorphosed pillow basalt, amphibolites with greenschist and blueschist overprints, and rare eclogites (Weiland, 1999). The ophiolite and underlying oceanic crustal rocks that were likely accreted from now-subducted oceanic lithosphere that existed north of the Australian margin lie overthrusted on continental metasedimentary rocks of the Ruffaer (or Derewo) unit that comprises slate and phyllites (Cloos et al., 2005), whose protoliths are likely the Jurassic and Cretaceous shales exposed in of the Irian fold-and-thrust belt and Arafura Platform to the south (Warren and Cloos, 2007). Radiometric ages from the structurally coherent ophiolite are lacking. However, K-Ar amphibole age of 57.9 ± 3.9 Ma from a gabbro float sample, and a 68.6 ± 1.1 Ma K-Ar white mica age from amygdules in a pillow basalt likely date the age of oceanic crust as they were probably derived from the ophiolite (Weiland, 1999).

The amphibolites underlying the ophiolites yielded different age clusters. The only available U/Pb zircon age yielded 66.4 ± 0.3 Ma (Weiland, 1999), which is similar to K-Ar ages of 68.4 ± 2.4 Ma (Weiland, 1999) and K-Ar hornblende ages between 61.4 ± 1.5 and 68.3 ± 1.5 Ma and a K-Ar whole-rock age of 62.8 ± 1.5 Ma obtained from amphibolite float samples (Bladon, 1988; Permana, 1995 in Weiland, 1999). These ages were interpreted by Weiland (1999) as a metamorphic sole age suggesting incipient subduction around 68 Ma. On the other hand, K-Ar ages of hornblende obtained from the amphibolites of 182.8 ± 8.0 Ma, $^{40}Ar/^{39}Ar$ ages between 94.2 ± 0.9 and 171.3 ± 8.1 Ma (Weiland, 1999) and a 147 ± 3.7 Ma K-Ar whole-rock age obtained by Permana (1995) and reported by Weiland (1999), reveal a wider and much older age range. These Jurassic amphibolite ages were interpreted as recording dynamic metamorphism that occurred at mid-ocean ridge during sea floor hydration, thus dating the protolith age, whereby Cretaceous ages are interpreted as partly reset ages (Weiland, 1999). Such a Jurassic seafloor spreading age is consistent with the interpreted break-up age of northern Australia, based on the stratigraphy of the Arafura Platform (Davies, 2012).

High-pressure metamorphism occurred in the Eocene: an eclogite-facies sample yielded a 48.4 ± 0.8 Ma K-Ar white mica

age and blueschist whole-rock K-Ar ages yielded an average age of 43.8 ± 2.2 Ma (Weiland, 1999). Permana (1995) reported K-Ar whole-rock ages from *meta*-gabbro and *meta*-dolerite of 49.5 ± 1.3 and 42.6 ± 1.4 Ma, showing that oceanic subduction continued through the middle Eocene. Lower grade metamorphism in the structurally underlying Ruffaer metamorphic belt to the south of the ophiolite yielded c. 35–20 Ma K-Ar whole-rock ages of metapelites and siliciclastic rocks (Weiland, 1999), indicating the Australian passive margin entered the trench below the ophiolites by latest Eocene to earliest Oligocene time.

To the north of, and likely overlying, the Irian Ophiolite are Oligocene-Miocene volcanic arc rocks that yielded K-Ar and U-Pb zircon ages of c. 35–24 and 12–10 Ma (Weiland, 1999). The older suite has an intra-oceanic arc geochemical signature, whereas the younger suite was interpreted as a volcanic arc that incorporated material derived from a continent (Weiland, 1999), consistent with the ages of the metamorphic rocks reported above.

The April Ophiolite (Fig. 7), commonly referred to as the April Ultramafics, occurs as thrusted slices of mainly peridotite with minor pyroxenite and gabbro and underlying partly metamorphosed sedimentary and volcanic rocks of up to middle to late Eocene age (Davies, 1982; Davies and Jaques, 1984). The ophiolitic crust is undated, but a Late Cretaceous age was assigned based on the presence of Upper Cretaceous (possibly Maastrichtian) foraminifera in limestone intercalated with pillow basalts (Ryburn, 1980). Similar to the Irian Ophiolite to the west, high pressure – low temperature metamorphic rocks (Om Formation and Tau Blueschists) are exposed south of and structurally below the ophiolite (Ryburn, 1980; Baldwin et al., 2012), with 40 – 45 Ma K-Ar ages obtained from sodic amphiboles from the Tau blueschists (Davies, 1982; Rogerson et al., 1987; Weiland, 1999). The Tau blueschists are predominantly mafic schists with a northward increasing metamorphic grade (Ryburn, 1980). Two amphibolites that occur close to the April Ophiolite have been dated, yielding K-Ar hornblende ages of 27.2 ± 0.6 and 23.8 ± 2.8 Ma (Page, 1976). Blueschist samples that were collected in the vicinity of the April Ophiolite yielded K-Ar mica ages of 28.0 ± 0.6 and 24.9 ± 0.4 Ma (Davies, 1982; Rogerson et al., 1987). To the north, the ultramafic complex is intruded by Early to Late Miocene arc plutons comprising mostly granodiorite and diorite (Davies, 1980a).

The Marum Ophiolite forms the easternmost ophiolite complex of Central New Guinea (Fig. 7). It consists mainly of peridotites and gabbros that to the south lie thrusted on a thrust sheet that contains pillow lavas, lava breccia, volcaniclastics, and argillite (Davies and Jaques, 1984). Based on geochemical differences between the basalt sheet (enriched in LREE, Ti, Zr; transitional MORB; Jaques et al., 1978, 1983) and the ophiolite (depleted in LREE, Ti, Zr, Y) the basalt sheet is thought to derive from oceanic lithosphere that subducted below the ophiolite (Davies and Jaques, 1984). The only radiometric ages were reported by Jaques (1981), which are a K-Ar age of 173 Ma of plagioclase separates from cumulus gabbros and a 59 ± 2.5 Ma age from hornblende in a granophyric diorite in the upper gabbro sequence. No analytical details were provided, but these ages fall in the cluster of ages that may represent the protolith of the subducted lithosphere, and the age of the oldest metamorphism interpreted as metamorphic sole-related in the Irian Ophiolite. The pillow basalts are intercalated with argilites that contain poorly preserved radiolaria of probable Eocene age (Jaques, 1981). There is no extensive metamorphic sequence found below the ophiolite, although some low-grade metasediments are present (Jaques, 1981). These shales, siltstones and limestones are of Late Cretaceous to Eocene age and are thought to be derived from the Australian continental margin (Davies and Jaques, 1984).

The total amount of shortening in Papua New Guinea was recently estimated to be c. 500 km based on a cross section balancing analysis (Martin et al., 2023). This includes 220 km of shortening related to ophiolite emplacement over the Australian continental margin between roughly 35 and 21 Ma, 190 km of shortening within the Australian passive margin sequence underneath the ophiolite between 21 and 9 Ma (Martin et al., 2023), and c. 100 km of shortening within the Papuan fold-and-thrust belt to the south of the ophiolite since 9 Ma, consistent with earlier estimates (Hill, 1991; Hobson 1986).

The Central Highlands of New Guinea is separated from the coastal mountain ranges by prominent strike-slip fault zones that form part of the northern plate boundary zone of Australia (Figs. 4 and 7). In the north, these strike-slip faults form the eastward continuation of the Sorong Fault Zone of the Bird's Head and include from west to east the Yapen Fault Zone and the Bewani-Torricelli Fault Zone. The Bewani-Torricelli Fault Zone connects eastwards to the ridge-transform plate boundary in the Bismarck Sea, which separates the North and South Bismarck microplates. The North Bismarck microplate is separated in the north and east from the Caroline and Pacific plates by the Manus and Kilinailai trenches (Fig. 4). The Manus Trench continues westwards as the New Guinea Trench. The South Bismarck microplate is separated from the Australian Plate by the onshore Ramu-Markham Fault Zone that connects eastwards with the New Britain Trench (Fig. 4; e.g., Holm et al., 2015). The Ramu-Markham Fault Zone accommodates eastwards increasing convergent motion between the New Guinea orogen and the South Bismarck Microplate (Koulali et al., 2015).

The amount of left-lateral displacement on the Sorong-Yapen-Bewani-Torricelli Fault system after the late Miocene-Pliocene is estimated at ~ 300–370 km based on the similar U-Pb detrital zircon age spectra and lithological similarities of the Tamrau Block of the Bird's Head Peninsula and rocks in the Lengguru fold-and-thrust belt farther east (Dow and Sukamto, 1984; Webb et al., 2019).

The coastal ranges also expose ophiolites, intruding and overlying magmatic rocks, and sedimentary rocks. The geology of the westernmost range, the Foja Range, is poorly known, but includes ultramafics as well as andesites, basalts and volcaniclastic sediments, presumed to be of Paleogene age, unconformably overlain by Neogene sediments (Davies, 2012). Biak Island, north of the Sorong Fault between the Bird's Head Peninsula and the northern ranges of Central New Guinea (Fig. 7), exposes an ophiolite overlain by Eocene to Lower Oligocene volcanics and Oligocene to recent shallow-marine carbonates and clastic erosion products thereof (Saragih et al., 2020). This stratigraphy is comparable to that of the northern Bird's Head Peninsula and Waigeo Island to the west.

The Cyclops Ophiolite**,** at the north coast of New Guinea (Fig. 7), comprises peridotites, cumulate gabbros, dolerites, and lavas including pillow basalts and minor boninites (Monnier et al., 1999). The ophiolite is deformed by S-dipping thrust faults and is underthrusted by undated greenschist to amphibolite facies metabasites (Monnier et al., 1999). The ophiolite is unconformably overlain by Miocene volcaniclastics and limestones. The geochemistry of the peridotites has been interpreted as supra-subduction zone affinity (Monnier et al., 1999; Zglinicki et al., 2020), and the crustal series have a geochemistry consistent with a back-arc basin origin (Monnier et al., 1999). K-Ar whole rock dating yielded a 43 ± 1 Ma age for the boninite sample, and 29.3 ± 0.7 and 29.5 ± 0.7 Ma ages of basalts with interpreted back-arc basin affinities (Monnier et al., 1999).

To the east of the Cyclops Ophiolite are the Bewani-Torricelli-Prince Alexander Mountains, which expose ultramafic, volcanic, and intrusive formations, unconformably overlain by Early Miocene to recent conglomerate, siltstone, and limestone formations (Hutchison and Norvick, 1978; Griffin, 1983; Doust, 1990). This mountain range has an ophiolitic basement, consisting of mafic and ultramafic rocks that returned an uncertain Jurassic K-Ar

whole-rock age of a gabbro (188 ± 55 Ma; Hutchison and Norvick, 1978). The basement is overlain by a Paleocene to earliest Miocene volcanic complex (Bliri Volcanics) and intruded by gabbros, dolerites, and diorites (Torricelli Intrusive Complex), from which some Late Cretaceous (75–70 Ma), but mostly Eocene to Early Miocene (42–18 Ma) K-Ar ages were obtained (Hutchison, 1975; Hutchison and Norvick, 1980; Griffin, 1983; Doust, 1990). Towards the east, the basement consists of highly deformed amphibolite facies orthogneiss and subordinate micaschist, intruded by andesite and pegmatite dikes (Griffin, 1983; Doust, 1990). K-Ar ages between 114 and 106 Ma were obtained from sheared granodiorite, while Upper Oligocene to Lower Miocene (25–20 Ma) ages were obtained from andesite and pegmatite dikes (Hutchison, 1975; Griffin, 1983). A metamorphosed sedimentary complex of unknown age is exposed to the south of the Bewani-Torricelli-Prince Alexander Mountains, referred to as the Ambunti Metamorphics (Doust, 1990). The complex consists of metapelites of mixed continental and oceanic origin (Crowhurst et al., 2004; Davies, 2012). The metamorphic grade is generally low to medium but increases northwards to locally high-grade amphibolite facies (Doust, 1990). The basement, the intrusives, and volcanics are, together with sediments of Early Miocene to Pleistocene age, exposed in top-to-the-south thrust sheets (Hutchison and Norvick, 1978, 1980).

Southeast of the Bewani-Torricelli-Prince Alexander Mountains and north of the Marum Ophiolite are the Adelbert and Finisterre ranges (Fig. 4). These comprise Eocene pelagic and hemipelagic sediments with subordinate volcanics overlain by Lower Oligocene to Lower Miocene volcanics, including basalt and andesite flow breccia, pillow lavas and tuff, sometimes intercalated with argillite, micrite and radiolarian chert (Jaques, 1976; Jaques and Robinson, 1980). The Paleogene sediments and volcanics form shallow north-dipping thrust-sheets and are in the south overlying low-grade Mesozoic metasediments that are also known to the south of the Ramu-Markham Fault (Jaques 1974; Jaques and Robinson, 1980). Both the Paleogene formations and the metamorphosed Mesozoic sediments are unconformably overlain by middle Miocene to Pliocene siliciclastics and carbonates (Jaques and Robinson, 1976).

In summary, the geology of the northern mountain ranges of New Guinea is generally similar to the geology of the Central Highlands. These mountain ranges comprise Mesozoic (Jurassic to Cretaceous) oceanic crust overlain and intruded by mostly Eocene to early Miocene volcanics and intrusives, thrusted towards the south over metamorphosed sediments. The exception is the Cyclops Ophiolite, which is exposed in south-dipping thrust sheets, and of which Eocene to Oligocene crystallization ages were obtained.

3.4.4.3. Papuan Peninsula. The geology of the Papuan Peninsula overall follows a similar logic as in central New Guinea. It exposes an ophiolite belt, underlain in the south by metamorphosed ocean- and continent-derived, accreted metasedimentary and *meta*-igneous thrust slices, and overlain by Paleogene and Neogene volcanics (Fig. 7). However, the architecture of the accreted thrust slices differs from Central New Guinea.

The ophiolite exposed on the Papuan Peninsula is referred to as the Papuan Ultramafic Belt (e.g., Davies and Smith, 1971; Davies, 1980b; Davies and Jaques, 1984; Lus et al., 2004). The most complete sequence of this ophiolite is exposed as a NE-ward dipping unit containing tectonite and cumulate ultramafic rock, gabbroic rock, sheeted dikes, and pillow basalts that are interbedded with calcareous pelagic sediments. Less complete parts of this ophiolite are found farther east on the D'Entrecasteaux and Louisiade islands, on the Moresby Seamount, and on Muyua/Woodlark Island (Davies and Smith, 1971; Davies and Warren, 1988; Monteleone et al., 2001; Little et al., 2011; Webb et al., 2014; Lindley, 2021). Geochemical signatures of basalts in the Papuan Ultramafic Belt are interpreted as varying between MORB and supra-subduction zone signature (Jaques and Chappell, 1980; Whattam et al., 2008; Whattam, 2009). A minimum age of the ophiolite is provided by 50–55 Ma K-Ar hornblende and plagioclase ages from plagiogranites and diorites that intrude the ophiolite (Davies and Smith, 1971). Late Paleocene (58.9 ± 1.1 Ma and 58.8 ± 0.8 Ma) $^{40}Ar/^{39}Ar$ whole rock ages were obtained from a tholeiitic lava and boninite from the Dabi Volcanics, which are exposed east of the main ophiolite body (Walker and McDougall, 1982). Others assigned a Late Cretaceous (Maastrichtian) age to the ophiolite based on the ages of foraminifera in sediments intercalated with basalts (Davies and Smith, 1971; Lus et al., 2004). The structural relationship between these stratigraphic units and the ophiolite is unclear, and as the age of the sediments is older than the crystallization ages of the crust of the ophiolite, we speculate that the basalts overlain by Maastrichtian sediments are from the unit that is structurally below the ophiolite. The ophiolite is overlain by Paleocene to Eocene carbonates, turbidites, and volcanics including pillow lavas, Upper Oligocene to middle Miocene platform carbonates, turbidites, submarine basalt and volcaniclastics and Miocene to recent continental clastics derived from contemporary volcanism (Davies and Smith, 1971).

The ophiolite nappe is thrusted over a metamorphic sole along the Owen Stanley Fault Zone. The metamorphic sole grades downwards from granulite to amphibolite facies rocks (Lus et al., 2004). The cooling of the metamorphic sole is dated to 58.3 ± 0.4 Ma, obtained from the mean $^{40}Ar/^{39}Ar$ age of five samples (Lus et al., 2004), i.e., the same age as the age of the SSZ ophiolitic crust, as is commonly observed worldwide (e.g., Van Hinsbergen et al., 2015). The Owen Stanley Fault thus originally formed as a subduction interface, but currently forms the plate boundary between the Australian and Solomon Sea plates (Davies and Jaques, 1984). The current relative motion along the Owen Stanley Fault transitions from transtentional in the southeast to strike-slip and transpressional in the northwest (Benyshek and Taylor, 2021).

A unit of mafic schists is thrusted below the metamorphic sole. This unit, referred to as the Emo Metamorphics, consists of metamorphic rocks ranging from prehnite-pumpellyite to greenschist facies, that locally overprint an older blueschist facies metamorphism (Pieters, 1978; Worthing and Crawford, 1996). Cooling of amphibolite minerals has been dated to ~ 34 Ma and ~ 14 Ma, based on $^{40}Ar/^{39}Ar$ ages (Worthing and Crawford, 1996). Protolith rock constituted gabbro, micro-gabbro and basalt, interbedded with minor volcanoclastic sediments (Davies and Jaques, 1984; Pieters, 1978; Worthing and Crawford, 1996; Smith, 2013). Basalts show a geochemical signature intermediate between E-MORB and N-MORB and were interpreted as back-arc basin-derived (Worthing and Crawford 1996; Smith, 2013; Österle et al., 2020). An age of the protolith has not been established.

A partly-metamorphosed body of continent-derived clastic rocks with minor metavolcanics is underthrusted below the Emo Metamorphics (Pieters, 1978; Worthing and Crawford, 1996). This unit, the Kagi Metamorphics, contains garnet-greenschist rock, which grade southwards to unmetamorphosed clastic sedimentary rock (Pieters, 1978; Johnson, 1979; Worthing and Crawford, 1996). The age of the protolith ranges from Middle Cretaceous to Early Eocene based on rare occurrences of planktonic foraminifera (Johnson, 1979; Worthing and Crawford, 1996; Davies, 2012).

The continent-derived Kagi Metamorphics are underlain by another unit of oceanic crustal rocks, known as the Milne Terrain, consisting of gabbro, dolerite, and basalt, with N-MORB to E-MORB geochemistry without a trace of arc or supra-subduction zone signature (Davies and Smith, 1971; Wai et al., 1994; Smith, 2013; Österle et al., 2020). Farther east, the Emo and Kagi metamorphics pinch out and the Milne Terrain is in direct structural contact with the Papuan Ultramafic Belt (Smith, 2013). Detrital zircons from

metasediments intercalated with metabasalts yielded maximum depositional ages of ~ 103 and ~ 72 Ma for two different samples (Österle et al., 2020). These basalts are intruded by low-grade tholeiitic *meta*-grabbroic and tonalitic rocks that yielded zircon U-Pb ages between 67.1 ± 2.5 and 53.6 ± 1.2 Ma (Österle et al., 2020). In addition, K-Ar hornblende ages of 56.3 ± 0.5 and 55.7 ± 1.5 Ma were obtained from gabbroic rocks (Rogerson and Hilyard, 1990). The fault separating the Milne Terrain from the Kagi Metamorphics is covered by an Upper Miocene (~5.7 Ma) basalt flow (Davies and Smith, 1971; Pain, 1983), providing a minimum age for emplacement of the continent-derived series over the ocean-derived series.

The southernmost, and structurally lowest, tectonic unit of the Papuan Peninsula is the Aure-Moresby fold-and-thrust belt. The Aure-Moresby fold-and-thrust belt and associated foreland basin formed since the late Miocene (Ott and Mann, 2015). Here, the orogen of the Papuan Peninsula is thrust over thinned continental crust of the Papuan and Eastern plateaus (Ott and Mann, 2015). The Papuan and Eastern Plateaus comprise pre-Mesozoic basement that was separated from Australia during opening of the Coral Sea Basin (Gaina et al., 1998). The thinned continental crust of these plateaus is covered with Upper Cretaceous to Paleocene *syn*-rift clastics, Paleocene to Oligocene post-rift deep water carbonates and Oligocene to recent pelagic sediments (Rogerson and Hilyard, 1990; Ott and Mann, 2015).

3.4.5. Louisiade Archipelago and Louisiade Ophiolite

The elevated ridge of the Papuan Peninsula (Pocklington Rise) continues to the east, mostly submerged with small islands known as the Louisiade Archipelago, with a southward convex shape (Fig. 4). The Pocklington Rise forms the southern margin of the Woodlark Basin and is in the east overthrust by the Solomon Islands at the San Cristobal Trench. Metamorphosed mafic volcanics and associated intrusives are exposed on the Deboyne Islands (Davies and Smith, 1971), and a mélange of ultramafic rocks is thrusted towards the SW over a metasedimentary schist unit (Webb et al., 2014). The majority of the Louisiade Archipelago comprises metasediments and intruding metagabbros, both of which underwent prehnite-pumpellyte to greenschist facies metamorphism (Webb et al., 2014). Based on detrital zircon U-Pb ages, it was inferred that the protoliths of the metasedimentary rocks are volcaniclastics derived from a Cretaceous silicic Large Igneous Province of the eastern Australian margin (Zirakparvar et al., 2013). This led to the interpretation that the metasediments of the Louisiade Archipelago represent a rifted fragment of the Australian passive margin that became separated from Australia during opening of the Coral Sea (Webb et al., 2014).

To the east of the Louisiade Archipelago, the Louisiade Ophiolite was recently identified based on dredging of the northern Louisiade Plateau (Figs. 4 and 7). This returned serpentinized peridotites, basalt breccia, and lavas, together with sedimentary rocks, and geochemical data suggest it is a supra-subduction zone ophiolite (McCarthy et al., 2022). Based on a seismic reflection transect, the ophiolite was interpreted as obducted towards the south onto the Louisiade Plateau, analogous to the Papuan Ultramafic Belt (Davies and Jaques, 1982; McCarthy et al., 2022).

3.4.6. Woodlark microplate

The Woodlark Basin is bounded by the Pocklington Rise in the south and by the Woodlark Rise in the north and contains the N-S spreading ridge that separates the Woodlark Microplate from Australia. The oldest unit exposed on Muyua/Woodlark Island, on the Woodlark Rise, comprises metamorphosed sandstones and chert beds, including turbidite and shallow marine shelf deposits of unknown age, in the southeast sometimes intercalated with basalt (Lindley, 2021). Based on the age of the unconformably overlying Upper Oligocene to Middle Miocene platform carbonates, the age of the oldest unit is inferred to be Paleocene to Eocene (Joseph and Finlayson, 1991; Lindley, 2021). Middle Miocene (14–12 Ma) volcanism is not straightforwardly linked to subduction, and may be extension-related (Lindley, 2021). This episode of post-middle Miocene extension may be related to the early opening of the Woodlark Basin.

The Woodlark Ridge produced ocean floor with magnetic anomalies initially interpreted as dating back C2A (3.5 Ma; Weissel et al., 1982). Taylor et al. (1999) subsequently identified additional anomalies back to C3A (6.2 Ma) in the southeast of the basin. Reconstructed spreading rates of the Woodlark plate decrease westward and define an Australia-Woodlark Plate Euler pole on the eastern Papuan Peninsula. To the west of this pole, the Woodlark-Australia plate boundary is likely formed by the Owen Stanley Fault Zone that ends in a triple junction with the New Britain Trench and the Ramu-Markham Fault Zone. The New Britain Trench connects to the San Cristobal Trench, which consumes the Woodlark Ridge (Fig. 4).

Towards the west, the amount of extension in the Woodlark Basin decreases and just east of the Woodlark-Australia Euler pole, on the D'Entrecasteaux Islands, the extension did not lead to oceanic spreading, but to extension of the orogen and exhumation of previously buried orogenic units. The D'Entrecasteaux Islands expose one of the youngest metamorphic core complexes and the youngest exhumed ultrahigh-pressure rock on Earth, which were at a depth of>90 km at about 8 Ma based on U-Pb zircon dating from eclogites and host gneisses, and garnet Lu-Hf ages on coesite eclogite (Baldwin et al., 1993, 2004, 2008; Monteleone et al., 2007; Zirakparvar et al., 2011). The metamorphic core complexes, exposing mafic eclogites, are separated from non-metamorphosed mafic and ultramafic rocks by Pliocene ductile shear zones and brittle fault zones (Davies and Warren, 1988; Baldwin et al., 1993; Hill, 1994). Final exhumation of the rocks to the surface occurred since the Plio-Pleistocene and extension is still active (Baldwin et al., 1993, 2004; Hill and Baldwin, 1993).

Metamorphic grade decreases southeastwards. On Misima Island, to the southeast of the D'Entrecasteaux Islands, upper amphibolite-facies felsic to mafic gneisses are juxtaposed against greenschist-facies schist and unmetamorphosed sediments along a low angle normal fault (Zirakparvar et al., 2013). The Louisiade Archipelago exposes prehnite-pumpellyte to greenschist facies metasediments and metagabbros (Webb et al., 2014). Conversely, $^{40}Ar/^{39}Ar$ cooling ages become younger westwards, which is thought to be related to the westward propagation of the Woodlark Rift (Baldwin et al., 2008). Based on Nd and Hf isotopic, U-Pb zircon geochronologic, and trace element data, Zirakparvar et al. (2013) inferred that the (U)HP basement gneisses of the D'Entrecasteaux Island were derived from the Cretaceous Large Igneous Province of eastern Australia, akin to the *meta*-sediments exposed in the Louisiade Archipelago. This connection between these islands with the Australian continent led to a tectonic model in which the metamorphosed rocks exposed on the D'Entrecasteaux Islands are derived from the thinned Australian continental margin that was subducted northwards, below the Papuan Ophiolite, and subsequently exhumed from below the ophiolite during extension in the Woodlark Rift (e.g., Baldwin et al., 2008). A 68.0 ± 3.6 Ma Lu-Hf age was obtained from a garnet porphyroblast within a Pleistocene amphibolite facies shear zone, which was interpreted to record subduction of stretched Australian continental rocks (Zirakparvar et al., 2011). A similar age of 66.4 ± 1.5 Ma was obtained using U-Pb zircon dating of a diabase sample obtained from a drill site on the Moresby Seamount (Monteleone et al., 2001), which is interpreted to have formed part of the upper plate during northwards subduction (Monteleone et al., 2001; Zirakparvar et al., 2013).

To the north of the D'Entrecasteaux Islands is the Trobriand Scarp that forms a marked northward deepening of bathymetry towards the Solomon Sea basin (Fig. 4). Marine magnetic anomalies were first identified in the Solomon Sea basin by Joshima et al. (1986). These authors developed different models that could fit the anomaly pattern, and then preferred a model in which the anomalies formed during chrons C12 to C9 (33–28 Ma), younging southwards. To explain the absence of a conjugate set of anomalies to the south (the ophiolites of the Papuan Peninsula and d'Entrecasteaux Islands are considerably older (~59 Ma; Davies and Smith, 1971; Walker and McDougall, 1982; Rogerson and Hilyard, 1990), they proposed that the Trobriand Scarp may have been a subduction zone that consumed the southern conjugate lithosphere. However, there is no clear fault or trench along the Trobriand Scarp, nor evidence for an accretionary prism. Later, Gaina and Müller (2007) reinterpreted the marine magnetic anomalies as chrons C19-C15 (41–35 Ma), younging northward. This would require that the northern conjugate lithosphere has subducted northward along the still-active San Cristobal and New Britain trenches. Extrapolating the spreading rates reconstructed from the Solomon Sea floor back in time could well explain the ages of the ophiolites on the Papuan Peninsula if these are part of the same oceanic lithosphere. Hence, in this scenario there is no need to invoke that subduction occurred along the Trobriand Scarp. Instead, this scarp likely represents the northern margin of the continental lithosphere of the Papuan and Eastern plateaus below the obducted Papuan ophiolites.

3.4.7. North and South Bismarck plates; New Britain; New Ireland

The Melanesian Borderlands occupy the zone of microplates that intervene the Australian and Pacific plates. This region includes the Bismarck Sea, the islands of Manus, New Britain, New Ireland, the Solomon Islands and Vanuatu (Fig. 4).

The Bismarck Sea hosts the Manus spreading ridge that is estimated to have started around 3.5 Ma based on the identification of active spreading and marine magnetic anomalies back to C2A (3 Ma; Taylor, 1979). This spreading ridge links up towards the west with the Bewani-Torricelli-Yapen-Sorong fault system. The opening of this basin thus constrains the amount of left-lateral strike-slip on these faults, which is within the range of the estimated 300–370 km based on lithological constraints (Dow and Sukamto, 1984; Webb et al., 2019.

New Britain is part of the South Bismarck Plate and is likely contiguous with the Adelbert and Finisterre ranges of the eastern Coastal Ranges of central New Guinea (e.g., Abott, 1995). On the North Bismarck Plate are the islands of Manus and New Ireland together with some smaller islands (Fig. 4). Prior to the late Neogene extension in the Manus Basin, all these islands were part of the same plate and the islands of the Bismarck plates have a similar tectono-sedimentary architecture. The oldest formations of these islands comprise Upper Eocene pillow basalts, andesite lavas, andesitic breccia and volcaniclastics interbedded with coralline and tuffaceous limestone (Francis, 1988; Lindley, 1988, 2006; Stewart and Sandy, 1988; Davies, 2005) that overlie an unknown, but presumably oceanic crust. The age of these formations is based on paleontological evidence and radiometric ages, including 49.0 ± 5.0 and 45.8 ± 5.0 K-Ar ages from Manus Island (Francis, 1988), and a 37.4 ± 1.7 K-Ar age from a dike intruding the oldest volcanics on New Ireland (Stewart and Sandy, 1988). On all three islands, these oldest volcanic units are overlain by Oligocene to middle Miocene volcaniclastics and limestone and intruded by upper Oligocene to lowermost Miocene arc plutons (Francis, 1988; Lindley, 1988; Stewart and Sandy, 1988; Davies, 2005; Lindley, 2006). Subsequently, extensive platform carbonates were deposited during a lull in magmatism from the middle to late Miocene (Francis, 1988; Lindley, 1988; Stewart and Sandy, 1988). Regional-scale volcanism became active again in the early Pliocene (Francis, 1988; Lindley, 1988; Stewart and Sandy, 1988). Recent volcanism on New Britain and on islands to the north of the main island, as well as the West Bismarck arc, is suggested to be related to subduction at the New Britain Trench (e.g. Weissel et al., 1982; Woodhead et al., 2010; Baldwin et al., 2012; Holm et al., 2016), while the extensional opening of the Manus Basin may be responsible for recent volcanism on the islands northeast of New Ireland (Lindley, 2016).

3.4.8. Solomon Islands

The modern North Bismarck Plate continues eastward towards the island of Bougainville (politically part of Papua New Guinea) and the Solomon Islands (Figs. 4 and 7). The Solomon Islands are in an upper plate position relative to the San Cristobal Trench that consumes the Woodlark microplate, and Australian Plate basins and ridges, such as the Santa Cruz Basin, along the southwestern margin of the archipelago. The northern boundary of the Solomon Islands is the North Solomon Trench which forms the continuation of the Manus and Kilinailai trenches (Tregoning et al., 1998). Oceanic crust of the Ontong Java Plateau on the Pacific Plate is being subducted below the Solomon Islands along this trench, although relative convergent motion is slow (~14–23 mm/yr; Tregoning et al., 1998; Phinney et al., 2004; Taira et al., 2004).

The Solomon Islands expose two basement terranes and two generations of arc volcanism. The uppermost basement terrane is an ophiolite, exposed on the islands of Choiseul, southern Santa Isabel, Guadalcanal, and Makira (Fig. 7). It comprises peridotites, some gabbro and dolerite, and abundant pillow lavas that are in places intercalated with cherts and pelagic limestones (Coulson and Vedder, 1986; Ridgway and Coulson, 1987; Berly, 2005; Tejada et al., 1996; Petterson et al., 1999, 2009). $^{40}Ar/^{39}Ar$ dating of basalt samples from Santa Isabel yielded five ages between 60.9 ± 1.2 Ma and 64.0 ± 1.1 Ma, as well as two ages of ~ 46.5 Ma (Tejada et al., 1996). A 46.5 ± 1.2 Ma zircon U-Pb age was obtained from a gabbro sample from Choiseul Island (Battan et al., 2022). The basalts display a wide range in geochemical signatures, but are generally MORB-like, with some lavas having characteristics of back-arc basin basalts (Tejada et al., 1996; Berly, 2005) A supra-subduction zone affinity was found in gabbros and peridotites on San Jorge and Santa Isabel islands (Berly, 2005; Berly et al., 2006).

The ultramafic section of the ophiolite overthrusts to the northeast a unit of volcanic rocks and schists with a metamorphic grade up to amphibolite facies, exposed on Choiseul and Santa Isabel (Ridgway and Coulson, 1987; Berly, 2005). This unit may represent the metamorphic sole of the ophiolite that formed during subduction initiation. Radiometric ages that constrain the metamorphism are sparse, but K-Ar ages of ~ 36.5 Ma and 44.7 ± 2.1 Ma of tremolite-actinolite-amphibolite from Nggela Island were obtained by Neef and McDougall (1976), and Richards et al. (1966) presented K-Ar ages between 32.4 ± 6.8 Ma and 51.5 ± 6.8 Ma, with a mean of 44 ± 18 Ma of amphibolite and schists from Choiseul. On Santa Isabel are also some blueschist occurrences reported, although with unknown age (Ota and Kaneko, 2010).

Exposed on the islands of Santa Isabel, Malaita, and Maramasike, to the northeast of the ophiolite, and structurally underlying the metamorphic rocks, is an OPS sequence comprising mainly of tholeiitic pillow and flow basalts and some minor gabbro, overlain by Cretaceous-Pliocene pelagic cherts and limestones (Petterson et al., 1999). $^{40}Ar/^{39}Ar$ ages of 120.8 ± 2.4 and 121.8 ± 2.9 were obtained from basalts exposed on Malaita, and ages of 122.9 ± 1.5 and between 90 and 95 Ma were obtained from basalts on Santa Isabel (Tejada et al., 1996). These ages are very similar to the 120.6 ± 0.9 Ma and 88–93 Ma $^{40}Ar/^{39}Ar$ ages obtained from drill holes on the Ontong Java Plateau (Tejada et al., 1996;

Mahoney et al., 1993). Based on these corresponding ages and identical isotopic ratios and geochemistry (transitional between tholeiitic N-MORB and E-MORB) of the Ontong Java Plateau (e.g., Kroenke et al., 1986; Mahoney et al., 1993; Tejada et al., 1996, 2002; Petterson et al., 1997; Phinney et al., 1999) this sequence is interpreted as accreted Ontong Java Plateau lavas (Petterson et al., 1999; Phinney et al., 2004). A 44.2 ± 0.2 Ma $^{40}Ar/^{39}Ar$ age obtained from basalts on Malaita was interpreted lavas that erupted onto the Ontong Java Plateau when it passed over the Samoan hotspot (Tejada et al., 1996). These accreted sequences are unconformably overlain by Upper Pliocene-Pleistocene clastic sedimentary formations (Petterson et al., 1997; Cowley et al., 2004), and accretion of Ontong Java Plateau rocks to the Solomon Islands thus occurred since c. 4 Ma (e.g., Mann and Taira, 2004; Phinney et al., 2004).

Overlying and intruding the Solomon ophiolite are arc complexes that formed during two periods separated by a lull. The older episode of arc volcanism occurred in the Oligocene-Early Miocene, the younger, currently active, episode started in the latest Miocene (Kroenke et al., 1986; Petterson et al., 1999). Tapster et al. (2014) reported 23.3–25.7 Ma U-Pb zircon ages from tonalite and diorites, in correspondence with the 24.4 ± 0.3 K-Ar age of a tonalite (Chivas and McDougall, 1978), both from Guadalcanal. The tonalite and dorite samples of Tapster et al. (2014) also include zircon xenocryst samples with c. 39–33 Ma and 71–63 Ma U-Pb ages, which may be recycled zircons from earlier arc volcanism or from the ophiolite. The oldest volcaniclastics in the Solomon Islands are of Late Oligocene age (Cowley et al., 2004). The oldest radiometric age reported for the younger volcanic arc sequence is a 6.4 ± 1.9 K-Ar age from Guadalcanal (Petterson et al., 1999).

3.4.9. Vanuatu; Vitiaz Trench; North Fiji Basin

Towards the east, the WNW-ESE trending San Cristobal trench changes its orientation and connects with the NNW-SSE trending New Hebrides trench. The Vanuatu archipelago to the east of this trench forms an active intra-oceanic arc above the NE-dipping New Hebrides subduction zone (Fig. 4). The active arc overlies an older arc basement, of which the oldest dated rocks returned 39 ± 5 and 36.7 ± 1 K-Ar ages of hornblende andesite (Taylor et al., 1985), a 35.4 ± 3.8 $^{40}Ar/^{39}Ar$ age of basaltic andesite and a 32.4 ± 0.57 U-Pb zircon age of dolerite (Buys et al., 2014). These ages are similar to the oldest zircon U-Pb ages reported from Fiji (38.6 ± 0.5 Ma; Rickard and Williams, 2013), which formed part of the same arc before opening of the North Fiji Basin since c. 10 Ma (Yan and Kroenke, 1993; Malahoff et al., 1994; Van de Lagemaat et al., 2018a). In addition to these late Eocene ages, several late Oligocene and early Miocene ages have been reported from the western belt of Vanuatu (e.g. Mitchell and Warden, 1971; Crawford et al., 2003; Buys et al., 2014), whereas magmatism in Fiji was most prominent between c. 15 and 5 Ma (Cluzel and Meffre, 2019). Furthermore, a dismembered ophiolite suite is exposed on Pentecost Island in eastern Vanuatu, which comprises peridotites and gabbros with lenses of amphibolites and green schist in serpentinites (Mitchell and Warden, 1971; Parrot and Dugas, 1980). An $^{40}Ar/^{39}Ar$ age of 44.9 ± 3.0 was obtained from a dolerite dyke within the ophiolite, while an amphibolitic mylonite and a metadolerite of greenschist facies, yielded $^{40}Ar/^{39}Ar$ ages of 33.4 ± 0.8 and 35.5 ± 0.6, respectively (Crawford et al., 2003).

The North Solomon Trench connects to the east with the Vitiaz Trench Lineament (Fairbridge and Stewart, 1960) that currently forms a transform plate boundary between Cretaceous crust of the Pacific Plate and Neogene crust of the North Fiji Basin (e.g., Pelletier and Auzende, 1996; Gill et al., 2022). Not much is known about this feature but it is generally thought that it formed originally as a subduction zone, where the Pacific Plate was being subducted (south)westwards since the Eocene, until a polarity switch in the Miocene that was likely associated with the arrival of the Ontong-Java Plateau in the trench (Brocher, 1985; Pelletier and Auzende, 1996; Crawford et al., 2003).

3.4.10. New Caledonia; Northland Ophiolite

Finally, the obduction front of ophiolites that is traced from the Papuan Peninsula to the Louisiade Ophiolites continues from the D'Entrecasteaux Ridge to the south, over New Caledonia towards the North Island of New Zealand (Fig. 4). The architecture and evolution of this belt was extensively described in Van de Lagemaat et al. (2018a), which we here summarize and update with recently published results. The New Caledonia Ophiolite (Figure S2), also referred to as the Peridotite Nappe, is interpreted to have formed in a supra-subduction zone setting (e.g., Maurizot et al., 2020b). The age of formation of the ophiolite's crust is not well constrained, as existing K-Ar ages are considered unreliable (Maurizot et a., 2020b). The age of the metamorphic sole is c. 56 Ma, based on $^{40}Ar/^{39}Ar$ hornblende and U-Pb zircon dating of amphibolites (Cluzel et al., 2012b). Timing of emplacement of the ophiolite is bracketed by 34 Ma age of the youngest sediments that are thrusted below the ophiolite (Cluzel et al., 2001), and the c. 27 Ma age of post-obduction plutons that intrude into the Peridotite Nappe (Paquette and Cluzel, 2007; Sevin et al., 2020). Based on geophysical modelling from seismic and gravity data, the Peridotite Nappe may be contiguous with the oceanic lithosphere that underlies the North Loyalty Basin to the north of the main island of New Caledonia (Collot et al., 1987; Patriat et al., 2018).

The ophiolite is the highest structural unit that is exposed in New Caledonia. Below the metamorphic sole of the ophiolite occur several units that were incorporated in the NE-dipping New Caledonia subduction complex (Maurizot et al., 2020b). The uppermost section comprises oceanic crust as well as a passive margin succession (Poya Terrane), which formed part of the South Loyalty Basin, the conceptual oceanic basin that was subducted at the New Caledonia subduction zone. Based on macro-fossils and detrital zircon provenance, the South Loyalty Basin likely opened in the Late Cretaceous (Campanian) - Paleocene, based on geochemistry as a back-arc basin (Cluzel et al., 2018). Structurally below the Poya Terrane is the Montagnes Blanches Nappe, which was derived from the sedimentary cover of passive margin of the Norfolk Ridge (Maurizot et al., 2020a, b) that forms the eastern margin of the extended continent Zealandia, the easternmost continental crust of the Australian Plate (Mortimer et al., 2017). A belt of HP-LT metamorphic rocks (eclogites and blueschists) of oceanic and continental passive margin origin is exposed in the northeast of the main island of New Caledonia (Maurizot et al., 2020b), which returned Lu/Hf ages of 38.4–36.5 Ma (Taetz et al., 2021), showing that subduction continued at least until the latest Eocene. Syntectonic trench-fill sediments were deposited during the Eocene, and unconformably overly a Cretaceous and older accretionary prism and overlying forearc basin, related to subduction below the entire East Gondwana margin (Maurizot, 2011; Maurizot and Cluzel, 2014).

The obduction front is inferred to continue submarine along the eastern margin of the Norfolk Ridge and western margin of the Three Kings Ridge to the southernmost exposures: the Northland Ophiolite in northernmost North Island, New Zealand (Figure S2). This ophiolite formed in a supra-subduction zone setting (Whattam et al., 2004, 2005) and its oceanic crust is thought to be of Paleocene age, based on radiolarians in limestones that are intercalated with pillow basalts (Hollis and Hanson, 1991). The ophiolite also returned Oligocene ages: between 25.1 ± 1.2 and 26.1 ± 1.0 based on $^{40}Ar/^{39}Ar$ dating of tholeiitic basalts and 31.6 ± 0.2 Ma 28.3 ± 0.2 based on U/Pb zircon dating of a gabbro and a plagiogranite (Whattam et al., 2005, 2006). The age of emplacement is constrained by the youngest upper Oligocene sediments

that are part of the ophiolite and the lower Miocene age of the oldest sediments sealing the basal thrust (Ballance and Spörli, 1979).

The New Caledonia and Northland ophiolites thrusted (south) westward over accretionary complexes that formed during long-lived, Mesozoic subduction below the East Gondwana margin (Mortimer, 2004; Mortimer et al., 2014b; Maurizot et al., 2020a, b). Westward Mesozoic subduction below the East Gondwana margin ended between 90 and 85 Ma at the New Caledonia margin and possibly ~ 79 Ma along New Zealand (Van de Lagemaat et al., 2023a).

4. Paleomagnetic data

We initially made the reconstruction based on marine geophysical and structural geological constraints without paleomagnetic data as input, after which we tested our reconstruction against paleomagnetic data. Where necessary, we then iterated the reconstruction within the previous constraints (see Van Hinsbergen et al. (2020a) for details on the approach).

There is only a limited amount of paleomagnetic data available in the Junction Region, and most of it was collected from the Philippine Sea Plate. We used the paleomagnetic data compilation of the Philippine Sea Plate of Van de Lagemaat et al. (2023b). In addition, paleomagnetic data relevant for the reconstruction are available from the Baliojong accreted OPS units of Sabah, North Borneo (Van de Lagemaat et al., 2023c) from accreted rocks of the Southern Palawan/Calatuigas Ophiolite (Almasco et al., 2000), and from the Eocene volcanic rocks of the Solomon Islands (Musgrave, 1990). (Supplementary Table S1).

As explained in Van de Lagemaat et al. (2023b), paleomagnetic data from the Junction Region either come from strongly deformed and uplifted plate margins, or from drill cores, and the declinations of those data that inform vertical axis rotations display strong regional differences owing to local deformation, or drill core rotation. We therefore only test our reconstruction against paleolatitude data computed from inclinations. In addition, we tested our reconstruction against paleolatitudes obtained from igneous data only, as the number of samples collected at sedimentary localities is insufficient to correct for inclination shallowing, which makes testing our reconstruction against sedimentary data problematic.

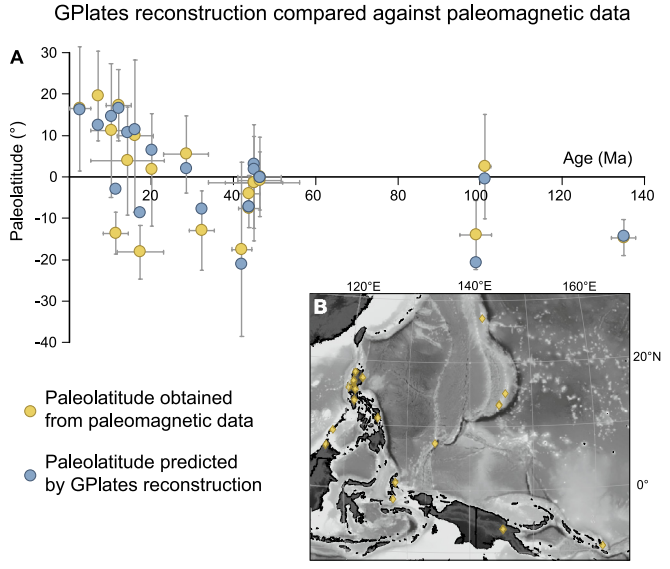

Fig. 8. A) Graph that compares the paleolatitudes of paleomagnetic sampling locations predicted in our GPlates reconstruction against paleomagnetically obtained paleolatitudes. B) Paleomagnetic sampling locations. The paleomagnetic compilation is provided in the Supporting Information as Table S1.

We use the global apparent polar wander path of Vaes et al. (2023) for the major plates surrounding the Junction Region (Eurasia, Australia, Pacific). For times prior to the 85 Ma connection of the Pacific Plate to Antarctica, we follow Boschman et al. (2019) in estimating the relative rotations of the Pacific Plate to South Africa using two mantle reference frames (Torsvik et al., 2019 for the Pacific, Van der Meer et al., 2010 for the Indo-Atlantic), and used this connection to predict the position of the Pacific and surrounding plates (e.g., Izanagi) in the paleomagnetic reference frame. The predicted paleolatitudes of the reconstruction that is described in section 5 compared to the paleomagnetic data in our compilation is given in Fig. 8.

5. Reconstruction

This section presents our reconstruction, which in principle straightforwardly follows from the reconstruction protocol explained in section 2, and the kinematic and geological constraints reviewed in section 3 and summarized in Table 1 and Fig. 9. GPlates reconstruction files are available in the Supporting Information. Here, we provide a description of the reconstruction (see Figs. 10 - 33) from the present back to the past, i.e., in order of increasing levels of interpretation. Each section describes a period back to a moment where we made a key choice or interpretation.

Our approach to the reconstruction of the Cenozoic Philippine Sea Plate differs fundamentally from previous reconstructions (Hall, 2002; Gaina and Müller, 2007; Seton and Müller, 2008; Zahirovic et al., 2014; Wu et al., 2016; Liu et al., 2023). The most important difference with most previous renditions is that we do not use paleomagnetic data as basis to infer vertical axis rotations of the Philippine Sea Plate. This is based on a critical re-appraisal of paleomagnetic data from the Philippine Sea Plate, which showed that the available datasets are small and do not unequivocally demonstrate whole-plate rotation, but may instead reflect regional deformation-associated rotations (Van de Lagemaat et al., 2023b).

Previous plate reconstructions that focus on the Junction Region generally only go back to the early Eocene (Hall, 2002; Gaina and Müller, 2007; Wu et al., 2016; Liu et al., 2023), as this is the classically inferred age of subduction initiation at the Izu-Bonin-Mariana trench (Stern and Bloomer, 1992; Reagan et al., 2010). Of the regional reconstructions, only those of Seton and Müller (2008) and Zahirovic et al. (2014) extend back to the Early Cretaceous. Global plate and paleogeographic reconstructions (e.g., Seton et al., 2012; Müller et al., 2019; Scotese, 2021) do go back to the early Mesozoic, but these do not describe the data or rationale behind their reconstruction of the Junction Region. Hence, our reconstruction is the first to consider the entire western Pacific/Panthalassa Plate system, starting from modern geological architecture and developing the reconstruction back in time using systematic plate boundary continuation, assuming the simplest plate tectonic scenario that satisfies geological observations.

At the end of each reconstruction section, we compare our reconstruction with the reconstructions of Hall (2002), Gaina and Müller (2007), Zahirovic et al. (2014), model 1 of Wu et al. (2016), and Liu et al. (2023) back to the Early Cretaceous. We do not compare our reconstruction to global plate reconstructions or the reconstruction of Seton and Müller (2008), as these lack detail in the description of the Junction Region, and the global plate reconstructions generally incorporate one of the regional reconstructions.

Table 1
Summary of kinematic data and predicted relative motions in our reconstruction.

Location	Interpretation	Type of data used	Anomalies	Timeframe (Ma)	Reference
Philippine Sea Plate					
Mariana trough	Back-arc extension	Marine magnetic anomalies	3n.3 - 0	4.8 - 0	Yamazaki et al. (2003)
Mariana trough	Start of extension	Magnetic vector analysis, DSDP Leg 60		6 - 4.8	Hussong and Uyeda (1982); Iwamoto et al. (2002); Yamazaki and Stern (1997)
Ogasawara trough	Back-arc extension	Stratigraphy		55 - 53	Ishizuka et al. (2006)
Shikoku Basin	Back-arc extension	Marine magnetic anomalies	C7.2n y - 5Dn y	24.47 - 17.24	Sdrolias et al. (2004b); Seton et al. (2014)
Parece Vela Basin	Back-arc extension	Marine magnetic anomalies	C9n - C5Dn	27.44 - 17.24	Sdrolias et al. (2004b); Seton et al. (2014)
Parece Vela & Shikoku basins	Beginning of extension	Age of arc magmatism along Kyushu - Palau ridge		30	Ishizuka et al. (2011b)
Parece Vela & Shikoku basins	End of extension	15.6 ± 0.1 Ma basalt from extinct spreading ridge		15	Ishizuka et al. (2010)
Guam and Northern Mariana Islands	Back-arc extension	Geometry (line up with Palau Ridge)		28 - 20	This study
West Philippine Basin	Oceanic spreading	Marine magnetic anomalies	C22n.2n y - C14n y	53.20 - 35.29	Hilde and Lee (1984); Deschamps and Lallemand (2002)
Okinawa Trough	Back-arc extension	Crustal structures (refraction data)		10 - 6 and 2 - 0	Sibuet et al. (1995); Miki (1995); Arai et al. (2017)
Kita Daito Basin	Back-arc extension	Crustal structures (refraction data)		46 - 41	Ishizuka et al. (2022)
Minami Daito Basin	Back-arc extension	51.3 - 42.8 Ma dredged basalts		52 - 48	Hickey-Vargas (1998); Ishizuka et al. (2013)
Amami Sankaku Basin	Back-arc extension	49.3 - 46.8 Ma drilled basalts		50 - 46	Ishizuka et al. (2018)
Palau Basin	Back-arc extension	Marine magnetic anomalies + Mindanao Fracture zone	C18n y - C16n.1n y	38.4 - 35.58	Sasaki et al. (2014); This study
Palau Basin	Back-arc extension	Geometry (Line up with Philippine Mobile Belt)		55 - 45	This study
Ayu Trough	Ultra slow spreading	Crustal structures (sedimentation rate) + reconstruction		15 - 0	Weissel and Anderson (1978); Fujiwara et al. (1995)
Ayu Trough	Subduction	Dredged arc lavas		> 15	Kumagai et al. (1996); This study
Huatung Basin	Back-arc extension	Marine magnetic anomalies + dredged samples		130 - 119	Deschamps et al. (2000)
Philippines					
Philippine fault zones	50–150 km left-lateral strike slip	Keep relative motion in north minimal, some subduction in the south		4 - 0	Aurelio et al. (1991); This study
Philippine Mobile Belt	Forearc spreading	Supra-subduction zone ophiolites		110 - 85	Dimalanta et al. (2020); This study. See main text for additional references
Proto-SE Bohol Trench	Subduction	Cebu arc lavas		130 - 110	This study. See main text for additional references
Lagonoy subduction zone	Subduction	Philippine ophiolites		156 - 85	Advokaat and Van Hinsbergen (2023); This study. See main text for additional references
Lagonoy subduction zone	Subduction initiation	Lagonoy ophiolite		156	Geary et al. (1988); This study
Tipuma-Jimi Basin	Back-arc extension	Philippine ophiolites and reconstruction of Argoland		156 - 110	Advokaat and Van Hinsbergen (2023); This study
Telkhinia subduction zone	Subduction	Paleomagnetic data		> 160 - 30 (?)	Van de Lagemaat et al. (2023c)
Philippine Mobile Belt	Clockwise rotation	Double relay ramp		62 - 45	This study.
Caroline Plate					
West Caroline Basin	Oceanic spreading	Marine magnetic anomalies	C16n.1n y - C11n.2n o	35.58 - 28.0	Gaina and Muller (2007)
East Caroline Basin	Oceanic spreading	Marine magnetic anomalies	C16n.1n y - C8n.2n o	35.58 - 25.0	Gaina and Muller (2007)
Caroline Plate	Caroline Plate fixed to Pacific	Overlapping Caroline Ridges		> 15	Wu et al. (2016); This study
Sorol Trough	250 km subduction	To avoid shortening at the New Guinea and Manus trenches; Paleomagnetic data		15 - 7	This study
Molucca Sea					
Molucca Sea	Back-arc extension	Eocene ophiolites in Philippine and Talaud, contiguous with Solomon Sea		45 - 30	This study

Table 1 (*continued*)

Location	Interpretation	Type of data used	Anomalies	Timeframe (Ma)	Reference
New Guinea					
Sorong-Yapen-Bewani Torricelli Fault	300 km left-lateral strike slip	Opening of Manus Basin		3.5 - 0	Taylor (1979); Webb et al. (2019); This study
New Guinea and Manus trenches	1200 km left-lateral strike slip	Avoid overlap with SE Asian Tethysides		15 - 3.5	This study
Central New Guinea	210 km shortening related to ophiolite emplacement	Balanced cross-sections		35 - 21	Martin et al. (2023)
Central New Guinea	190 km shortening of the Australian margin underneath the ophiolite	Balanced cross-sections		21 - 9	Martin et al. (2023)
Central New Guinea	100 km shortening in the Papuan & Irian Jaya Fold-and-thrust belt	Balanced cross-sections		9 - 0	Hobson (1986); Hill (1991); Martin et al. (2023)
Central New Guinea	Counterclockwise rotation New Guinea obduction front	Avoid overlap with SE Asian Tethysides		30 - 15	This study
New Guinea ophiolites	Northward subduction initiation	Metamorphic sole age of the Papuan Ultra Mafic Belt and global plate circuit		62	Lus et al. (2004); This study
Melanesian Borderlands					
Bismarck Sea	Back-arc extension	Marine magnetic anomalies	C2A - present-day	3.5 - 0	Taylor (1979)
Solomon Sea	Back-arc extension	Marine magnetic anomalies	C19n o - C16n.1n y	41.18 - 35.58	Gaina and Müller (2007)
Solomon Sea	End of spreading	New Guinea ophiolite obduction		30	This study
Woodlark Basin	Subducting plate spreading	Marine magnetic anomalies	C3A - present-day	6.3 - 0	Weissel et al. (1982); Taylor et al. (1990)
Santa Cruz Basin/South Rennell Trough	Subducting plate spreading	Marine magnetic anomalies	C19n o - C13n o	40.07 - 30	Seton et al. (2016)
Coral Sea Basin	Marginal basin formation	Marine magnetic anomalies	C27n o - C24n o	63 - 52	Gaina et al. (1999)
Louisiade Trough	Marginal basin formation	Marine magnetic anomalies		63 - 52	Gaina et al. (1999); Seton et al. (2016)
Solomon - Vitiaz - Tonga arc	Southward subduction initiation	Ages of Solomon and Pentecost Islands ophiolites		45	Neef and McDougall (1976); Crawford et al. (2003)
Townsville Basin	Marginal basin formation	Stratigraphy		156 - 110	Falvey and Taylor (1974); Struckmeyer and Symonds (1997); This study
SW Pacific					
Lau Basin	Back-arc extension	Marine magnetic anomalies	C3A - present-day	7 - 0	Yan and Kroenke (1993)
Havre Trough	Back-arc extension	In tandem with Lau Basin		7 - 0	Yan and Kroenke (1993); Van de Lagemaat et al. (2018a)
North Fiji Basin	Back-arc extension	Marine magnetic anomalies	C4 - present-day	10 - 0	Yan and Kroenke (1993)
South Fiji Basin	Back-arc extension	Marine magnetic anomalies	C9n o - C6n o	27.44 - 15	Herzer et al. (2009, 2011); Sdrolias et al. (2003); Van de Lagemaat et al. (2018a)
Norfolk Basin	Back-arc extension	In tandem with South Fiji Basin		30 - 15	Herzer et al. (2009, 2011); Sdrolias et al. (2003); Van de Lagemaat et al. (2018a)
North Loyalty Basin	Back-arc extension	Marine magnetic anomalies	C20n o - C16n o	43.45 - 35	Sdrolias et al. (2003)
South Loyalty Basin	Marginal basin formation	Misfit North and South Zealandia		79 - 62	Van de Lagemaat et al. (2023a)
Fairway-Aotea and New Caledonia basins	Marginal basin formation	Crustal thickness estimates		92 - 84	Grobys et al. (2008); Van de Lagemaat et al. (2023a)
Tasman Sea	Marginal basin formation	Marine magnetic anomalies	C33n o - C24n o	95 - 52	Gaina et al. (1998); Grobys et al. (2008); Van de Lagemaat et al. (2023a)
New Caledonia	Subduction initiation	Metamorphic sole age of the Peridotite Nappe and global plate circuit			Cluzel et al. (2012b); This study

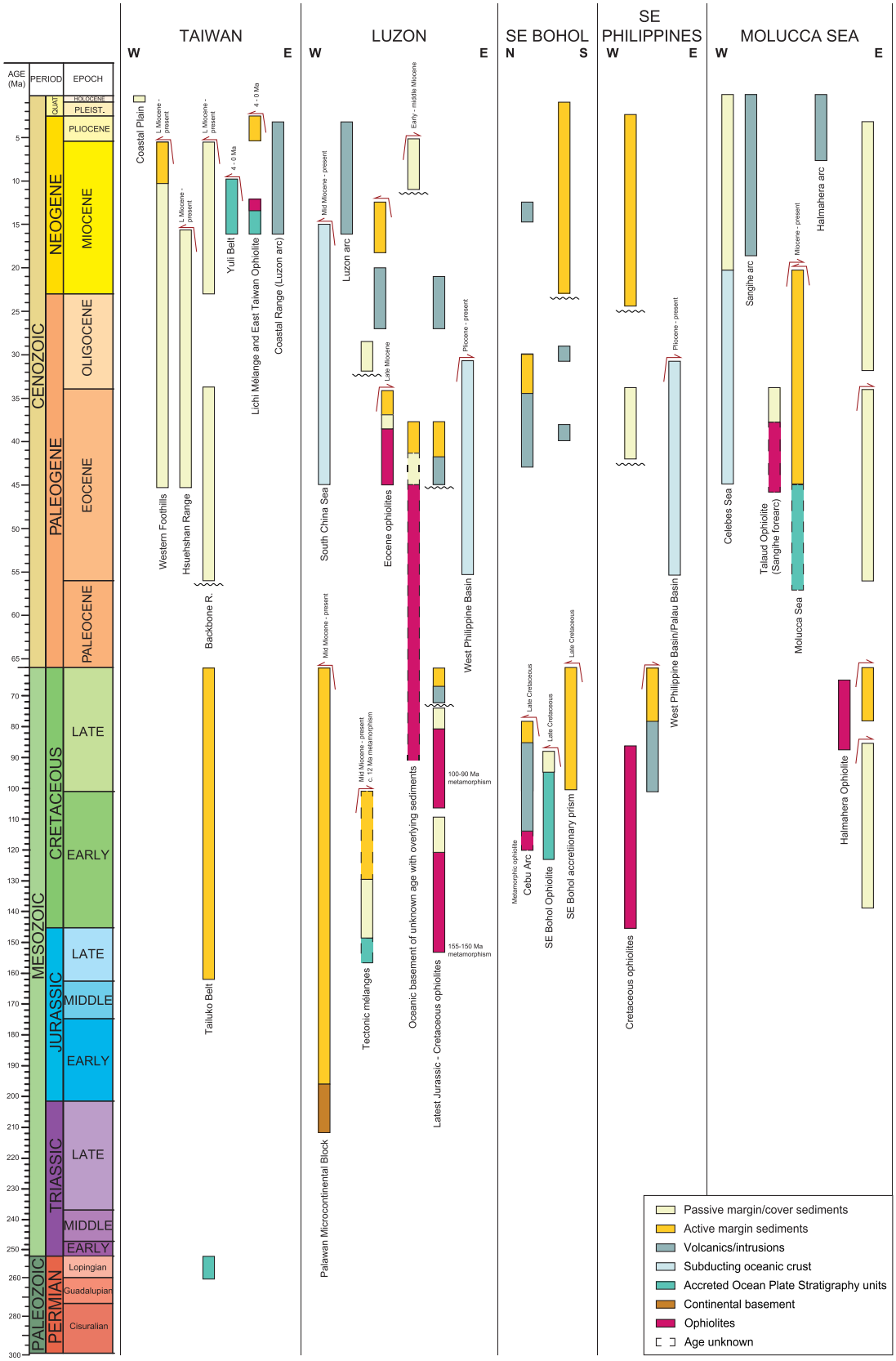

Fig. 9. Tectonostratigraphic diagrams of orogens in the Junction Region.

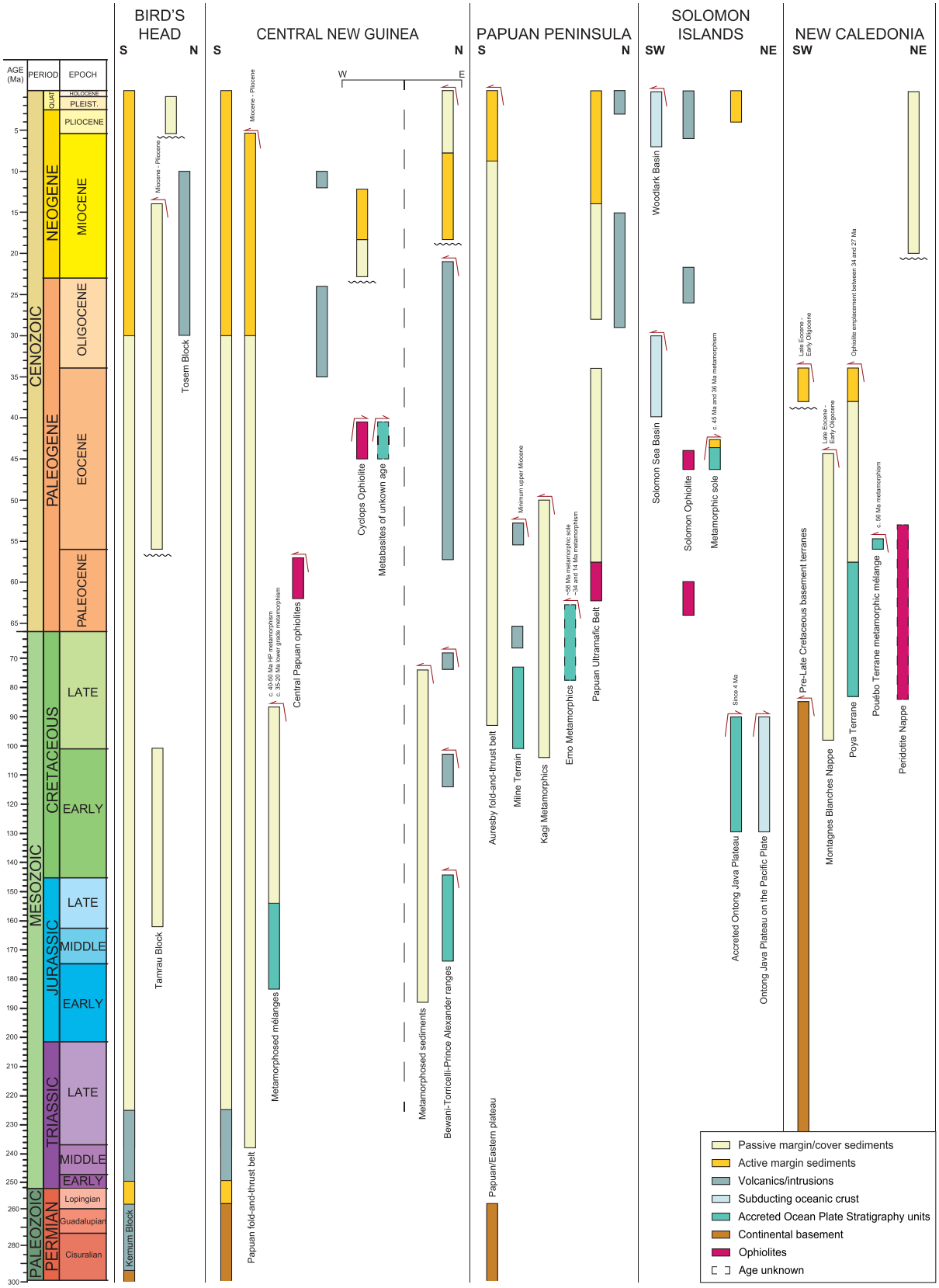

Fig. 9 (*continued*)

Fig. 10. Tectonic map at 0 Ma. The colors mark the plate tectonic affinity of lithosphere. The shaded areas behind the colors are continental crust or thickened oceanic crust, i.e., island arcs and oceanic plateaus. Present-day coastlines are shown throughout the reconstruction (Figs. 10 - 33) for reference. Reconstruction is shown in the paleomagnetic reference frame of Vaes et al. (2023).

5.1. 0 – 15 Ma

The first key interpretation step in our reconstruction coincides with the onset of opening of the Ayu Trough, estimated to have started sometime between 25 and 15 Ma (Weissel and Anderson, 1978; Fujiwara et al., 1995). Since that opening, the Philippine Sea Plate was connected to the Caroline Plate. Before that time, arc rocks dredged from the margins of the Ayu Trough suggest that it was a subduction zone (Kumagai et al., 1996). The youngest of these (c. 20 Ma) shows that subduction must have continued to at least 20 Ma, and our reconstruction assumed that the Ayu Trough's opening started on the young end of the estimated range, around 15 Ma (Figs. 10 – 12). This age corresponds to the oldest ages of arc magmatism of the Luzon arc that are related to westward subduction at the Manila Trench (c. 14 Ma; Maleterre et al., 1988; Defant et al., 1990). We initially assumed that the Sorol Trough and Mussau Trench/Lyra Trough that bound the Caroline Plate from the Pacific Plate did not accommodate motion in the last 15 Ma and use the resulting reconstruction to re-evaluate that assumption below.

Fig. 11. Snapshot of the kinematic reconstruction at 5 Ma.

The reconstruction of the Ayu Trough restores a ~ 25° clockwise rotation of the Palau Basin (the southernmost basin of the Philippine Sea Plate) relative to the Caroline Plate (Figs. 10 – 12). Just north of the Ayu Trough Euler pole, this rotation reconstructs sufficient convergence at the Yap trench to restore an amount of lithosphere that is large enough to contain the eastern conjugate lithosphere that formed during formation of the Parece Vela Basin, of which only the western part remains west of Yap Island (Figs. 10 - 12). Our reconstruction thus infers that the onset of extensional opening of the Ayu Trough, in combination with oblique opening of the Parece Vela basin after c. 20 Ma, initiated subduction at the Yap trench at the southernmost end of the Parece Vela ridge, locally consuming the forearc lithosphere.

In the northwest, subduction of the Philippine Sea Plate oceanic basins is restored at the Nankai and Ryukyu trenches and the extensional opening in the Mariana Trough, active in the last 6 Ma (Yamazaki et al., 2003), as well as subduction of the West Philippine Basin below the Philippine Mobile Belt, since 4 Ma (Figs. 10 and 11). The amount of convergence accommodated by this subduction zone decreases both northwards and southwards, as subduction did not occur to the north of Luzon or to the east of Halmahera. Reconstructing this lateral gradient in convergence led us to reconstruct a small (~3°) clockwise rotation of eastern Mindanao and the Palau Basin relative to the West Philippine Basin, accommodated along the Philippine Fault and Mindanao Fracture Zone. Within the Philippines, we restore left-lateral strike

Fig. 12. Snapshot of the kinematic reconstruction at 10 Ma.

slip faulting of 100–200 km since 4 Ma along the Philippine Fault, East Luzon Transform Fault, and Sibuyan Sea Fault in line with geological estimates (Aurelio et al. 1991; Barrier et al., 1991; Mitchell et al., 1986; Cole et al., 1989). The reconstructed strike-slip faulting ensures that subduction at the Philippine Trench decreased both north and southward.

In the south, the restoration of the Ayu Trough combined with the assumption that the Caroline Plate was rigidly connected to the Pacific Plate leads to eastward restoration of the west Philippine plate boundary, reconstructing the now-subducted Molucca Sea Plate between the Sangihe and Halmahera trenches. This eastward restoration of the Philippine Sea Plate is accommodated along the Sorong-Yapen-Bewani Torricelli fault system back to 3.5, and along the New Guinea and Manus trenches north of New Guinea before 3.5 Ma. At 6 Ma, the Halmahera trench lines up with the western boundary of the obduction front of the Papuan ophiolites, interpreted as a transform fault. To test whether the west Philippine/Halmahera trenches continued into New Guinea before 6 Ma, we initially connected the Philippine Sea Plate to the Papuan ophiolites at this time and restored the New Guinea obduction since ~ 30 Ma according to kinematic constraints provided by Martin et al. (2023). However, this leads to large overlap between the western Philippine Sea Plate domain and the SE Asian Tethysides before 6 Ma, which is clearly inconsistent with the geological record. This overlap is avoided when the Philippine Sea Plate and the western trenches are reconstructed with the westward moving

Fig. 13. Snapshot of the kinematic reconstruction at 15 Ma.

Pacific Plate, generating 1200 km of left-lateral transform motion along the northern margin of New Guinea, presently occupied by the New Guinea and Manus trenches, between 6 and 15 Ma. This transform motion reconstructs a 1900 km wide Molucca Sea basin at 15 Ma, which reconstructs as a triangular basin between the southward obducting Papuan ophiolites and the westward moving southern Philippines/Halmahera ophiolites (Fig. 12).

Within New Guinea, we reconstruct 100 km of shortening in the New Guinea fold-and-thrust belt since 9 Ma following the balanced cross-sections of Hill (1991) and Hobson (1986). The Sorong-Fault-Bewani-Torricelli fault zone is reconstructed as part of the North Bismarck Microplate and the relative motion at the transform fault system thus follows from the marine magnetic anomaly constraints in the Manus Basin (Figs. 10 and 11). This leads to c. 300 km of left-lateral transform motion within northern New Guinea since 3.5 Ma, in line with geological data (Dow and Sukamto, 1984; Webb et al., 2019). The Woodlark Basin opening since 6.5 Ma is reconstructed, which is balanced by resurfacing the northern conjugate oceanic lithosphere of the Solomon Sea that was consumed by subduction at the San Cristobal Trench. Restoring the western propagation of the Woodlark Basin buries the upper Neogene core complexes of the D'Entrecasteaux Islands back to their UHP conditions as part of the down-going Australian lithosphere below the obducting Papuan Ultramafic Belt. In addition,

Fig. 14. Snapshot of the kinematic reconstruction at 20 Ma.

we restore southeastward roll-back of the New Britain trench, which infers ~ 225 km of right-lateral strike-slip faulting at the Ramu-Markham fault zone (Figs. 10 and 11). The amount of roll-back follows from the constraint that motion of the North Bismarck Plate relative to the Papuan ophiolites is pure strike-slip.

Whereas restoring the westward motion of the Philippine Sea Plate in the last 15 Ma together with the Pacific Plate avoids overlaps between the western Philippine Sea Plate and the SE Asian Tethysides, assuming that there was no relative motion between the Pacific and Caroline Plates back to 15 Ma introduces two other kinematic problems. Firstly, an underlap (gap) of about 350 km forms between the Caroline Plate and the New Guinea and Manus trenches along northern New Guinea. This requires that a south-dipping slab should be present below the northern New Guinea margin, and while this boundary is accommodating some thrusting alongside dominantly transform motion, there is no evidence for a tomographically resolvable slab. Secondly, this scenario predicts paleolatitudes for the Philippine Sea Plate that systematically offset to the north compared to paleolatitude data obtained from igneous rocks of the Philippine Sea Plate. This problem may be overcome by restoring the Philippine Sea Plate ~ 3-4° southwards at 15 Ma relative to the Pacific Plate, which is permitted by, and actually improves, the paleomagnetically predicted paleolatitudes for the Philippine Sea Plate. Candidate structures to accommodate this motion are the margin between the Philippine Sea Plate and the Caroline Plate east of the Ayu Trough, and the Izu-Bonin-Marianas trenches farther to the north, or the Sorol Trough-Lyra Trough boundaries between the Caroline Plate and the Pacific

Fig. 15. Snapshot of the kinematic reconstruction at 25 Ma.

Plate. The first option would require N-S extension between the Pacific Plate and the Philippine Sea Plate on the E-W trending segments of the Philippine Sea Plate-Pacific plate boundary, e.g., connecting the Mariana Trough and the Yap Trench, that should be still present today, whereas it is not. In addition, while this scenario does resolve the underlap at the New Guinea trench, the gap north of the Manus Trench remains and this scenario leads to overlap between the Philippine Sea Plate and SE Asian Tethysides after 15 Ma. Hence, we favor the second option, which infers a short-lived south-dipping subduction zone at the Sorol Trough, since 15 Ma, with the Lyra Trough acting as a transform plate boundary between the Caroline and Pacific plates during this time (Figs. 12 and 13). The asymmetric, southward deepening Sorol Trough was previously interpreted as a rift (Weissel and Anderson, 1978; Altis, 1999), even though its morphology is highly asymmetric and normal faults are only found on the southern part of the rift (Weissel and Anderson, 1978; Dong et al., 2018). We tentatively infer that these normal faults may instead result from plate bending. There is currently no subducting slab connected to the Pacific Plate at the Sorol Trough, but a subducted slab has long been interpreted from tomography below the Caroline Plate (the Caroline Slab; Hall and Spakman, 2002; Van der Meer et al. 2018), which may represent (part of) this subducted lithosphere. If subduction occurred, it must thus have ceased sufficiently long ago for the slab

Fig. 16. Snapshot of the kinematic reconstruction at 30 Ma.

to sink to the mantle transition zone, and we model the cessation of subduction at 7 Ma, although this could be a few million years earlier or later.

The largest difference between our reconstructions and previous ones in this time interval is that we reconstruct subduction at the Sorol Trough to avoid major convergence along the northern margin of New Guinea. Gaina and Müller (2007), Zahirovic et al. (2014), and Wu et al. (2016) reconstruct up to c. 1000 km of convergence within New Guinea between the ophiolites and arcs, since 15 Ma. Hall (2002) accommodates the convergence between the southern margin of the Caroline Plate and the New Guinea arcs (without drawing a subduction zone plate boundary), while Liu et al. (2023) divide the convergence between a subduction zone in between the ophiolites and the arc and between the arc and the southern margin of the Caroline Plate. In addition, Hall (2002) reconstructs major strike slip motion within New Guinea.

5.2. 15 – 30 Ma

From 15 Ma back in time, we reconstructed the (northern) Caroline Plate as part of the Pacific Plate. The Philippine Sea plate motion chain (i.e., the collection of the Philippine Sea microplates that are reconstructed relative to each other with preserved magnetic anomalies) is prior to 15 Ma disconnected from the Caroline (Pacific) Plate, accommodated by subduction below the eastern margin of the Ayu Trough (Figs. 13 – 16), where arc rocks of early Miocene have been dredged (Kumagai et al., 1996). Instead, we reconstructed the Philippine Sea Plate as connected to the

Fig. 17. Snapshot of the kinematic reconstruction at 35 Ma.

ophiolites that were overthrusting the northern Australian margin of New Guinea since 30 Ma (Martin et al., 2023) and evaluated whether that assumption led to configurations and plate motions elsewhere that conflict with data. With this logic, the relative motion between the Philippine Sea Plate and the surrounding major plates is constrained back to the start of ophiolite obduction on New Guinea, which is estimated to have occurred around 30 Ma based on metamorphic ages of continent-derived rocks (Martin et al., 2023; Weiland, 1999).

The reconstruction at 30 Ma displays westward subduction of the Caroline/Pacific plates along a subduction system that spans from the Izu-Bonin-Mariana trench and its triple junction with the Japan and Nankai Trenches, via the Ayu Trench, to the North Solomon and Vitiaz Trenches, and from there to the Tonga-Kermadec-Hikurangi subduction zone (Fig. 16). At 30 Ma, the south Caroline Plate is a separate plate that is spreading relative to the Pacific Plate in the north (Gaina and Müller, 2007), bounded by the Lyra Trough in the east, the North Solomon Trench in the south, and the Ayu Trench in the west (Fig. 16). Geological data from New Zealand's North Island show that the Hikurangi subduction zone initiated around 30 Ma, or shortly thereafter (Van de Lagemaat et al., 2022), and from that moment onwards, the west Pacific plate boundary transitioned through the Alpine Fault transform to the Puysegur plate boundary (Kamp, 1986; Lebrun et al., 2000) that ends in a triple junction in the Southern Ocean (Figs. 10 - 16).

At 30 Ma, the c. 400 km of shortening related to ophiolite obduction onto the Australian continental margin of northern New Guinea (Martin et al., 2023) is fully restored (Fig. 16). The exact shortening direction of the New Guinea obduction is not well constrained. We initially assumed N-S, margin-perpendicular

Fig. 18. Snapshot of the kinematic reconstruction at 40 Ma.

shortening, and kept Halmahera, connected to the Philippine Sea Plate, fixed relative to the Papuan ophiolites. This led to overlap of the Philippines with the SE Asian Tethysides, showing that the Philippines must have undergone a westward motion component between 15 and 30 Ma. We therefore reconstructed the ophiolite obduction with a NNE-SSW shortening direction, and restored westward-increasing shortening, leading to a small counterclockwise rotation relative to Australia of the Papua ophiolites and the Philippine Sea Plate between 30 and 21 Ma (Figs. 14 – 16). This satisfies all available structural evidence, avoids overlaps, and predicts mostly transform motion and some minor extension along the western margin of Luzon, which accommodates relative motion between the Philippine Mobile Belt and the SE Asian Tethysides.

The limited convergence between the Philippine Sea Plate and the Australian Plate, which was restricted to the shortening documented on New Guinea, is in line with the paleolatitudes predicted from paleomagnetic data of the Philippine Sea Plate (Fig. 8; Van de Lagemaat et al., 2023b). The bulk oceanic crust consumed by post-30 Ma subduction is thus restored to the north of the Philippine Sea Plate, where it was subducted at the Nankai and Ryukyu trenches. Within the Philippine Sea Plate, opening of the Shikoku and Parece Vela Basins is restored (Sdrolias et al., 2004b), which results in a much smaller Philippine Sea Plate mosaic by 30 Ma (Fig. 16).

A key difference between our reconstruction and others in the 15–30 Ma interval is that we treat the Philippine Mobile belt as a rigid terrane, while other reconstructions incorporate relative

Fig. 19. Snapshot of the kinematic reconstruction at 45 Ma.

motions between different parts of the Philippines, except for Zahirovic et al. (2014). Wu et al. (2016) and Liu et al. (2023) reconstruct relative convergence between the east and west Philippines, accommodated at the location of the present-day Philippine Fault. Hall (2002) and Gaina and Müller (2007), on the other hand, reconstruct relative convergence between the north and south Philippines already before c. 10 Ma, accommodated to the south of Luzon.

Further differences between the existing reconstructions in the 15–30 Ma interval are the configuration and polarity of subduction zone plate boundaries in the New Guinea-Melanesian region. Hall (2002) and Gaina and Müller (2007) reconstruct a similar northward-dipping subduction zone below the Papuan ophiolites, but in their models, the Australian margin enters the trench around 25 Ma, and no convergence is reconstructed in the 15–25 Ma interval. Moreover, in their models, this subduction zone does not connect with the New Caledonia subduction zone, as this trench does not exist, or only until 45 Ma. In the model of Zahirovic et al. (2014), the New Caledonia trench does exist, but is connected to the New Guinea trench through extensional plate boundaries. In contrast to the other reconstructions, including ours, the reconstructions of Wu et al. (2016) and Liu et al. (2023) include southward subduction. Liu et al. (2023) incorporate southward subduction of oceanic crust below the entire northern margin of New Guinea, while Wu et al. (2016) reconstruct southward intra-oceanic subduction between New Guinea and the Philippine Sea Plate as well as southward subduction to the east of New Guinea, at the Trobriand Trough and farther to the east. While the

Fig. 20. Snapshot of the kinematic reconstruction at 50 Ma.

Trobriand Trough has been interpreted as the site of southward subduction by others (Joshima et al., 1986), we interpreted the bathymetric depression as a scarp that represents the northern margin of underthrusted continental lithosphere below the Papuan ophiolites.

5.3. 30 – 45 Ma

There is in the circum-Junction Region that we reviewed no evidence for continental underthrusting below oceanic or continental lithosphere before 30 Ma. Instead, all accretionary orogenic records reveal oceanic subduction. In addition to subduction below Japan, these restore to two main subduction systems: northward subduction of Australian Plate oceanic lithosphere, and westward subduction of the Pacific Plate, which both occurred contemporaneously below a plate system that includes the precursors of the Philippine Sea Plate, the Papuan ophiolites and Molucca Sea basin, and the Melanesian arcs and marginal basins (including the Solomon Sea basin). This pre-30 Ma plate configuration formed around 45 Ma, which marks the time that westward subduction of the Pacific Plate started at the North Solomon and Vitiaz trenches as inferred from metamorphic sole age estimates on the Solomon and Vanuatu ophiolites (Neef and McDougall, 1976, Richards et al., 1966; Crawford et al., 2003).

Despite the lack of kinematic data that demonstrate relative plate motion amount and direction at the Junction Region trenches

Fig. 21. Snapshot of the kinematic reconstruction at 55 Ma.

in the 30–45 Ma interval, there is enough geological data for a well-constrained reconstruction (Figs. 16 – 19). At first, we assumed a simplest-case scenario in which a single plate intervened the Pacific and Australian plate in the Junction Region, bounded on either side by trenches. This plate includes the Philippine Sea Plate, the Papuan ophiolites and the Molucca Sea lithosphere that was reconstructed between the Papuan ophiolites and the southern Philippines and Halmahera at 15 Ma, the eastern continuations of the Papuan ophiolites in the form of the Louisiade and New Caledonia ophiolites, and the eastern Philippine Sea Plate arcs (Izu-Bonin-Mariana) and Melanesian arcs (Solomon, Vitiaz/New Hebrides, Tonga), as well as intervening oceanic basins (Solomon Sea and North Loyalty Basin) (Fig. 13). We restored the available marine magnetic anomaly evidence for opening of oceanic basins, but there is no direct field evidence for a plate boundary that cut through this composite series of arcs and basins during this time interval.

First, we reconstructed where the system of two opposing subduction zones must have terminated. There is positive evidence for subduction below the Solomon Sea ophiolites since 45 Ma (Neef and McDougall, 1976, Richards et al., 1966) and the oldest dated arc rocks on Fiji are 39 Ma (Rickard and Williams, 2013), showing that the Pacific trench must have continued beyond Fiji southwards, to the Tonga Trench. However, farther south, subduction at the Hikurangi trench did not start before c. 28–30 Ma (Van de Lagemaat et al., 2022), and also at the Alpine Fault there is no evi-

Fig. 22. Snapshot of the kinematic reconstruction at 60 Ma.

dence for significant pre-30 Ma dextral motion (Furlong and Kamp, 2013; Kamp, 1986). Instead, at the longitude of the Hikurangi trench, relative plate motion between the Australian and Pacific plates was only accommodated through eastward subduction of the Australian Plate before c. 30 Ma, at the subduction zone below the New Caledonia-Northland ophiolites (Van de Lagemaat et al., 2018a). We thus infer that the Solomon-Fiji-Tonga trench ended against a transform fault to the south of the North Loyalty Basin, which we tentatively connect to the Cook transform fault that bounded the Norfolk Basin during its opening (Figs. 17 - 19; Sdrolias et al., 2004a; Van de Lagemaat et al., 2018a), which is still present in the Tasman Sea, to the north of New Zealand (Fig. 4).

Our reconstruction thus infers that to the south of the Cook Fault, there was only one subduction zone (the Three Kings Ridge trench segment of the New Caledonia subduction zone) before 30 Ma, and that the oceanic lithosphere that obducted onto Zealandia, including the Northland Ophiolite, moved as part of the Pacific Plate. The position of this plate boundary therefore follows directly from Pacific-Australia motion before the moment of obduction (which we model at 30 Ma following Van de Lagemaat et al., 2018a). We reconstruct the Solomon-Vitiaz arc at 45 Ma to a position that lines up the Papuan Peninsula-Louisiade trench with the New Caledonia trench (Fig. 19). This position of the Melanesian arc requires that we restore some clockwise rotation of the Tonga trench segment to avoid overlap with the New Caledonia trench at 45 Ma.

In the northwest of the Junction Region, our reconstruction ensures that there is convergence and thus subduction of both

Fig. 23. Snapshot of the kinematic reconstruction at 65 Ma.

the Pacific and Australian plates with the Philippine Sea Plate and Melanesian arcs. The reconstruction positions the entire Philippine-Melanesian plate system from the Tonga-New Caledonia region in the southeast to the northwest Philippines in the northwest such that there is no major convergence between the Philippine Sea Plate and the SE Asian Tethysides after ~ 40 Ma because there is little geological evidence for significant subduction on the northern Philippines after this time in this region. This reconstruction is in correspondence with paleomagnetic data from the Philippine Sea Plate (Fig. 8), and allows for the opening of the Solomon Sea basin, as dictated by the preserved magnetic anomalies (Gaina and Müller, 2007) between the two major bounding subduction zones (Figs. 16 - 19).

Within the above-described tectonic framework, we reconstructed the Molucca Sea as a back-arc basin behind the Papuan ophiolites and arcs between 45 and 30 Ma (Figs. 16 - 19). As the Molucca Sea has been completely consumed after 15 Ma, there are no preserved marine magnetic anomalies that corroborate this reconstruction, but a 45–30 Ma age of formation is in line with Eocene radiolarian chert that is preserved in the tectonic mélange of Talaud Island (Moore et al., 1981) and the Talaud Ophiolite which was interpreted to have a back-arc basin geochemical signature (Evans et al., 1983). The Eocene oceanic crust of the Zambales, Angat, and Antique ophiolites in Luzon and possibly the Polanco ophiolite on Mindanao (Fig. 5; Encarnación et al., 1993; Yumul et al., 2000a; Marcelles et al., 2018) reconstructs as part of this

Fig. 24. Snapshot of the kinematic reconstruction at 70 Ma.

same back-arc basin. Molucca Sea back-arc basin is reconstructed as a larger, westward equivalent of the Solomon Sea basin (Figs. 16 - 19).

In our reconstruction, the closure of the Molucca Sea reconstructs the Papuan ophiolites and the arc rocks of northern New Guinea adjacent to the Cretaceous crust and arc remnants of the southern Philippine Mobile Belt (Fig. 19). The reconstruction of the Molucca Sea in this way solves and explains several issues: First, it reconstructs sufficient oceanic crust north of the Australian continental margin for a subduction zone to have existed from 45 to 30 Ma. Second, this scenario explains why there are no late Eocene arc volcanics preserved in the southern Philippines, while they are present in the north: this southern continuation of the arc rifted off during opening of the Molucca Sea and remained active but is now found on New Guinea. Third, the reconstruction of the Molucca Sea in this way provides an explanation for the origin of the Cyclops Ophiolite of New Guinea, from which ages between 43 and 30 Ma were obtained (Monnier et al., 1999). The reconstruction also explains the abrupt termination of the Papuan ophiolites just east of the Bird's Head as a transform (STEP) fault (Figs. 16 - 19) and infers that Miocene subduction initiation of the Halmahera subduction zone occurred on the northeastern margin of the Molucca Sea back-arc basin (Fig. 13).

By 45 Ma, opening of the West Philippine Basin is largely restored (Hilde and Lee, 1984), which leads to a much smaller Philippine Sea Plate and the N-S length of the Kyushu-Palau ridge west of the Izu-Bonin Mariana-Palau subduction zone is also significantly reduced (Fig. 19). The extension of the Kyushu-Palau

Fig. 25. Snapshot of the kinematic reconstruction at 80 Ma.

intra-oceanic arc towards the north at 45 Ma is unknown, but we reconstruct a limited northwestward continuation of the Izu-Bonin Mariana-Palau trench. We infer that the Pacific Plate was subducting below Japan at the Nankai and Ryukyu trenches and that the Izu-Bonin Mariana trench ended in a triple junction with transform faults with perhaps minor convergent components between the Philippine Sea Plate and the SE Asian Tethysides to the south, and the Pacific Plate and the Proto-South China Sea embayment to the north.

At 45 Ma, the main difference between existing reconstructions is the amount of restored clockwise vertical-axis rotation of the Philippine Sea Plate. All reconstructions, including ours, restore a rotation of the Philippine Sea Plate at 45 Ma, but to a variable extent. Gaina and Müller (2007), Wu et al. (2016), and Liu et al. (2023) all restore c. 90° rotation, to the extent that spreading in the West Philippine Basin occurs in a NW-SE direction. In the reconstruction of Hall (2002) the amount of restored rotation at 45° is about 60°, but additional clockwise rotation is restored between 45 and 52 Ma, so that the total amount of restored vertical axis rotation is also around 90° at 52 Ma. In our reconstruction and that of Zahirovic et al. (2014), on the other hand, the amount of vertical axis rotation restored for most of the Philippine Sea Plate is only ~ 30°. Unlike us, Zahirovic et al. (2014) restored additional rotation of the Philippine Mobile Belt relative to the rest of the

Fig. 26. Snapshot of the kinematic reconstruction at 90 Ma.

Philippine Sea Plate, between 14 and 6 Ma, which results in the restoration of a total of 50° clockwise rotation of the Philippine Mobile Belt at 45 Ma, where it is 30° in our reconstruction.

Another key difference between our reconstruction and the others is the location of (south)westward subduction initiation at the Solomon-Vitiaz-Tonga trench. All previous models reconstruct this subduction zone close to the continental margin at subduction initiation, and subsequently reconstruct trench-roll back and the formation of a back-arc basin, i.e., the Solomon Sea. Our reconstruction is the only one that reconstructs this subduction zone to start intra-oceanic (Fig. 19) and model the opening of the Solomon Sea in between two opposing subduction zones. Wu et al. (2016), in addition to their subduction zone that forms along the New Guinea continental margin, also reconstruct a west-dipping intra-oceanic subduction zone, which is subsequently consumed when the subduction zone that hosts the Solomon Arc rolls back.

5.4. 45 – 62 Ma

The logical next step in our reconstruction would be 52 Ma, which corresponds to the age of the oldest supra-subduction oceanic lithosphere of the Izu-Bonin-Mariana forearc and is the widely inferred age for the onset of subduction at the Izu-Bonin Mariana trench (Ishizuka et al., 2011a; Stern et al., 2012; Reagan et al., 2013, 2019). However, as geological data from the Solomon Islands, Vanuatu, Fiji, and Tonga suggest that southwestward

Fig. 27. Snapshot of the kinematic reconstruction at 100 Ma. Note the more southerly projection compared to the previous figures.

subduction of the Pacific Plate beneath these arcs did not start before c. 45 Ma (Neef and McDougall, 1976; Richards et al., 1966; Bloomer et al., 1995; Crawford et al., 2003), it is not straightforward where the Izu-Bonin Mariana plate boundary continued, or where and why it would have ended. Therefore, we chose as next step in our reconstruction 62 Ma. North- and eastward subduction of the Australian Plate at the New Caledonia-New Guinea trench started around 60 Ma as revealed by metamorphic sole ages of the Papuan and New Caledonia ophiolites (Lus et al., 2004; Cluzel et al., 2012b). We incorporate a 62 Ma subduction initiation age at the southwestern Philippine Sea Plate/Melanesian (New Caledonia-New Guinea) subduction zone because at this time a small change in relative plate motion between the Pacific and Australian plates occurred that follows from the global plate circuit. We use the constraints from the Papuan and New Caledonia ophiolites to restore relative motions at the Izu-Bonin Mariana trench from this perspective (Figs. 19 – 23).

As (south)westward subduction of the Pacific Plate south of the Philippine Sea Plate (Halmahera) did not start before 45 Ma, we reconstruct the Solomon Islands, Vanuatu, and Tonga, as well as intra-oceanic highs and basins east of the Louisiade-New Caledonia trench, such as the Three Kings Ridge (Figs. 19 - 23), as part of the Pacific Plate. The New Guinea-New Caledonia subduction zone ended in a zone of diffuse and distributed deformation around

Fig. 28. Snapshot of the kinematic reconstruction at 110 Ma.

New Zealand, close to the Pacific-Australia Euler pole, and around 40 Ma connected with the Emerald Basin spreading center (Van de Lagemaat et al., 2018a),

To the north of the Solomon Islands, the Philippine Mobile Belt formed the overriding plate to the New Guinea-New Caledonia subduction, which was not part of the Pacific Plate before 45 Ma, as the Izu-Bonin Mariana subduction zone accommodated subduction of the Pacific Plate below the Philippine Sea Plate. There is no evidence for a discrete plate boundary between the Philippine Mobile Belt (south of Halmahera) and the Solomon arc that may have accommodated the inevitable relative motion between the two. We therefore reconstruct that between 62 and 45 Ma, the Philippines acted as a major relay ramp between two subduction systems that laterally decreased convergence in opposite direction. The Izu-Bonin Mariana subduction zone accommodated all Pacific-Australia convergence at the position of the northern Philippines. The amount of convergence accommodated by this subduction zone decreased southwards towards Halmahera, and to the southeast, all Australian-Pacific convergence was accommodated by the New Caledonia-New Guinea subduction zone. We accommodate this evolution by reconstructing a clockwise rotation of the Philippine Mobile Belt relative to the Solomon Islands between 62 and 52 Ma that avoids relative convergence between southern Halmahera and the Pacific Plate. Our restoration of clockwise rotation of the Philippines also ensures that the amount of convergence accommodated by the New Caledonia-New Guinea subduction

Fig. 29. Snapshot of the kinematic reconstruction at 120 Ma.

zone decreased northwards and transitioned into a transform fault with both the Australian Plate and farther north with the SE Asian Tethysides (Figs. 20 - 22). This explains the absence of evidence of subduction beyond the Papuan ophiolites. After 52 Ma, subduction of the Pacific Plate at the Izu-Bonin-Mariana subduction zone is sustained through opening of the West Philippine and Palau Basins (Hilde and Lee, 1984; Sasaki et al., 2014). Our reconstruction thus implies that the Izu-Bonin Mariana subduction zone was already forming by 62 Ma, at a time that the Philippine Sea Plate only consisted of Cretaceous and latest Jurassic oceanic crust and arc rocks of the small Huatung Basin (Deschamps et al., 2000) and the Philippine Mobile Belt (e.g., Geary et al., 1988; Suerte et al., 2005; Dimalanta et al., 2020). We will return to this element of our reconstruction in the discussion section.

Subduction of the Pacific-Izanagi Ridge below Japan is restored to have occurred at 50 Ma following e.g., Wu and Wu (2019), and at 62 Ma, the Izanagi Plate was subducting below the Eurasian continental margin of Japan (Figs. 20 and 23). We reconstruct the western termination of this subduction zone along the continental margin around the Kerama Gap in the central Ryukyu Islands, corresponding to the Qingdao line of Wu et al. (2022), to the west of which there is no evidence for post-85 Ma subduction or accretion (see also Van de Lagemaat et al., 2023c). Instead, the plate boundary continued southwards along the eastern margin of the Proto-South China Sea embayment (Figs. 20 - 23). Wu et al. (2022) postulated that the Qingdao Line may have been a transform fault, but relative plate motions that follow from the global plate circuit combined with the reconstructed orientation of the plate boundary

Fig. 30. Snapshot of the kinematic reconstruction at 130 Ma.

rather suggests that this plate boundary accommodated oblique subduction of the Izanagi and later Pacific plates below the Proto-South China Sea. This oblique trench ended in the triple junction with the northern extension of the Izu-Bonin Mariana subduction zone and the western Philippine transform-dominated plate boundary (Figs. 20 - 23).

5.5. 62 – 85 Ma

Whereas there are records of subduction that accommodated the convergence of the Pacific plate system and the Tethyan plate system after 62 Ma and before 85 Ma (e.g., East Gondwana subduction in New Zealand and New Caledonia (Van de Lagemaat et al., 2023a), and the arcs of the Philippines and the circum-Proto-South China Sea embayment (section 3; see also Van de Lagemaat et al., 2023c), evidence for subduction in the Junction Region in the intervening period is sparse. The next step in our reconstruction is therefore 85 Ma.

The global plate circuit straightforwardly explains the tectonic quiescence in the 62–85 Ma interval (Figs. 24 and 25). This time interval is bracketed between two major plate motion changes, around 85 Ma and ~ 50 Ma (as explained, the 62–50 Ma interval accommodated only minor convergence), and relative motions between the major plates were limited. Australia moved only ~ 600 km to the NE relative to Eurasia. Relative motion between the Pacific and Australian plates was slow, and divergent in the south, accommodated at the Tasman Ridge (Figs. 24 - 26). The northward decrease in extension at the Tasman Ridge indicates that the Euler Pole of Australia-Pacific motion was located around the northeast corner of the Australian continental margin,

Fig. 31. Snapshot of the kinematic reconstruction at 140 Ma.

around the Coral Sea. To the north, the Pacific Plate moved in the 85–62 Ma time interval some ~ 700 km to the northwest. Prior to the initiation of subduction of the Australian Plate below the Philippine Sea Plate at the New Caledonia-New Guinea trench at 62 Ma, we reconstruct the Philippine Mobile Belt as part of the Australian Plate (Figs. 24 – 26). Because this reconstruction predicts a NW-SE trend of the Philippine Mobile Belt at 62 Ma, the boundary between the Philippine Mobile Belt and the Pacific Plate in the 62–85 Ma interval was predominantly a transform fault with perhaps some obliquely subduction of the Pacific Plate below the Australian Plate. This oblique subduction may explain the sparse Campanian accretionary prism rocks identified on Halmahera (Hall et al., 1988) and the 77 Ma diorite intrusion into the Rapu-Rapu ophiolite in the Philippines (David et al., 1997).

With limited Australia-Eurasia motion, the transform-dominated plate boundary east of the Philippine Mobile Belt, which eventually develops into the Izu-Bonin Mariana trench, aligned with the Qingdao Line, where oblique subduction was accommodated. To the east, the Izanagi-Pacific ridge migrated towards the eastern Eurasian margin and formed a triple junction that moved along the east-Philippine Mobile Belt and Qingdao Line (Figs. 20 - 26).

The model of Zahirovic et al. (2014) is the only previous regional reconstruction that extends this far back in time. In our model, the Philippine Mobile Belt still acts as a rigid plate, now part of the Australian Plate, whereas the model of Zahirovic et al. (2014) connects the northernmost Cretaceous arc of the Philippine Sea Plate (the Amami Plateau) to the Pacific Plate at 65 Ma and reconstruct extension between the Cretaceous arcs between 65 and 85 Ma, which we restored during the Eocene based on the age constraints in the intervening basins (Hickey-Vargas, 1998; Ishizuka et al., 2013, 2018). The reconstruction of Zahirovic et al. (2014) suggests

Fig. 32. Snapshot of the kinematic reconstruction at 150 Ma.

that subduction of the Australian Plate below the Papuan ophiolites already started at 85 Ma, while the ophiolites of New Guinea and New Caledonia suggest a c. 60 Ma onset of subduction.

5.6. Before 85 Ma, back to the Permian

Prior to 85 Ma, the western Panthalassa Ocean was surrounded by subduction zones, from Antarctica to Japan (Figs. 26 – 33). Along the east Gondwana margins of New Zealand and New Caledonia, accretionary prisms formed during subduction of the Phoenix Plate and its daughter plates that broke up during emplacement of the Ontong-Java-Nui large igneous province (Van de Lagemaat et al., 2023a, and references therein). Some marginal basin development may have affected the New Zealand margin in the Triassic-Jurassic (Howell, 1980; Roser et al., 2002; Van de Lagemaat et al., 2018b), but this is not of consequence for the reconstruction of the Junction Region. For the Japan margin, major back-arc basin opening, and closure has recently been postulated for Jurassic and Cretaceous time based on combining marine magnetic anomaly reconstructions of the northwestern Pacific Plate with analyses of OPS sequences (Boschman et al., 2021a). However, subduction and arc magmatism along the eastern Eurasian margins of Indochina and South China west of the Qingdao Line was continuous from the Jurassic until ~ 85 Ma and upper plate deformation remained restricted to Basin & Range-style extension, and prior to that Andean-style orogenesis in the South China Block (Jahn et al., 1990; Lapierre et al., 1997; Li et al., 2012; Li et al., 2014b). Finally, to the west, the SE Asian Tethysides experienced a northward journey from the northwest Australian margin to the Indochina margin from middle Jurassic to ~ 85 Ma, accommodated by the closure

Fig. 33. Snapshot of the kinematic reconstruction at 160 Ma.

and opening of Neotethyan oceanic basins (Hall, 2012; Advokaat and Van Hinsbergen, 2023). The plate reconstruction of the Junction Region thus hinges on interpretations of the geology from the Philippines and New Guinea, and the remains of the Proto-South China Sea lithosphere.

5.6.1. Philippine Mobile Belt

The pre-85 Ma geological record of the Philippine Mobile Belt reveals supra-subduction zone oceanic lithosphere of Late Cretaceous age (~100–85 Ma) overlain by arc volcanic rocks of similar age (Dimalanta et al., 2020), and fragments of older oceanic lithosphere of Early Cretaceous (e.g., the Huatung Basin; Deschamps et al., 2000; Ghong et al., 2021) and Late Jurassic age (the Lagonoy and Tacloban ophiolites; Geary et al., 1988; Suerte et al., 2005; Dimalanta et al., 2020). Moreover, the Cebu arc and associated accretionary prims demonstrate that the northern and southern Philippine Mobile Belt were part of two separate plates that converged parallel to the trend of the Philippine Mobile Belt between ~ 135 and ~ 110 Ma, accommodated at the proto-SE Bohol Trench (Faustino et al., 2003; Deng et al., 2015, 2019; Gong et al., 2021). The accretionary prisms below the Papua ophiolites reveal that the ocean basin that separated the Philippine Mobile Belt from Australia contained Upper Jurassic oceanic crust (Permana, 1995; Weiland, 1999) that formed after extension affected the northern Australian margin of the Fry and Arafura plateaus (Home et al., 1990; Pigram and Symonds, 1991; Davies, 2012), during which time small microcontinental blocks may have locally separated from this margin (Davies, 2012). Prior to the Late Jurassic, the oceanic crust of the Philippine Mobile Belt did not exist yet, and a volcanic arc was located in Permian and Triassic

time on the northern Australian continental margin of south New Guinea (Amiruddin, 2009; Crowhurst et al., 2004: Webb and White, 2016; Jost et al., 2018). This Permian and Triassic arc magmatism is also known from the SW Borneo Block of the SE Asian Tethysides (Burton-Johnson et al., 2020; Wang et al., 2023) which was reconstructed to the west of New Guinea (Advokaat and Van Hinsbergen, 2023) and which we infer was the continuation of the pre-Jurassic north Gondwana arc. We used these constraints to propose the following reconstruction.

We consider the Philippine Mobile Belt as the arc and forearc crust that formed above a southwest-dipping subduction zone that consumed oceanic crust of the Panthalassa Ocean (Figs. 26 – 33). We refer to this 'proto-Izu-Bonin Mariana' subduction zone as the Lagonoy subduction zone, after the oldest ophiolite exposed in the Philippines. In Permian to Triassic time this subduction zone was located along the north Australian margin (Fig. 33), but in Late Jurassic time it started to roll back, opening a forearc basin that developed into a back-arc basin, with some trench-parallel convergence accommodated at the SE Bohol trench (Figs. 28 – 33). After 110 Ma, extension jumped back to the forearc. This may either have occurred because of trench-parallel extension above an oblique subduction zone, such as documented for the Andaman Sea (Curray, 2005) or the Jurassic Californian ophiolites (Arkula et al., 2023), or trench-normal, analogous to the ridge jump from the Parece Vela Basin to the Mariana Trough, or from the South Fiji Basin to the Lau Basin. The Upper Cretaceous crust of the eastern Philippine Mobile Belt formed shortly after the jump in extension and was subsequently overlain by arcs. Trench-parallel extension may have played a role at 135 Ma as suggested by the E-W trending magnetic anomalies of the Huatung Basin (Deschamps et al., 2000), although this basin may also have opened as a back-arc basin above the proto-SE Bohol Trench. In our reconstruction, we model a 'Mariana Trough style' ridge jump around 110 Ma, inferring trench-normal extension between 110 and 85 Ma for the Philippine Mobile Belt (Figs. 26 – 28), which may be tested in the future with paleomagnetic data from sheeted dyke sequences (see e.g., Maffione et al., 2017). This extension and roll-back ceased when the Pacific changed plate motion at 85 Ma, and the margin became transform dominated (Fig. 25).

In our reconstruction of 110 Ma, the opening of a Mariana-style forearc basin is reconstructed, and of the Philippine Mobile Belt and the Molucca Islands, only the pre-110 Ma crust is left. Before 110 Ma, the northward (or in reconstructed coordinates, northwestward) subduction at the proto-SE Bohol Trench is reconstructed by connecting the upper plate of the SE Bohol subduction zone, including the northern Philippine Mobile Belt, to the SW Borneo Block as reconstructed by Advokaat and Van Hinsbergen (2023). This connection infers that the Late Jurassic-Cretaceous Lagonoy subduction zone was continuous with the subduction zone of NW Borneo, which formed the Kuching Zone (Figs. 28 - 33). Restoring these in tandem reconstructs the northern Philippines adjacent to the Australian continental margin of west New Guinea and the Bird's Head at 156 Ma (Fig. 33), when the SW Borneo Block, as part of the greater Argoland microcontinental Archipelago, was separated from the NW Australian margin (Veevers et al., 1991; Hall, 2002; Advokaat and Van Hinsbergen, 2023). Reconstructing the Philippines as an oceanic part of the Argoland Plate thus straightforwardly explains the latest Jurassic ages of the Lagonoy and Tacloban ophiolites (Geary et al., 1988; Suerte et al., 2005) and the oceanic crustal remains below the Papuan ophiolites (Permana, 1995; Weiland, 1999). We reconstruct the southeastern, down-going plate of the SE Bohol subduction zone, including Mindanao and Halmahera, as an independent plate against the northeastern point of the Australian continental margin at 156 Ma. Applying a constant rotation rate whereby we keep the trench lined up with the northwestern continuation, a small change in plate motion of the SW Borneo Block in the reconstruction of Advokaat and Van Hinsbergen (2023) generates relative convergence across the SE Bohol Trench at 130 Ma, satisfying the geological constraints from the Cebu arc and accretionary prism.

5.6.2. Proto-South China Sea lithosphere

Prior to the arrest of subduction of Proto-South China Sea lithosphere around 85 Ma, convergence between the Panthalassic plates, and the Eurasian and the 'Tethyan' plates was at least in part accommodated by subduction at the trenches surrounding the later Proto-South China Sea, below Borneo, Indochina, and South China. Paleomagnetic data from 135 Ma old pillow lavas from OPS units of NW Borneo that accreted just prior to ~ 85 Ma subduction cessation (Van de Lagemaat et al., 2023c) show that this Proto-South China Sea lithosphere cannot have been part of the Izanagi Plate. Predicting the paleolatitude of the Proto-South China Sea lithosphere by reconstructing it as part of the Izanagi Plate before 85 Ma predicts paleolatitudes of ~ 30°S at 135 Ma, ~15-25° south of the measured paleolatitude (Van de Lagemaat et al., 2023c). The Proto-South China Sea lithosphere must therefore have been part of a plate that was subducting below the Eurasian and Tethyan plates, but that was not the Izanagi Plate. Paleomagnetic data show that this plate moved ~ 15° northward between 135 and 85 Ma, and it must have had a westward motion component to have been able to subduct below the Tethyan and Eurasian plates. The plate boundary with the Izanagi Plate must have been a subduction zone with the Proto-South China Sea lithosphere as upper plate. Remains of an arc on the eastern Proto-South China Sea lithosphere have been reported from undated rocks in the accretionary prism of Luzon, and 100 Ma old volcanic rocks in the accretionary prism below the Palawan ophiolite (Pasco et al., 2019; Dycoco et al., 2021; see Van de Lagemaat et al., 2023c). Such a configuration of subduction zones surrounding a lithospheric domain between the major Pacific realm and the Tethyan realm was previously inferred from lower mantle seismic tomographic images of anomalies of deeply subducted slabs, imaged at a depth of > 2000 km in the mantle below the west-central Pacific Ocean (Van der Meer et al., 2012). At shallower depths, their tomographic model had no resolution, but they inferred from the slab remnants at > 2000 km depth that an intra-oceanic subduction system must have been active in at least Triassic-Jurassic time, separating the Panthalassa realm into two plate systems. Those authors named the western lithospheric system enclosed by these subduction zones the 'Pontus Ocean' and Van de Lagemaat et al. (2023c) therefore referred to the plate carrying the Proto-South China Sea lithosphere as the 'Pontus Plate'. We refer to the subduction zone of the Izanagi Plate below the Pontus Plate as the 'Telkhinia' subduction zone, following Van der Meer et al. (2012).

Our reconstruction at 110 Ma illustrates that the Pontus Plate must have been a major plate (or, farther back in time, plate system) in the Mesozoic (Fig. 28). The Telkhinia subduction zone ended in the south at a trench-trench-trench triple junction with the Lagonoy subduction zone (proto-Izu-Bonin Mariana subduction zone), with the Pontus Plate in a downgoing plate position (Figs. 26 - 33). In the north, the Telkhinia subduction zone must have had a triple junction with the subduction zones along the South China Block, and we model a triple junction location around the Kerama Gap/Qingdao Line.

For times back to 156 Ma, we reconstruct the motion of the Pontus Plate as such that we avoid extension with the Izanagi Plate. The Telkhinia trench that accommodated subduction of the Izanagi Plate restores farther into the Panthalassa Ocean back in time, and as a result, its north–south extent becomes longer in older reconstruction slices (Figs. 26 - 33). The triple junction at e.g., 135 Ma was located farther southeastwards along the East Gondwana

margin, and the Telkhinia subduction zone likely also accommodated the subduction of the Izanagi-Phoenix ridge, or even part of the Pacific Plate (Figs. 28 - 33).

The age of the oldest lithosphere in the Pontus Plate, and hence the maximum age of the Telkhinia subduction zone, is unknown. Accreted units below the eastern margin of the Pontus Plate have likely all been lost to subduction. The accreted seamount in the South China margin with an age of ~ 154 Ma (Xu et al., 2022) show that the plate contained lithosphere of at least Late Jurassic age. For ages older than 135 Ma, we have no direct kinematic constraints left from rocks of the Pontus Plate, and it is possible that the Pontus 'Ocean' *sensu* Van der Meer et al. (2012) contained multiple plates, separated by ridges. In our reconstruction prior to 135 Ma, we keep the Telkhinia subduction zone more or less mantle stationary, following the tomography-based interpretations of the lower mantle below the Pacific Ocean of Van der Meer et al. (2012).

The Pontus Plate (or further back in time, probably plate system) thus formed a Junction Region in between the Panthalassa and Tethys domains. The westernmost plate boundary of the Panthalassa Ocean (or the 'Thalassa Ocean' *sensu* Van der Meer et al., 2012) was formed by the Telkhinia subduction zone, that connected the subduction zone below Japan with the subduction zone below East Gondwana. To the west, the subduction zones along the Philippine Mobile Belt (Lagonoy subduction zone) and the Kuching Zone adjacent to the SW Borneo Block must have connected through an intra-oceanic trench system to the trenches along Sundaland and South China. Such trenches were also inferred for Jurassic and older times based on seismic tomographic images of the lowermost mantle by Van der Meer et al. (2012), but geological relics of these trenches have not been identified yet. Such relics would have been consumed by subduction below the SW Borneo Block in the south, the West Sulawesi and Sibumasu terranes of Sundaland, and depending on how far this subduction zone reached westwards, perhaps even in de Bangong-Nujiang suture zone between the Lhasa and Qiangtang terranes of western Burma. Future analysis of accretionary prisms in SE Asia may identify further constraints on the intra-oceanic subduction systems that must have existed between the Pontus and Neotethys oceans. The reconstruction at 160 Ma (Fig. 33) satisfies all presently available geological constraints on intra-oceanic subduction that we are aware of from the Junction Region.

The key difference with the reconstruction of Zahirovic et al. (2014) in the oldest part of our reconstruction is the location of the plate boundary that separates the Panthalassa plates from the Junction. Where we follow the constraints of Wu et al. (2022) and Van de Lagemaat et al. (2023c) to infer a subduction zone that extends from the East Gondwana northwards to the Qingdao Line, and the subduction of the Pontus Plate below the SE China and Indochina margins, Zahirovic et al. (2014) incorporate the widely held view that the Izanagi Plate subducted below the entire Eurasian margin. Moreover, their model opens the Proto-South China Sea as a back-arc basin between c. 65 and 35 Ma, while geological data from surrounding regions indicate that the oceanic lithosphere of this basin was of Cretaceous age (Dycoco et al., 2021; Xu et al., 2022; Wang et al., 2023; Van de Lagemaat et al., 2023c).

6. Discussion: Geodynamic implications

Our kinematic reconstruction is based on the modern geological architecture of the Junction Region, in which we assumed a simplest plate model with the least amount of plate boundaries necessary to explain the present-day geology. In this section we briefly discuss the geodynamic implications that follow from our reconstruction, and how they may contribute to a better understanding of geodynamics.

6.1. Small oceanic basins opening in the downgoing plate close to trenches

An interesting finding of our plate reconstruction is that the Junction Region hosts several examples of relatively small oceanic basins that opened within a down-going plate, in the proximity of and at ridges parallel to a subduction zone. Opening of oceanic basins above subduction zones is a common phenomenon, as illustrated by the numerous forearc and back-arc basins of the West and Southwest Pacific realms, such as the Mariana Trough, Ogasawara Trough, Parece-Vela Basin, South Fiji Basin, or Lau Basin (Fig. 1). Examples of oceanic basins that opened in a down-going plate are the South China Sea basin, the Santa Cruz Basin, and the Woodlark Basin (Fig. 34). We speculate that there may be causal relationships between opening of these basins and the nearby subduction zones. The South China Sea basin opened from the late Eocene to mid-Miocene, during southward subduction of the Proto-South China Sea, partly contemporaneous with the Sulu Sea that started opening as back-arc basin in the upper plate (e.g., Advokaat and Van Hinsbergen, 2023). It was recently suggested that the Proto-South China Sea may have been underlain by an oceanic plateau that initially stopped subduction in the Mesozoic (Van de Lagemaat et al., 2023c). Those authors tentatively suggested that when this oceanic plateau was eventually forced to subduct during counterclockwise vertical-axis rotation of Borneo, the eclogitization of thickened oceanic crust may have caused an especially strong slab pull, that resulted in the extension and eventual break-up of the down-going plate and the formation of the South China Sea.

The Santa Cruz Basin formed in the Eocene during eastward subduction at the New Caledonia subduction zone, while the North Loyalty back-arc basin opened contemporaneously and in a parallel orientation in the overriding plate (Seton et al., 2016; Van de Lagemaat et al., 2018a). The eastern margin of the Santa Cruz Basin is flanked by the West Torres Plateau. In the case of the Santa Cruz Basin, however, extension in the down-going plate ceased in the early Oligocene, while subduction of the plateau is presently occurring at the New Hebrides trench. Moreover, it is unknown whether the West Torres Plateau was being subducted during opening of the Santa Cruz Basin, because its original eastward extension is unknown.

The Woodlark Basin also recently started forming in the down-going Australian Plate, but at a higher angle to the subduction zone owing to rotational opening around an Euler pole not far west of the d'Entrecasteaux Islands. In this basin, there is no evidence of the presence of an oceanic plateau, but it is attached to older, Eocene, oceanic crust of the Solomon Sea. Similar to the tectonic settings of the South China Sea and Santa Cruz basins, there is also a back-arc basin in the northwest (the Manus Basin) that forms in an overriding plate position to the Woodlark Basin. However, in the case of the South China Sea and Santa Cruz Basin, their opening was preceded a few Ma by the opening of the back-arc basin, while in the case of the Woodlark Basin, the back-arc basin is younger than the subducting plate basin. Moreover, where the back-arc and subducting plate basins opened roughly parallel in the case of the South China Sea and Santa Cruz basins, the orientation of the Manus Basin is at a higher angle with the Woodlark Basin.

Other than the fact that all these basins formed in a down-going plate in the proximity and roughly parallel to a subduction zone, the most striking resemblance between the South China Sea and Santa Cruz basins is that both formed parallel to a back-arc basin in the overriding plate that started forming a few Ma earlier, but this similarity is not shared with the Woodlark Basin. The basins that opened in subducting plates all formed in pre-existing weak zones of that plate; the South China Sea formed within the South China margin accretionary prism, and the Santa Cruz and

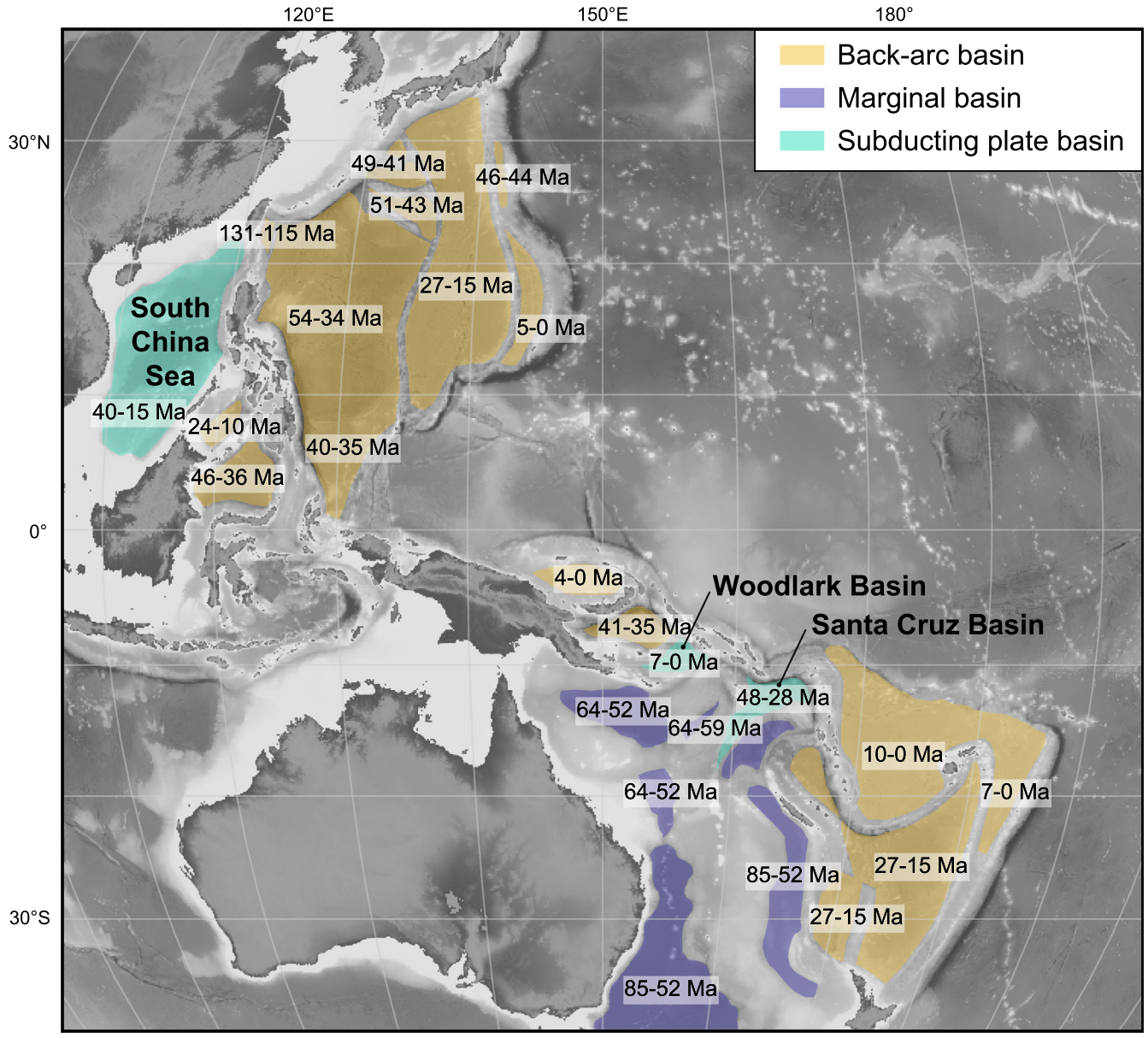

Fig. 34. Map of the oceanic basins in the Junction Region colored by their tectonic setting. Back-arc basins formed above active subduction zones. Marginal basins formed by breaking of a continental margin in absence of a subduction zone. The marginal basins east of Australia formed after the end of Mesozoic subduction and before the onset of Tonga-Kermadec subduction. The subducting plate basins formed at ridges that were created within a downgoing plate close to a subduction zone.

Woodlark basis formed at an obducted continent-ocean transition zone of the Australian Plate.

The consequence of back-arc basins that form during slab roll-back is that subduction rates exceed the convergence rates between the plates that were originally interacting at the plate boundary, an effect that is in these cases caused or enhanced by the formation of subducting plate basins. The reason behind this effect related to the formation of subducting-plate basins and its connection to subduction zone dynamics are topics that may be explored further through geodynamic modeling.

Finally, the Coral Sea and Caroline Plate basins also opened in a down-going plate position, and roughly parallel to the San Cristobal North Solomon subduction zone, respectively, but at a far larger distance and at a larger scale than the aforementioned basins. A causal relationship between the opening of the basin and the subduction zone may therefore be less straightforward. We consider the Coral Sea Basin as a northward extension of the Tasman Sea, which formed as a marginal basin during continental break-up. Previously, the Caroline Plate was considered a back-arc basin (e.g., Weissel and Anderson, 1978; Gaina and Müller, 2007; Wu et al., 2016), but in our reconstruction the plate is separated from the north-dipping New Guinea subduction zone by the south-dipping North Solomon-Vitiaz subduction zone and the basin is therefore not in a back-arc position. As the large igneous provinces on the Caroline Plate clearly indicate its interaction with a mantle plume, we suspect that the formation of Caroline Plate basins may be related to weakening by a mantle plume, with spreading driven by slab pull of the already subducting slab.

6.2. Absolute plate and slab motion

Placing our reconstruction in a mantle reference frame provides insight into the absolute motions of plates and subducted slabs (known as ‘slab dragging’; Spakman et al., 2018), during

subduction and after slab break-off. Van de Lagemaat et al. (2018a) showed that the Tonga-Kermadec slab was dragged northward, laterally through the mantle over about 1200 km since 30 Ma, resulting from the northward, trench-parallel component of the absolute motion of Pacific Plate. Our reconstruction now assigns an earlier age of subduction initiation of the Tonga segment of the subduction zone of 45 Ma, which increases the amount of Tonga slab dragging since subduction initiation to 1600 km (~3.5 cm/yr). The accompanying northward motion of the Australian Plate resulted in also northward motion of the Tonga-Kermadec trench and upper plate (Fig. 35). Slab dragging is not restricted to trenches that accommodate subduction between two plates that also share a trench-parallel absolute plate motion component. Slab dragging also occurs during highly oblique subduction below near-mantle-stationary upper plates, e.g., the northward dragging of the Burma slab as part of the Indian Plate (Le Dain et al., 1984; Parsons et al., 2021). In addition to trench-parallel slab dragging, slab dragging also occurs during trench-perpendicular absolute motion; the motion of upper plates (and hence trenches) relative to the mantle may result in slab retreat or slab advance, which causes flat-lying and steep (or even overturned) slabs, respectively (e.g., Qayyum et al., 2022). We here assess the motion of trenches and slabs relative to the mantle as the result of absolute plate motion, and how this may have influenced slab geometry, by placing our reconstruction of the Junction Region in the global moving hotspot reference frame of Doubrovine et al. (2012).

The rapid Australian absolute plate motion must mean that the New Hebrides slab, which has been subducting and rolling back below Vanuatu, has experienced northward slab dragging since its formation (c. 10 Ma ago, Yan and Kroenke, 1993). The clockwise rotation of the trench has resulted in a larger amount of absolute trench motion in the south than in the north, and a larger northward component of the northern part of the trench. This slab dragging component may provide a straightforward explanation for the incipient subduction at the Hunter fracture zone that started in the Plio-Pleistocene (Patriat et al., 2015; 2019; Lallemand and Arcay, 2021). This transform formed as a STEP fault accommodating New Hebrides trench roll-back. We foresee that the resistance of the New Hebrides slab against northward slab dragging, which is known to cause trench-parallel shortening in the downgoing plate (Spakman et al., 2018), may contribute to the incipient subduction at the Hunter fracture zone.

The Tonga-Kermadec trench was connected northwards with the Solomon-Vitiaz trench, which also accommodated Pacific-Australia relative motion. The motion of the Pacific Plate relative to the mantle since 45 Ma is roughly towards the WNW, similar to the orientation of the North Solomon trench. The subduction of the Pacific Plate at the North Solomon trench is thus purely the result of the 2200 km (~4.9 cm/yr) northward motion of the North Solomon trench since 45 Ma, as part of the Australian Plate (Fig. 35). The northward motion of the North Solomon trench leads to slab retreat.

Farther north, the Izu-Bonin Mariana subduction zone also has a N-S orientation. The Philippine Sea Plate underwent a strong northward motion component (see section 5; also Van de Lagemaat et al., 2023b). Like the Tonga-Kermadec slab, the Izu-Bonin Mariana slab is located due west of the present-day trench (Miller et al., 2004; Wu et al., 2016; Van der Meer et al., 2018), but the subduction zone originated much farther southward (Fig. 35). Slab dragging at the Mariana trench was c. 3000 km (~6.6 cm/yr), i.e., almost twice as fast as the Tonga-Kermadec subduction zone since 45 Ma. We suggest that the N-S opening of the West Philippine Basin and the NE-SW opening of the Parece Vela Basin accommodated additional slab dragging of the Izu-Bonin section driven by absolute motion of the Pacific Plate. Moreover, as subduction here initiated earlier than in the Tonga-Kermadec case, the total amount of slab dragging is much larger, in the order of ~ 4000 km for the northernmost Izu-Bonin trench since 52 Ma (~7.7 cm/yr) and ~ 3000 km for the central Mariana trench (~5.8 cm/yr). The recent clockwise rotation of the Philippine Sea Plate accommodated by extensional motion in the Ayu Trough since 15 M, has resulted in slab advance of the southern portion of the trench, which explains the steep nature of the Mariana slab (e.g., Spakman et al., 1989; Van der Hilst, 1991; Miller et al., 2004). This also suggests that the Mariana Trough back-arc did not open because of slab roll-back, but rather due to slab resistance against overriding plate retreat.

In the north of the Philippine Sea Plate, the position of the trenches along the Eurasian margin have been comparatively stable relative to the mantle since the Late Cretaceous. The total amount of trench retreat of the Ryukyu arc since 70 Ma is about 750 km (~1.1 cm/yr). However, the opening of the Shikoku Basin in the Philippine Sea Plate, which was accompanied by trench retreat of the Izu-Bonin trench, has resulted in large-scale (~1600 km since 30 Ma) trench-parallel slab dragging at the Nankai trench, analogous to the Burma slab.

The Manila and the Halmahera trenches that form the western plate boundary of the Philippine Sea Plate have experienced large absolute trench motions since subduction initiation around 15 Ma. In this case, however, the position of the down-going plate relative to the mantle has been almost stationary throughout the subduction history. So even though the Manila trench's upper plate underwent large scale northward, trench-parallel, motion, lateral slab dragging is minimal here.

In addition to the presently active subduction zones, we may also analyze former trenches in our reconstruction and make inferences about where we may find slab remnants in the mantle. The north- and eastward dipping New Guinea-New Caledonia subduction zones have been subject to slab dragging (Fig. 35). Like most trenches in the Junction Region, these trenches and slabs underwent northward absolute motion, which resulted in trench-parallel dragging at the New Caledonia trench. Van de Lagemaat et al. (2018a) showed that the South Loyalty Slab, identified by Schellart et al. (2009), is in a position that is just north of the reconstructed 30 Ma location of the New Caledonia trench, at which time northward subduction ceased and the slab likely detached. After the end of subduction, the slab sank vertically into the mantle, and the inactive trench subsequently overrode the slab during northward motion of the Australian Plate. The change in orientation from roughly N-S at the New Caledonia trench to roughly E-W at the New Guinea trench resulted in slab advance rather than lateral dragging of the slab at the New Guinea trench (Fig. 35). During the Eocene, however, slab advance in the New Guinea sector was largely cancelled by roll-back such that the trench remained in a more or less mantle-stationary position. The opening of the Molucca Sea and Solomon Sea back-arc basins occurred mostly due to northward absolute motion components of the Philippine Sea Plate relative to this mantle-stationary trench. Subsequent slab advance during northward motion of the New Guinea trench may have resulted in a steeply dipping or overturned slab. Depending on how the geometry of the slab was affected by slab advance, both the Arafura and Carpentaria slabs of Van der Meer et al. (2018) may be correlated to the New Guinea subduction zone. Following slab break-off, Australia overrode these slabs, and their mantle wedges. Previously, Van Hinsbergen et al. (2020b) inferred that Australia overriding a former mantle wedge above the Arafura slab led to the enigmatic arc-signature in the Pliocene Ertsberg and Grasberg magmatic centers in Central New Guinea, close to the obduction front. Those authors used the reconstructions of Hall (2002) and Zahirovic et al. (2014) who suggested that the Arafura slab formed entirely at an intra-oceanic subduction zone far north of Australia, prior to ~ 30 Ma. Our reconstruction instead suggests that the only

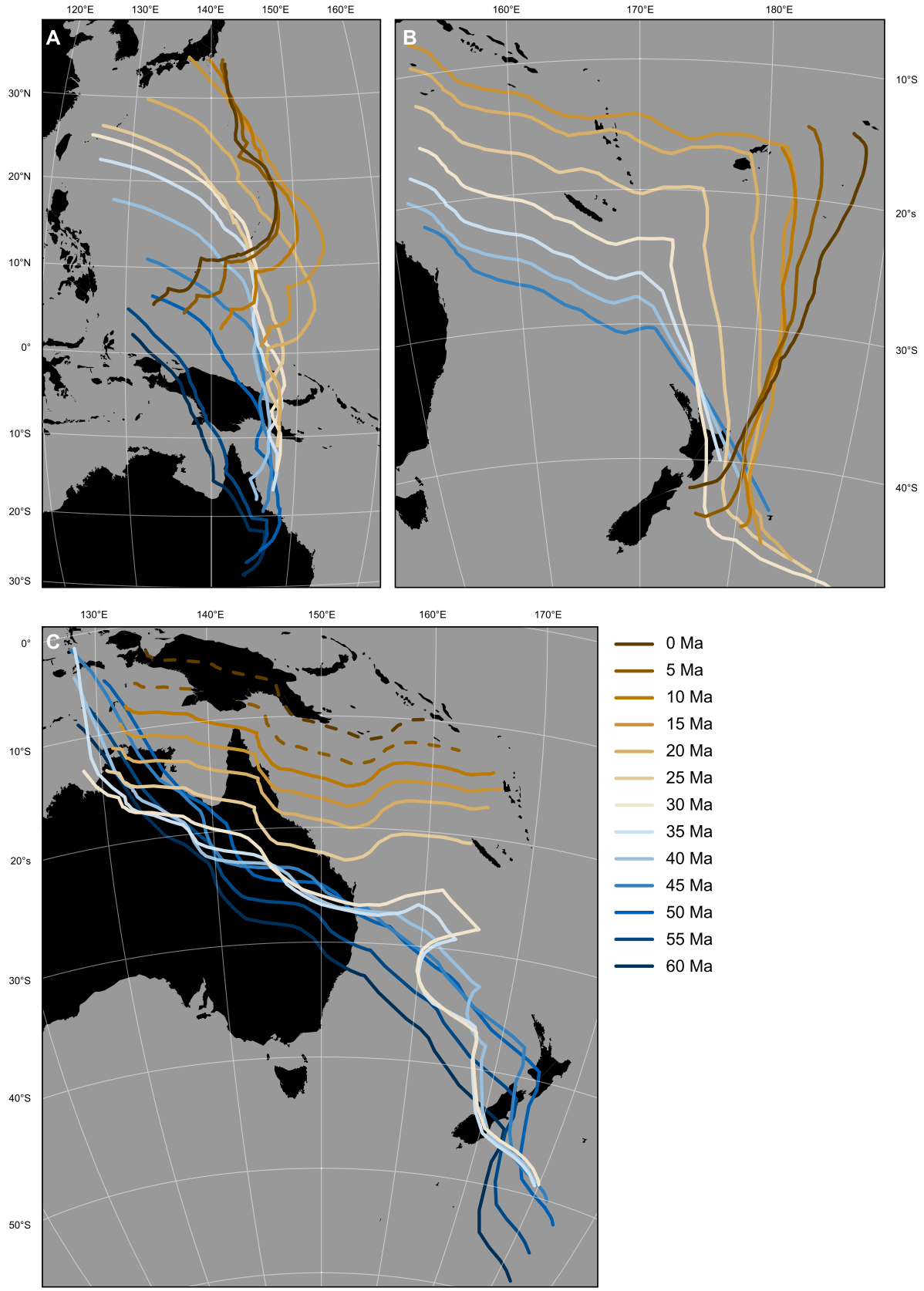

Fig. 35. Maps showing the locations of subduction zones through time in the mantle reference frame of Doubrovine et al. (2012). A) Izu-Bonin Mariana subduction zone; B) Tonga-Kermadec(-Vitiaz-Solomon) subduction zone; C) New Guinea-New Caledonia subduction zone.

candidate to have formed the Arafura slab is the subduction zone that led to the obduction of the Papuan ophiolite. The timing of its break-off may have occurred anytime after 30 Ma, but the position of the slab suggests that this occurred around 10 Ma, and that the time delay between mantle wedge formation and plowing of the Australian margin through the mantle is shorter than interpreted by Van Hinsbergen et al. (2020b).

In the Cretaceous, the Lagonoy subduction zone underwent trench retreat, as well as northward trench-parallel slab dragging. Slab dragging at the Telkhinia trench was dominated by slab advance. During roll-back of the Lagonoy subduction zone, the Telkhinia subduction zone was progressively consumed by the Lagonoy subduction zone, and we therefore expect that the Telkhinia slab may have broken in several instances. This may explain some of the slab remnants that are present in the mantle below the eastern margin of eastern Australia. One of the slab remnants below Australia is the Lake Eyre slab, which is in the lower mantle below Lake Eyre, Australia. This slab was previously interpreted using the reconstruction of Hall (2002) as the detached slab that formed during northward subduction of the Australian Plate below the Papuan ophiolites (Schellart and Spakman, 2015). In their interpretation subduction there ceased around 50 Ma, based on the c. 54 Ma age of the metamorphic sole below the Papuan Ultramafic Belt (Lus et al., 2004). However, as the metamorphic sole forms during subduction initiation rather than subduction termination, this age does not represent the end of subduction but the start, and the geology of New Guinea indicates that oceanic subduction continued into the Oligocene and obduction until the late Miocene. In light of our reconstruction, it is unlikely that the Lake Eyre slab is correlated to a 60-less than30 Ma New Guinea subduction zone. Instead, when putting our reconstruction in de slab references frame of Van der Meer et al. (2010), the Lake Eyre slab is in a location that could correspond to the location of the Lagonoy subduction zone around 85 Ma, just prior to when this plate boundary became dominated by transform motion owing to the change in absolute motion of the Pacific plate from west to north (Fig. 36). The change in relative plate motion at the plate boundary may have resulted in slab detachment which subsequently sank vertically into the mantle. This interpretation would suggest that the Lake Eyre slab is much older than previously thought.

Our analysis of slab dragging in the west Pacific region shows that lateral slab dragging such as previously shown for the Tonga-Kermadec (Van de Lagemaat et al., 2018a) is a rule rather than an exception. Lateral slab dragging is a common phenomenon that occurs in all subduction zones where the down-going plate has a trench-parallel component. In addition, the absolute motion of upper plates relative to slabs is a key driver of upper plate deformation (Van Hinsbergen and Schouten, 2021). Slab dragging can only be correctly analyzed in an absolute plate motion frame, because the absolute plate motion of both the upper plate and down-going plate as well as their interaction at the trench determine the amount and type of slab dragging. In addition, as illustrated by the example of the Lake Eyre slab, our reconstruction sheds a new light on the plate boundary evolution in the Junction Region that requires a reinterpretation of the geological history of upper and especially lower mantle slabs, such as those listed in the Atlas of the Underworld (Van der Meer et al., 2018).

6.3. Subduction initiation

The Izu-Bonin Mariana subduction zone is one of the best-studied subduction zones on Earth, particularly to understand subduction initiation (e.g., Stern and Bloomer, 1992; Stern et al., 2003, 2012; Reagan et al., 2010; Ishizuka et al., 2011a; Arculus et al., 2015). The age of subduction initiation at the Izu-Bonin Mariana trench is generally inferred from the oldest supra-subduction zone gabbros and basalts recovered from the Izu-Bonin-Mariana forearc, which are ~ 52 Ma old (Ishizuka et al., 2011a; Reagan et al., 2010, 2013, 2019). This inference is based on the assumption that the catastrophic extension that led to the overriding plate spreading centers at which these basalts and gabbros formed along the strike of the Izu-Bonin-Mariana forearc signals spontaneous subduction initiation (Stern and Bloomer, 1992; Stern et al., 2012). In such a setting, the area consumed by initial subduction resulting from the gravitationally driven lithospheric collapse of the down-going plate must be instantaneously compensated by upper plate extension, and the magmatic rocks formed during that extension must thus be synchronous with subduction initiation (e.g., Stern and Bloomer, 1992; Stern, 2004; Arculus et al., 2015). However, the Semail Ophiolite of Oman comprises similar forearc crust that formed through catastrophic extension because of lithospheric collapse, but there, rocks that formed at the incipient subduction plate boundary are exhumed as metamorphic sole rocks, which are about 8 Ma older than the age of forearc basalts (Guilmette et al., 2018). Similar and even larger time delays between the formation of the metamorphic sole and the formation of forearc crust have been shown since for the Coast Range Ophiolite in California (Mulcahy et al., 2018), the Halilbağı Complex in Turkey (Pourteau et al., 2019) and the Xigaze Ophiolite in Tibet (Guilmette et al., 2023). These time lags between metamorphic sole and subsequent forearc crust formation can only exist in subduction zones that formed due to far-field-forced convergence, as the subduction interface formed before lithospheric collapse occurred (Guilmette et al., 2018). The metamorphic sole of the Izu-Bonin Mariana subduction zone remains buried below the Izu-Bonin Mariana forearc and it is therefore impossible to determine its age that would directly resolve the debate of whether subduction initiation occurred spontaneously or was forced. In this case, a kinematic reconstruction provides the next best insight into the question of whether subduction initiation at the Izu-Bonin Mariana trench must have been spontaneous or may have been induced.

Based on our reconstruction, we find that there is no need to assume that subduction initiation at the Izu-Bonin Mariana trench must have been spontaneous. Instead, our reconstruction shows that it is more likely that subduction initiation at the Izu-Bonin Mariana trench was forced and occurred around 62 Ma linked to the slow Pacific-Australian plate convergence that also led to the formation of the New Guinea-New Caledonia subduction zone. If correct, subduction initiation occurred about 10 Ma before lithospheric collapse and extension in the Izu-Bonin Mariana forearc, a similar delay as in the Tethyan and Californian examples. This is based on the reconstructed 62–52 Ma clockwise rotation of the Philippine Mobile Belt that is required for the northward decrease of convergence to avoid subduction of the Australian Plate beyond the Papuan ophiolite belt.

In addition to the cause of subduction initiation, also the nature of the Izu-Bonin Mariana plate boundary before it became a subduction zone has been subject of debate. The most common suggestion is that subduction initiated along a transform fault between two mid-ocean ridge segments (e.g., Casey and Dewey, 1984; Dewey and Casey, 2011), whether it be spontaneous or induced (e.g., Stern and Bloomer, 1992; Hall et al., 2003). This suggestion was mostly based on the interpretation that extension and spreading in the West Philippine Basin predated subduction initiation, but it did not explain the presence of oceanic crust in the overriding Philippine Sea Plate that is up to 100 Ma older (the Lagonoy Ophiolite) at time of subduction initiation. Our reconstruction shows that the Izu-Bonin Mariana trench initiated along a pre-existing weakness zone indeed, which had accommodated mostly transform motion for about 20 Ma resulting from relative

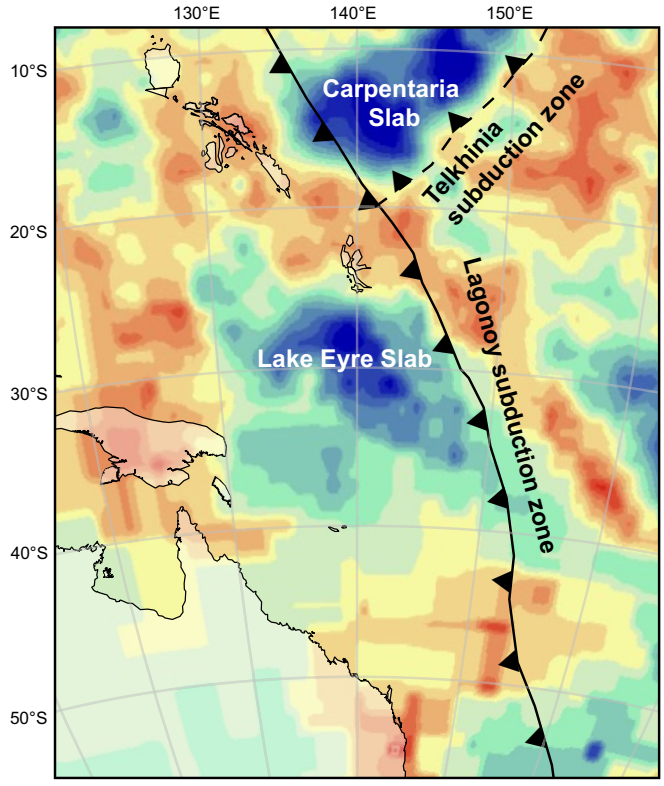

Fig. 36. Reconstructed position of the Lagonoy and Telkhinia subduction zones during the mid to late Cretaceous in the slab reference frame of Van der Meer et al. (2010) projected on a seismic tomographic image of the present-day mantle structure at a depth of 1050 km, based on the UU-P07 tomographic model (Amaru, 2007).

plate motion changes around 85 Ma, but that was a subduction zone before that time: our 'Lagonoy' subduction zone that was active in the Mesozoic.

If the Izu-Bonin Mariana trench formed through forced subduction initiation that resulted from a small change in Australia-Pacific relative plate motion at 62 Ma together with the New Guinea-New Caledonia subduction zone, the 52 Ma lithospheric collapse may signal the effective onset of slab pull, and thus may have been a trigger for the Eocene change in Pacific Plate motion that resulted in the formation of the Hawaii-Emperor Bend (Torsvik et al., 2017). Izu-Bonin Mariana subduction initiation as driver for the change in absolute plate motion of the Pacific Plate was previously suggested based on geodynamic modelling (Faccenna et al., 2012). Moreover, the possibility that the initiation of effective slab pull that is reflected in lithospheric collapse following subduction initiation may cause absolute plate motion changes was tested and shown for the forced subduction initiation event below the Oman and Anatolia ophiolites that caused a change in African plate motion (Gürer et al., 2022). Our reconstruction shows that it is feasible that the sequence of events from forced subduction initiation to lithospheric collapse and a subsequent change in absolute plate motion applies to the Izu-Bonin Mariana trench and Pacific Plate. To what extent the subduction initiation at the Izu-Bonin Mariana trench was responsible for the change in absolute plate motion of the Pacific Plate is uncertain, as the NW Pacific was the location of other drastic plate tectonic changes, including subduction of the Izanagi-Pacific Ridge that led to the first demonstrable subduction of Pacific Plate lithosphere (Seton et al., 2015; Wu and Wu, 2019) and a subduction polarity reversal after the collision of the Olyutorsky arc with Kamchatka (Domeier et al., 2017; Vaes et al., 2019). Based on the reconstructed 45 Ma age of the Solomon-Vitiaz-Tonga subduction zone, we find it most likely that subduction initiation there was a result of the change in absolute plate motion change of the Pacific Plate rather than a cause, but after it happened, it will have contributed to a more westerly course of absolute Pacific Plate motion. However, if future age constraints provide evidence for an older age of subduction initiation there, it may have played an active role in changing the absolute motion of the Pacific Plate.

7. Conclusions

We developed a kinematic restoration of the Junction Region back to the Jurassic, based on the present-day orogenic record of the circum-Philippine Sea Plate and Australasian region. We presented a comprehensive review of the orogens of southwestern Japan, Taiwan, the Philippines and northern Molucca Islands, New Guinea, and the Solomon Islands and adjacent archipelagoes and ocean basins. Our reconstruction is based on a systematic restoration of the tectonic motions that are inferred from these orogenic and marine geophysical records, cast in context of relative motions of the Australian, Eurasian, and Pacific plates, and in context of a recent restoration of orogenesis in the Tethyan belts of SE Asia. We present our reconstruction in a series of maps from the present back to the Jurassic and provide GPlates reconstruction files that can be placed in mantle or paleomagnetic reference frames as basis for geodynamic or paleoclimatic analysis, respectively. Our conclusions are plentifold, but include the following:

- The Molucca Sea as well as the Eocene ophiolites of the Philippines and the Cyclops Ophiolite in New Guinea formed as part of an Eocene back-arc basin above a northward dipping subduction zone that consumed the Australian Plate. Subduction at this trench initiated around 62 Ma, was contiguous with the New Caledonia subduction zone, and ended in the Oligocene.
- The latest Jurassic oceanic crust that is preserved in the Philippines originated from the northern margin of the Australian Plate where continental margin subduction was active during the Permian and Triassic. The formation of the ophiolites records the onset of oceanic spreading and the formation of an Early Cretaceous back-arc basin behind a proto-Izu-Bonin Mariana subduction zone which we refer to as the Lagonoy subduction zone. The Late Cretaceous ophiolites formed when extension relocated to the forearc.
- Trench-parallel slab dragging as well as slab retreat and advance are common features of subduction zones. The previously identified Lake Eyre slab is not related to the New Guinea subduction zone, but instead may be related to slab break-off at the Lagonoy subduction zone around 85 Ma, when this plate boundary became a transform fault. Instead, the Arafura or possibly the Carpentaria slabs may have formed at the New Guinea subduction zone. A careful re-evaluation of modern mantle structure of the western Pacific in light of our reconstruction is timely.
- There is no necessity for spontaneous subduction initiation at the Izu-Bonin Mariana trench. Our reconstruction predicts forced subduction initiation around 62 Ma, which subsequently resulted in lithospheric collapse and the formation of the Izu-Bonin Mariana forearc around 52 Ma. The lithospheric collapse may have been a trigger of the change in absolute plate motion of the Pacific Plate that caused the formation of the Hawaii-Emperor Bend.

Declaration of Competing Interest

The authors declare that they have no known competing financial interests or personal relationships that could have appeared to influence the work reported in this paper.

Acknowledgements

SHAvdL and DJJvH were funded by NWO Vici grant 865.17.001 to DJJvH. We thank an anonymous reviewer for valuable comments.

Appendix A. Supplementary material

Supplementary data to this article can be found online at https://doi.org/10.1016/j.gr.2023.09.013.

References

Abbott, L.D., 1995. Neogene tectonic reconstruction of the Adelbert-Finisterre-New Britain collision, northern Papua New Guinea. J. SE Asian Earth Sci. 11 (1), 33–51.

Advokaat. E. L., & Van Hinsbergen, D. J. J., (2023). Finding Argoland: reconstructing a lost continent in SE Asia. Submitted to *Gondwana Research*.

Advokaat, E.L., Hall, R., White, L.T., Watkinson, I.M., Rudyawan, A., BouDagher-Fadel, M.K., 2017. Miocene to recent extension in NW Sulawesi, Indonesia. J. Asian Earth Sci. 147, 378–401.

Advokaat, E.L., Marshall, N.T., Li, S., Spakman, W., Krijgsman, W., van Hinsbergen, D. J., 2018. Cenozoic rotation history of Borneo and Sundaland, SE Asia revealed by paleomagnetism, seismic tomography, and kinematic reconstruction. Tectonics 37 (8), 2486–2512.

Almasco, J.N., Rodolfo, K., Fuller, M., Frost, G., 2000. Paleomagnetism of Palawan, Philippines. J. Asian Earth Sci. 18 (3), 369–389.

Altis, S., 1999. Origin and tectonic evolution of the Caroline Ridge and the Sorol Trough, western tropical Pacific, from admittance and a tectonic modeling analysis. Tectonophysics 313 (3), 271–292.

Alvarez-Marron, J., Brown, D., Camanni, G., Wu, Y.M., Kuo-Chen, H., 2014. Structural complexities in a foreland thrust belt inherited from the shelf-slope transition: Insights from the Alishan area of Taiwan. Tectonics 33 (7), 1322–1339.

Amaru, M.L., 2007. Global travel time tomography with 3-D reference models. Utrecht University, the Netherlands. Ph. D thesis,.

Amiruddin, A., 2009. A review on Permian to triassic active or convergent margin in southeasternmost gondwanaland: possibility of exploration target for tin and hydrocarbon deposits in the Eastern Indonesia. Indonesian Journal on Geoscience 4 (1), 31–41.

Andal, E.S., Arai, S., Yumul Jr, G.P., 2005. Complete mantle section of a slow-spreading ridge-derived ophiolite: An example from the Isabela ophiolite in the Philippines. Isl. Arc 14 (3), 272–294.

Arai, R., Kodaira, S., Yuka, K., Takahashi, T., Miura, S., Kaneda, Y., 2017. Crustal structure of the southern Okinawa Trough: Symmetrical rifting, submarine volcano, and potential mantle accretion in the continental back-arc basin. J. Geophys. Res. Solid Earth 122 (1), 622–641.

Arcilla, C.A., Ruelo, H.B., Umbal, J., 1989. The Angat ophiolite, Luzon, Philippines: lithology, structure, and problems in age interpretation. Tectonophysics 168 (1–3), 127–135.

Arculus, R.J., Ishizuka, O., Bogus, K.A., Gurnis, M., Hickey-Vargas, R., Aljahdali, M.H., Zhang, Z., 2015. A record of spontaneous subduction initiation in the Izu–Bonin–Mariana arc. Nat. Geosci. 8 (9), 728–733.

Arkula, C., Lom, N., Wakabayashi, J., Rea-Downing, G., Qayyum, A., Dekkers, M.J., van Hinsbergen, D.J., 2023. The forearc ophiolites of California formed during trench-parallel spreading: Kinematic reconstruction of the western USA Cordillera since the Jurassic. Earth Sci. Rev. 237, 104275.

Aurelio, M.A., 2000. Shear partitioning in the Philippines: constraints from Philippine Fault and global positioning system data. Isl. Arc 9 (4), 584–597.

Aurelio, M.A., Barrier, E., Rangin, C., Müller, C., 1991. The Philippine Fault in the late Cenozoic tectonic evolution of the Bondoc-Masbate-N. Leyte area, central Philippines. J. SE Asian Earth Sci. 6 (3–4), 221–238.

Aurelio, M.A., Forbes, M.T., Taguibao, K.J.L., Savella, R.B., Bacud, J.A., Franke, D., Carranza, C.D., 2014. Middle to Late Cenozoic tectonic events in south and central Palawan (Philippines) and their implications to the evolution of the south-eastern margin of South China Sea: Evidence from onshore structural and offshore seismic data. Mar. Pet. Geol. 58, 658–673.

Bailly, V., Pubellier, M., Ringenbach, J.C., De Sigoyer, J., Sapin, F., 2009. Deformation zone 'jumps' in a young convergent setting; the Lengguru fold-and-thrust belt. New Guinea Island. Lithos 113 (1–2), 306–317.

Baker, S., Malaihollo, J., 1996. Dating of Neogene igneous rocks in the Halmahera region: arc initiation and development. Geol. Soc. Lond. Spec. Publ. 106 (1), 499–509.

Baldwin, S.L., Lister, G.S., Hill, E.J., Foster, D.A., McDougall, I., 1993. Thermochronologic constraints on the tectonic evolution of active metamorphic core complexes, D'Entrecasteaux Islands. Papua New Guinea. Tectonics 12 (3), 611–628.

Baldwin, S.L., Monteleone, B.D., Webb, L.E., Fitzgerald, P.G., Grove, M., June Hill, E., 2004. Pliocene eclogite exhumation at plate tectonic rates in eastern Papua New Guinea. Nature 431 (7006), 263–267.

Baldwin, S.L., Webb, L.E., Monteleone, B.D., 2008. Late Miocene coesite-eclogite exhumed in the Woodlark Rift. Geology 36 (9), 735–738.

Baldwin, S.L., Fitzgerald, P.G., Webb, L.E., 2012. Tectonics of the New Guinea region. Annu. Rev. Earth Planet. Sci. 40, 495–520.

Ballance, P.F., Spörli, K.B., 1979. Northland allochthon. J. R. Soc. N. Z. 9 (2), 259–275.

Ballantyne, P.D., 1990. The petrology of the ophiolitic rocks of the Halmahera region, Indonesia. UCL (University College London). Doctoral thesis (Ph.D),.

Ballantyne, P., 1991. Petrological constraints upon the provenance and genesis of the East Halmahera ophiolite. J. SE Asian Earth Sci. 6 (3–4), 259–269.

Balmater, H.G., Manalo, P.C., Faustino-Eslava, D.V., Queaño, K.L., Dimalanta, C.B., Guotana, J.M.R., Yumul Jr, G.P., 2015. Paleomagnetism of the Samar Ophiolite: Implications for the Cretaceous sub-equatorial position of the Philippine island arc. Tectonophysics 664, 214–224.

Barrier, E., Huchon, P., Aurelio, M., 1991. Philippine fault: A key for Philippine kinematics. Geology 19 (1), 32–35.

Batara, B., Xu, C., 2022. Evolved magmatic arcs of South Borneo: Insights into Cretaceous slab subduction. Gondw. Res. 111, 142–164.

Battan, R., Chung, S. L., Komiya, T., Maruyama, S., Lin, A. T., Lee, H. Y., & Iizuka, Y. (2022, December). Zircon U-Pb Ages and Geochemical Characteristics of Magmatic Rocks from Choiseul and Santa Isabel, Solomon Islands: Implications for the Magmatic and Tectonic Evolution in SW Pacific. In *AGU Fall Meeting Abstracts* (Vol. 2022, pp. V12C-0058).

Beiersdorf, H., Bach, W., Delisle, G., Faber, E., Gerling, P., Hinz, K., & Dheeradilok, P. (1997). Age and possible modes of formation of the Celebes Sea basement, and thermal regimes within the accretionary complexes off SW Mindanao and N Sulawesi. In *Proceedings of the International Conference on Stratigraphy and Tectonic Evolution of Southeast Asia and the South Pacific* (pp. 369-387).

Bellon, H., Rangin, C., 1991. Geochemistry and isotopic dating of Cenozoic volcanic arc sequences around the Celebes and Sulu Seas. Proc. ODP Sci. Results 124, 321–338.

Bellon, H., Yumul Jr, G.P., 2000. Mio-Pliocene magmatism in the Baguio Mining District (Luzon, Philippines): age clues to its geodynamic setting. Comptes Rendus de l'Académie des Sciences-Series IIA-Earth and Planetary Science 331 (4), 295–302.

Benyshek, E.K., Taylor, B., 2021. Tectonics of the Papua-Woodlark Region. Geochem. Geophys. Geosyst. 22 (1). e2020GC009209.

Bergman, S.C., Hutchison, C.S., Swauger, D.A., Graves, J.E., 2000. K: Ar ages and geochemistry of the Sabah Cenozoic volcanic rocks. Geological society of Malaysia Bulletin 44, 165–171.

Berly, T., 2005. Ultramafic and mafic rock types from Choiseul, Santa Isabel and santa Jorge (Northeastern Solomon Islands): origins and significance. Université Joseph-Fourier-Grenoble I). Doctoral dissertation,.

Berly, T.J., Hermann, J., Arculus, R.J., Lapierre, H., 2006. Supra-subduction zone pyroxenites from San Jorge and Santa Isabel (Solomon Islands). J. Petrol. 47 (8), 1531–1555.

Bernard, A., Munschy, M., Rotstein, Y., Sauter, D., 2005. Refined spreading history at the Southwest Indian Ridge for the last 96 Ma, with the aid of satellite gravity data. Geophys. J. Int. 162 (3), 765–778.

Billedo, E.B., Stephan, J.F., Delteilt, J., Bellon, H., Sajona, F., Feraud, G., 1996. The pre-Tertiary ophiolitic complex of northeastern Luzon and the Polillo group of islands, Philippines. Journal of the Geological Society of the Philippines 51, 95–114.

Bird, P., 2003. An updated digital model of plate boundaries. Geochem. Geophys. Geosyst. 4 (3).

Bladon, G.M., 1988. Catalogue, appraisal and significance of K-Ar isotopic ages determined for igneous and metamorphic rocks in Irian Jaya. Geological Research and Development Centre, Bandung, Indonesia, Preliminary Geological Report, p. 86.

Boschman, L.M., Van der Wiel, E., Flores, K.E., Langereis, C.G., van Hinsbergen, D.J., 2019. The Caribbean and Farallon plates connected: Constraints from stratigraphy and paleomagnetism of the Nicoya Peninsula, Costa Rica. J. Geophys. Res. Solid Earth 124 (7), 6243–6266.

Boschman, L.M., Van Hinsbergen, D.J., 2016. On the enigmatic birth of the Pacific Plate within the Panthalassa Ocean. Sci. Adv. 2 (7). e1600022.

Boschman, L.M., van Hinsbergen, D.J., Torsvik, T.H., Spakman, W., Pindell, J.L., 2014. Kinematic reconstruction of the Caribbean region since the Early Jurassic. Earth Sci. Rev. 138, 102–136.

Boschman, L.M., van Hinsbergen, D.J., Spakman, W., 2021a. Reconstructing Jurassic-Cretaceous Intra-Oceanic Subduction Evolution in the Northwestern Panthalassa Ocean Using Ocean Plate Stratigraphy From Hokkaido, Japan. Tectonics 40 (8). e2019TC005673.

Boschman, L.M., Van Hinsbergen, D.J., Langereis, C.G., Flores, K.E., Kamp, P.J., Kimbrough, D.L., Spakman, W., 2021b. Reconstructing lost plates of the Panthalassa Ocean through paleomagnetic data from circum-Pacific accretionary orogens. Am. J. Sci. 321 (6), 907–954.

Boyden, J.A., Müller, R.D., Gurnis, M., Torsvik, T.H., Clark, J.A., Turner, M., Cannon, J.S., 2011. Next-generation plate-tectonic reconstructions using GPlates. Geoinformatics: Cyberinfrastructure for the Solid Earth Sciences. Cambridge University Press, Cambridge 2011, 95–113.

Breitfeld, H.T., Hall, R., Galin, T., Forster, M.A., BouDagher-Fadel, M.K., 2017. A Triassic to Cretaceous Sundaland-Pacific subduction margin in West Sarawak, Borneo. Tectonophysics 694, 35–56.
Breitfeld, H.T., Hall, R., Galin, T., BouDagher-Fadel, M.K., 2018. Unravelling the stratigraphy and sedimentation history of the uppermost Cretaceous to Eocene sediments of the Kuching Zone in West Sarawak (Malaysia), Borneo. J. Asian Earth Sci. 160, 200–223.
Briais, A., Patriat, P., Tapponnier, P., 1993. Updated interpretation of magnetic anomalies and seafloor spreading stages in the South China Sea: Implications for the Tertiary tectonics of Southeast Asia. J. Geophys. Res. Solid Earth 98 (B4), 6299–6328.
Brocher, T.M., 1985. On the formation of the Vitiaz Trench lineament and North Fiji Basin. Geological investigations of the Northern Melanesian Borerland, Circum-Pacific Council for Energy and Mineral Resources Earth Science Series 3, 13–33.
Brown, D., Ryan, P.D., Byrne, T., Chan, Y.C., Rau, R.J., Lu, C.Y., Wang, Y.J., 2011. The arc–continent collision in Taiwan. Arc-continent collision, 213–245.
Brown, D., Alvarez-Marron, J., Biete, C., Kuo-Chen, H., Camanni, G., Ho, C.W., 2017. How the structural architecture of the Eurasian continental margin affects the structure, seismicity, and topography of the south central Taiwan fold-and-thrust belt. Tectonics 36 (7), 1275–1294.
Brown, D., Alvarez-Marron, J., Camanni, G., Biete, C., Kuo-Chen, H., Wu, Y.M., 2022. Structure of the south-central Taiwan fold-and-thrust belt: Testing the viability of the model. Earth Sci. Rev. 231, 104094.
Burton-Johnson, A., Macpherson, C.G., Millar, I.L., Whitehouse, M.J., Ottley, C.J., Nowell, G.M., 2020. A Triassic to Jurassic arc in north Borneo: Geochronology, geochemistry, and genesis of the Segama Valley Felsic Intrusions and the Sabah ophiolite. Gondw. Res. 84, 229–244.
Buys, J., Spandler, C., Holm, R.J., Richards, S.W., 2014. Remnants of ancient Australia in Vanuatu: Implications for crustal evolution in island arcs and tectonic development of the southwest Pacific. Geology 42 (11), 939–942.
Camanni, G., Ye, Q., 2022. The significance of fault reactivation on the Wilson cycle undergone by the northern South China Sea area in the last 60 Myr. Earth Sci. Rev. 225, 103893.
Cande, S.C., Stock, J.M., 2004. Pacific—Antarctic—Australia motion and the formation of the Macquarie Plate. Geophys. J. Int. 157 (1), 399–414.
Cande, S.C., Patriat, P., Dyment, J., 2010. Motion between the Indian, Antarctic and African plates in the early Cenozoic. Geophys. J. Int. 183 (1), 127–149.
Cao, L., Shao, L., Qiao, P., Cui, Y., Zhang, G., Zhang, X., 2021. Formation and paleogeographic evolution of the Palawan continental terrane along the Southeast Asian margin revealed by detrital fingerprints. Bulletin 133 (5–6), 1167–1193.
Cao, L., Shao, L., van Hinsbergen, D.J., Jiang, T., Xu, D., Cui, Y., 2023. Provenance and evolution of East Asian large rivers recorded in the East and South China Seas: A review. Geological Society of America Bulletin.
Casey, J.F., Dewey, J.F., 1984. Initiation of subduction zones along transform and accreting plate boundaries, triple-junction evolution, and forearc spreading centres—implications for ophiolitic geology and obduction. Geol. Soc. Lond. Spec. Publ. 13 (1), 269–290.
Chambers, L.M., Pringle, M.S., Fitton, J.G., 2004. Phreatomagmatic eruptions on the Ontong Java Plateau: an Aptian 40Ar/39Ar age for volcaniclastic rocks at ODP Site 1184. Geol. Soc. Lond. Spec. Publ. 229 (1), 325–331.
Chandler, M.T., Wessel, P., Taylor, B., Seton, M., Kim, S.S., Hyeong, K., 2012. Reconstructing Ontong Java Nui: Implications for Pacific absolute plate motion, hotspot drift and true polar wander. Earth Planet. Sci. Lett. 331, 140–151.
Charlton, T.R., Hall, R., Partoyo, E., 1991. The geology and tectonic evolution of Waigeo Island, NE Indonesia. J. SE Asian Earth Sci. 6 (3–4), 289–297.
Chen, W.S., Huang, Y.C., Liu, C.H., Feng, H.T., Chung, S.L., Lee, Y.H., 2016. UPb zircon geochronology constraints on the ages of the Tananao Schist Belt and timing of orogenic events in Taiwan: Implications for a new tectonic evolution of the South China Block during the Mesozoic. Tectonophysics 686, 68–81.
Chen, W.S., Chung, S.L., Chou, H.Y., Zugeerbai, Z., Shao, W.Y., Lee, Y.H., 2017. A reinterpretation of the metamorphic Yuli belt: Evidence for a middle-late Miocene accretionary prism in eastern Taiwan. Tectonics 36 (2), 188–206.
Chivas, A.R., McDougall, I., 1978. Geochronology of the Koloula porphyry copper prospect, Guadalcanal. Solomon Islands. Economic Geology 73 (5), 678–689.
Chung, S.L., Sun, S.S., 1992. A new genetic model for the East Taiwan Ophiolite and its implications for Dupal domains in the Northern Hemisphere. Earth Planet. Sci. Lett. 109 (1–2), 133–145.
Cloos, M., Sapiie, B., van Ufford, A.Q., Weiland, R.J., Warren, P.Q., McMahon, T.P., 2005. Collisional delamination in New Guinea: The geotectonics of subducting slab breakoff. GSA Special Papers.
Cluzel, D., Meffre, S., 2019. In search of Gondwana heritage in the Outer Melanesian Arc: no pre-upper Eocene detrital zircons in Viti Levu river sands (Fiji Islands). Aust. J. Earth Sci. 66 (2), 265–277.
Cluzel, D., Aitchison, J.C., Picard, C., 2001. Tectonic accretion and underplating of mafic terranes in the Late Eocene intraoceanic fore-arc of New Caledonia (Southwest Pacific): geodynamic implications. Tectonophysics 340 (1–2), 23–59.
Cluzel, D., Jourdan, F., Meffre, S., Maurizot, P., Lesimple, S., 2012a. The metamorphic sole of New Caledonia ophiolite: 40Ar/39Ar, U-Pb, and geochemical evidence for subduction inception at a spreading ridge. Tectonics 31 (3).
Cluzel, D., Maurizot, P., Collot, J., Sevin, B., 2012b. An outline of the Geology of New Caledonia; from Permian-Mesozoic Southeast Gondwanaland active margin to Cenozoic obduction and supergene evolution. Episodes J. Int. Geosci. 35 (1), 72–86.
Cluzel, D., Whitten, M., Meffre, S., Aitchison, J.C., Maurizot, P., 2018. A Reappraisal of the Poya Terrane (New Caledonia): Accreted Late Cretaceous-Paleocene Marginal Basin Upper Crust, Passive Margin Sediments, and Early Eocene E-MORB Sill Complex. Tectonics 37 (1), 48–70.
Cogné, J.P., Kravchinsky, V.A., Halim, N., Hankard, F., 2005. Late Jurassic-Early Cretaceous closure of the Mongol-Okhotsk Ocean demonstrated by new Mesozoic palaeomagnetic results from the Trans-Baikal area (SE Siberia). Geophys. J. Int. 163 (2), 813–832.
Cole, W.S., 1950. Larger foraminifers from the Palau Islands. US Geological Survey Professional Paper, B 221, 21–26.
Cole, J., McCabe, R., Moriarty, T., Malicse, J.A., Delfin, F.G., Tebar, H., Ferrer, H.P., 1989. A preliminary Neogene paleomagnetic data set from Leyte and its relation to motion on the Philippine fault. Tectonophysics 168 (1–3), 205–220.
Collot, J., Herzer, R., Lafoy, Y., Geli, L., 2009. Mesozoic history of the Fairway-Aotea Basin: Implications for the early stages of Gondwana fragmentation. Geochem. Geophys. Geosyst. 10 (12).
Collot, J.Y., Malahoff, A., Récy, J., Latham, G., Missègue, F., 1987. Overthrust emplacement of New Caledonia ophiolite: geophysical evidence. Tectonics 6 (3), 215–232.
Collot, J., Vendé-Leclerc, M., Rouillard, P., Lafoy, Y., Géli, L., 2012. Map helps unravel complexities of the southwestern Pacific Ocean. Eos Trans. AGU 93 (1), 1–2.
Conand, C., Mouthereau, F., Ganne, J., Lin, A.T.S., Lahfid, A., Daudet, M., Mesalles, L., Giletycz, S., Bonzani, M., 2020. Strain partitioning and exhumation in oblique Taiwan collision: Role of rift architecture and plate kinematics. Tectonics 39 (4). e2019TC005798.
Cosca, M., Arculus, R., Pearce, J., Mitchell, J., 1998. 40Ar/39Ar and K-Ar geochronological age constraints for the inception and early evolution of the Izu–Bonin–Mariana arc system. Isl. Arc 7 (3), 579–595.
Coulson, F.I., Vedder, J.G., 1986. Geology of the central and western Solomon Islands. Geology and Offshore Resources of Pacific Island Arcs–central and western Solomon Islands 4, 59–87.
Cowley, S., Mann, P., Coffin, M.F., Shipley, T.H., 2004. Oligocene to Recent tectonic history of the Central Solomon intra-arc basin as determined from marine seismic reflection data and compilation of onland geology. Tectonophysics 389 (3–4), 267–307.
Cox, A., Hart, R.B., 1986. Plate Tectonics: How It Works. Blackwell Scientific Publications, Inc, Boston, p. 392.
Crameri, F., Magni, V., Domeier, M., Shephard, G.E., Chotalia, K., Cooper, G., Thielmann, M., 2020. A transdisciplinary and community-driven database to unravel subduction zone initiation. Nat. Commun. 11 (1), 3750.
Crawford, A.J., Meffre, S., Symonds, P.A., 2003. 120 to 0 Ma tectonic evolution of the southwest Pacific and analogous geological evolution of the 600 to 220 Ma Tasman Fold Belt System. Geological Society of Australia Special Publication 22, 377–397.
Croon, M.B., Cande, S.C., Stock, J.M., 2008. Revised Pacific-Antarctic plate motions and geophysics of the Menard Fracture Zone. Geochem. Geophys. Geosyst. 9 (7).
Crowhurst, P.V., Maas, R., Hill, K.C., Foster, D.A., Fanning, C.M., 2004. Isotopic constraints on crustal architecture and Permo-Triassic tectonics in New Guinea: Possible links with eastern Australia. Aust. J. Earth Sci. 51 (1), 107–122.
Curray, J.R., 2005. Tectonics and history of the Andaman Sea region. J. Asian Earth Sci. 25 (1), 187–232.
David Jr, S., Stephan, J.F., Delteil, J., Müller, C., Butterlin, J., Bellon, H., Billedo, E., 1997. Geology and tectonic history of Southeastern Luzon. Philippines. Journal of Asian Earth Sciences 15 (4–5), 435–452.
Davies, H.L., 1980a. Aitape-Vanimo - 1: 250 ,000 Geological Series. Geological Survey of Papua New Guinea. Dept. of Minerals and Energy, Port Moresby.
Davies, H.L., 1980b. Folded thrust fault and associated metamorphism in the Suckling-Dayman massif, Papua New Guinea. Am. J. Sci. 280A, 171–191.
Davies, H.L., 1982. Mianmin – 1: 250 000 geological series. Geological Survey of Papua New Guinea, Dept. of Minerals and Energy, Port Moresby.
Davies, H.L., 2005. The geology of Bougainville. Bougainville before the conflict (eds AJ Regan & HM Griffin), 20–30.
Davies, H.L., 2012. The geology of New Guinea-the cordilleran margin of the Australian continent. Episodes Journal of International Geoscience 35 (1), 87–102.
Davies, H.L., Jaques, A.L., 1984. Emplacement of ophiolite in Papua New Guinea. Geol. Soc. Lond. Spec. Publ. 13 (1), 341–349.
Davies, H.L., Smith, I.E., 1971. Geology of eastern Papua. Geol. Soc. Am. Bull. 82 (12), 3299–3312.
Davies, H.L., Warren, R.G., 1988. Origin of eclogite-bearing, domed, layered metamorphic complexes ("core complexes") in the D'Entrecasteaux islands. Papua New Guinea. Tectonics 7 (1), 1–21.
De Jesus, J.V., Yumul, G.P., Faustino, D.V., 2000. The Cansiwang Melange of southeast Bohol (central Philippines): origin and tectonic implications. Isl. Arc 9 (4), 565–574.
Decker, J., Ferdian, F., Morton, A., Fanning, M., & White, L. T. (2017). New geochronology data from eastern Indonesia–An aid to understanding sedimentary provenance in a frontier region.
Defant, M.J., Jacques, D., Maury, R.C., de Boer, J., Joron, J.L., 1989. Geochemistry and tectonic setting of the Luzon arc. Philippines. Geological Society of America Bulletin 101 (5), 663–672.
Defant, M.J., Maury, R., Joron, J.L., Feigenson, M.D., Leterrier, J., Bellon, H., Richard, M., 1990. The geochemistry and tectonic setting of the northern section of the Luzon arc (the Philippines and Taiwan). Tectonophysics 183 (1–4), 187–205.
DeMets, C., Gordon, R.G., Argus, D.F., 2010. Geologically current plate motions. Geophys. J. Int. 181 (1), 1–80.

DeMets, C., Iaffaldano, G., Merkouriev, S., 2015. High-resolution Neogene and quaternary estimates of Nubia-Eurasia-North America plate motion. Geophys. J. Int. 203 (1), 416–427.
DeMets, C., Merkouriev, S., Sauter, D., 2021. High resolution reconstructions of the Southwest Indian Ridge, 52 Ma to present: implications for the breakup and absolute motion of the Africa plate. Geophys. J. Int. 226 (3), 1461–1497.
Deng, J., Yang, X., Zhang, Z.F., Santosh, M., 2015. Early Cretaceous arc volcanic suite in Cebu Island, Central Philippines and its implications on paleo-Pacific plate subduction: Constraints from geochemistry, zircon U-Pb geochronology and Lu–Hf isotopes. Lithos 230, 166–179.
Deng, J., Yang, X., Qi, H., Zhang, Z.F., Mastoi, A.S., Sun, W., 2017. Early Cretaceous high-Mg adakites associated with Cu-Au mineralization in the Cebu Island, Central Philippines: Implication for partial melting of the paleo-Pacific Plate. Ore Geol. Rev. 88, 251–269.
Deng, J., Yang, X., Qi, H., Zhang, Z.F., Mastoi, A.S., Al Emil, G.B., Sun, W., 2019. Early Cretaceous adakite from the Atlas porphyry Cu-Au deposit in Cebu Island, Central Philippines: Partial melting of subducted oceanic crust. Ore Geol. Rev. 110, 102937.
Deng, J., Yang, X., Zhang, L.P., Duan, L., Mastoi, A.S., Liu, H., 2020. An overview on the origin of adakites/adakitic rocks and related porphyry Cu-Au mineralization, Northern Luzon. Philippines. Ore Geology Reviews 124, 103610.
Deschamps, A., Lallemand, S., 2002. The West Philippine Basin: An Eocene to early Oligocene back arc basin opened between two opposed subduction zones. Journal of Geophysical Research: Solid. Earth 107 (B12), EPM-1.
Deschamps, A., Monié, P., Lallemand, S., Hsu, S.K., Yeh, K.Y., 2000. Evidence for Early Cretaceous oceanic crust trapped in the Philippine Sea Plate. Earth Planet. Sci. Lett. 179 (3–4), 503–516.
Dewey, J.F., Casey, J.F., 2011. The origin of obducted large-slab ophiolite complexes. Arc-continent collision, 431–444.
Diegor, W.G., 1996. The ophiolitic basement complex of Cebu. Journal of the Geological Society of the Philippines 51, 48–60.
Dimalanta, C.B., Suerte, L.O., Yumul, G.P., Tamayo, R.A., Ramos, E.G.L., 2006. A Cretaceous supra-subduction oceanic basin source for Central Philippine ophiolitic basement complexes: Geological and geophysical constraints. Geosci. J. 10, 305–320.
Dimalanta, C.B., Ramos, E.G.L., Yumul Jr, G.P., Bellon, H., 2009. New features from the Romblon Island Group: Key to understanding the arc–continent collision in Central Philippines. Tectonophysics 479 (1–2), 120–129.
Dimalanta, C.B., Faustino-Eslava, D.V., Gabo-Ratio, J.A.S., Marquez, E.J., Padrones, J.T., Payot, B.D., Yumul Jr, G.P., 2020. Characterization of the proto-Philippine Sea Plate: Evidence from the emplaced oceanic lithospheric fragments along eastern Philippines. Geosci. Front. 11 (1), 3–21.
Domeier, M., Shephard, G.E., Jakob, J., Gaina, C., Doubrovine, P.V., Torsvik, T.H., 2017. Intraoceanic subduction spanned the Pacific in the Late Cretaceous-Paleocene. Science. Advances 3 (11), eaao2303.
Dong, D., Zhang, Z., Bai, Y., Fan, J., Zhang, G., 2018. Topographic and sedimentary features in the Yap subduction zone and their implications for the Caroline Ridge subduction. Tectonophysics 722, 410–421.
Doo, W.B., Hsu, S.K., Yeh, Y.C., Tsai, C.H., Chang, C.M., 2015. Age and tectonic evolution of the northwest corner of the West Philippine Basin. Mar. Geophys. Res. 36, 113–125.
Doubrovine, P.V., Steinberger, B., Torsvik, T.H., 2012. Absolute plate motions in a reference frame defined by moving hot spots in the Pacific, Atlantic, and Indian oceans. J. Geophys. Res. Solid Earth 117 (B9).
Doust, H. (1990). Geology of the Sepik basin, Papua New Guinea (PNG) *Proceedings of the First PNG Petroleum Convention,* 461-478.
Dow, D.B., Sukamto, R., 1984. Western Irian Jaya: the end-product of oblique plate convergence in the late Tertiary. Tectonophysics 106 (1–2), 109–139.
Dycoco, J.M.A., Payot, B.D., Valera, G.T.V., Labis, F.A.C., Pasco, J.A., Perez, A.D., Tani, K., 2021. Juxtaposition of Cenozoic and Mesozoic ophiolites in Palawan island, Philippines: New insights on the evolution of the Proto-South China Sea. Tectonophysics 819, 229085.
Encarnación, J., 2004. Multiple ophiolite generation preserved in the northern Philippines and the growth of an island arc complex. Tectonophysics 392 (1–4), 103–130.
Encarnación, J.P., Mukasa, S.B., Obille Jr, E.C., 1993. Zircon U-Pb geochronology of the Zambales and Angat Ophiolites, Luzon, Philippines: Evidence for an Eocene arc-back arc pair. J. Geophys. Res. Solid Earth 98 (B11), 19991–20004.
Engebretson, D.C., Cox, A., Gordon, R.G., 1985. Relative motions between oceanic and continental plates in the Pacific basin. GSA Special Papers 206.
Evans, C.A., Hawkins, J.W., Moore, G.F., 1983. Petrology and geochemistry of ophiolitic and associated volcanic rocks on the Talaud Islands, Molucca Sea Collision Zone, northeast Indonesia. Geodynamics of the Western Pacific-Indonesian Region 11, 159–172.
Fabbri, O., Monié, P., Fournier, M., 2004. Transtensional deformation at the junction between the Okinawa trough back-arc basin and the SW Japan island arc. Geol. Soc. Lond. Spec. Publ. 227 (1), 297–312.
Faccenna, C., Becker, T.W., Lallemand, S., Steinberger, B., 2012. On the role of slab pull in the Cenozoic motion of the Pacific plate. Geophys. Res. Lett. 39 (3).
Fairbridge, R. W., & Stewart Jr, H. B. (1960). Alexa Bank, a drowned atoll on the Melanesian Border Plateau. *Deep Sea Research (1953), 7*(2), 100-116.
Falvey, D.A., Taylor, L.W., 1974. Queensland Plateau and Coral Sea Basin: structural and time-stratigraphic patterns. Explor. Geophys. 5 (4), 123–126.
Faure, M., Ishida, K., 1990. The Mid-Upper Jurassic olistostrome of the west Philippines: a distinctive key-marker for the North Palawan block. J. SE Asian Earth Sci. 4 (1), 61–67.
Faustino, D.V., Yumul, G.P., De Jesus, J.V., Dimalanta, C.B., Aitchison, J.C., Zhou, M.F., De Leon, M.M., 2003. Geology of southeast Bohol, central Philippines: accretion and sedimentation in a marginal basin. Aust. J. Earth Sci. 50 (4), 571–583.
Fisher, D.M., Lu, C.-Y., Chu, H.-T., 2002. Taiwan slate belt: Insights into the ductile interior of an arc-continent collision. Geol. Soc. Am. Spec. Pap. 358, 93–106.
Francis, G., 1988. Stratigraphy of Manus Island, Western New Ireland Basin, Papua New Guinea. Geology and Offshore Resources of Pacific Island Arcs-New Ireland and Manus Region, Papua New Guinea 9, 31–40.
Fujiwara, T., Tamaki, K., Fujimoto, H., Ishii, T., Seama, N., Toh, H., Kinoshita, H., 1995. Morphological studies of the Ayu trough, Philippine sea–Caroline plate boundary. Geophys. Res. Lett. 22 (2), 109–112.
Fuller, M., Haston, R., Almasco, J., 1989. Paleomagnetism of the Zambales ophiolite, Luzon, northern Philippines. Tectonophysics 168 (1–3), 171–203.
Fuller, M., Haston, R., Lin, J.L., Richter, B., Schmidtke, E., Almasco, J., 1991. Tertiary paleomagnetism of regions around the South China Sea. J. SE Asian Earth Sci. 6 (3–4), 161–184.
Furlong, K.P., Kamp, P.J.J., 2013. Changes in plate boundary kinematics: Punctuated or smoothly varying—Evidence from the Mid-Cenozoic transition from lithospheric extension to shortening in New Zealand. Tectonophysics 608, 1328–1342.
Gaina, C., Müller, D., 2007. Cenozoic tectonic and depth/age evolution of the Indonesian gateway and associated back-arc basins. Earth Sci. Rev. 83 (3–4), 177–203.
Gaina, C., Müller, D.R., Royer, J.Y., Stock, J., Hardebeck, J., Symonds, P., 1998. The tectonic history of the Tasman Sea: a puzzle with 13 pieces. J. Geophys. Res. Solid Earth 103 (B6), 12413–12433.
Gaina, C., Müller, R.D., Royer, J.Y., Symonds, P., 1999. Evolution of the Louisiade triple junction. J. Geophys. Res. Solid Earth 104 (B6), 12927–12939.
Gans, P.B., Mortimer, N., Patriat, M., Turnbull, R.E., Crundwell, M.P., Agranier, A., Collot, J., 2023. Detailed 40Ar/39Ar geochronology of the Loyalty and Three Kings Ridges clarifies the extent and sequential development of Eocene to Miocene southwest Pacific remnant volcanic arcs. Geochem. Geophys. Geosyst. 24 (2). e2022GC010670.
Garrison, R.E., Espiritu, E., Horan, L.J., Mack, L.E., 1979. Petrology, sedimentology, and diagenesis of hemipelagic limestone and tuffaceous turbidities in the Aksitero Formation, central Luzon, Philippines. *U.S.* Geological Survey Professional Papers 1112, 1–16.
Geary, E.E., 1986. Tectonic significance of basement complexes and ophiolites in the northern Philippines: Results of geological, geochronological and geochemical investigations. Cornell University, Ithaca, New York, p. 221 p.. Ph.D. thesis)..
Geary, E.E., Kay, R.W., 1989. Identification of an early cretaceous ophiolite in the Camarines Norte-Calaguas Islands basement complex, eastern Luzon. Philippines. Tectonophysics 168 (1–3), 109–126.
Geary, E.E., Harrison, T.M., Heizler, M., 1988. Diverse ages and origins of basement complexes, Luzon. Philippines. Geology 16 (4), 341–344.
Gill, J., Todd, E., Hoernle, K., Hauff, F., Price, A.A., Jackson, M.G., 2022. Breaking up is hard to do: Magmatism during oceanic arc breakup, subduction reversal, and cessation. Geochem. Geophys. Geosyst. 23 (12). e2022GC010663.
Gong, L., Hollings, P., Zhang, Y., Tian, J., Li, D., Chen, H., 2021. Contribution of an Eastern Indochina-derived fragment to the formation of island arc systems in the Philippine Mobile Belt. GSA Bull. 133 (9–10), 1979–1995.
Granot, R., Dyment, J., 2018. Late Cenozoic unification of East and West Antarctica. Nat. Commun. 9 (1), 3189.
Granot, R., Cande, S.C., Stock, J.M., Damaske, D., 2013. Revised Eocene-Oligocene kinematics for the West Antarctic rift system. Geophys. Res. Lett. 40 (2), 279–284.
Griffin, T.J., Moresby, P., 1983. Granitoids of the Tertiary continent-island are collision zone, Papua New Guinea. Geological Society of America. Memoir i59, 61–76.
Grobys, J.W., Gohl, K., Eagles, G., 2008. Quantitative tectonic reconstructions of Zealandia based on crustal thickness estimates. Geochem. Geophys. Geosyst. 9 (1).
Guilmette, C., van Hinsbergen, Smit, M.A., Godet, A., Fournier-Roy, F., Butler, J.P. ... Hodges, K., 2023. Formation of the Xigaze Metamorphic Sole under Tibetan continental lithosphere reveals generic characteristics of subduction initiation. Communications Earth & Environment 4 (1), 339.
Guilmette, C., Smit, M.A., van Hinsbergen, D.J., Gürer, D., Corfu, F., Charette, B., Savard, D., 2018. Forced subduction initiation recorded in the sole and crust of the Semail Ophiolite of Oman. Nat. Geosci. 11 (9), 688–695.
Gungor, A., Lee, G.H., Kim, H.J., Han, H.C., Kang, M.H., Kim, J., Sunwoo, D., 2012. Structural characteristics of the northern Okinawa Trough and adjacent areas from regional seismic reflection data: geologic and tectonic implications. Tectonophysics 522, 198–207.
Guotana, J.M.R., Payot, B.D., Dimalanta, C.B., Ramos, N.T., Faustino-Eslava, D.V., Queaño, K.L., Yumul Jr, G.P., 2017. Arc and backarc geochemical signatures of the proto-Philippine Sea Plate: Insights from the petrography and geochemistry of the Samar Ophiolite volcanic section. J. Asian Earth Sci. 142, 77–92.
Guotana, J.M.R., Payot, B.D., Dimalanta, C.B., Ramos, N.T., Faustino-Eslava, D.V., Queaño, K.L., Yumul Jr, G.P., 2018. Petrological and geochemical characteristics of the Samar Ophiolite ultramafic section: implications on the origins of the ophiolites in Samar and Leyte islands. Philippines. International Geology Review 60 (4), 401–417.
Gürer, D., Granot, R., van Hinsbergen, D.J., 2022. Plate tectonic chain reaction revealed by noise in the Cretaceous quiet zone. Nat. Geosci. 15 (3), 233–239.
Gurnis, M., Hall, C., Lavier, L., 2004. Evolving force balance during incipient subduction. Geochem. Geophys. Geosyst. 5 (7).

Hall, R., 1996. Reconstructing Cenozoic SE Asia. Geol. Soc. Lond. Spec. Publ. 106 (1), 153–184.
Hall, R., 2002. Cenozoic geological and plate tectonic evolution of SE Asia and the SW Pacific: computer-based reconstructions, model and animations. J. Asian Earth Sci. 20 (4), 353–431.
Hall, R., 2012. Late Jurassic-Cenozoic reconstructions of the Indonesian region and the Indian Ocean. Tectonophysics 570, 1–41.
Hall, R., Breitfeld, H.T., 2017. Nature and demise of the proto-South China Sea. Bull. Geol. Soc. Malaysia 63, 61–76.
Hall, C.E., Gurnis, M., Sdrolias, M., Lavier, L.L., Müller, R.D., 2003. Catastrophic initiation of subduction following forced convergence across fracture zones. Earth Planet. Sci. Lett. 212 (1–2), 15–30.
Hall, R., Spakman, W., 2002. Subducted slabs beneath the eastern Indonesia-Tonga region: insights from tomography. Earth Planet. Sci. Lett. 201 (2), 321–336.
Hall, R., Audley-Charles, M.G., Banner, F.T., Hidayat, S., Tobing, S.L., 1988. Basement rocks of the Halmahera region, eastern Indonesia: a Late Cretaceous-Early Tertiary arc and fore-arc. J. Geol. Soc. London 145 (1), 65–84.
Haston, R., Fuller, M., Schmidtke, E., 1988. Paleomagnetic results from Palau, West Caroline Islands: a constraint on Philippine Sea plate motion. Geology 16 (7), 654–657.
Hawkins, J.W., 1985. Geology of the composite terranes of east and central Mindanao. Circum Pacific Council Publications, Earth Science Series 1, 437–463.
Hawkins, J., Batiza, R., 1977. Metamorphic rocks of the Yap arc-trench system. Earth Planet. Sci. Lett. 37 (2), 216–229.
Hawkins, J.W., Evans, C.A., 1983. Geology of the Zambales Range, Luzon, Philippine Islands: Ophiolite derived from an island arc-back arc basin pair. Washington DC American Geophysical Union Geophysical Monograph Series 27, 95–123.
Hawkins, J.W., Ishizuka, O., 2009. Petrologic evolution of Palau, a nascent island arc. Isl. Arc 18 (4), 599–641.
Hegarty, K.A., Weissel, J.K., Hayes, D.E., 1983. Convergence at the Caroline-Pacific plate boundary: collision and subduction. Washington DC American Geophysical Union Geophysical Monograph Series 27, 326–348.
Herzer, R.H., Mascle, J., 1996. Anatomy of a continent-backarc transform—The Vening Meinesz Fracture Zone northwest of New Zealand. Mar. Geophys. Res. 18 (2–4), 401–427.
Herzer, R.H., Barker, D.H.N., Roest, W.R., Mortimer, N., 2011. Oligocene-Miocene spreading history of the northern South Fiji Basin and implications for the evolution of the New Zealand plate boundary. Geochemistry, Geophysics, Geosystems 12, Q02004.
Herzer, R.H., Davy, B.W., Mortimer, N., Quilty, P.G., Chaprioniere, G.C.H., Jones, C.M., Crawford, A.J., Hollis, C.J., 2009. Seismic stratigraphy and structure of the Northland Plateau and the development of the Vening Meinesz transform margin. SW Pacific Ocean. Marine Geophysical Researches 30 (1), 21–60.
Hickey-Vargas, R., 1998. Origin of the Indian Ocean-type isotopic signature in basalts from Philippine Sea plate spreading centers: An assessment of local versus large-scale processes. J. Geophys. Res. Solid Earth 103 (B9), 20963–20979.
Hickey-Vargas, R., 2005. Basalt and tonalite from the Amami Plateau, northern West Philippine Basin: New Early Cretaceous ages and geochemical results, and their petrologic and tectonic implications. Isl. Arc 14 (4), 653–665.
Hickey-Vargas, R., Ishizuka, O., Bizimis, M., 2013. Age and geochemistry of volcanic clasts from DSDP Site 445, Daito Ridge and relationship to Minami-Daito Basin and early Izu-Bonin arc magmatism. J. Asian Earth Sci. 70, 193–208.
Hilde, T.W., Lee, C.S., 1984. Origin and evolution of the West Philippine Basin: a new interpretation. Tectonophysics 102 (1–4), 85–104.
Hill, K.C., 1991. Structure of the Papuan fold belt. Papua New Guinea. AAPG bulletin 75 (5), 857–872.
Hill, E.J., 1994. Geometry and kinematics of shear zones formed during continental extension in eastern Papua New Guinea. J. Struct. Geol. 16 (8), 1093–1105.
Hill, E.J., Baldwin, S.L., 1993. Exhumation of high-pressure metamorphic rocks during crustal extension in the D'Entrecasteaux region, Papua New Guinea. J. Metam. Geol. 11 (2), 261–277.
Hill, K.C., Gleadow, A.J.W., 1989. Uplift and thermal history of the Papuan Fold Belt, Papua New Guinea: Apatite fission track analysis. Aust. J. Earth Sci. 36 (4), 515–539.
Hill, K.C., Hall, R., 2002. Mesozoic-Cainozoic evolution of Australia's New Guinea margin in a West Pacific context. Defining Australia: the Australian Plate as Part of Planet Earth: Geological Society of America and Geological Society of Australia, joint publication, special paper, 1–43.
Hill, K.C., Raza, A., 1999. Arc-continent collision in Papua Guinea: Constraints from fission track thermochronology. Tectonics 18 (6), 950–966.
Hinz, K., Block, M., Kudrass, H.R., Meyer, H., 1991. Structural elements of the Sulu Sea, Philippines. *AAPG Bull.* 78.
Ho, C.S., 1969. Geological significance of potassium-argon ages of the Chimei igneous complex in eastern Taiwan. Bull. Geol. Surv. Taiwan 20, 63–74.
Ho, C.S., 1986. A synthesis of the geologic evolution of Taiwan. Tectonophysics 125 (1–3), 1–16.
Hobson, D.M., 1986. A thin skinned model for the Papuan thrust belt and some implications for hydrocarbon exploration. The APPEA Journal 26 (1), 214–225.
Hollings, P., Wolfe, R., Cooke, D.R., Waters, P.J., 2011. Geochemistry of Tertiary igneous rocks of northern Luzon, Philippines: Evidence for a back-arc setting for alkalic porphyry copper-gold deposits and a case for slab roll-back? Econ. Geol. 106 (8), 1257–1277.
Hollis, C.J., Hanson, J.A., 1991. Well-preserved late Paleocene Radiolaria from Tangihua Complex, Camp Bay, eastern Northland. Tane 33, 65–76.
Holm, R.J., Spandler, C., Richards, S.W., 2015. Continental collision, orogenesis and arc magmatism of the Miocene Maramuni arc. Papua New Guinea. Gondwana Research 28 (3), 1117–1136.
Holm, R.J., Rosenbaum, G., Richards, S.W., 2016. Post 8 Ma reconstruction of Papua New Guinea and Solomon Islands: Microplate tectonics in a convergent plate boundary setting. Earth Sci. Rev. 156, 66–81.
Home, P.C., Dalton, D.G., Brannan, J., 1990. Geological evolution of the western Papuan basin. In: Proceedings of the First PNG Petroleum Convention, pp. 107–117.
Honza, E., Fujioka, K., 2004. Formation of arcs and backarc basins inferred from the tectonic evolution of Southeast Asia since the Late Cretaceous. Tectonophysics 384 (1–4), 23–53.
Hou, Y., Shao, L., Cui, Y., Allen, M.B., Zhu, W., Qiao, P., Goh, T.L., 2022. Sediment features and provenance analysis of the late Mesozoic–early Cenozoic strata of the Ryukyu Islands: Implications for palaeogeography of East China Sea. Mar. Pet. Geol. 145, 105840.
Howell, D.G., 1980. Mesozoic accretion of exotic terranes along the New Zealand segment of Gondwanaland. Geology 8 (10), 487–491.
Huang, C.Y., Yuan, P.B., Tsao, S.J., 2006. Temporal and spatial records of active arc-continent collision in Taiwan: A synthesis. Geol. Soc. Am. Bull. 118 (3–4), 274–288.
Huang, C.Y., Chen, W.H., Wang, M.H., Lin, C.T., Yang, S., Li, X., Harris, R., 2018. Juxtaposed sequence stratigraphy, temporal-spatial variations of sedimentation and development of modern-forming forearc Lichi Mélange in North Luzon Trough forearc basin onshore and offshore eastern Taiwan: An overview. Earth Sci. Rev. 182, 102–140.
Huang, C.Y., Wang, P., Yu, M., You, C.F., Liu, C.S., Zhao, X., Yumul Jr, G.P., 2019. Potential role of strike-slip faults in opening up the South China Sea. Natl. Sci. Rev. 6 (5), 891–901.
Hussong, D.M., Uyeda, S., 1982. Tectonic processes and the history of the Mariana Arc: A synthesis of the results of deep-sea drilling project Leg 60. Initial Rep. Deep Sea Drill. Proj. 60, 909–929.
Hutchison, D.S., 1975. Basement geology of the North Sepik region. Papua New Guinea, Bureau of Mineral Resources, Australia, Record, p. 162.
Hutchison, D. S., & Norvick, M. (1978). Wewak, Papua New Guinea 1: 250,000 geological series. Geological Survey of Papua New Guinea, Dept. of Minerals and Energy, Port Moresby.
Hutchison, C.S., Bergman, S.C., Swauger, D.A., Graves, J.E., 2000. A Miocene collisional belt in north Borneo: uplift mechanism and isostatic adjustment quantified by thermochronology. J. Geol. Soc. London 157 (4), 783–793.
Hutchison, D.S., Norvick, M., 1980. Geology of the North Sepik region. Papua New Guinea, Bureau of Mineral Resources.
Imai, A., 2001. Generation and evolution of ore fluids for porphyry Cu-Au mineralization of the Santo Tomas II (Philex) deposit. Philippines. Resource Geology 51 (2), 71–96.
Ishizuka, O., Kimura, J.I., Li, Y.B., Stern, R.J., Reagan, M.K., Taylor, R.N., Haraguchi, S., 2006. Early stages in the evolution of Izu-Bonin arc volcanism: New age, chemical, and isotopic constraints. Earth Planet. Sci. Lett. 250 (1–2), 385–401.
Ishizuka, O., Yuasa, M., Tamura, Y., Shukuno, H., Stern, R.J., Naka, J., Taylor, R.N., 2010. Migrating shoshonitic magmatism tracks Izu–Bonin–Mariana intra-oceanic arc rift propagation. Earth Planet. Sci. Lett. 294 (1–2), 111–122.
Ishizuka, O., Tani, K., Reagan, M.K., Kanayama, K., Umino, S., Harigane, Y., Dunkley, D.J., 2011a. The timescales of subduction initiation and subsequent evolution of an oceanic island arc. Earth Planet. Sci. Lett. 306 (3–4), 229–240.
Ishizuka, O., Taylor, R.N., Yuasa, M., Ohara, Y., 2011b. Making and breaking an island arc: A new perspective from the Oligocene Kyushu-Palau arc, Philippine Sea. Geochem. Geophys. Geosyst. 12 (5).
Ishizuka, O., Taylor, R.N., Ohara, Y., Yuasa, M., 2013. Upwelling, rifting, and age-progressive magmatism from the Oki-Daito mantle plume. Geology 41 (9), 1011–1014.
Ishizuka, O., Tani, K., Harigane, Y., Yamazaki, T., Ohara, Y., 2015. Geologic and geochronological constraints on the Philippines Sea tectonics around 50 Ma. JpGU. 2015 Abstract.
Ishizuka, O., Hickey-Vargas, R., Arculus, R.J., Yogodzinski, G.M., Savov, I.P., Kusano, Y., Sudo, M., 2018. Age of Izu–Bonin–Mariana arc basement. Earth Planet. Sci. Lett. 481, 80–90.
Ishizuka, O., Tani, K., Taylor, R.N., Umino, S., Sakamoto, I., Yokoyama, Y., Sekimoto, S., 2022. Origin and age of magmatism in the northern Philippine Sea basins. Geochem. Geophys. Geosyst. 23 (4).
Isozaki, Y., Maruyama, S., Furuoka, F., 1990. Accreted oceanic materials in Japan. Tectonophysics 181 (1–4), 179–205.
Isozaki, Y., Aoki, K., Nakama, T., Yanai, S., 2010. New insight into a subduction-related orogen: A reappraisal of the geotectonic framework and evolution of the Japanese Islands. Gondw. Res. 18 (1), 82–105.
Ito, T., Kojima, Y., Kodaira, S., Sato, H., Kaneda, Y., Iwasaki, T., Ikawa, T., 2009. Crustal structure of southwest Japan, revealed by the integrated seismic experiment Southwest Japan 2002. Tectonophysics 472 (1–4), 124–134.
Iwamoto, H., Yamamoto, M., Seama, N., Kitada, K., Matsuno, T., Nogi, Y., Goto, T., Fujiwara, T., Suyehiro, K., Yamazaki, T., 2002. Tectonic evolution of the central Mariana Trough. *Eos Trans. AGU* 83 (47). Fall Meet. Suppl., abstract T72A-1235, 2002.
Jahn, B.M., 1986. Mid-ocean ridge or marginal basin origin of the East Taiwan Ophiolite: chemical and isotopic evidence. Contrib. Miner. Petrol. 92 (2), 194–206.

Jahn, B.M., Martineau, F., Comichet, J., 1984. Chronological significance of Sr isotopic compositions in the crystalline limestones of the Central Range Taiwan. Memoirs Geol. Soc. China 6, 295–301.
Jahn, B.M., Zhou, X.H., Li, J.L., 1990. Formation and tectonic evolution of southeastern China and Taiwan: isotopic and geochemical constraints. Tectonophysics 183 (1–4), 145–160.
Jahn, B.M., Chi, W.R., Yui, T.F., 1992. A Late Permian formation of Taiwan (marbles from Chia-Li well No. 1): Pb-Pb isochron and Sr isotopic evidence, and its regional geological significance. J. Geol. Soc. China 35, 193–218.
Jaques, A.L., 1976. High-K2O island-arc volcanic rocks from the Finisterre and Adelbert Ranges, northern Papua New Guinea. Geol. Soc. Am. Bull. 87 (6), 861–867.
Jaques, A.L., 1981. Petrology and petrogenesis of cumulate peridotites and gabbros from the Marum ophiolite complex, northern Papua New Guinea. J. Petrol. 22 (1), 1–40.
Jaques, A. L., & Robinson, G.P. (1976). Madang - Papua New Guinea 1: 250,000 geological series. Geological Survey of Papua New Guinea, Dept. of Minerals and Energy, Port Moresby.
Jaques, A. L., & Robinson, G.P. (1980). Bogia - Papua New Guinea 1: 250,000 geological series. Geological Survey of Papua New Guinea, Dept. of Minerals and Energy, Port Moresby.
Jaques, A.L., Chappell, B.W., 1980. Petrology and trace element geochemistry of the Papuan ultramafic belt. Contrib. Miner. Petrol. 75 (1), 55–70.
Jaques, A.L., Chappell, B.W., Taylor, S.R., 1983. Geochemistry of cumulus peridotites and gabbros from the Marum Ophiolite Complex, northern Papua New Guinea. Contrib. Miner. Petrol. 82, 154–164.
Jaques, A. L., & BW, C. (1978). Geochemistry of LIL-element enriched tholeiites from the Marum ophiolite complex, northern Papua New Guinea. Australian J. Geol. Geophys. 3(4), 297-310.
Johnson, T.L., 1979. Alternative model for emplacement of the Papuan ophiolite. Papua New Guinea. Geology 7 (10), 495–498.
Jolivet, L., Tamaki, K., Fournier, M., 1994. Japan Sea, opening history and mechanism: A synthesis. J. Geophys. Res. Solid Earth 99 (B11), 22237–22259.
Joseph, L.E., Finlayson, E.J., 1991. A revised stratigraphy of Muyua (Woodlark Island). Geological Survey of Papua New Guinea.
Joshima, M., Okuda, Y., Murakami, F., Kishimoto, K., Honza, E., 1986. Age of the Solomon Sea Basin from magnetic lineations. Geo-Mar. Lett. 6, 229–234.
Jost, B.M., Webb, M., White, L.T., 2018. The Mesozoic and Palaeozoic granitoids of north-western New Guinea. Lithos 312, 223–243.
Kamp, P.J.J., 1986. The mid-Cenozoic Challenger Rift System of western New Zealand and its implications for the age of Alpine fault inception. Geological Society of America Bulletin 97 (3), 255–281.
Karig, D.E., 1971. Structural history of the Mariana island arc system. Geol. Soc. Am. Bull. 82 (2), 323–344.
Karig, D.E., 1983. Accreted terranes in the northern part of the Philippine archipelago. Tectonics 2 (2), 211–236.
Keenan, T.E., Encarnación, J., Buchwaldt, R., Fernandez, D., Mattinson, J., Rasoazanamparany, C., Luetkemeyer, P.B., 2016. Rapid conversion of an oceanic spreading center to a subduction zone inferred from high-precision geochronology. Proc. Natl. Acad. Sci. 113 (47), E7359–E7366.
Kiminami, K., Miyashita, S., Kawabata, K., 1994. Ridge collision and in situ greenstones in accretionary complexes: An example from the Late Cretaceous Ryukyu Islands and southwest Japan margin. Isl. Arc 3 (2), 103–111.
Kimura, G., Hashimoto, Y., Kitamura, Y., Yamaguchi, A., Koge, H., 2014. Middle Miocene swift migration of the TTT triple junction and rapid crustal growth in southwest Japan: A review. Tectonics 33 (7), 1219–1238.
Kizaki, K., 1986. Geology and tectonics of the Ryukyu Islands. Tectonophysics 125 (1–3), 193–207.
Klimetz, M.P., 1987. The Mesozoic Tectonostratigraphic Terranes and Accretionary Heritage of South-Eastern Mainland Asia. Terrane Accretion and Orogenic Belts 19, 221–234.
Knittel, U., 1983. Age of the Cordon Syenite Complex and its implication on the Mid-Tertiary history of North Luzon. Philippine Geol 37 (2), 22–31.
Knittel, U., Walia, M., Suzuki, S., Dimalanta, C.B., Tamayo, R., Yang, T.F., Yumul Jr, G. P., 2017. Diverse protolith ages for the Mindoro and Romblon Metamorphics (Philippines): Evidence from single zircon U-Pb dating. Isl. Arc 26 (1), e12160.
Kobayashi, K., Fujioka, K., Fujiwara, T., Iwabuchi, Y., Kitazato, H., 1997. Why is the Palau Trench so deep? Deep-sea trench without plate convergence. Proceedings of the Japan Academy, Series B 73 (6), 89–94.
Koulali, A., Tregoning, P., McClusky, S., Stanaway, R., Wallace, L., Lister, G., 2015. New Insights into the present-day kinematics of the central and western Papua New Guinea from GPS. Geophys. J. Int. 202 (2), 993–1004.
Kravchinsky, V.A., Cogné, J.P., Harbert, W.P., Kuzmin, M.I., 2002. Evolution of the Mongol-Okhotsk Ocean as constrained by new palaeomagnetic data from the Mongol-Okhotsk suture zone. Siberia. Geophysical Journal International 148 (1), 34–57.
Kroenke, L., 1981. Site 451: East edge of the West Mariana Ridge. Initial Report of the Deep Sea Drilling Project 59, 405–483.
Kroenke, L.W., Eade, J.V., 1982. Three Kings Ridge: A west-facing arc. Geo-Mar. Lett. 2 (1–2), 5–10.
Kroenke, L.W., Resig, J.M., Cooper, P.A., 1986. Tectonics of the Southeastern Solomon Islands: Formation of the Malaita Anticlinorium. Geology and Offshore Resources of Pacific Island Arcs–central and western Solomon Islands 4, 109–116.
Kumagai, H., Kaneoka, I., Ishii, T., 1996. The active period of the Ayu Trough estimated from K-Ar ages: The southeastern spreading center of Philippine Sea Plate. Geochem. J. 30 (2), 81–87.
Lafoy, Y., Géli, L., Klingelhoefer, F., Vially, R., Sichler, B., Nouzé, H., 2005. Discovery of continental stretching and oceanic spreading in the Tasman Sea. Eos Trans. AGU 86 (10), 101–105.
Lai, Y.M., Song, S.R., Lo, C.H., Lin, T.H., Chu, M.F., Chung, S.L., 2017. Age, geochemical and isotopic variations in volcanic rocks from the Coastal Range of Taiwan: Implications for magma generation in the Northern Luzon Arc. Lithos 272, 92–115.
Lallemand, S., Arcay, D., 2021. Subduction initiation from the earliest stages to self-sustained subduction: Insights from the analysis of 70 Cenozoic sites. Earth Sci. Rev. 221, 103779.
Landmesser, C., Andrews, J., Packham, G., 1973. Aspects of the geology of the eastern Coral Sea and the western New Hebrides Basin. Init. Rep. Deep Sea Drilling Proj. 30, 647–662.
Lapierre, H., Jahn, B.M., Charvet, J., Yu, Y.W., 1997. Mesozoic felsic arc magmatism and continental olivine tholeiites in Zhejiang Province and their relationship with the tectonic activity in southeastern China. Tectonophysics 274 (4), 321–338.
Lapouille, A., 1982. Etude des bassins marginaux fossiles du Sud-Ouest Pacifique: bassin Nord d'Entrecasteaux, bassin Nord-Loyaute, bassin Sud-Fidjien. *Contribution a l'etude geodynamique du Sud-Ouest Pacifique*, Travaux et Documents de l'ORSTOM 147, 409–438.
Larson, R.L., Chase, C.G., 1972. Late Mesozoic evolution of the western Pacific Ocean. Geol. Soc. Am. Bull. 83 (12), 3627–3644.
Launay, J., Dupont, J., Lapouille, A., 1982. The Three Kings Ridge and the Norfolk Basin (southwest Pacific): An attempt at structural interpretation. South Pacific Marine Geological Notes 2, 121–130.
Le Dain, A.Y., Tapponnier, P., Molnar, P., 1984. Active faulting and tectonics of Burma and surrounding regions. J. Geophys. Res. Solid Earth 89 (B1), 453–472.
Lebrun, J.F., Lamarche, G., Collot, J.Y., Delteil, J., 2000. Abrupt strike-slip fault to subduction transition: The Alpine fault-Puysegur trench connection. New Zealand. Tectonics 19 (4), 688–706.
Lee, T.Y., Lawver, L.A., 1994. Cenozoic plate reconstruction of the South China Sea region. Tectonophysics 235 (1–2), 149–180.
Lee, T.Y., Lawver, L.A., 1995. Cenozoic plate reconstruction of Southeast Asia. Tectonophysics 251 (1–4), 85–138.
Lee, C.S., Shor Jr, G.G., Bibee, L.D., Lu, R.S., Hilde, T.W., 1980. Okinawa Trough: Origin of a back-arc basin. Mar. Geol. 35 (1–3), 219–241.
Letouzey, J., Kimura, M., 1986. The Okinawa Trough: genesis of a back-arc basin developing along a continental margin. Tectonophysics 125 (1–3), 209–230.
Li, Z.X., Li, X.H., Chung, S.L., Lo, C.H., Xu, X., Li, W.X., 2012. Magmatic switch-on and switch-off along the South China continental margin since the Permian: Transition from an Andean-type to a Western Pacific-type plate boundary. Tectonophysics 532, 271–290.
Li, C.F., Xu, X., Lin, J., Sun, Z., Zhu, J., Yao, Y., Zhang, G.L., 2014a. Ages and magnetic structures of the South China Sea constrained by deep tow magnetic surveys and IODP Expedition 349. Geochem. Geophys. Geosyst. 15 (12), 4958–4983.
Li, J., Zhang, Y., Dong, S., Johnston, S.T., 2014b. Cretaceous tectonic evolution of South China: A preliminary synthesis. Earth Sci. Rev. 134, 98–136.
Lin, C.T., Harris, R., Sun, W.D., Zhang, G.L., 2019. Geochemical and geochronological constraints on the origin and emplacement of the East Taiwan Ophiolite. Geochem. Geophys. Geosyst. 20 (4), 2110–2133.
Lindley, D., 1988. Early Cainozoic stratigraphy and structure of the Gazelle Peninsula, east New Britain: An example of extensional tectonics in the New Britain arc-trench complex. J. Geol. Soc. Aust. 35 (2), 231–244.
Lindley, I.D., 2006. New Britain Trench, Papua New Guinea: An extensional element in a regional sinistral strike-slip system. New Concepts in Global Tectonics Newsletter 41, 15–27.
Lindley, I.D., 2016. Plate flexure and volcanism: late cenozoic tectonics of the tabar–lihir–tanga–feni alkalic province, new Ireland basin, Papua New Guinea. Tectonophysics 677, 312–323.
Lindley, I.D., 2021. Cenozoic volcanism, tectonics and mineralisation of Woodlark Island (Muyuw), eastern Papua. Aust. J. Earth Sci. 68 (5), 609–627.
Ling, H.Y., Hall, R., Nichols, G.J., 1991. Early Eocene Radiolaria from Waigeo Island, Eastern Indonesia. J. SE Asian Earth Sci. 6 (3–4), 299–305.
Little, T.A., Hacker, B.R., Gordon, S.M., Baldwin, S.L., Fitzgerald, P.G., Ellis, S., Korchinski, M., 2011. Diapiric exhumation of Earth's youngest (UHP) eclogites in the gneiss domes of the D'Entrecasteaux Islands. Papua New Guinea. Tectonophysics 510 (1–2), 39–68.
Liu, B., Li, S.Z., Suo, Y.H., Li, G.X., Dai, L.M., Somerville, I.D., Yu, S., 2016. The geological nature and geodynamics of the Okinawa Trough, Western Pacific. Geol. J. 51, 416–428.
Liu, J., Li, S., Cao, X., Dong, H., Suo, Y., Jiang, Z., Zhou, J., Li, X., Zhang, R., Liu, L., Foulger, G.R., 2023. Back-Arc Tectonics and Plate Reconstruction of the Philippine Sea-South China Sea Region Since the Eocene. Geophys. Res. Lett. 50 (5). e2022GL102154.
Liu, B., Wu, J.H., Li, H., Wu, Q.H., Evans, N.J., Kong, H., Xi, X.S., 2020. Geochronology, geochemistry and petrogenesis of the Dengfuxian lamprophyres: Implications for the early Cretaceous tectonic evolution of the South China Block. Geochemistry 80 (2), 125598.
Lo, Y.C., Chih-Tung, C., Lo, C.H., Sun-Lin, C., 2020. Ages of ophiolitic rocks along plate suture in Taiwan orogen: Fate of the South China Sea from subduction to collision. TAO. Terr. Atmos. Ocean. Sci. 31 (4), 3.

Lo, C.H., Onstott, T.C., Chen, C.H., Lee, T., 1994. An assessment of $^{40}Ar/^{39}Ar$ dating for the whole-rock volcanic samples from the Luzon Arc near Taiwan. Chem. Geol. 114 (1–2), 157–178.
Lus, W.Y., McDougall, I., Davies, H.L., 2004. Age of the metamorphic sole of the Papuan Ultramafic Belt ophiolite. Papua New Guinea. Tectonophysics 392 (1–4), 85–101.
Maac, Y.O., Ylade, E.D., 1988. Stratigraphic and paleontologic studies of Tablas, Romblon. Report of Research and Development Cooperation ITIT Project 8319, 44–67.
Maffione, M., van Hinsbergen, D.J., de Gelder, G.I., van der Goes, F.C., Morris, A., 2017. Kinematics of Late Cretaceous subduction initiation in the Neo-Tethys Ocean reconstructed from ophiolites of Turkey, Cyprus, and Syria. J. Geophys. Res. Solid Earth 122 (5), 3953–3976.
Mahoney, J.J., Storey, M., Duncan, R.A., Spencer, K.J., Pringle, M., 1993. Geochemistry and age of the Ontong Java Plateau. *The Mesozoic Pacific: Geology, Tectonics, and Volcanism*. Geophys. Monogr. Ser. 77, 233–261.
Malahoff, A., Feden, R.H., Fleming, H.S., 1982. Magnetic anomalies and tectonic fabric of marginal basins north of New Zealand. J. Geophys. Res. 87 (B5), 4109–4125.
Malahoff, A., Kroenke, L.W., Cherkis, N., Brozena, J., 1994. Magnetic and tectonic fabric of the North Fiji Basin and Lau Basin. Basin Formation, Ridge Crest Processes, and Metallogenesis in the North Fiji Basin, 49–61.
Malaihollo, J.F., Hall, R., 1996. The geology and tectonic evolution of the Bacan region, east Indonesia. Geol. Soc. Lond. Spec. Publ. 106 (1), 483–497.
Maleterre, P. (1988). The Southern Central Cordillera of Luzon; a multistage Upper Eocene to Pleistocene arc-deformed on the northern end of the Philippine strike-slip fault. In *International Symposium on the Geodynamic Evolution of Eastern Eurasian Margin (Abstracts), Paris 13-20 September 1988*.
Manalo, P.C., Dimalanta, C.B., Faustino-Eslava, D.V., Payot, B.D., Ramos, N.T., Queaño, K.L., Yumul Jr, G.P., 2015. Geochemical and Geophysical Characteristics of the Balud Ophiolitic Complex (BOC), Masbate Island, Philippines: Implications for its Generation, Evolution and Emplacement. Terr. Atmos. Ocean. Sci. 26 (6).
Marchadier, Y., Rangin, C., 1990. Polyphase tectonics at the southern tip of the Manila trench, Mindoro-Tablas Islands. Philippines. Tectonophysics 183 (1–4), 273–287.
Martin, A.K., 2011. Double saloon door tectonics in the Japan Sea, Fossa magna, and the Japanese Island arc. Tectonophysics 498 (1–4), 45–65.
Martin, P.E., Macdonald, F.A., McQuarrie, N., Flowers, R.M., Maffre, P.J., 2023. The rise of New Guinea and the fall of Neogene global temperatures. Proceedings of the National Academy of Sciences 120 (40), e2306492120.
Matthews, K.J., Müller, R.D., Wessel, P., Whittaker, J.M., 2011. The tectonic fabric of the ocean basins. J. Geophys. Res. Solid Earth 116 (B12).
Maurizot, P., 2011. First sedimentary record of the pre-obduction convergence in New Caledonia: formation of an Early Eocene accretionary complex in the north of Grande Terre and emplacement of the 'Montagnes Blanches' nappe. Bulletin de la Société Géologique de France 182 (6), 479–491.
Maurizot, P., Cluzel, D., Meffre, S., Campbell, H.J., Collot, J., Sevin, B., 2020a. Pre-Late Cretaceous basement terranes of the Gondwana active margin of New Caledonia. Geol. Soc. Lond. Mem. 51 (1), 27–52.
Maurizot, P., Cluzel, D., Patriat, M., Collot, J., Iseppi, M., Lesimple, S., Davies, H.L., 2020b. The Eocene subduction–obduction complex of New Caledonia. Geol. Soc. Lond. Mem. 51 (1), 93–130.
McCabe, R., Almasco, J., Diegor, W., 1982. Geologic and paleomagnetic evidence for a possible Miocene collision in western Panay, central Philippines. Geology 10 (6), 325–329.
Mccaffrey, R., Silver, E.A., Raitt, R.W., 1980. Crustal structure of the Molucca Sea collision zone, Indonesia. In The tectonic and geologic evolution of Southeast Asian seas and islands, Geophysical Monograph 23, 161–177.
McCarthy, A., Magri, L., Sauermilch, I., Fox, J., Seton, M., Mohn, G., Whittaker, J.M., 2022. The Louisiade ophiolite: a missing link in the western Pacific. Terra Nova 34 (2), 146–154.
Meijer, A., Reagan, M., Ellis, H., Shafiqullah, M., Sutter, J., Damon, P., Kling, S., 1983. Chronology of volcanic events in the eastern Philippine Sea. Washington DC American Geophysical Union Geophysical Monograph Series 27, 349–359.
Mesalles, L., Walia, M., Lee, H., & Lee, Y. H. (2018, December). Cenozoic evolution of the Panay Island, Philippines: magmatic chronology and arc-continent collision. In *AGU Fall Meeting Abstracts* (Vol. 2018, pp. T23A-0343).
Metcalfe, I., 2013. Gondwana dispersion and Asian accretion: Tectonic and palaeogeographic evolution of eastern Tethys. J. Asian Earth Sci. 66, 1–33.
Miki, M., 1995. Two-phase opening model for the Okinawa Trough inferred from paleomagnetic study of the Ryukyu arc. J. Geophys. Res. Solid Earth 100 (B5), 8169–8184.
Miller, M.S., Kennett, B.L.N., Lister, G.S., 2004. Imaging changes in morphology, geometry, and physical properties of the subducting Pacific plate along the Izu–Bonin–Mariana arc. Earth Planet. Sci. Lett. 224 (3–4), 363–370.
Mitchell, A.H.G., Warden, A.J., 1971. Geological evolution of the New Hebrides island arc. J. Geol. Soc. London 127 (5), 501–529.
Mitchell, A.H.G., Hernandez, F.T., Dela Cruz, A.P., 1986. Cenozoic evolution of the Philippine Archipelago. J. SE Asian Earth Sci. 1 (1), 3–22.
MMAJ-JICA, 1977. Report on geological survey of northeastern Luzon. *Phase III: Metal Mining*. Agency of Japan and Japan International Cooperation Agency, Tokyo.
MMAJ-JICA. (1987). Report on the mineral exploration, mineral deposits and tectonics of two contrasting geological environments in the Philippines, Phase 3 (part1), northern Sierra Madre area. *Government of Japan*, 403.
MMAJ-JICA, 1986. Report on Mineral Exploration, Mineral Deposits and Tectonics of Two Contrasting Geologic Environments in the Republic of the Philippines, Phase II. Masbate and Leyte Areas.
Monnier, C., Girardeau, J., Maury, R.C., Cotten, J., 1995. Back-arc basin origin for the East Sulawesi ophiolite (eastern Indonesia). Geology 23 (9), 851–854.
Monnier, C., Girardeau, J., Pubellier, M., Polvé, M., Permana, H., Bellon, H., 1999. Petrology and geochemistry of the Cyclops ophiolites (Irian Jaya, East Indonesia): consequences for the Cenozoic evolution of the north Australian margin. Mineral. Petrol. 65 (1–2), 1–28.
Monteleone, B.D., Baldwin, S.L., Ireland, T.R., Fitzgerald, P.G., 2001. Thermochronologic constraints for the tectonic evolution of the Moresby seamount, Woodlark Basin, Papua New Guinea. Proc. ODP, Sci. Results, Vol. 180. Ocean Drilling Program, pp. 1–34.
Monteleone, B.D., Baldwin, S.L., Webb, L.E., Fitzgerald, P.G., Grove, M., Schmitt, A.K., 2007. Late Miocene-Pliocene eclogite facies metamorphism, D'Entrecasteaux Islands, SE Papua New Guinea. J. Metam. Geol. 25 (2), 245–265.
Moore, G.F., Kadarisman, D., Evans, C.A., Hawkins, J.W., 1981. Geology of the Talaud islands, Molucca sea collision zone, northeast Indonesia. J. Struct. Geol. 3 (4), 467–475.
Morishita, T., Tani, K.I., Soda, Y., Tamura, A., Mizukami, T., Ghosh, B., 2018. The uppermost mantle section below a remnant proto-Philippine Sea island arc: Insights from the peridotite fragments from the Daito Ridge. American Mineralogist: Journal of Earth and Planetary Materials 103 (7), 1151–1160.
Morrice, M.G., Jezek, P.A., Gill, J.B., Whitford, D.J., Monoarfa, M., 1983. An introduction to the Sangihe arc: Volcanism accompanying arc—arc collision in the Molucca Sea, Indonesia. J. Volcanol. Geoth. Res. 19 (1–2), 135–165.
Mortimer, N., 2004. New Zealand's geological foundations. Gondwana research 7 (1), 261–272.
Mortimer, N., Herzer, R.H., Gans, P.B., Parkinson, D.L., Seward, D., 1998. Basement geology from Three Kings Ridge to West Norfolk Ridge, southwest Pacific Ocean: evidence from petrology, geochemistry and isotopic dating of dredge samples. Mar. Geol. 148 (3–4), 135–162.
Mortimer, N., Herzer, R.H., Gans, P.B., Laporte-Magoni, C., Calvert, A.T., Bosch, D., 2007. Oligocene-Miocene tectonic evolution of the South Fiji Basin and Northland Plateau, SW Pacific Ocean: Evidence from petrology and dating of dredged rocks. Mar. Geol. 237 (1–2), 1–24.
Mortimer, N., Gans, P.B., Palin, J.M., Herzer, R.H., Pelletier, B., Monzier, M., 2014a. Eocene and Oligocene basins and ridges of the Coral Sea-New Caledonia region: Tectonic link between Melanesia, Fiji, and Zealandia. Tectonics 33 (7), 1386–1407.
Mortimer, N., Rattenbury, M.S., King, P.R., Bland, K.J., Barrell, D.J.A., Bache, F., Turnbull, R.E., 2014b. High-level stratigraphic scheme for New Zealand rocks. N. Z. J. Geol. Geophys. 57 (4), 402–419.
Mortimer, N., Campbell, H.J., Tulloch, A.J., King, P.R., Stagpoole, V.M., Wood, R.A., Seton, M., 2017. Zealandia: Earth's hidden continent. GSA Today 27 (3), 27–35.
Mouthereau, F., Lacombe, O., 2006. Inversion of the Paleogene Chinese continental margin and thick-skinned deformation in the Western Foreland of Taiwan. J. Struct. Geol. 28 (11), 1977–1993.
Mouthereau, F., Lacombe, O., Deffontaines, B., Angelier, J., Brusset, S., 2001. Deformation history of the southwestern Taiwan foreland thrust belt: insights from tectono-sedimentary analyses and balanced cross-sections. Tectonophysics 333 (1–2), 293–322.
Mueller, C.O., Jokat, W., 2019. The initial Gondwana break-up: a synthesis based on new potential field data of the Africa-Antarctica Corridor. Tectonophysics 750, 301–328.
Mulcahy, S.R., Starnes, J.K., Day, H.W., Coble, M.A., Vervoort, J.D., 2018. Early onset of Franciscan subduction. Tectonics 37 (5), 1194–1209.
Müller, R.D., Royer, J.Y., Cande, S.C., Roest, W.R., Maschenkov, S., 1999. New constraints on the Late Cretaceous/Tertiary plate tectonic evolution of the Caribbean. Sedimentary basins of the world 4, 33–59.
Müller, R.D., Cannon, J., Qin, X., Watson, R.J., Gurnis, M., Williams, S., Zahirovic, S., 2018. GPlates: building a virtual Earth through deep time. Geochem. Geophys. Geosyst. 19 (7), 2243–2261.
Müller, R.D., Zahirovic, S., Williams, S.E., Cannon, J., Seton, M., Bower, D.J., Tetley, M. G., Heine, C., Le Breton, E., Liu, S., Russel, S.H.J., Yang, T., Leonard, J., Gurnis, M., 2019. A global plate model including lithospheric deformation along major rifts and orogens since the Triassic. Tectonics 38 (6), 1884–1907.
Musgrave, R.J., 1990. Paleomagnetism and tectonics of Malaita. Solomon Islands. Tectonics 9 (4), 735–759.
Nakanishi, M., Winterer, E.L., 1998. Tectonic history of the Pacific-Farallon-Phoenix triple junction from Late Jurassic to Early Cretaceous: an abandoned Mesozoic spreading system in the central Pacific basin. J. Geophys. Res. Solid Earth 103 (B6), 12453–12468.
Nakanishi, M., Tamaki, K., Kobayashi, K., 1992. Magnetic anomaly lineations from Late Jurassic to Early Cretaceous in the west-central Pacific Ocean. Geophys. J. Int. 109 (3), 701–719.
Neef, G., McDougall, I., 1976. Potassium-argon ages on rocks from Small Nggela Island. British Solomon Islands, SW Pacific, *Pacific Geology* 11, 81–86.
Nichols, G., Hall, R., 1999. History of the Celebes Sea Basin based on its stratigraphic and sedimentological record. J. Asian Earth Sci. 17 (1–2), 47–59.
Nishimura, T., 2011. Back-arc spreading of the northern Izu-Ogasawara (Bonin) Islands arc clarified by GPS data. Tectonophysics 512 (1–4), 60–67.
Nong, A.T., Hauzenberger, C.A., Gallhofer, D., Dinh, S.Q., 2021. Geochemistry and zircon UPb geochronology of Late Mesozoic igneous rocks from SW Vietnam–SE Cambodia: Implications for episodic magmatism in the context of the Paleo-Pacific subduction. Lithos 390, 106101.

Nong, A.T., Hauzenberger, C.A., Gallhofer, D., Skrzypek, E., Dinh, S.Q., 2022. Geochemical and zircon U-Pb geochronological constraints on late mesozoic Paleo-Pacific subduction-related volcanism in southern Vietnam. Mineral. Petrol. 116 (5), 349–368.
Ogg, J.G., 2020. Geomagnetic polarity time scale. In: Geologic time scale 2020. Elsevier, pp. 159–192.
Okada, A., 1973. On the quaternary faulting along the median tectonic line. The Median Tectonic Line 46, 49–86.
Olfindo, V.S.V., Payot, B.D., Valera, G.T.V., Gadot Jr, E.G., Villaplaza, B.R.B., Tani, K., Yumul Jr, G.P., 2019. Petrographic and geochemical characterization of the crustal section of the Pujada Ophiolite, southeastern Mindanao, Philippines: Insights to the tectonic evolution of the northern Molucca Sea Collision Complex. J. Asian Earth Sci. 184, 103994.
O'Neill, C., Müller, D., Steinberger, B., 2005. On the uncertainties in hot spot reconstructions and the significance of moving hot spot reference frames. Geochem. Geophys. Geosyst. 6 (4).
Österle, J.E., Little, T.A., Seward, D., Stockli, D.F., Gamble, J., 2020. The petrology, geochronology and tectono-magmatic setting of igneous rocks in the Suckling-Dayman metamorphic core complex, Papua New Guinea. Gondw. Res. 83, 390–414.
Ota, T., Kaneko, Y., 2010. Blueschists, eclogites, and subduction zone tectonics: Insights from a review of Late Miocene blueschists and eclogites, and related young high-pressure metamorphic rocks. Gondw. Res. 18, 167–188.
Ott, B., Mann, P., 2015. Late Miocene to Recent formation of the Aure-Moresby fold-thrust belt and foreland basin as a consequence of Woodlark microplate rotation, Papua New Guinea. Geochem. Geophys. Geosyst. 16 (6), 1988–2004.
Pacle, N.A.D., Dimalanta, C.B., Ramos, N.T., Payot, B.D., Faustino-Eslava, D.V., Queaño, K.L., Yumul Jr, G.P., 2017. Petrography and geochemistry of Cenozoic sedimentary sequences of the southern Samar Island, Philippines: clues to the unroofing history of an ancient subduction zone. J. Asian Earth Sci. 142, 3–19.
Page, R.W., 1976. Geochronology of Igneous and Metamorphic Rocks in the New Guinea Highlands. Bureau of Mineral Resources, Canberra, Australia.
Pain, C.F., 1983. Volcanic rocks and surfaces as indicators of landform age: The Astrolabe Agglomerate. Papua New Guinea. Australian Geographer 15 (6), 376–381.
Paquette, J.L., Cluzel, D., 2007. U-Pb zircon dating of post-obduction volcanic-arc granitoids and a granulite-facies xenolith from New Caledonia. Inference on Southwest Pacific geodynamic models. Int. J. Earth Sci. 96, 613–622.
Parrot, J.F., Dugas, F., 1980. The disrupted ophiolitic belt of the Southwest Pacific: evidence of an Eocene subduction zone. Tectonophysics 66 (4), 349–372.
Parsons, A.J., Sigloch, K., Hosseini, K., 2021. Australian Plate Subduction is Responsible for Northward Motion of the India-Asia Collision Zone and~ 1,000 km Lateral Migration of the Indian Slab. Geophys. Res. Lett. 48 (18). e2021GL094904.
Pasco, J.A., Dycoco, J.M.A., Valera, G.T.V., Payot, B.D., Pillejera, J.D.B., Uy, F.A.A.E., Dimalanta, C.B., 2019. Petrogenesis of ultramafic-mafic clasts in the Dos Hermanos Mélange, Ilocos Norte: insights to the evolution of western Luzon. Philippines. Journal of Asian Earth Sciences 184, 104004.
Patriat, M., Collot, J., Danyushevsky, L., Fabre, M., Meffre, S., Falloon, T., Fournier, M., 2015. Propagation of back-arc extension into the arc lithosphere in the southern New Hebrides volcanic arc. Geochem. Geophys. Geosyst. 16 (9), 3142–3159.
Patriat, M., Collot, J., Etienne, S., Poli, S., Clerc, C., Mortimer, N., ... & VESPA scientific voyage team. (2018). New Caledonia obducted Peridotite Nappe: offshore extent and implications for obduction and postobduction processes. *Tectonics*, *37*(4), 1077–1096.
Patriat, M., Falloon, T., Danyushevsky, L., Collot, J., Jean, M.M., Hoernle, K., Feig, S.T., 2019. Subduction initiation terranes exposed at the front of a 2 Ma volcanically-active subduction zone. Earth Planet. Sci. Lett. 508, 30–40.
Pelletier, B., Auzende, J.M., 1996. Geometry and structure of the Vitiaz trench lineament (SW Pacific). Mar. Geophys. Res. 18, 305–335.
Permana, H., 1995. Etude des ophiolites des Weylands (Irian Jaya): origine et âge de mise en place. Mémoire DEA, Université de Brest, France, Comparaison avec celles de la Haute Chaîne centrale.
Petterson, M.G., Neal, C.R., Mahoney, J.J., Kroenke, L.W., Saunders, A.D., Babbs, T.L., McGrail, B., 1997. Structure and deformation of north and central Malaita, Solomon Islands: tectonic implications for the Ontong Java Plateau-Solomon arc collision, and for the fate of oceanic plateaus. Tectonophysics 283 (1–4), 1–33.
Petterson, M.G., Babbs, T., Neal, C.R., Mahoney, J.J., Saunders, A.D., Duncan, R.A., Natogga, D., 1999. Geological–tectonic framework of Solomon Islands, SW Pacific: crustal accretion and growth within an intra-oceanic setting. Tectonophysics 301 (1–2), 35–60.
Petterson, M.G., Coleman, P.J., Tolia, D., Mahoa, H., Magu, R., 2009. Application of terrain modelling of the Solomon Islands, Southwest Pacific, to the metallogenesis and mineral exploration in composite arc-ocean floor terrain collages. Pacific Minerals in the New Millennium. Science, Exploration, Mining, and Community, 99–120.
Phinney, E.J., Mann, P., Coffin, M.F., Shipley, T.H., 1999. Sequence stratigraphy, structure, and tectonic history of the southwestern Ontong Java Plateau adjacent to the North Solomon Trench and Solomon Islands arc. J. Geophys. Res. Solid Earth 104 (B9), 20449–20466.
Phinney, E.J., Mann, P., Coffin, M.F., Shipley, T.H., 2004. Sequence stratigraphy, structural style, and age of deformation of the Malaita accretionary prism (Solomon arc–Ontong Java Plateau convergent zone). Tectonophysics 389 (3–4), 221–246.
Pieters, P. E., Pigram, C. J., Trail, D. S., Dow, D. B., Ratman, N., & Sukamto, R. (1983). The stratigraphy of western Irian Jaya. *Proceedings Indonesian Petroleum Association, Twelfth Annual Convention.* 229-261.
Pieters, P. E., Hartono, U., & Amri, C. (1989). Geology of the Mar sheet area, Irian Jaya. *Geological Research and Development Centre, Bandung (62pp.).*
Pieters, P.E., 1978. Port Moresby-Kalo-Aroa - Papua New Guinea 1: 250,000 geological series. Geological Survey of Papua New Guinea, Dept. of Minerals and Energy, Port Moresby.
Pigram, C.J., Symonds, P.A., 1991. A review of the timing of the major tectonic events in the New Guinea Orogen. J. SE Asian Earth Sci. 6 (3–4), 307–318.
Pourteau, A., Scherer, E.E., Schorn, S., Bast, R., Schmidt, A., Ebert, L., 2019. Thermal evolution of an ancient subduction interface revealed by Lu–Hf garnet geochronology, Halilbağı Complex (Anatolia). Geosci. Front. 10 (1), 127–148.
Pubellier, M., Quebral, R., Rangin, C., Deffontaines, B., Muller, C., Butterlin, J., Manzano, J., 1991. The Mindanao collision zone: a soft collision event within a continuous Neogene strike-slip setting. J. SE Asian Earth Sci. 6 (3–4), 239–248.
Pubellier, M., Bader, A.G., Rangin, C., Deffontaines, B., Quebral, R., 1999. Upper plate deformation induced by subduction of a volcanic arc: the Snellius Plateau (Molucca Sea, Indonesia and Mindanao, Philippines). Tectonophysics 304 (4), 345–368.
Pubellier, M., Monnier, C., Maury, R., Tamayo, R., 2004. Plate kinematics, origin and tectonic emplacement of supra-subduction ophiolites in SE Asia. Tectonophysics 392 (1–4), 9–36.
Qayyum, A., Lom, N., Advokaat, E.L., Spakman, W., Van Der Meer, D.G., van Hinsbergen, D.J., 2022. Subduction and Slab Detachment Under Moving Trenches During Ongoing India-Asia Convergence. Geochem. Geophys. Geosyst. 23 (11). e2022GC010336.
Qian, X., Yu, Y., Wang, Y., Gan, C., Zhang, Y., Asis, J.B., 2022. Late Cretaceous Nature of SW Borneo and Paleo-Pacific Subduction: New Insights from the Granitoids in the Schwaner Mountains. Lithosphere 2022 (1), 8483732.
Qian, S., Zhang, X., Wu, J., Lallemand, S., Nichols, A.R., Huang, C., Zhou, H., 2021. First identification of a Cathaysian continental fragment beneath the Gagua Ridge, Philippine Sea, and its tectonic implications. Geology 49 (11), 1332–1336.
Quarles van Ufford, A., Cloos, M., 2005. Cenozoic tectonics of New Guinea. AAPG Bull. 89 (1), 119–140.
Queaño, K.L., 2005. Upper Miocene to Lower Pliocene Sigaboy formation turbidites, on the Pujada Peninsula, Mindanao, Philippines: internal structures, composition, depositional elements and reservoir characteristics. J. Asian Earth Sci. 25 (3), 387–402.
Queaño, K.L., Ali, J.R., Aitchison, J.C., Yumul, G.P., Pubellier, M., Dimalanta, C.B., 2008. Geochemistry of Cretaceous to Eocene ophiolitic rocks of the Central Cordillera: Implications for Mesozoic-early Cenozoic evolution of the northern Philippines. Int. Geol. Rev. 50 (4), 407–421.
Queaño, K.L., Marquez, E.J., Aitchison, J.C., Ali, J.R., 2013. Radiolarian biostratigraphic data from the Casiguran Ophiolite, northern Sierra Madre, Luzon, Philippines: stratigraphic and tectonic implications. J. Asian Earth Sci. 65, 131–142.
Queaño, K.L., Dimalanta, C.B., Yumul Jr, G.P., Marquez, E.J., Faustino-Eslava, D.V., Suzuki, S., Ishida, K., 2017a. Stratigraphic units overlying the Zambales Ophiolite Complex (ZOC) in Luzon, (Philippines): Tectonostratigraphic significance and regional implications. J. Asian Earth Sci. 142, 20–31.
Queaño, K.L., Marquez, E.J., Dimalanta, C.B., Aitchison, J.C., Ali, J.R., Yumul Jr, G.P., 2017b. Mesozoic radiolarian faunas from the northwest Ilocos Region, Luzon, Philippines and their tectonic significance. Isl. Arc 26 (4), e12195.
Queaño, K.L., Yumul Jr, G.P., Marquez, E.J., Gabo-Ratio, J.A., Payot, B.D., Dimalanta, C. B., 2020. Consumed tectonic plates in Southeast Asia: Markers from the Mesozoic to early Cenozoic stratigraphic units in the northern and central Philippines. Journal of Asian Earth Sciences: X 4, 100033.
Quebral, R.D., Pubellier, M., Rangin, C., 1996. The onset of movement on the Philippine Fault in eastern Mindanao: A transition from a collision to a strike-slip environment. Tectonics 15 (4), 713–726.
Raimbourg, H., Augier, R., Famin, V., Gadenne, L., Palazzin, G., Yamaguchi, A., Kimura, G., 2014. Long-term evolution of an accretionary prism: The case study of the Shimanto Belt, Kyushu. Japan. Tectonics 33 (6), 936–959.
Rangin, C., 1991. The Philippine Mobile Belt: a complex plate boundary. J. SE Asian Earth Sci. 6 (3–4), 209–220.
Rangin, C., Stephan, J.F., Muller, C., 1985. Middle Oligocene oceanic crust of South China Sea jammed into Mindoro collision zone (Philippines). Geology 13 (6), 425–428.
Rangin, C., Bellon, H., Benard, F., Letouzey, J., Muller, C., Sanudin, T.A.H.I.R., 1990. Neogene arc-continent collision in Sabah, northern Borneo (Malaysia). Tectonophysics 183 (1–4), 305–319.
Rangin, C., Stephan, J.F., Butterlin, J., Bellon, H., Muller, C., Chorowicz, J., Baladad, D., 1991. Collision néogène d'arcs volcaniques dans le centre des Philippines: stratigraphie et structure de la chaîne d'Antique (île de Panay). Bulletin Societe Géologique du France 162 (3), 465–477.
Rangin, C., Dahrin, D., Quebral, R., Party, M.S., 1996. Collision and strike-slip faulting in the northern Molucca Sea (Philippines and Indonesia): preliminary results of a morphotectonic study. Geol. Soc. Lond. Spec. Publ. 106 (1), 29–46.
Rangin, C., Spakman, W., Pubellier, M., Bijwaard, H., 1999. Tomographic and geological constraints on subduction along the eastern Sundaland continental margin (South-East Asia). Bulletin de la Société géologique de France 170 (6), 775–788.
Reagan, M.K., Hanan, B.B., Heizler, M.T., Hartman, B.S., Hickey-Vargas, R., 2008. Petrogenesis of volcanic rocks from Saipan and Rota, Mariana Islands, and implications for the evolution of nascent island arcs. J. Petrol. 49 (3), 441–464.

Reagan, M.K., Ishizuka, O., Stern, R.J., Kelley, K.A., Ohara, Y., Blichert-Toft, J., Woods, M., 2010. Fore-arc basalts and subduction initiation in the Izu-Bonin-Mariana system. Geochem. Geophys. Geosyst. 11 (3).
Reagan, M.K., McClelland, W.C., Girard, G., Goff, K.R., Peate, D.W., Ohara, Y., Stern, R. J., 2013. The geology of the southern Mariana fore-arc crust: Implications for the scale of Eocene volcanism in the western Pacific. Earth Planet. Sci. Lett. 380, 41–51.
Reagan, M.K., Heaton, D.E., Schmitz, M.D., Pearce, J.A., Shervais, J.W., Koppers, A.A., 2019. Forearc ages reveal extensive short-lived and rapid seafloor spreading following subduction initiation. Earth Planet. Sci. Lett. 506, 520–529.
Récy, J. (1977). Fossil subduction zones: examples in the South West Pacific, *International Symposium Geodynamics in S.W. Pacific,* 345-356.
Ren, J., Niu, B., Wang, J., Jin, X., Zhao, L., Liu, R., 2013. Advances in research of Asian geology—A summary of 1: 5M International Geological Map of Asia project. J. Asian Earth Sci. 72, 3–11.
Richard, M., Bellon, H., Maury, R., Barrier, E., Wen-Shing, J., 1986. Miocene to recent calc-alkalic volcanism in eastern Taiwan: K-Ar ages and petrography. Tectonophysics 125 (1–3), 87–102.
Richards, J.R., Cooper, J.A., Webb, A.W., Coleman, P.J., 1966. Potassium-Argon Measurements of the Age of Basal Schists in the British Solomon Islands. Nature 211, 1251–1252.
Rickard, M.J., Williams, I.S., 2013. No zircon U-Pb evidence for a Precambrian component in the Late Eocene Yavuna trondhjemite Fiji. Australian J. Earth Sci. 60 (4), 521–525.
Ridgway, J., Coulson, F.I.E., 1987. The Geology of Choiseul and the Shortland Islands, Solomon Islands, Vol. 8. HM Stationery Office.
Ridley, W. I., Rhodes, J. M., REID, A. M., Jakes, P., Shih, C. Y., & Bass, M. N. (1974). Basalts from leg 6 of the deep-sea drilling project. *J. Petrol. 15*(1), 140–159.
Ringenbach, J.C., Stephan, J.F., Maleterre, P., Bellon, H., 1990. Structure and geological history of the Lepanto-Cervantes releasing bend on the Abra River fault, Luzon Central Cordillera. Philippines. Tectonophysics 183 (1–4), 225–241.
Rioux, M., Bowring, S., Kelemen, P., Gordon, S., Miller, R., Dudás, F., 2013. Tectonic development of the Samail ophiolite: High-precision U-Pb zircon geochronology and Sm-Nd isotopic constraints on crustal growth and emplacement. J. Geophys. Res. Solid Earth 118, 2085–2101.
Rodrigo, J.D., Gabo-Ratio, J.A.S., Queaño, K.L., Fernando, A.G.S., de Silva Jr, L.P., Yonezu, K., Zhang, Y., 2020. Geochemistry of the Late Cretaceous Pandan Formation in Cebu Island, Central Philippines: sediment contributions from the Australian plate margin during the Mesozoic. The Depositional Record 6 (2), 309–330.
Rodrigo, J., Schlagintweit, F., 2022. The Lower Cretaceous Tuburan Limestone of Cebu Island, Philippines: Microfacies, micropalaeontology, biostratigraphy, and palaeogeographic perspectives. Carnets Geol. 22 (14), 661–679.
Rodrigo, J., Tsutsumi, Y., Tani, K., Haga, T., Aira, J., 2021. Tectonostratigraphy of the basement complex of Cebu Island, central Philippines: New constraints from petrography, micropaleontology and geochronology. In The Second International Symposium of the International Geoscience Programme Project 679, 19.
Rodriguez-Roa, F.A., Wiltschko, D.V., 2010. Thrust belt architecture of the central and southern Western Foothills of Taiwan. Geol. Soc. Lond. Spec. Publ. 348 (1), 137–168.
Roeser, H. A. (1991). Age of the crust of the southeast Sulu Sea basin based on magnetic anomalies and age determined at site 768. In *Proceedings of the Ocean Drilling Program, Scientific Results* 124, 339-343.
Rogerson, R.J., Hilyard, D.B., 1990. Scrapland: a suspect composite terrane in Papua New Guinea. Petroleum Convention Proceedings, Papua New Guinea (PNG).
Rogerson, R. (1987). *The geology and mineral resources of the Sepik headwaters region, Papua New Guinea* (Vol. 12). Geological Survey of Papua New Guinea.
Roser, B.P., Coombs, D.S., Korsch, R.J., Campbell, J.D., 2002. Whole-rock geochemical variations and evolution of the arc-derived Murihiku Terrane. New Zealand. Geological Magazine 139 (6), 665–685.
Ruellan, E., Delteil, J., Wright, I., Matsumoto, T., 2003. From rifting to active spreading in the Lau Basin-Havre Trough backarc system (SW Pacific): Locking/unlocking induced by seamount chain subduction. Geochem. Geophys. Geosyst. 4 (5), 8909.
Ryburn, R.J., 1980. Blueschists and associated rocks in the south Sepik region, Papua New Guinea; field relations, petrology, mineralogy, metamorphism and tectonic setting. University of Auckland. Doctoral dissertation.
Rytuba, J.J., Miller, W.R., 1990. Geology and geochemistry of epithermal precious metal vein systems in the intra-oceanic arcs of Palau and Yap, western Pacific. J. Geochem. Explor. 35 (1–3), 413–447.
Saito, M., 2008. Rapid evolution of the Eocene accretionary complex (Hyuga Group) of the Shimanto terrane in southeastern Kyushu, southwestern Japan. Isl. Arc 17 (2), 242–260.
Sajona, F.G., Bellon, H., Maury, R.C., Pubellier, M., Quebral, R.D., Cotten, J., Pamatian, P., 1997. Tertiary and quaternary magmatism in Mindanao and Leyte (Philippines): geochronology, geochemistry and tectonic setting. J. Asian Earth Sci. 15 (2–3), 121–153.
Sandmann, S., Nagel, T.J., Froitzheim, N., Ustaszewski, K., Münker, C., 2015. Late Miocene to Early Pliocene blueschist from Taiwan and its exhumation via forearc extraction. Terra Nova 27 (4), 285–291.
Santos, R. A. (2014). Mineral Resource Estimate Report of the Islands of Nonoc, Awasan, and Hanigad and Part of South Dinagat for Pacific Nickel Philippines Inc. (PNPI). MPSA No. 072-1997-XIII.
Saputra, A., Hall, R., White, L.T., 2014. Development of the Sorong Fault Zone North of Misool, Eastern Indonesia. *Indonesian Petroleum Association, 38th Annual Convention Proceedings*, IPA, 14-G-086.
Saragih, R. Y., Sunan, H. L., Slameto, E., & Nurdiana, I. (2020, December). Rifting and Lifting Neogene Age in Biak-Yapen Basin Based on Structural Trajectory Analogy in Biak and Supiori Island. In *IOP Conference Series: Materials Science and Engineering* (Vol. 982, No. 1, p. 012042). IOP Publishing.
Sarewitz, D.R., Karig, D.E., 1986. Processes of allochthonous terrane evolution, Mindoro Island. Philippines. Tectonics 5 (4), 525–552.
Sasaki, T., Yamazaki, T., Ishizuka, O., 2014. A revised spreading model of the West Philippine Basin. Earth Planets Space 66, 1–9.
Sato, T., Kasahara, J., Katao, H., Tomiyama, N., Mochizuki, K., Koresawa, S., 1997. Seismic observations at the Yap Islands and the northern Yap Trench. Tectonophysics 271 (3–4), 285–294.
Schellart, W.P., Lister, G.S., Toy, V.G., 2006. A Late Cretaceous and Cenozoic reconstruction of the Southwest Pacific region: tectonics controlled by subduction and slab rollback processes. Earth Sci. Rev. 76 (3–4), 191–233.
Schellart, W.P., Kennett, B.L.N., Spakman, W., Amaru, M., 2009. Plate reconstructions and tomography reveal a fossil lower mantle slab below the Tasman Sea. Earth Planet. Sci. Lett. 278 (3–4), 143–151.
Schellart, W.P., Spakman, W., 2015. Australian plate motion and topography linked to fossil New Guinea slab below Lake Eyre. Earth Planet. Sci. Lett. 421, 107–116.
Schlüter, H.U., Hinz, K., Block, M., 1996. Tectono-stratigraphic terranes and detachment faulting of the South China Sea and Sulu Sea. Mar. Geol. 130 (1–2), 39–78.
Schweller, W.J., Karig, D.E., Bachman, S.D., 1983. The Tectonic and Geologic Evolution of Southeast Asian Seas and Islands: Part 2. American Geophysical Union Geophysical Monograph Series 27, 95–123.
Scotese, C.R., 2021. An atlas of Phanerozoic paleogeographic maps: the seas come in and the seas go out. Annu. Rev. Earth Planet. Sci. 49, 679–728.
Sdrolias, M., Müller, R.D., Gaina, C., 2003. Tectonic evolution of the southwest Pacific using constraints from backarc basins. GSA Special Papers 372, 343–360.
Sdrolias, M., Müller, R.D., Mauffret, A., Bernardel, G., 2004a. Enigmatic formation of the Norfolk Basin, SW Pacific: A plume influence on back-arc extension. Geochem. Geophys. Geosyst. 5, Q06005.
Sdrolias, M., Roest, W.R., Müller, R.D., 2004b. An expression of Philippine Sea plate rotation: the Parece Vela and Shikoku basins. Tectonophysics 394 (1–2), 69–86.
Seton, M., Müller, R.D., 2008. Reconstructing the junction between Panthalassa and Tethys since the Early Cretaceous. PESA Eastern Australian Basin Symposium III abstract, 263–266.
Seton, M., Müller, R.D., Zahirovic, S., Gaina, C., Torsvik, T., Shephard, G., Talsma, A., Gurnis, M., Turner, M., Maus, S., Chandler, M., 2012. Global continental and ocean basin reconstructions since 200 Ma. Earth Sci. Rev. 113 (3–4), 212–270.
Seton, M., Whittaker, J.M., Wessel, P., Müller, R.D., DeMets, C., Merkouriev, S., Williams, S.E., 2014. Community infrastructure and repository for marine magnetic identifications. Geochem. Geophys. Geosyst. 15 (4), 1629–1641.
Seton, M., Flament, N., Whittaker, J., Müller, R.D., Gurnis, M., Bower, D.J., 2015. Ridge subduction sparked reorganization of the Pacific plate-mantle system 60–50 million years ago. Geophys. Res. Lett. 42 (6), 1732–1740.
Seton, M., Mortimer, N., Williams, S., Quilty, P., Gans, P., Meffre, S., Matthews, K.J., 2016. Melanesian back-arc basin and arc development: Constraints from the eastern Coral Sea. Gondw. Res. 39, 77–95.
Sevin, B., Maurizot, P., Cluzel, D., Tournadour, E., Etienne, S., Folcher, N., Patriat, M., 2020. Post-obduction evolution of New Caledonia. Geol. Soc. Lond. Mem. 51 (1), 147–188.
Shao, L., Cao, L., Qiao, P., Zhang, X., Li, Q., van Hinsbergen, D.J., 2017. Cretaceous-Eocene provenance connections between the Palawan Continental Terrane and the northern South China Sea margin. Earth Planet. Sci. Lett. 477, 97–107.
Shiraki, K., 1971. Metamorphic basement rocks of Yap Islands, western Pacific: Possible oceanic crust beneath an island arc. Earth Planet. Sci. Lett. 13 (1), 167–174.
Sibuet, J.C., Letouzey, J., Barbier, F., Charvet, J., Foucher, J.P., Hilde, T.W., Stéphan, J.F., 1987. Back arc extension in the Okinawa Trough. J. Geophys. Res. Solid Earth 92 (B13), 14041–14063.
Sibuet, J.C., Hsu, S.K., Shyu, C.T., Liu, C.S., 1995. Structural and kinematic evolutions of the Okinawa Trough backarc basin. Tectonics and Magmatism, Backarc Basins, pp. 343–379.
Silver, E. A., & Rangin, C. (1991). Leg 124 Tectonic synthesis. In *Proceedings of the Ocean Drilling Program*, 124, 3-9.
Silver, E.A., Moore, J.C., 1978. The Molucca sea collision zone, Indonesia. J. Geophys. Res. Solid Earth 83 (B4), 1681–1691.
Smith, I.E., 2013. The chemical characterization and tectonic significance of ophiolite terrains in southeastern Papua New Guinea. Tectonics 32 (2), 159–170.
Smith, R.B., Betzler, C., Brass, G.W., Huang, Z., Linsley, B.K., Menill, D., Spadea, P., 1990. Depositional history of the Celebes Sea from ODP Sites 767 and 770. Geophys. Res. Lett. 17 (11), 2061–2064.
Spakman, W., Stein, S., van der Hilst, R., Wortel, R., 1989. Resolution experiments for NW Pacific subduction zone tomography. Geophys. Res. Lett. 16 (10), 1097–1100.
Spakman, W., Chertova, M.V., van den Berg, A., van Hinsbergen, D.J., 2018. Puzzling features of western Mediterranean tectonics explained by slab dragging. Nat. Geosci. 11 (3), 211–216.
Srivastava, S. P., & Roest, W. R. (1996). Comment on "Porcupine plate hypothesis" by MF Gerstell and JM Stock (Marine Geophysical Researches 16, pp. 315–323, 1994). *Marine Geophysical Researches*, *18*(5), 589-593.

Stampfli, G.M., Borel, G.D., 2002. A plate tectonic model for the Paleozoic and Mesozoic constrained by dynamic plate boundaries and restored synthetic oceanic isochrons. Earth Planet. Sci. Lett. 196 (1–2), 17–33.
Stern, R.J., 2004. Subduction initiation: spontaneous and induced. Earth Planet. Sci. Lett. 226 (3–4), 275–292.
Stern, R.J., Bloomer, S.H., 1992. Subduction zone infancy: examples from the Eocene Izu-Bonin-Mariana and Jurassic California arcs. Geol. Soc. Am. Bull. 104 (12), 1621–1636.
Stern, R.J., Gerya, T., 2018. Subduction initiation in nature and models: A review. Tectonophysics 746, 173–198.
Stern, R.J., Fouch, M.J., Klemperer, S.L., 2003. An overview of the Izu-Bonin-Mariana subduction factory. Geophysical Monograph, American Geophysical Union 138, 175–222.
Stern, R.J., Reagan, M., Ishizuka, O., Ohara, Y., Whattam, S., 2012. To understand subduction initiation, study forearc crust: To understand forearc crust, study ophiolites. Lithosphere 4 (6), 469–483.
Stewart, W.D., Sandy, M.J., 1988. Geology of New Ireland and Djaul Islands, northeastern Papua New Guinea. Geology and Offshore Resources of Pacific Island Arcs-New Ireland and Manus Region, Papua New Guinea 9, 13–30.
Struckmeyer, H.I.M., Symonds, P.A., 1997. Tectonostratigraphic evolution of the Townsville Basin, Townsville Trough, offshore northeastern Australia. Aust. J. Earth Sci. 44 (6), 799–817.
Suerte, L.O., Yumul, G.P., Tamayo, R.A., Dimalanta, C.B., Zhou, M.F., Maury, R.C., Balce, C.L., 2005. Geology, geochemistry and U-Pb SHRIMP age of the Tacloban Ophiolite Complex, Leyte Island (Central Philippines): Implications for the existence and extent of the proto-Philippine Sea Plate. Resour. Geol. 55 (3), 207–216.
Sugiyama, Y., 1994. Neotectonics of Southwest Japan due to the right-oblique subduction of the Philippine Sea plate. Geofis. Int. 33 (1), 53–76.
Suppe, J.O.H.N., 1980. A retrodeformable cross section of northern Taiwan. In Proc. Geol. Soc. China 23, 46–55.
Suppe, J., Chi, W.R., 1985. Tectonic implications of Miocene sediments of Lan-Hsu island, northern Luzon arc. Petroleum Geology of Taiwan 21, 93–106.
Sutherland, R., Collot, J., Bache, F., Henrys, S., Barker, D., Browne, G.H., et al., 2017. Widespread compression associated with Eocene Tonga-Kermadec subduction initiation. Geology 45, 355–358.
Taetz, S., Scherer, E.E., Bröcker, M., Spandler, C., John, T., 2021. Petrological and Lu-Hf age constraints for eclogitic rocks from the Pam Peninsula New Caledonia. *Lithos* 388–389, 106073.
Taira, A., Okada, H., Whitaker, J.H., Smith, A.J., 1982. The Shimanto Belt of Japan: Cretaceous-lower Miocene active-margin sedimentation. Geol. Soc. Lond. Spec. Publ. 10 (1), 5–26.
Taira, A., Mann, P., Rahardiawan, R., 2004. Incipient subduction of the Ontong Java Plateau along the North Solomon trench. Tectonophysics 389 (3–4), 247–266.
Taira, A. (1988). The Shimanto belt in Shikoku, Japan-evolution of Cretaceous to Miocene accretionary prism. *The Shimanto belt, Southwest Japan-Studies on the evolution of an accretionary prism*.
Tamayo, R.J., Yumul Jr., G.P., Santos, R.A., Jumawan, F., Rodolfo, K.S., 1998. Petrology and mineral chemistry of a back-arc upper mantle suite: Example from the Camarines Norte Ophiolite complex, South Luzon. J. Geol. Soc. Philippines 51, 1–23.
Tamayo, R.A., Yumul, G.P., Maury, R.C., Bellon, H., Cotten, J., Polvé, M., Querubin, C., 2000. Complex origin for the south-western Zamboanga metamorphic basement complex, Western Mindanao. Philippines. Island Arc 9 (4), 638–652.
Tamayo Jr, R.A., Yumul Jr, G.P., Maury, R.C., Polvé, M., Cotten, J., Bohn, M., 2001. Petrochemical investigation of the Antique Ophiolite (Philippines): Implications on volcanogenic massive sulfide and podiform chromitite deposits. Resour. Geol. 51 (2), 145–164.
Tamayo Jr, R.A., Maury, R.C., Yumul Jr, G.P., Polvé, M., Cotten, J., Dimantala, C.B., Olaguera, F.O., 2004. Subduction-related magmatic imprint of most Philippine ophiolites: implications on the early geodynamic evolution of the Philippine archipelago. Bulletin de la Société Géologique de France 175 (5), 443–460.
Tanaka, G., Nomura, S.I., 2009. Late Miocene and Pliocene Ostracoda from the Shimajiri Group, Kume-jima Island, Japan: Biogeographical significance of the timing of the formation of back-arc basin (Okinawa Trough). Palaeogeogr. Palaeoclimatol. Palaeoecol. 276 (1–4), 56–68.
Tapster, S., Roberts, N.M.W., Petterson, M.G., Saunders, A.D., Naden, J., 2014. From continent to intra-oceanic arc: Zircon xenocrysts record the crustal evolution of the Solomon island arc. Geology 42 (12), 1087–1090.
Taylor, B., 1979. Bismarck Sea: evolution of a back-arc basin. Geology 7 (4), 171–174.
Taylor, B., 2006. The single largest oceanic plateau: Ontong Java–Manihiki–Hikurangi. Earth Planet. Sci. Lett. 241 (3–4), 372–380.
Taylor, B., Goodliffe, A.M., Martinez, F., 1999. How continents break up: insights from Papua New Guinea. J. Geophys. Res. Solid Earth 104 (B4), 7497–7751.
Taylor, F.W., Jouannic, C., Bloom, A.L., 1985. Quaternary uplift of the Torres Islands, northern New Hebrides frontal arc: Comparison with Santo and Malekula Islands, central New Hebrides frontal arc. J. Geol. 93 (4), 419–438.
Tejada, M.L.G., Castillo, P.R., 2002. In search of a common ground: Geochemical study of ancient oceanic crust in eastern Luzon. Philippines. *Geochimica et Cosmochimica Acta* 56 (66), 767.
Tejada, M.L.G., Mahoney, J.J., Duncan, R.A., Hawkins, M.P., 1996. Age and geochemistry of basement and alkalic rocks of Malaita and Santa Isabel, Solomon Islands, southern margin of Ontong Java Plateau. J. Petrol. 37 (2), 361–394.
Tejada, M.L.G., Mahoney, J.J., Neal, C.R., Duncan, R.A., Petterson, M.G., 2002. Basement geochemistry and geochronology of Central Malaita, Solomon Islands, with implications for the origin and evolution of the Ontong Java Plateau. J. Petrol. 43 (3), 449–484.
Torsvik, T., & Cocks, L. (2017). *Earth History and Palaeogeography*. Cambridge: Cambridge University Press. doi:10.1017/9781316225523.
Torsvik, T.H., Müller, R.D., Van der Voo, R., Steinberger, B., Gaina, C., 2008. Global plate motion frames: toward a unified model. Rev. Geophys. 46 (3).
Torsvik, T.H., Van der Voo, R., Preeden, U., Mac Niocaill, C., Steinberger, B., Doubrovine, P.V., Cocks, L.R.M., 2012. Phanerozoic polar wander, palaeogeography and dynamics. Earth Sci. Rev. 114 (3–4), 325–368.
Torsvik, T.H., Doubrovine, P.V., Steinberger, B., Gaina, C., Spakman, W., Domeier, M., 2017. Pacific plate motion change caused the Hawaiian-Emperor Bend. Nat. Commun. 8 (1), 15660.
Torsvik, T.H., Steinberger, B., Shephard, G.E., Doubrovine, P.V., Gaina, C., Domeier, M., Sager, W.W., 2019. Pacific-Panthalassic reconstructions: Overview, errata and the way forward. Geochem. Geophys. Geosyst. 20 (7), 3659–3689.
Tregoning, P., Tan, F., Gilliland, J., McQueen, H., Lambeck, K., 1998. Present-day crustal motion in the Solomon Islands from GPS observations. Geophys. Res. Lett. 25 (19), 3627–3630.
Ujiie, K., 1997. Off-scraping accretionary process under the subduction of young oceanic crust: The Shimanto Belt of Okinawa Island. Ryukyu Arc. Tectonics 16 (2), 305–322.
Ujiie, K., 2002. Evolution and kinematics of an ancient décollement zone, mélange in the Shimanto accretionary complex of Okinawa Island, Ryukyu Arc. J. Struct. Geol. 24 (5), 937–952.
Vaes, B., Van Hinsbergen, D.J., Boschman, L.M., 2019. Reconstruction of subduction and back-arc spreading in the NW Pacific and Aleutian Basin: Clues to causes of Cretaceous and Eocene plate reorganizations. Tectonics 38 (4), 1367–1413.
Vaes, B., Van Hinsbergen, D.J.J., Van de Lagemaat, S.H.A., Van der Wiel, E., Lom, N., Advokaat, E., Langereis, C., 2023. A global apparent polar wander path for the last 320 Ma calculated from site-level paleomagnetic data. Earth Sci. Rev. 245, 104547.
Van de Lagemaat, S.H.A., Boschman, L.M., Kamp, P.J.J., Langereis, C.G., van Hinsbergen, D.J.J., 2018a. Post-remagnetisation vertical axis rotation and tilting of the Murihiku Terrane (North Island, New Zealand). N. Z. J. Geol. Geophys. 61 (1), 9–25.
Van de Lagemaat, S.H.A., Van Hinsbergen, D.J.J., Boschman, L.M., Kamp, P.J.J., Spakman, W., 2018b. Southwest Pacific absolute plate kinematic reconstruction reveals major Cenozoic Tonga-Kermadec slab dragging. Tectonics 37 (8), 2647–2674.
Van de Lagemaat, S.H.A., Swart, M.L., Vaes, B., Kosters, M.E., Boschman, L.M., Burton-Johnson, A., Bijl, P.K., Spakman, W., Van Hinsbergen, D.J., 2021. Subduction initiation in the Scotia Sea region and opening of the Drake Passage: When and why? Earth Sci. Rev. 215, 103551.
Van de Lagemaat, S.H.A., Mering, J.A., Kamp, P.J.J., 2022. Geochemistry of syntectonic carbonate veins within Late Cretaceous turbidites, Hikurangi Margin (New Zealand): Implications for a mid-Oligocene age of subduction initiation. Geochem. Geophys. Geosyst. 23 (5). e2021GC010125.
Van de Lagemaat, S.H.A., Kamp, P.J.J., Boschman, L.M., Van Hinsbergen, D.J.J., 2023a. Reconciling the Cretaceous breakup and demise of the Phoenix Plate with East Gondwana orogenesis in New Zealand. Earth Sci. Rev. 236, 104276.
Van de Lagemaat, S.H.A., Pastor-Galán, D., Zanderink, B.B.G., Villareal, M.J., Jenson, J. W., Dekkers, M.J., van Hinsbergen, D.J.J., 2023b. A critical reappraisal of paleomagnetic evidence for Philippine Sea Plate rotation. Tectonophysics 863, 230010.
Van de Lagemaat, S. H. A., Cao, L., Asis, J., Advokaat, E.L., Mason, P.R.D., Xu, D., Dekkers, M.J., and van Hinsbergen, D.J.J., (2023c). Causes of Late Cretaceous subduction termination below South China and Borneo: Was the Proto-South China Sea underlain by an oceanic plateau? Submitted to *Geoscience Frontiers*. Preprint: https://doi.org/10.31223/X5ZW9G.
Van den Broek, J.M., Gaina, C., 2020. Microcontinents and continental fragments associated with subduction systems. Tectonics 39 (8). e2020TC006063.
Van der Hist, R., Engdahl, R., Spakman, W., Nolet, G., 1991. Tomographic imaging of subducted lithosphere below northwest Pacific island arcs. Nature 353 (6339), 37–43.
Van der Meer, D.G., Spakman, W., Van Hinsbergen, D.J., Amaru, M.L., Torsvik, T.H., 2010. Towards absolute plate motions constrained by lower-mantle slab remnants. Nat. Geosci. 3 (1), 36–40.
Van der Meer, D.G., Torsvik, T.H., Spakman, W., Van Hinsbergen, D.J.J., Amaru, M.L., 2012. Intra-Panthalassa Ocean subduction zones revealed by fossil arcs and mantle structure. Nat. Geosci. 5 (3), 215–219.
Van der Meer, D.G., Van Hinsbergen, D.J., Spakman, W., 2018. Atlas of the underworld: Slab remnants in the mantle, their sinking history, and a new outlook on lower mantle viscosity. Tectonophysics 723, 309–448.
Van der Voo, R., van Hinsbergen, D.J., Domeier, M., Spakman, W., Torsvik, T.H., 2015. Latest Jurassic–earliest Cretaceous closure of the Mongol-Okhotsk Ocean: A paleomagnetic and seismological-tomographic analysis. Geol. Soc. Am. Spec. Paper 513, 589–606.
Van Hinsbergen, D.J., Peters, K., Maffione, M., Spakman, W., Guilmette, C., Thieulot, C., Kaymakcı, N., 2015. Dynamics of intraoceanic subduction initiation: 2. Suprasubduction zone ophiolite formation and metamorphic sole exhumation in context of absolute plate motions. Geochem. Geophys. Geosyst. 16 (6), 1771–1785.

Van Hinsbergen, D.J.J., Schouten, T.L., 2021. Deciphering paleogeography from orogenic architecture: constructing orogens in a future supercontinent as thought experiment. Am. J. Sci. 321 (6), 955–1031.
Van Hinsbergen, D.J., Spakman, W., de Boorder, H., Van Dongen, M., Jowitt, S.M., Mason, P.R., 2020b. Arc-type magmatism due to continental-edge plowing through ancient subduction-enriched mantle. Geophys. Res. Lett. 47 (9). e2020GL087484.
Van Hinsbergen, D.J.J., Torsvik, T.H., Schmid, S.M., Maţenco, L.C., Maffione, M., Vissers, R.L., Gürer, D., Spakman, W., 2020a. Orogenic architecture of the Mediterranean region and kinematic reconstruction of its tectonic evolution since the Triassic. Gondw. Res. 81, 79–229.
Van Hinsbergen, D.J.J., Steinberger, B., Guilmette, C., Maffione, M., Gürer, D., Peters, K., Spakman, W., 2021. A record of plume-induced plate rotation triggering subduction initiation. Nat. Geosci. 14 (8), 626–630.
Van Horne, A., Sato, H., Ishiyama, T., 2017. Evolution of the Sea of Japan back-arc and some unsolved issues. Tectonophysics 710, 6–20.
Veevers, J.J., Powell, C.M., Roots, S.R., 1991. Review of seafloor spreading around Australia. I. Synthesis of the patterns of spreading. Aust. J. Earth Sci. 38 (4), 373–389.
Vissers, R.L.M., Meijer, P.T., 2012a. Mesozoic rotation of Iberia: Subduction in the Pyrenees? Earth Sci. Rev. 110 (1–4), 93–110.
Vissers, R.L.M., Meijer, P.T., 2012b. Iberian plate kinematics and Alpine collision in the Pyrenees. Earth Sci. Rev. 114 (1–2), 61–83.
Wai, K.M., Abbott, M.J., Grady, A.E., 1994. The Sadowa Igneous Complex, Eastern Papua New Guinea: Ophiolite or not? Goldschmidt Conference Edinburgh, 949–950.
Wakita, K., 2015. OPS mélange: A new term for mélanges of convergent margins of the world. Int. Geol. Rev. 57 (5–8), 529–539.
Wakita, K., Metcalfe, I., 2005. Ocean plate stratigraphy in East and Southeast Asia. J. Asian Earth Sci. 24 (6), 679–702.
Walker, D.A., McDougall, I., 1982. $^{40}Ar/^{39}Ar$ and K-Ar dating of altered glassy volcanic rocks: the Dabi Volcanics. PNG. Geochimica et Cosmochimica Acta 46 (11), 2181–2190.
Wallis, S.R., Yamaoka, K., Mori, H., Ishiwatari, A., Miyazaki, K., Ueda, H., 2020. The basement geology of Japan from A to Z. Isl. Arc 29 (1), e12339.
Walther, H.W., 1981. Early Cretaceous porphyry copper mineralization on Cebu Island, Philippines, dated with K-Ar and R-Sr methods. Geol. Jahrb. 48, 21–35.
Wang, X., Cao, L., Zhao, M., Cheng, J., He, X., 2022. What conditions promote atypical subduction: Insights from the Mussau Trench, the Hjort Trench, and the Gagua Ridge. Gondw. Res.
Wang, Y., Qian, X., Asis, J.B., Cawood, P.A., Wu, S., Zhang, Y., Lu, X., 2023. "Where, when and why" for the arc-trench gap from Mesozoic Paleo-Pacific subduction zone: Sabah Triassic-Cretaceous igneous records in East Borneo. Gondw. Res. 117, 117–138.
Warren, P.Q., Cloos, M., 2007. Petrology and tectonics of the Derewo metamorphic belt, west New Guinea. Int. Geol. Rev. 49 (6), 520–553.
Waters, P.J., Cooke, D.R., Gonzales, R.I., Phillips, D., 2011. Porphyry and epithermal deposits and 40Ar/39Ar geochronology of the Baguio district. Philippines. Economic Geology 106 (8), 1335–1363.
Watts, A.B., Weissel, J.K., Larson, L.R., 1977. Sea-floor spreading in marginal basins of the western Pacific. Tectonophysics 37 (1–3), 167–181.
Webb, L.E., Baldwin, S.L., Fitzgerald, P.G., 2014. The Early-Middle Miocene subduction complex of the Louisiade Archipelago, southern margin of the Woodlark Rift. Geochem. Geophys. Geosyst. 15 (10), 4024–4046.
Webb, M., White, L.T., 2016. Age and nature of Triassic magmatism in the Netoni Intrusive Complex, West Papua, Indonesia. J. Asian Earth Sci. 132, 58–74.
Webb, M., White, L.T., Jost, B.M., Tiranda, H., 2019. The Tamrau Block of NW New Guinea records late Miocene-Pliocene collision at the northern tip of the Australian Plate. J. Asian Earth Sci. 179, 238–260.
Webb, M., White, L.T., Jost, B.M., Tiranda, H., BouDagher-Fadel, M., 2020. The history of Cenozoic magmatism and collision in NW New Guinea-New insights into the tectonic evolution of the northernmost margin of the Australian Plate. Gondw. Res. 82, 12–38.
Weiland Jr, R.J., 1999. Emplacement of the Irian ophiolite and unroofing of the Ruffaer metamorphic belt of Irian Jaya, Indonesia. The University of Texas at Austin. PhD Thesis..
Weissel, J.K., 1980. Evidence for Eocene oceanic crust in the Celebes Basin. Washington DC American Geophysical Union Geophysical Monograph Series 23, 37–47.
Weissel, J.K., Anderson, R.N., 1978. Is there a Caroline plate? Earth Planet. Sci. Lett. 41 (2), 143–158.
Weissel, J.K., Watts, A.B., 1979. Tectonic evolution of the Coral Sea basin. J. Geophys. Res. Solid Earth 84 (B9), 4572–4582.
Weissel, J.K., Taylor, B., Karner, G.D., 1982. The opening of the Woodlark Basin, subduction of the Woodlark spreading system, and the evolution of northern Melanesia since mid-Pliocene time. Tectonophysics 87 (1–4), 253–277.
Wessel, P., Matthews, K.J., Müller, R.D., Mazzoni, A., Whittaker, J.M., Myhill, R., Chandler, M.T., 2015. Semiautomatic fracture zone tracking Vol. 16(7, 2462–2472.
Whattam, S.A., 2009. Arc-continent collisional orogenesis in the SW Pacific and the nature, source and correlation of emplaced ophiolitic nappe components. Lithos 113 (1–2), 88–114.
Whattam, S.A., Malpas, J.G., Ali, J.R., Smith, I.E., Lo, C.H., 2004. Origin of the Northland Ophiolite, northern New Zealand: discussion of new data and reassessment of the model. N. Z. J. Geol. Geophys. 47 (3), 383–389.
Whattam, S.A., Malpas, J., Ali, J.R., Lo, C.H., Smith, I.E., 2005. Formation and emplacement of the Northland ophiolite, northern New Zealand: SW Pacific tectonic implications. J. Geol. Soc. London 162 (2), 225–241.
Whattam, S.A., Malpas, J., Smith, I.E.M., Ali, J.R., 2006. Link between SSZ ophiolite formation, emplacement and arc inception, Northland, New Zealand: U-Pb SHRIMP constraints; Cenozoic SW Pacific tectonic implications. Earth Planet. Sci. Lett. 250 (3–4), 606–632.
Whattam, S.A., Malpas, J., Ali, J.R., Smith, I.E.M., 2008. New SW Pacific tectonic model: Cyclical intraoceanic magmatic arc construction and near-coeval emplacement along the Australia-Pacific margin in the Cenozoic. Geochem. Geophys. Geosyst. 9, Q03021.
Whittaker, J.M., Muller, R.D., Leitchenkov, G., Stagg, H., Sdrolias, M., Gaina, C., Goncharov, A., 2007. Major Australian-Antarctic plate reorganization at Hawaiian-Emperor bend time. Science 318 (5847), 83–86.
Whittaker, J.M., Goncharov, A., Williams, S.E., Müller, R.D., Leitchenkov, G., 2013. Global sediment thickness data set updated for the Australian-Antarctic Southern Ocean. Geochem. Geophys. Geosyst. 14 (8), 3297–3305.
Williams, S.E., Whittaker, J.M., Müller, R.D., 2011. Full-fit, palinspastic reconstruction of the conjugate Australian-Antarctic margins. Tectonics 30 (6).
Wintsch, R.P., Li, X.H., 2014. Hf and O isotopic evidence for metamorphic crystallization of zircon during contact metamorphism of Fenniaolin metabasalts, Tananao complex. Taiwan. Lithos 205, 142–147.
Wintsch, R.P., Yang, H.J., Li, X.H., Tung, K.A., 2011. Geochronologic evidence for a cold arc–continent collision: The Taiwan orogeny. Lithos 125 (1–2), 236–248.
Woodhead, J., Hergt, J., Sandiford, M., Johnson, W., 2010. The big crunch: Physical and chemical expressions of arc/continent collision in the Western Bismarck arc. J. Volcanol. Geoth. Res. 190 (1–2), 11–24.
Worthing, M.A., Crawford, A.J., 1996. The igneous geochemistry and tectonic setting of metabasites from the Emo Metamorphics, Papua New Guinea; a record of the evolution and destruction of a backarc basin. Mineral. Petrol. 58 (1–2), 79–100.
Wright, N.M., Müller, R.D., Seton, M., Williams, S.E., 2015. Revision of Paleogene plate motions in the Pacific and implications for the Hawaiian-Emperor bend. Geology 43 (5), 455–458.
Wright, N.M., Seton, M., Williams, S.E., Mueller, R.D., 2016. The Late Cretaceous to recent tectonic history of the Pacific Ocean basin. Earth Sci. Rev. 154, 138–173.
Wu, J., Suppe, J., Lu, R., Kanda, R., 2016. Philippine Sea and East Asian plate tectonics since 52 Ma constrained by new subducted slab reconstruction methods. J. Geophys. Res. Solid Earth 121 (6), 4670–4741.
Wu, J., Lin, Y.A., Flament, N., Wu, J.T.J., Liu, Y., 2022. Northwest Pacific-Izanagi plate tectonics since Cretaceous times from western Pacific mantle structure. Earth Planet. Sci. Lett. 583, 117445.
Wu, J.T.J., Wu, J., 2019. Izanagi-Pacific ridge subduction revealed by a 56 to 46 Ma magmatic gap along the northeast Asian margin. Geology 47 (10), 953–957.
Xu, Y., Yan, Q., Shi, X., Jichao, Y., Deng, X., Xu, W., Jing, C., 2022. Discovery of Late Mesozoic volcanic seamounts at the ocean-continent transition zone in the Northeastern margin of South China Sea and its tectonic implication. Gondw. Res.
Yamazaki, T., Seama, N., Okino, K., Kitada, K., Joshima, M., Oda, H., Naka, J., 2003. Spreading process of the northern Mariana Trough: Rifting-spreading transition at 22 N. Geochem. Geophys. Geosyst. 4 (9).
Yamazaki, T., Stern, R.J., 1997. Topography and magnetic vector anomalies in the Mariana Trough. JAMSTEC J. Deep Sea Res. 13, 31–45.
Yan, C.Y., Kroenke, L.W., 1993. A plate reconstruction of the southwest Pacific 0–100 Ma. In Proceedings of Ocean Drilling Program, Scientific Results 130, 697–709.
Yan, S., Yan, Q., Shi, X., Yuan, L., Liu, Y., Yang, G., Ye, X., 2022. The dynamics of the Sorol Trough magmatic system: Insights from bulk-rock chemistry and mineral geochemistry of basaltic rocks. Geol. J. 57 (10), 4074–4089.
Yang, K.M., Huang, S.T., Jong-Chang, W., Ting, H.H., Wen-Wei, M., Lee, M., Chang-Jie, L., 2007. 3D geometry of the Chelungpu thrust system in central Taiwan: Its implications for active tectonics. TAO. Terr. Atmos. Ocean. Sci. 18 (2), 143.
Yang, K.M., Rau, R.J., Chang, H.Y., Hsieh, C.Y., Ting, H.H., Huang, S.T., Tang, Y.J., 2016. The role of basement-involved normal faults in the recent tectonics of western Taiwan. Geol. Mag. 153 (5–6), 1166–1191.
Yang, T.F., Tien, J.L., Chen, C.H., Lee, T., Punongbayan, R.S., 1995. Fission-track dating of volcanics in the northern part of the Taiwan-Luzon Arc: eruption ages and evidence for crustal contamination. J. SE Asian Earth Sci. 11 (2), 81–93.
Yeh, K.Y., Cheng, Y.N., 2001. The first finding of early Cretaceous radiolarians from Lanyu, the Philippine Sea Plate. Collection and Research 13, 111–145.
Yu, M., Dilek, Y., Yumul Jr, G.P., Yan, Y., Dimalanta, C.B., Huang, C.Y., 2020. Slab-controlled elemental–isotopic enrichments during subduction initiation magmatism and variations in forearc chemostratigraphy. Earth Planet. Sci. Lett. 538, 116217.
Yui, T.F., Maki, K., Lan, C.Y., Hirata, T., Chu, H.T., Kon, Y., Yokoyama, T.D., Jahn, B.M., Ernst, W.G., 2012. Detrital zircons from the Tananao metamorphic complex of Taiwan: Implications for sediment provenance and Mesozoic tectonics. Tectonophysics 541, 31–42.
Yumul Jr, G.R., 1989. Petrological characterization of the residual-cumulate sequences ofthe Zambales ophiolite complex, Luzon, Philippines. Ofioliti 14, 253–291.
Yumul Jr, G.P., 1993. Angat Ophiolitic Complex, Luzon, Philippines: a Cretaceous dismembered marginal basin ophiolitic complex. J. SE Asian Earth Sci. 8 (1–4), 529–537.
Yumul Jr, G.P., 2007. Westward younging disposition of Philippine ophiolites and its implication for arc evolution. Isl. Arc 16 (2), 306–317.

Yumul Jr., G.P., Balce, G.R., Dimalanta, C.B., Datuin, R.T., 1997. Distribution, geochemistry and mineralization potentials of Philippine ophiolite and ophiolitic sequences. Ofioliti 22, 47–56.
Yumul Jr, G.P., Dimalanta, C.B., Jumawan, F.T., 2000a. Geology of the southern Zambales ophiolite complex, Luzon. Philippines. Island Arc 9 (4), 542–555.
Yumul, Dimalanta, C.B., Salapare, R.C., Queano, K.L., Faustino-Eslava, D.V., Marquez, E.J. ... Suzuki, S., 2020. Slab rollback and microcontinent subduction in the evolution of the Zambales Ophiolite Complex (Philippines): A review. Geoscience Frontiers 11 (1), 23–36.
Yumul Jr, G.P., Dimalanta, C.B., Tamayo, R.A., Barretto, J.A.L., 2000b. Contrasting morphological trends of islands in Central Philippines: speculation on their origin. Isl. Arc 9 (4), 627–637.
Yumul Jr, G.P., Dimalanta, C.B., Maglambayan, V.B., Tamayo Jr, R.A., 2003. Mineralization controls in island arc settings: Insights from Philippine metallic deposits. Gondw. Res. 6 (4), 767–776.
Yumul Jr, G.P., Dimalanta, C.B., Tamayo Jr, R.A., Maury, R.C., Bellon, H., Polvé, M., Cotten, J., 2004. Geology of the Zamboanga Peninsula, Mindanao, Philippines: An enigmatic South China continental fragment? Geol. Soc. Lond. Spec. Publ. 226 (1), 289–312.
Yumul Jr, G.P., Dimalanta, C.B., Tamayo Jr, R.A., Zhou, M.F., 2006. Geology and geochemistry of the Rapu-Rapu ophiolite complex, eastern Philippines: possible fragment of the proto-Philippine Sea Plate. Int. Geol. Rev. 48 (4), 329–348.
Yumul Jr, G.P., Jumawan, F.T., Dimalanta, C.B., 2009. Geology, geochemistry and chromite mineralization potential of the Amnay Ophiolitic Complex, Mindoro. Philippines. Resource geology 59 (3), 263–281.
Yumul Jr, G.P., Dimalanta, C.B., Tamayo Jr, R.A., Faustino-Eslava, D.V., 2013. Geological features of a collision zone marker: the Antique Ophiolite Complex (Western Panay, Philippines). J. Asian Earth Sci. 65, 53–63.
Zahirovic, S., Seton, M., Müller, R.D., 2014. The Cretaceous and Cenozoic tectonic evolution of Southeast Asia. Solid Earth 5 (1), 227–273.
Zamoras, L.R., Matsuoka, A., 2001. The Malampaya Sound Group in the Calamian Islands, North Palawan Block (Philippines). J. Geol. Soc. Jpn 107 (5), XI-XII.
Zamoras, L.R., Matsuoka, A., 2004. Accretion and postaccretion tectonics of the Calamian Islands, North Palawan block. Philippines. Island Arc 13 (4), 506–519.
Zglinicki, K., Szamałek, K., Górska, I., 2020. The Cyclops Ophiolite as a Source of High-Cr Spinels from Marine Sediments on the Jayapura Regency Coast (New Guinea, Indonesia). Minerals 10 (9), 735.
Zhang, G., Zhang, J., Wang, S., Zhao, J., 2020. Geochemical and chronological constraints on the mantle plume origin of the Caroline Plateau. Chem. Geol. 540, 119566.
Zhang, J., Zhang, G., 2020. Geochemical and chronological evidence for collision of proto-Yap arc/Caroline plateau and rejuvenated plate subduction at Yap trench. Lithos 370, 105616.
Zirakparvar, N.A., Baldwin, S.L., Vervoort, J.D., 2011. Lu–Hf garnet geochronology applied to plate boundary zones: Insights from the (U) HP terrane exhumed within the Woodlark Rift. Earth Planet. Sci. Lett. 309 (1–2), 56–66.
Zirakparvar, N.A., Baldwin, S.L., Vervoort, J.D., 2013. The origin and geochemical evolution of the Woodlark Rift of Papua New Guinea. Gondw. Res. 23 (3), 931–943.
NOAA National Centers for Environmental Information, 2022. ETOPO 2022 15 Arc-Second Global Relief Model. NOAA National Centers for Environmental Information. https://doi.org/10.25921/fd45-gt74.

Suzanna van de Lagemaat recently received her PhD from Utrecht University, the Netherlands. Her PhD research focused on the plate tectonic evolution of the western and southern Panthalassa realm, spanning from Japan to Patagonia. Van de Lagemaat uses a combination of field-based research, including paleomagnetism and geochronology, and extensive literature research to make kinematic reconstructions of plate tectonics and orogenesis in the Panthalassa realm during the Mesozoic and Cenozoic. She is also interested in using these kinematic reconstructions to make inferences about geodynamic processes.

Douwe van Hinsbergen (PhD, Utrecht University, 2004) is full professor of global tectonics and paleogeography at Utrecht University, the Netherlands, where he has taught since 2012. Van Hinsbergen studies and kinematically reconstructs plate tectonics, orogenesis, and paleogeography across the globe. He closely collaborates with seismologists to reconstruct mantle convection and with modelers of geodynamics and paleoclimate to advance understanding in the physics driving geological processes particularly related to plate tectonics. Van Hinsbergen is author or co-author of over 200 articles in peer-reviewed international journals.